Clemens Walther · Dharmendra K. Gupta
Editors

Radionuclides in the Environment

Influence of chemical speciation and plant uptake on radionuclide migration

Springer

Radionuclides in the Environment

Clemens Walther • Dharmendra K. Gupta
Editors

Radionuclides in the Environment

Influence of chemical speciation and plant uptake on radionuclide migration

Springer

Editors

Clemens Walther
Gottfried Wilhelm Leibniz Universität Hannover
Institut für Radioökologie und Strahlenschutz (IRS)
Hannover
Germany

Dharmendra K. Gupta
Gottfried Wilhelm Leibniz Universität Hannover
Institut für Radioökologie und Strahlenschutz (IRS)
Hannover
Germany

ISBN 978-3-319-22170-0 ISBN 978-3-319-22171-7 (eBook)
DOI 10.1007/978-3-319-22171-7

Library of Congress Control Number: 2015955144

Springer Cham Heidelberg New York Dordrecht London

Printed on acid-free paper

Springer International Publishing AG Switzerland is part of Springer Science+Business Media (www.springer.com)

Preface

The natural and artificial radionuclides, which are present in the upper soil, in drinking water, in food, and in the atmosphere, are the main sources of radiation exposure for living organisms. On a global average, 79 % of the radiation to which general public is exposed are from natural sources, 19 % from therapeutic application, and the remaining 2 % are from fallout of nuclear weapons testing and from use of nuclear power. 438 nuclear power plants exist in 31 countries as of June 1, 2015 with an installed electric net capacity of about 379 GW. 67 plants with planned installed capacity of 65 GW are under construction in 16 countries. More than 200 different radioactive isotopes are generated during the operation of a typical reactor, most of the them relatively short-lived and decay to low levels within a few decades. During normal operation, only a negligible fraction is set free; however, the volatile and short-lived isotopes such as I-131 can commit considerable dose to man.

Uranium is ubiquitous in nature and uranium concentrations of 1–10 mg kg^{-1} are not uncommon. By weathering of U-bearing minerals like uraninite, coffinite, pitchblende, and carnotite, uranium in its hexavalent state can be mobilized. Oxidative dissolution of minerals by the action of water releases soluble uranyl (UO_2^{2+}). Besides, U(VI) valance states III, IV, and V exist, of which IV and VI are the most common valance states at natural conditions. The oxidation of organic matter or iron in soil can reduce hexavalent uranium to the hardly soluble U(IV), which is strongly adsorbed by soil particles and forms stable complexes (hydroxides, hydrated fluorides, and phosphates) immobile in soils. In contrast, U(VI) has a high solubility. U(VI) is readily complexed by fluoride, sulfate, carbonate, as well as phosphate. U(IV) is predominant in soils with high water content at $Eh < 200$ mV, whereas U(VI) prevails in adequately aerated soils. Vertical U migration in soil is a long-term process and has two possible pathways: upward, in the case of water deficit, and downward, as a result of leaching.

Dissolved radionuclide ions can bind to solid surfaces by a number of processes often classified under sorption. The radioactive nuclides' relocation rate in soil is defined as an average velocity of downward migration after the deposition to the soil surface.

In summary, the behavior and ultimate radiological impacts of radionuclides in soils are largely controlled by their chemical form and speciation, which strongly affects their mobility, the residence time within the soil rooting zone, and availability for uptake by biota. The basic processes controlling mobility of radionuclides (and other trace elements) in soil include convective transport by flowing water, dispersion caused by spatial variations of convection velocities, diffusive movement within the fluid, and physicochemical interactions with the soil matrix.

The low concentration of radionuclides in soil makes formation of intrinsic polymeric species and formation of their pure solid phases an unlikely process. Instead, mixed phases and complexes are the dominating species. Exceptions are release of radionuclides already in particulate form such as in the case of reactor accidents or from fuel fabrication plants. However, humus and low-molecular weight are significantly involved in the mobility of radionuclides in soil. Soil redox potential, pH, the content, and composition of the organic matter and the sorption to mineral soil constituents represent the main factors controlling the chemical form of radionuclides in soil.

To achieve information on radionuclide species such as (pseudo-)colloids and particles, advanced analytical methods including nano- and micro-analytical techniques are required for the identification, isolation, and characterization of “hot” particles. Measurement of radioactivity alone is not sufficient for understanding the fundamental molecular mechanisms of environmental concern, such as migration, plant uptake, and transfer. Additional dedicated techniques such as X-ray-based high-resolution imaging or spatially resolved mass spectrometry give valuable additional information.

Transfer of radionuclides along food chains has been studied widely in the last 50 years following civilian use of nuclear energy, releases from military sites, and nuclear weapons testing on a global scale. The transfer factor (TF) for the uptake of any radionuclide from soil to plant is defined as the ratio of the dry weight concentration in plants to the dry weight concentration in a specified soil layer. The dry weight was used to reduce uncertainty, with the exception of fruits. The TF also regularly referred to as concentration ratio (CR) is the most common parameter to quantify radionuclide soil to plant transfer, when uptake by plant roots is the only process affecting transfer and wet or dry deposition on leaves is not taken into account.

The primary application of soil-to-plant transfer factors is in biosphere models used for calculating radiological consequences from routine or accidental release of radioactive substances into the environment. These models usually are designed to give conservative assessments. However, the migration and accumulation of radionuclides in the soil plant system is a complicated phenomenon, involving, e.g., leaching, capillary rise, runoff, sorption, root uptake, and resuspension into aquifer or atmosphere.

The uptake of any radioactive ion is regulated by a number of factors, i.e., physicochemical properties of the radioactive ions, the growth stage on the agricultural crop at the time of radionuclide contamination, the total amount of precipitation, the intensity of the precipitation, and the ability of the agricultural crops to hold water. The concentration of radioactive ions in agricultural crops will be different depending on the growth stage. Usually at a well-developed growth stage, the majority of deposited radionuclides will be taken up directly by areal parts of the plant.

Sometimes chelating agents and/or organic compounds also increase the radionuclide ion mobility in plant systems and reduce soil retention, which leads to an overall enhanced radionuclide uptake. Moreover, chelating agents also enhance the translocation ability within the plant itself. For remediation purposes, plants' nutrient deficiencies are beneficial because they decrease soil retention, therefore increasing plant uptake. However, the opposite, i.e., high nutrient concentration, is desirable to avoid intake into the food chain. Effectiveness depends on soil properties (especially soil pH), chemical form of the radionuclide, and the nature and concentration of chelating agent.

In any plants, radionuclides do not easily enter through the cuticular layer of the epidermis of leaves. It is rather through cracks and defects in the cuticle layer that radionuclide can enter the leaves. Alternatively, radionuclides may enter into the plant system through the stomata as well, but this pathway contributes to the total uptake only to a smaller extent. Once radionuclide entered inside the cuticle layer, specialized epidermal cells (surface veins consisting of thin-walled parenchyma tissue) are easily penetrated. Radionuclides are then actively transported inside the plant cells through the symplastic pathway (the inner side of the plasma membrane in which water can freely diffuse) and also by an exchange apparatus between phloem and xylem (vascular bundle) through the vascular rays.

Plant tolerance to radionuclides largely depends on plant competence in uptake, translocation, and sequestration of radionuclide in specialized tissues or in trichomes and cell organelles. Radionuclides which are complexed and sequestered in cellular structures become unavailable to shoots via translocation. Radionuclide binding/complexing to the cell wall is not the only plant mechanism responsible for radionuclides' immobilization into roots and subsequent inhibition of ion translocation to above ground parts. In general, vacuoles are generally considered to be the main storage site for radionuclides in plant cells and there is some evidence that phytochelatin (low-molecular binding peptides)–metal complexes are pumped into the vacuole.

The significant features of this book are related to how radionuclides are released into the environment and how the chemical speciation does influence the radionuclide migration in soil and uptake in plant system. The first four chapters deal with bioavailability of radionuclide mobility in soil. The rest of the chapters focus on radiotracers and biotransformation of radionuclides, uptake and retention of radionuclide after natural/artificial radionuclide fallout, analysis of certain radionuclide in environmental samples, methods of decreasing radionuclide transfer in the plant system from soil, and some case studies on modeling. Furthermore, the information compiled in this book will bring in-depth knowledge and enhancement in the field of radionuclide uptake and its toxicity in plants after Chernobyl and Fukushima nuclear power plants accidents.

Prof. Clemens Walther and Dr. Dharmendra K. Gupta personally thank the authors for contributing their valuable time, knowledge, and eagerness to bring this book into in this shape.

Hannover, Germany

Clemens Walther
Dharmendra K. Gupta

Contents

Sources Contributing to Radionuclides in the Environment: With Focus on Radioactive Particles

Brit Salbu, Lindis Skipperud, and Ole Christian Lind

Contents

Abstract To assess environmental impact and risks associated with radioactive contamination of ecosystems, links must be established between the source term and deposition, ecosystem transfer, biological uptake and effects in exposed organisms. In transport, dose, impact and risk models, information on the source term and the deposition densities is therefore an essential input. Following severe nuclear events, a major fraction of refractory radionuclides can be present as radioactive particles. The particle characteristics will depend on the source and the release scenarios, and such information should be included in the source term. Furthermore, assessments are traditionally based on average bulk mass or surface activity concentrations of radionuclides in environmental compartments (Bq/kg, Bq/m^2 or

B. Salbu (✉) • L. Skipperud • O.C. Lind
CERAD, Department of Environmental Sciences, Norwegian University of Life Sciences, 1432 Aas, Norway
e-mail: brit.salbu@nmbu.no

C. Walther, D.K. Gupta (eds.), *Radionuclides in the Environment*,
DOI 10.1007/978-3-319-22171-7_1

Bq/L), assuming that a limited number of samples are representative. Localised heterogeneities such as particles will, however, be unevenly distributed, and representative sampling can be questionable. Due to structural properties, dissolution of radionuclides from particles prior to measurements may be partial. For areas affected by particle contamination, the inventories can be underestimated, and impact and risk assessments may suffer from unacceptable large uncertainties if radioactive particles are ignored. The present chapter will focus on key sources contributing to radioactivity in the environment, especially radioactive particles, and will summarise the most important particle characterisation techniques available.

Keywords Nuclear sources releasing particles • Particle characterisation techniques • Linking sources to particle characteristics

1 Release of Radioactivity in the Environment

A series of sources has contributed to radioactivity in the environment, and naturally occurring radioactive materials (NORMs) and artificially produced radionuclides are present in all ecosystems. In addition to NORM from natural processes such as the weathering of uranium (U)- or thorium (Th)-rich minerals, additional contributions originate from man-made activities associated with the front end of the nuclear weapon and fuel cycles (U mining) and from non-nuclear industries (e.g., oil and gas industries). Since 1945, a series of nuclear and radiological sources have also contributed to the release of artificially produced radionuclides into the environment, in particular sources associated with the nuclear weapon and fuel cycles.

To put the contribution of the different sources into perspective, the relative (%) contribution to the radiological consequences, expressed as the average annual radiation dose per person (mSv), can be utilised. According to the National Council on Radiation Protection and Measurement (NCRPM 2009), the average annual radiation dose per person in the USA is 6.2 mSv, while 3.0 mSv on a global scale. The contribution of different sources to the annual average person dose can be distingushed. NORM sources such as cosmic radiation and contribution from the ground including daughter nuclides like the radon and thoron gases contribute to more than 50 % of the annual dose. The exposure from man-made sources (48 %) is predominately attributed to medical diagnostics and treatments. The estimated contribution from the nuclear weapon and fuel cycle amounts to about 0.02 mSv also on the global scale. However, the natural and artificial background radiation levels are unevenly distributed and vary according to geology and altitude and especially to the distance from nuclear accidental or nuclear test sites.

To put the contribution of different sources included in the nuclear weapon and fuel cycles into perspective, UNSCEAR (2000) has estimated their contribution to

Table 1 Collective effective dose to the public from radionuclides released from the nuclear weapon and fuel cycles (UNSCEAR 2000)

Source	Normalised collective effective dose (manSv/GW_ey)
Local and regional effects	1995–1997
Mining	0.19
Milling	0.008
Mine and mill tailings (releases over 5 years)	0.04
Fuel fabrication	0.003
Reactor operation	
Atmospheric	0.4
Aquatic	0.04
Reprocessing	
Atmospheric	0.04
Aquatic	0.09
Transportation	<0.1
Total (rounded)	0.91
Solid waste disposal and global effects	
Mine and mill tailings	
Releases of radon over 10000 y	7.5
Reactor operation	
Low-level waste disposal	0.00005
Intermediate-level waste disposal	0.5
Reprocessing solid waste disposal	0.05
Globally dispersed radionuclides (truncated to 10000 years)	40
Total (rounded)	50

the collective effective dose to members of the public, normalised according to energy produced per year (mSv/GW_ey). As demonstrated in Table 1, the major contributors to environmental contaminations are the global dispersion (atmospheric nuclear weapons tests, release from nuclear accidents) and mining. In contrast to NORM which includes naturally occurring isotopes of a limited number of stable elements, a series of radionuclides is produced in weapon tests and in reactors. Fission products, activation products and transuranics are signatures of the weapon and fuel cycle, while the contribution of the "NORM" nuclides ^{3}H and ^{14}C also is substantial.

To assess environmental impact and risks associated with radioactive contamination of ecosystems, links must be established between the source term and deposition, ecosystem transfer, biological uptake and effects in exposed organisms. In transport, dose, impact and risk models, information on the source term and the deposition densities is needed as input. The source term is usually a qualitative and quantitative description of radionuclides released from a source, used as input to models describing the air or water transport, dispersion and deposition of radionuclides in affected ecosystems. The source term is most often estimated from the source inventory (% released) and provides information on the amount of radionuclides released (Bq), the time development of the release, plume height and energy content of the release. In most air dispersion models, the source term input as Bq is assumed to represent aerosol transport (e.g. similar to sulphate aerosols adapted from acid rain research), while in most marine transport models, Bq refers to simple chemical species behaving conservatively. When refractory radionuclides such as uranium (U) and plutonium (Pu) are released during nuclear events, however, a major fraction is associated with particles, ranging from submicrons to fragments.

Radiological assessments are also most often based on average bulk mass or surface activity concentrations of radionuclides in water (Bq L^{-1}), soils, sediments (Bq kg^{-1} or Bq/m^2) or biota (Bq kg^{-1}), assuming that radionuclides are homogeneously distributed as simple chemical species and that a limited number of samples are representative of the deposition. It is generally not recognised that releases can include radioactive particles that often contain a significant fraction of the bulk sample activity present in the environment (IAEA 2011). Furthermore, localised heterogeneities such as particles will be unevenly distributed and the assumption of representative sampling can be questionable. Due to structural properties, dissolution of radionuclides from particles prior to measurements may also be partial (Oughton et al. 1993). Furthermore, the inherent differences in transport, mobility and bioavailability of particle-bound radionuclides compared with radionuclide species such as molecules, ions or complexes have largely been ignored in radiochemistry, radioecology and radiation dosimetry. For areas affected by particle contamination, the inventories can be underestimated, and the assessment of impact and risk to human health and the long-term ecological consequences can suffer from unacceptable large uncertainties if radioactive particles are ignored (Salbu 2009; Salbu et al. 2004).

Radionuclides released from a source and deposited in different ecosystems can be present in different physico-chemical forms, such as low molecular mass (LMM) species, colloids or nanoparticles as well as pseudocolloids, particles and fragments (Salbu 2000a, b). LMM species are believed to be mobile and potentially bioavailable, colloids are mobile, while particles can be retained in sinks such as soils and sediments. Due to remobilization processes, however, contaminated soils and sediments can act as diffuse sources of radionuclides in the future. Thus, information of radionuclide species released from a source and deposited in the environment as well as transformation of radionuclide species over time is essential for assessing ecosystem transfer and uptake in exposed organisms (Fig. 1).

Radioactive particles are defined as a localised aggregation of radioactive atoms that give rise to an inhomogeneous distribution of radionuclides significantly different from that of the matrix background (IAEA 2011). In water, particles are defined as entities having diameters larger than 0.45 μm, i.e. entities that will settle due to gravity. Radionuclide species within the size range 0.001–0.45 μm are referred to as radioactive colloids or pseudocolloids, while species less than 1 nm (10^3 Da) is referred to as low molecular mass (LMM) species. For soils and sediments, grain-size analysis differentiates between categories of sand (0.062–2 mm), silt (4–62.5 μm) and clays (1–4 μm), and particles larger than 2 mm should

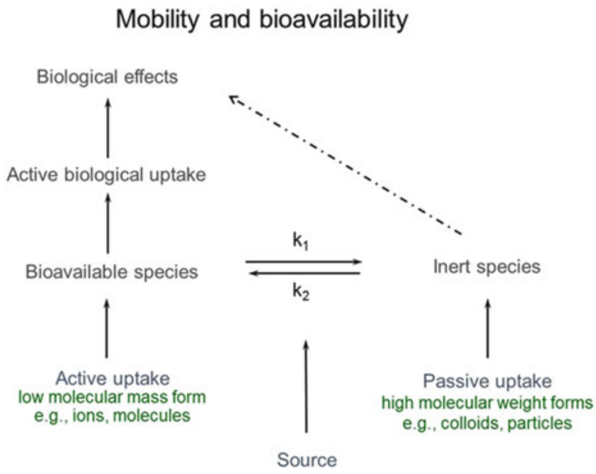

Fig. 1 Radionuclides released from a source can be present in different physico-chemical forms. LMM species are believed to be potentially bioavailable, while particles can be retained in, for instance, filtering organisms. The system is dynamic; due to transformation processes, the fraction of LMM species can decrease due to interactions with soil compartment; due to particle weathering, LLM species can be produced over time. The distribution of radionuclide species and kinetics are essential for assessing uptake, effects, impact and risks (Salbu 2000b)

be referred to as fragments. In air, radioactive particles ranging from submicrons in aerosols to fragments are classified according to the aerodynamic diameters, where particles less than 10 μm are considered respiratory. These categories are operationally based, and there are gradual transitions between categories. Due to interactions and transformation processes in the environment, particle growth mechanisms and dispersion processes will alter the original distribution of radionuclide species deposited in an ecosystem. The presence of radioactive species ranging from micrometre-sized particles to fragments can be identified by imaging techniques such as digital autoradiography (Salbu 2000b), reflecting their inhomogeneous distributions in water, sediments and soils. To obtain information on radionuclide species including particle characteristics, more advanced analytical techniques are needed (Sect. 2).

Following historical nuclear events, refractory radionuclides such as U and Pu were to a certain extent associated with particles, ranging from submicrons to fragments, containing fission products, activation products and transuranics (Sect. 3). Severe nuclear events include nuclear weapon tests and nuclear reactor explosions or fires. Conventional detonation of nuclear weapons, safety trials and the use of depleted uranium ammunition include the release of matrix particles, often ranging from submicron to fragments. Reprocessing facilities and civil reactors are also sources of radioactive colloids and particles via authorised or accidental releases. Furthermore, radioactive particles are identified in sediments in the close vicinity of radioactive waste dumped at sea. In addition, radioactive particles containing U, Th or progenies are identified at NORM sites such as U mining sites or associated with scale from the oil and gas industry. Thus, whenever refractory radionuclides are released following nuclear events, radioactive particles should also be expected.

Radioactive particles are formed due to critical (explosions, fires) or subcritical (corrosion processes) destruction of fuel, weapon matrices and other nuclear or radiological materials. During nuclear events under high-temperature and high-pressure conditions such as nuclear weapon tests (e.g., Semipalatinsk, Kazakhstan; Marshall Islands), the particle formation depends on the weapon materials and other major components such as metals (iron) in the fireball, as well as the yield and altitude of the blast. During the blast, fission and activation products as well as transuranics are formed. When the fireball temperature decreases, condensation processes take place as well as decay processes of the produced radionuclides. Due to differences in volatility, chemical properties and half-lives, the particle composition will depend on fractionation of produced radionuclides, and daughter nuclides can be depleted in particles. Thus, isotope or atom ratios of transuranic elements can be used for source identification. The particle size distribution, morphology and structure are also dependent on the type of explosion. Near-surface detonations produce large glassy soil containing often highly radioactive particles. Bursts at high altitudes in the atmosphere will produce small spherical particles which can remain suspended for considerable periods of time. Following conventional detonation of nuclear weapon (e.g., Thule, Greenland; Palomares, Spain) or the use of depleted uranium ammunition, particles are made from the mechanical destruction of weapon materials and the containment. Similarly, at high-temperature and high-pressure release scenarios (reactor explosion, fire), solid materials can liquefy, volatiles will escape, while refractory transuranics and fission and activation products can remain when droplets are solidified. Furthermore, interactions with construction materials such as moderator and zircaloy in reactors are essential for the products formed, i.e. the formation of metal–metal crystalline structures such as U–Zr or U–carbide compounds as observed after the Chernobyl accident (Salbu et al. unpublished). In contrast to hydrogen explosions, the presence of air during a fire will influence on the structure and oxidation states of released radionuclides. Thus, the composition of particles released in a nuclear reactor accident will reflect the characteristics of refractory elements in the source (burn-up) and its containment, while the release scenario (temperature, pressure and presence of oxygen) will influence the particle size distribution, crystallographic structures and oxidation states (Sect. 3) of relevance for ecosystem transfer.

Releases under low-temperature conditions are most often associated with corrosion processes damaging the source containment and allowing releases to occur. The extent of corrosion depends on physical conditions of containments as well as on the surroundings (e.g., water pH, redox, temperature). Due to corrosion of depleted uranium (DU) ammunition penetrators buried in sand, oxidised DU particles were released (Lind et al. 2009; Salbu et al. 2005). Due to corrosion, leakages of waste from containers dumped in the fjords of Novaya Zemlya are significant (Salbu et al. 1997). Due to corrosion of U–Al fuel misplaced in air ducts at the Windscale Pile, about 20 kg of U as U–Al particles were released through the air-cooled ducts (Salbu 2000a). Particles and colloids have also been released from nuclear installations as authorised discharges via pipelines to the sea (Sellafield and La Hague reprocessing facilities) (Salbu et al. 1993, 2003). Such particles can reflect the composition of the waste streams as well as represent reminiscences of the industrial processes (residues from exchange resins). The characteristics of particles obtained under low-temperature conditions will be distinctly different from those released under high-temperature–pressure conditions (Sect. 3).

The source and release scenarios, including physical characteristics such as temperature, pressure and redox conditions, are important determinants of the physico-chemical forms of released and deposited radionuclides and thereby their mobility, biological uptake and effects of consequences for affected ecosystems. To obtain information on particle characteristics, advanced techniques and equipment are needed (Sect. 2). Using such techniques, information on particle characteristics associated with different nuclear and radiological sources and different release scenarios can be obtained (Sect. 3).

2 Particle Characterisation Techniques

Key particle characteristics influencing mobility and ecosystem transfer, biological uptake and effects include particle size distributions, surface and bulk (3D) elemental composition, morphology, structure, density and oxidation state influencing the particle weathering rates (Salbu 2001). Due to their small sizes, often in the range of submicron to micrometres, radioactive particles can be difficult to locate, identify and characterise. It is likely that the lack of a reliable procedure for particle identification often leads to negligence of radioactive particles and thereby underestimation of the role they play in environmental contamination. When located, isolated and extracted, several solid-state speciation techniques can be utilised to characterise particles identified in the environment. In addition, atom or isotopic ratios can be utilised for source identification purposes.

A number of analytical tools have been applied in radioactive particle research (Table 2) as also discussed in IAEA (2011). For radionuclides in waters, filtration (<0.45 μm) and ultrafiltration (nm to μm range membranes) combined with radioanalytical techniques may be applied to distinguish ionic species and colloidal and particulate material (Salbu 2000b). To separate particles from air and provide estimates on the size distribution, cascade impactors with membranes having different cut-off levels (μm to mm) are frequently used in combination with radioanalytical methods. In contaminated areas, hot spots can be identified using portable detectors. In the laboratory, radioactive heterogeneities may be identified using imaging techniques, repeated sample mixing (Bunzl 1998; Bunzl and Tschiersch 2001) or splitting (Bunzl 1997) combined with gamma spectrometry. For contaminated soils and sediments, biological material and filters from air or water fractionation procedures, imaging techniques such as digital phosphor

Table 2 Analytical tools available in radioactive particle research

	Method	Information obtained	Comments
Identification	Size fractionation in water followed by radioanalytical techniques	Size distribution	
	Cascade impactor with aerosol filters followed by radioanalytical techniques	Size distribution (AMAD)	
	Portable monitors in the field	Hot spot identification	
	Digital autoradiography	Distribution of radioactivity	Easy and time saving Non-destructive
	Real-time imaging techniques	Distribution of radioactivity	Easy and time saving Non-destructive
	Repeated sample splitting combined with γ-spectrometry	Elevated activities in subsamples indicate heterogeneities	Non-destructive
	Repeated sample mixing combined with γ-spectrometry	Skewed frequency distribution of the counts indicates heterogeneities	Non-destructive
Isolation	Repeated sample splitting combined with light microscope and GM tube, γ-spectrometry or autoradiography	Elevated activity in subsamples indicates heterogeneities	Non-destructive
	Direct identification in SEM confirmation by XRMA	High atomic number elements identified as bright areas in BEI mode	Non-destructive
	FIB-SEM	Microsurgery or micromanipulation of particles	
Characterisation of particles	Scanning electron microscopy with XRMA	Size distribution, surface morphology, elemental composition and distribution	Non-destructive
	Analytical TEM (transmission electron microscopy)/STEM with XRMA, electron diffraction, EELS, HAADF	Size distribution of colloids. Element composition, crystalline structure, chemical bonding and Z-contrast imaging	Often time-consuming sample preparation Thin sections prepared by ultramicrotome
	Nano- and microfocused XRF	Elemental composition and 2D distribution (depth information)	Non-destructive
	Confocal μ-XRF	Elemental composition and 3D distribution	Non-destructive

(continued)

Table 2 (continued)

	Method	Information obtained	Comments
	Nano- and microfocused XANES	Oxidation state (distribution)	Non-destructive Synchrotron based
	Nano- and microfocused XRD	Crystallographic structures	Non-destructive
	Nano- and microfocused tomography	Spatial distribution of density, elements, oxidation states	Non-destructive Laboratory based (nano-CT) or synchrotron based
	EXAFS	Structure of noncrystalline materials	Synchrotron based
	Microfocused PIXE	Elemental composition and distribution	Semi-destructive
	Nano-SIMS, SIMS	Size distribution and isotope ratios	Semi-destructive
	LA-ICP-MS, LAMMA	Elemental and isotopic composition	Semi-destructive
	Leaching experiments	Solubility/weathering rates	Gradually destructive. Results depend on extraction agent
	Isotope or atom ratios by MS techniques (ICP-MS, AMS, RIMS, TIMS, SIMS)	Source identification of individual particles (isotope ratios)	Destructive techniques
	γ-spectrometry and X-ray spectrometry	Activity concentrations, activity ratios	Non-destructive
	α-, β-spectrometry	Source identification (activity ratios)	Destructive techniques

imaging (digital autoradiography) have proved especially useful for locating radioactive particles. Hot spots reflect particles, and further separations of subsamples using radiation detectors and microscopes are needed prior to the use of surface (and to certain extent subsurface)-sensitive EM techniques. Using conventional (SEM) or environmental scanning electron microscopes (ESEM) in backscattered electron imaging (BEI) mode, bright areas reflect the presence of high atomic number elements, while the composition and distribution of elements in the upper particle surface layer are attained using energy-dispersive X-ray analysis (EDX). The structure of particles is characterised from images acquired in secondary electron imaging mode. SEM and ESEM also serve as screening techniques prior to further detailed studies using other nanometre- or micrometre-sized beam techniques.

To obtain information on the distribution of elements and species below the surface of particles, microanalytical techniques with greater penetration depths such as proton (or particle)-induced X-ray emission (μ-PIXE) and secondary ion mass spectrometry (SIMS) as well as synchrotron radiation (SR)-based nano- or micro-X-ray techniques are needed. Using high-flux monochromatic X-ray beams, synchrotron radiation (SR)-based X-ray techniques have proved most useful for characterisation of individual particles. Nanoscopic or microscopic X-ray fluorescence analysis (μ-XRF) provides information on two-dimensional or three-dimensional (μ-tomography) elemental distributions within individual particles, while nano-/micro-X-ray diffraction (XRD) gives information on the crystallographic structures of solid particles. Nano- or micro-X-ray absorption near-edge structure (XANES) spectrometry provides information on the oxidation state on corresponding nanometre or micrometre scales, while extended X-ray absorption fine structure (EXAFS) analysis could potentially provide information on the coordination number and the distance to neighbouring atoms, if detailed knowledge on atoms involved is available (Conradson 2000).

Following solid-state (non-destructive) speciation techniques, leaching experiments may provide important data on solubility and weathering rates, which can be linked to the particle characteristics. Finally, the particles may be fully dissolved and subjected to α-, β- and/or mass spectrometry determining activity concentrations and isotopic ratios to identify the source of particles.

2.1 Identification and Isolation of Radioactive Particles

The usual identification procedure includes the collection of air filters (cascade impactors) or in-field monitoring of anomalously high radioactivity (hot spots), sampling of bulk material and preparation of thin layers of solutions or spreading thin layers of solid material on sheets for autoradiography. For any sample type, particle distribution can be determined only in layers sufficiently thin to allow the emitted radiation to pass without being fully absorbed. Large particles having certain colours can be extracted under microscope, while physical extraction represents a challenge for small particles. Sample splitting and counting techniques can be utilised to reduce the volume of soil and sediments to be searched, prior to autoradiography. Using phosphorous imaging and long exposure time, submicron in homogeneities can be identified and extracted under microscope using micromanipulators. Equipment for manipulation of single particles in the size range down to μm is available for investigations in light microscopes and for scanning electron microscopes (Admon 2009).

2.2 Nano- and Microfocusing Analytical Techniques

Following the isolation and extraction of particles, beam-based methods are commonly used, e.g. SEM, TEM and STEM interfaced with X-ray microscopic techniques for the characterisation of 2D elemental composition (IAEA 2011). The elemental composition of micrometre-sized particles can also be determined by other X-ray emission techniques, i.e. μ-X-ray fluorescence (μ-XRF), μ-particle-

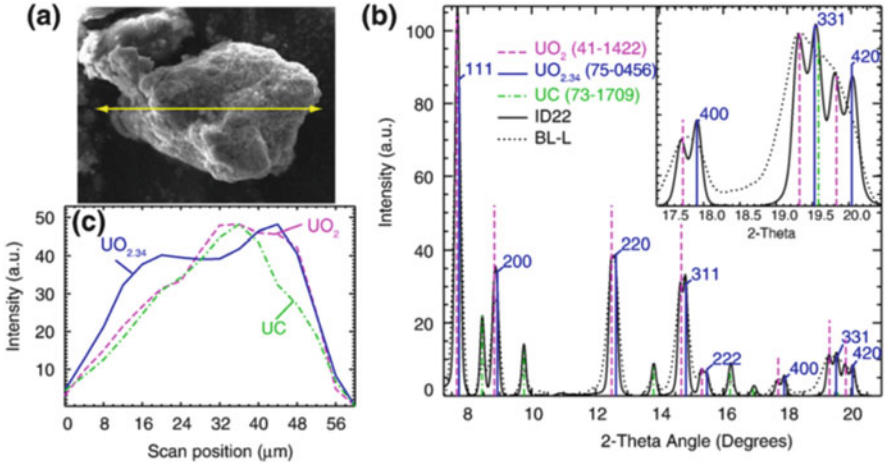

Fig. 2 Micro-X-ray diffraction analysis of a DU particle at two different beam lines, i.e. ID22, ESRF, and BL-L, HASYLAB (De Nolf et al. 2009). (**a**) Electron micrograph of a DU particle; a series of X-ray fluorescence/X-ray powder diffraction measurements were performed along the horizontal line, 60-μm long. (**b**) X-ray diffractograms from the middle of the particle using the ID22 (*full line*) and BL-L setups (dotted line, data rescaled to match the 2θ-scale of the ID22 experiment). Inset: detail of the (400), (331) and (420) reflections from UO_2 and $UO_{2.34}$ highlighting the superior resolution of the ID22 setup. Additionally UC is present. (**c**) Relative phase intensity distribution of the three uranium species along the line shown in (**a**)

induced X-ray emission (μ-PIXE) and electron probe microanalysis (EPMA). These three methods differ in the type of primary beam used to eject core-level electrons from the target atoms. In recent years, there has been a strong focus on improving the resolution of synchrotron-based X-ray techniques down to low nm level (Denecke et al. 2012). The combination of synchrotron-based μ-XRF, μ-XRD, μ-XANES and 3D tomo XAS applied on one single radioactive particle was first presented in 2001 (Salbu et al. 2001a).

X-ray micro-diffraction (μ-XRD) is applicable for the analysis of crystalline materials. Crystal structures can be determined, the phases can be identified and defects can be characterised. Conventional XRD studies can be made on single crystals or on powdered crystalline materials. Typically, samples are irradiated by monochromatic X-rays, and the diffracted radiation is detected either by photographic or electronic technique. Distances between adjacent crystal planes are calculated from X-ray wavelength and diffraction angles according to the Laue or Bragg equations. μ-XRD experiments have been performed using either continuum or monochromatic X-rays produced by synchrotron sources (Fig. 2). The number of applications of μ-XRD is increasing. Electron diffraction technique is also widely used for the characterisation of crystalline materials. However, synchrotron-based nano- and micro-diffraction is non-destructive. Synchrotron-based μ-XRD, most often in combination with μ-XRF, has been used for characterisation of particles from a series of sites (Lind et al. 2009, 2011a, b, 2013a, 2014; Salbu et al. 2001a; Crean et al. 2014; Batuk et al. 2015).

When the absorption of condensed matter is measured near to an absorption edge, an oscillatory behaviour is observed on the high-energy side of the absorption edge, i.e. the absorption fine structure. X-ray absorption fine structure (XAFS) analysis is subdivided into two parts:

1. The structure observed above the absorption edge (on the high-energy side, 500–1000 eV above the edge) is called the extended X-ray absorption fine structure (EXAFS).
2. That observed at the low-energy side of the edge (up to about 50 eV above the edge) is called the X-ray absorption near-edge structure (XANES).

Signals in the first part reflect the local atomic structure arrangements, and those of the second part relates to the electronic structure of the neighbouring atoms.

EXAFS analysis is useful for noncrystalline materials where XRD is not applicable (for amorphous materials, solutions, polymers). From the measured spectra, quantitative information about the distance from the central atom to the neighbouring atoms, the coordination numbers and the atomic vibrations can be drawn, provided that the elemental composition is well known (IAEA 2011). Batuk and co-workers recently reported EXAFS data for radioactive particles from several sites (Batuk et al. 2015).

Using XANES, the fine structure and position of the absorption edge can reveal information on the oxidation state of the element and its chemical surrounding. Usually the XANES spectrum is compared with a reference spectrum of an oxidation state standard and the shift of the photoelectric absorption edge is used to estimate the oxidation state of the atoms. μ-XANES spectra of particles collected in the Chernobyl region (Fig. 3) were first determined by Salbu and co-workers at the

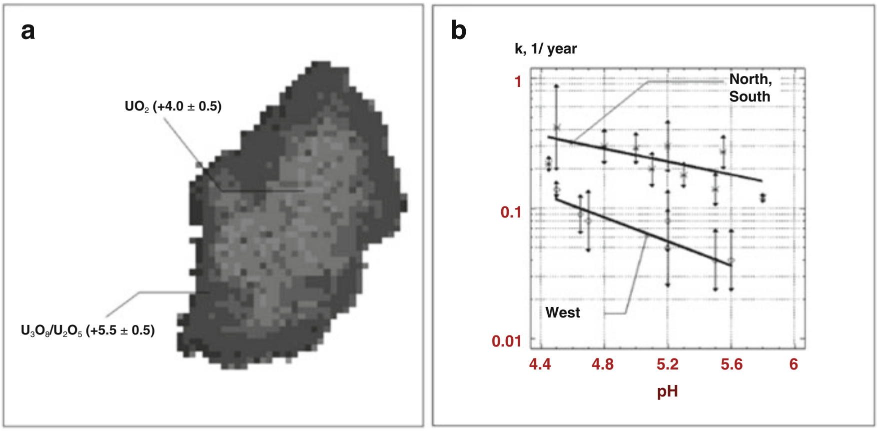

Fig. 3 Particles released from the Chernobyl reactor and associated weathering rates. (**a**) Oxidised fuel particle (UO_2 cores with oxidised U_3O_8 and U_2O_5 layers) released during the reactor fire obtained from 2D micro-XANES (Salbu et al. 2000, 2001a, b). (**b**) Weathering rate constants as functions of pH for fuel particles released during the explosion (*lower*) and during the fire (*upper*) (Kasparov et al. 1999)

ESRF facility (Salbu et al. 2001a). Although XANES has proved to be the most useful technique in determining oxidation states of radionuclides contained in single particles, results should be confirmed using, for instance, μ-XRD.

In computed microtomography (CMT), an analogue to the transmission technique of computed tomography of bulk materials, the beam passes through the sample, and the transmitted X-ray intensities depend on the density, the thickness and the elemental composition of the sample. A series of two-dimensional data are converted to three-dimensional data by means of a back-projection algorithm, thus obtaining a three-dimensional image of the sample. The image contrast usually originates from X-ray absorption. Recently, a phase contrast X-ray CT has been developed to enhance contrasts for weakly absorbing materials consisting of light elements. μ-XAS and CMT studies were first performed on particles collected in the Chernobyl region by Salbu et al. using the ESRF synchrotron facility (Salbu et al. 2000, 2001a).

Tomographic reconstruction of 3D images and computerised slicing demonstrated inhomogeneous distribution of U within the particles. Microtomographic images of radioactive particles from the Chernobyl exclusion zone showed also differences in the structures of particles depending on the different release scenarios. Recently, laboratory-based X-ray absorption tomography with resolutions of a few hundred nm (nano-computerised tomography) has been utilised by Lind and co-workers on several hundred μm-sized heterogeneous radioactive particles to identify inclusions of dense material such as actinides (Lind et al. 2011a, b, 2014).

2.3 *Identification of Isotope Ratios for Source Identification of Single Particles Using MS Techniques*

Radiometric determination methods, such as alpha spectrometry, require long counting times when low activities are to be determined. Mass spectrometric techniques as inductively coupled plasma mass spectrometry (ICP-MS), thermal ionisation mass spectrometry (TIMS), secondary ion mass spectrometry (SIMS) and accelerator mass spectrometry (AMS) have shown several advantages compared to traditional methods when measuring long-lived radionuclides including very low actinide concentrations in single particles. Since Pu and U isotope ratios depend on factors such as nuclear fuel burn-up, reactor type and operating history, neutron flux and weapon yield, etc., they can be used to identify the origin of particle contamination (Lind 2006; Lind et al. 2007, 2011a, b; Salbu et al. 2005; Wendel et al. 2013; Eriksson et al. 2008), calculate inventories or follow particle-associated radionuclides in ecosystem processes (Lind et al. 2006). Due to the low specific activity of long-lived radionuclides, many of these are preferentially analysed using mass spectrometric techniques. Mass spectrometry also enables the individual determination of ^{239}Pu and ^{240}Pu, which cannot be obtained by alpha spectrometry (Oughton et al. 2000, 2004; Skipperud and Oughton 2004; Skipperud et al. 2004).

A. Inductively Coupled Mass Spectrometry The use of inductively coupled plasma mass spectrometry (ICP-MS) to determine the concentration of plutonium and other long-lived radionuclides (including other actinides) has increased in the last decade (Eroglu et al. 1998; Sturup et al. 1998; Baglan et al. 2000, 2004; Pointurier et al. 2004; Skipperud and Oughton 2004; Skipperud et al. 2004). ICP-MS is an analytical technique that performs elemental analysis with excellent sensitivity and high sample throughput. ICP-MS systems rely on the introduction of sample molecules into argon plasma at temperatures of 6000–10,000 K, where they are dissociated and the resulting atoms ionised. Normally, liquid samples (a purified actinide in an appropriate acid medium) are transferred by a peristaltic pump to a nebulizer, which feeds a fine aerosol of analyte droplets into the plasma. Analyte ions are extracted from the plasma into a mass spectrometer (held at high vacuum) through a pair of orifices, known as sampling and skimmer cones. These ions are focused by a series of ion lenses into a magnetic quadrupole analyser, which separates the ions on the basis of their mass/charge ratio. ICP-MS has successfully been used to determine U and Pu activity concentrations as well as atom ratios in single particles (Lind 2006; Lind et al. 2007; Salbu et al. 2005; Eriksson et al. 2008; Boulyga and Becker 2001).

B. Accelerator Mass Spectrometry In recent years, the field of AMS has expanded into many areas of science, and a number of authors working in this area have presented comprehensive reviews of the technology involved and applications possible (Fifield 1999, 2000). Skipperud and Oughton (2004) reviewed a variety of applications of AMS of samples from the marine environment, focusing particularly on recent developments and applications. AMS is an ultrasensitive technique for isotopic analysis in which atoms extracted from a sample are ionised; accelerated to high energies (MeV); separated according to their momentum, charge and energy; and then individually counted (after having been identified as having the correct atomic number or mass). The principal difference between AMS and conventional mass spectrometry is the energy to which the ions are accelerated (MeV as compared to keV in conventional mass spectrometry). The practical consequence of having higher energies is that ambiguities in identification of atomic and molecular ions with the same mass are removed, which has enabled AMS to be used to measure isotopic ratios for a specific element to a level of 1 in 10^{15} (a factor of 10^5 better than in most other mass spectrometry systems). Moreover, this sensitivity can be achieved for sample sizes of 1 mg or less (containing as few as 10^6 atoms of the isotope of interest) within a measurement time of 1 h. Thus, AMS is extremely useful for analysis of individual low-level radioactive particles (Salbu et al. 2005; Lind 2006; Lind et al. 2011a, b).

C. Secondary Ion Mass Spectrometry SIMS is essentially a destructive technique often used to determine the composition of solid surfaces and thin films by sputtering the surface of the specimen with a focused primary ion beam and collecting and analysing ejected secondary ions. The mass/charge ratios of these secondary ions are measured with a mass spectrometer to determine the elemental, isotopic or molecular composition of the surface to a depth of 1–2 nm. Due to the large variation in ionisation probabilities among different materials, SIMS is generally considered to be a qualitative technique, although quantitation is possible with the use of standards. SIMS is the most sensitive surface analysis technique, with elemental detection limits ranging from parts per million to parts per billion. SIMS, however, suffers from isobaric interferences, and interpretation of spectra is not straightforward for mixed U and Pu materials (Ranebo et al. 2007). Nano-SIMS provides significantly better resolution and has successfully been applied to characterise Pu and U adsorbed to colloids from Mayak groundwater (Novikov et al. 2006).

D. Resonance Ionisation Mass Spectrometry Selective determination of extremely small amounts of long-lived radionuclides and their isotope ratios can be performed by atom counting using selective laser-based resonance ionisation in combination with conventional mass spectrometry—resonance ionisation mass spectrometry (RIMS). Due to the elemental selectivity of laser excitation and ionisation and the mass selectivity of the mass spectrometer, isobaric interferences are suppressed, and high to ultrahigh isotopic selectivity is achieved (Gruning et al. 2004). High detection efficiency results from the high cross sections for optical excitations. RIMS has the advantage of being a fast technique if sample preparation time is not included.

E. Thermal Ionisation Mass Spectrometry TIMS is a highly sensitive isotope mass spectrometry characterisation technique that exploits the thermal ionisation effect, in which a chemically purified sample is heated to cause ionisation of the atoms of the sample. The ions are focused into a beam by an electromagnet and then separated into individual beams based on the mass/charge ratio of the ions. The technique is used extensively in isotope geochemistry, in geochronology and in cosmochemistry. TIMS is a magnetic sector mass spectrometry technique in which ions are separated as a function of their charge and velocity or mass in a magnetic field. Variants of this technique are ID-TIMS (ID = isotope dilution) and CA-TIMS (CA = chemical abrasion). The relative abundances of different isotopes are then used to describe the chemical fractionation of different isotopes, travel in different reservoirs of non-radiogenic isotopes and age or origins of solar system objects by the presence of radiogenic daughter isotopes (Lehto and Hou 2011).

3 Linking Sources and Particle Characteristics

Since 1945, a series of sources associated with the nuclear weapon and fuel cycles have contributed to radioactive contamination of the environment, from the extraction of uranium from bedrock ores, via enrichment plants and fabrication to nuclear weapon tests, nuclear reactor accidents to reprocessing and waste disposal including dumping at sea. In most contaminated sites, investigated radioactive heterogeneities have been observed, indicating the presence of radioactive particles and colloids. During the last 10 years, radioactive particles and colloids collected at different sites have been identified and characterised (IAEA 2011). The present results demonstrate that the composition of radionuclides as well as stable elements in radioactive particles is source related, while particle characteristics essential for ecosystem transfer and biological uptake such as particle size distribution, crystallographic structures, oxidation states and solubility depend mostly on the release conditions.

3.1 Particles Originating from Testing of Nuclear Weapons

Totally more than 2300 weapon tests have been performed, where radioactive debris from a total of 520 atmospheric tests has entered the global environment, while surface, underground and underwater nuclear weapon tests as well as subcritical safety trials with conventional explosives have entered the environment locally (UNSCEAR 1993). According to Heft (1970), all radionuclides (except ^{3}H, ^{14}C and the long-lived rare gases) produced in such tests are accounted for as radioactive particles. During the late 1950s and 1960s, attention was put on the local deposition of radioactive particles at US test sites (Crocker et al. 1966). Reports on radioactive particles deposited within a series of test sites (e.g., Marshall Islands, Nevada Test Site, Johnston Atoll, Novaya Zemlya, Maralinga, Mururoa) are also available in open literature. In the 1950s and 1960s, long-range transport of radioactive particles originating from distant nuclear tests has been identified in Norway (Semipalatinsk), Sweden (Novaya Zemlya, Russia) and Japan (Lop Nor, China, and Semipalatinsk, Kazakhstan). The presence of radioactive particles is also expected at several other test sites such as underground nuclear test sites, safety trial sites and sites where peaceful nuclear explosions (PNE) were used for civil purposes (Amchitka Island, USA; Kraton-3 and Crystal, Republic of Sakha, Russia; In Ekker and Reggane, Algeria; Montebello Islands, Australia; Pokhran, India; and Ras Koh, Pakistan), but no information seems to be available in open literature.

A. Semipalatinsk Nuclear Test Site, Kazakhstan A total of 456 nuclear weapon tests have been conducted during the period from 1949 to 1989 (IAEA 1998) in the Semipalatinsk Test Site (STS), northeast of Kazakhstan. Digital phosphor imaging of dried and homogenised surface soils from several detonation sites demonstrates highly heterogeneous radioactive contamination (Salbu and Lind 2011). Glass-like vitrified particles were observed in soil samples from the Balapan (Lind 2006), Degelen (Solodukhin 2005) and Ground Zero (Lind 2006) sites, whereas soil particles with U and Pu coexisting in highly concentrated small grains (tens of μm in size) were found at the Tel'kem craters (Lind 2006). Spherical, uniformly coloured, reddish brown or black radioactive particles with optical diameters up to about 15 μm originating from the STS tests were identified in Japan in 1961–1962 (Mamuro et al. 1962, 1966). Furthermore, direct tropospheric transport of radioactive debris from specific nuclear detonations at the STS to Norway has been demonstrated, based on hot spots in air filters, Pu atom ratios and real-time meteorological data (Wendel et al. 2013). Thus, long-distance tropospheric transport from test sites during 1950–1960 may at least periodically have played a more important role for the radionuclide depositions in Europe than previously anticipated.

B. Novaya Zemlya, Russia During 1950–1990, 88 atmospheric, 39 underground and at least three underwater nuclear weapon tests took place at Novaya Zemlya. Significant contamination including hot spots and localised heterogeneities has been observed within the three major test areas (Amap 1997; Smith et al. 2000). While information on particle characteristics in the near field is scarce, a large number of radioactive particles originating from atmospheric weapon tests at Novaya Zemlya were collected in October 1958 by aircraft at high altitude (up to about 13 km) over central Sweden (Sisefsky 1961). These studies showed that the activity of the spherical, translucent and colourless to reddish particles was roughly proportional to the volume.

C. Marshall Islands During 1946–1958, the USA performed 23 nuclear weapon tests in the atmosphere and at ground surface at the Bikini and Enewetak Atolls, Marshall Islands. According to Simon et al. (1995), localised heterogeneities reflected particles deposited in soils. Autoradiography of samples from ground surface shots showed large spherical particles (0.5–1 mm) with uniform distribution of radionuclides and irregular several mm-sized particles with surface contamination. Crocker et al. (1966) reported that particle characteristics such as size distribution, shape and colour depended on devices and shot conditions. Leaching of spherical particles from high-altitude detonations showed that Pu associated with the particles was inert in water, while high water solubility is reported for Pu associated with algal crust of the atoll soils and the debris from coral surface bursts. Fragments with plain Pu matrix found at Fig-Quince zone, Runit Island, Enewetak Atoll, are assumed to originate from the 1958 Quince safety trial (Hamilton et al. 2009). Si-/O-rich matrix particles with Pu existing as particle-like structures or Pu distributed in the Si-/O-rich matrix probably originate from the low-fission yield test at the same site.

D. Nevada Test Site, USA During 1951–1992, 86 atmospheric weapon tests (UNSCEAR 2000) and 828 underground tests (Kersting et al. 1999) took place in Nevada Test Site, USA. Autoradiography demonstrated hot spots and heterogeneities, indicating the presence of radioactive particles (Anspaugh and Church 1986). According to Kersting et al. (1999), the majority of the refractory radionuclides involved in underground nuclear tests are incorporated into melt glass that forms at the bottom of the test cavities. Reported particle properties vary largely and include fused or partially fused particles, vesicle-shaped particles and large agglomerates consisting of individual small particles differing in colour, specific activity, density and magnetic properties. The particle size distributions are reported to depend on the device and shot conditions (Crocker et al. 1966). Thus, high-altitude detonations resulted in spherical small-sized dense particles with high specific activity, while ground surface shots produced large irregularly shaped particles with lower density and specific activities, probably due to the inclusion of soil. Leaching experiments showed that the solubility of particle-associated gamma- and beta-emitting radionuclides depended on device and shot conditions, matrix composition, particle size and type. Particles originating from shots at high altitudes were more inert than those from ground detonations. Gamma- and beta-emitting radionuclides in airburst debris were dissolved in 0.1 M HCl. Colloids or pseudocolloids containing Pu have also been identified in groundwaters within the Nevada Test Site (Kersting et al. 1999). Due to sorption to colloidal clays, silica and zeolites, the colloid-facilitated transport of Pu in groundwaters seems to play an important role within the test site. Thus, in contaminated sites more attention should be paid to the colloidal behaviour of surface-reactive radionuclides.

E. Maralinga and Emu, Australia In the period 1953–1963, nine nuclear weapon tests and several hundred smaller-scale weapon trials as well as several safety trials took place at the Maralinga and Emu sites in Southern Australia as part of the UK nuclear weapon programme (Burns et al. 1994, 1995; Cooper et al. 1994). The major part of the radioactive particle contamination is due to the 12 “Vixen B” safety trials at the Taranaki part of the Maralinga nuclear test site (Cooper et al. 1994). These trials involved either burning or explosive dispersal of 22.2 kg Pu and 47.3 kg U. Cooper et al. (1994) found that particles within the 250–500 μm fraction was predominant, while finely dispersed particles as well as fragments up to several hundred microns were identified, also as contaminated soil particles and contaminated coatings on device reminiscences. Based on gamma spectrometry and proton-induced X-ray emission spectroscopy, Pu and U were localised on surfaces of individual large particles. The solubility of quite porous particles from the Taranaki site was quite low, but in 0.16 M HCl, mimicking stomach fluid, the solubility varied from 1 to 96 % over a period of 40 days (Burns et al. 1994). A 1957 low-fission yield test at the Tadje area of Maralinga contaminated an area close to the detonation site with both small-sized particles and glassy spherical particles containing Pu and Am (Cooper et al. 1994).

F. Fangataufa and Mururoa Atolls, French Polynesia Between 1966 and 1996, 193 nuclear tests (178 nuclear detonations and 15 safety trials) were conducted by French authorities above and below ground at the Mururoa and Fangataufa Atolls in French Polynesia. The presence of relatively large (200–1000 μm) Pu-containing particles originating from five safety test trials performed between 1966 and 1974 has been confirmed at the safety test sites at Colette, northern part of Mururoa (Danesi et al. 2002). An individual Mururoa particle was characterised by Eriksson and co-workers (2005) as a Pu inclusion (~100 μm) attached to a coral matrix. The activity levels of ^{239}Pu and ^{241}Am in the particles ranged from 5 kBq to about 1 MBq and 0.2–5.6 kBq, respectively. (Danesi et al. 2002) also reported that 99.9 % of the mass and 95.8 % of the activity were associated with particles larger than 250 μm. However, the presence of particles smaller than 10 μm with ^{239}Pu activities of several hundred Bq could not be excluded (Danesi 1998). In vitro dissolution studies of individual particles in simulated serum showed very low solubility (0.07 %) of Pu, similar to particles from the Maralinga nuclear test site (Danesi 1998).

G. Lop Nor, China The Chinese nuclear weapon testing programme included 22 atmospheric tests between 1964 and 1980 at the Lop Nor Test Site in Gansu, China (UNSCEAR 2000). Information on local deposition is not available. However, spherical (7–22 μm) radioactive particles were identified in Japan 3–4 days after the first test (small-scale land surface burst) at Lop Nor in 1964 (Mamuro et al. 1965).

3.2 Particles Released During Nuclear Accidents

A. Windscale Releases, UK Two air-cooled graphite-moderated metal U reactors operated from 1951 to 1957, when both were shut down due to the fire in Pile No. 1. Already in the mid-1950s, fuel particles containing actinides and fission products were dispersed due to low-temperature oxidation and corrosion of spent fuel elements misplaced in the air-cooled ducts leading to the discharge stack with inefficient filtering system (Salbu and Kudo 2001). The total release has been estimated to about 20 kg U as large (up to 700 μm in length) particles with a flake-like structure significantly different from those observed in the Chernobyl fallout (Jakeman 1986; Salbu et al. 1994). The particles were inert towards leaching with 1 M HCl (Oughton et al. 1993). Following the graphite fire in 1957, about 180 TBq ^{137}Cs, 0.75 TBq ^{90}Sr and 20 GBq of ^{239}Pu were released (Garland and Wakeford 2007), probably associated with U fuel particles (Arnold 1992; Chamberlain and Dunster 1958). Particles in the size range 20–500 μm were observed up to 4 km from the site, but were considered of little relevance to public health (Appleby and Luttrell 1993).

B. Chernobyl Accident, Ukraine As a result of the Chernobyl accident in 1986, particles of at least 5 different categories were released (Dobrovolsky and Lyalko 1995; Salbu and Lind 2011). According to new estimates by Kashparov et al. (2003), about 3–4 tonnes of U fuel with variable burn-up were released into the atmosphere, either as more or less pure U oxide particles (category 1) or fuel construction particles (category 2), i.e. particles with a matrix of nuclear fuel mixed with reactor construction material. A lot of rather inert (Zr, U)O_x particles have been found inside the 30-km exclusion zone around the Chernobyl Nuclear Power Plant, both to the west and to the north of the reactor. Category 1 and 2 particles are carriers of the major part of the refractory radionuclides released. Construction particles (category 3) are composed of reactor construction materials and are carriers of some radionuclides. Particles of hybrid type (category 4) were mainly derived from the interaction of fuel and reactor construction material with fire extinguishing material, etc. The U fuel particle includes the presence of “white inclusions”, containing Ru and analogues. A fifth category comprises single element (Ru, Cs) particles such as those found as far away as Norway, 2000 km from Chernobyl (Salbu et al. 1988). In many cases, particle of different categories contained a thin layer of stable Pb from the Pb containing fire distinguishing materials.

As a consequence of the initial explosion in the reactor on April 26, mechanical destruction of the UO_2 fuel occurred under high pressure and high temperatures (>2000 °C immediately prior to the explosion and reaching 2400–2600 °C in local regions of the reactor), and deposition of fuel particles took place to the west of the reactor. During the subsequent fire on April 26–30, volatile fission products and U fuel particles were released under moderate temperatures (330–930 °C) and oxidising conditions (Kasparov et al. 1999), and deposition of particles occurred to the north, northeast and south of the plant. From April 30 to May 6, the temperature was further lowered (Kasparov et al. 1999). The particle weathering rate constant (k year^{-1}) of U fuel particles in Chernobyl ranged from 0.04 to 0.4 y^{-1} indicating that varying weathering rates could be related to different particle characteristics as well as varying soil pH (Kasparov et al. 1999). Uranium fuel particles deposited to the west of the reactor featured significantly slower weathering rates than for particles deposited to the north and south of the reactor (Kasparov et al. 1999). Based on synchrotron-based radiation X-ray microanalytical techniques such as μ-XANES and μ-XRD/XRF, Salbu and co-workers (2001) showed that fuel particles released during the initial explosion were not oxidised and some particles contained apparently inert, reduced forms of U associated with Zr or carbide (Salbu et al. 2001a). Furthermore, it was demonstrated that a particle released during the reactor fire (north of the reactor) was characterised by a UO_2 core surrounded by oxidised U (a layer of U_2O_5/U_3O_8 and possibly other intermediate forms) as demonstrated in Fig. 4. Thus, differences in elemental composition, crystallographic structures and oxidation states of U in fuel particles explain the observed differences in weathering kinetics, mobility and soil-to-vegetation transfer coefficients of radionuclides associated with particles located west and north of the Chernobyl reactor. Based on the experiences from the Chernobyl accident, characteristics of U fuel particles released from an RBMK-type nuclear reactor with graphite moderator are also assumed to vary according to the release conditions. Moderate temperatures and oxidising conditions (fire) would result in amorphous structures, oxidised states of matrix elements and enhanced weathering, whereas high temperatures and reducing conditions such as in an explosion would result in reduced or non-oxidised states of matrix elements and delay in ecosystem transfer (Lind 2006).

C. Fukushima Daiichi Nuclear Power Plant (FNPP), Japan The atmospheric releases of radionuclides from the Fukushima accident were predominantly volatiles such as radioactive noble gases, iodine and Cs isotopes. In addition, refractory radionuclides like Pu have been observed relatively close to the site (Schneider et al. 2013). Findings of radioactive particles originating from the damaged Fukushima reactors have also been claimed by Abe, Adachi and co-workers (Abe et al. 2014; Adachi et al. 2013). They identified, partially isolated and analysed spherical glassy particles containing low levels of radiocaesium, stable Cs and U as well as other metals. These particles are, however, remarkably similar to particles observed in coal combustion (Ault et al. 2012), and U in fly ash particles should be expected as previously reported (Utsunomiya et al. 2002). Thus, it is likely that the reported radio Cs carrying particles could reflect surface adsorption of radiocaesium from the Fukushima releases on fly ash and on other atmospheric particles, e.g. due to condensation processes. Highly contaminated black-coloured road dust material has also been reported in Japan after the Fukushima accident (Sakaguchi 2014). However, the presence of fuel particles has not yet been fully confirmed.

3.3 Particles Originating from Nuclear Reprocessing Activities

Nuclear fuel reprocessing is conducted in order to recover U and Pu from spent nuclear fuel for civil or military use. During reprocessing, the spent fuel is brought into solution thereby increasing the potential for release as liquid waste discharges. Reports on U fuel particles found in the vicinity of reprocessing sites indicate that the dissolution of fuel may be incomplete (Dennis et al. 2007; Bolsunovsky and Tcherkezian 2001; Voilleque et al. 2002; Maucec et al. 2004) and that residual fuel fragments and particles are released through discharges.

3.3.1 Particles Released from North American Sites

A. Hanford, USA In the late 1940s and early 1950s, episodic releases of physically large radioactive particles to the air occurred at the nuclear Hanford Site (Voilleque et al. 2002). The first particle releases occurred due to corrosion of the canals in the exhaust system during the early years of reprocessing plant operations. Contaminated corrosion particles contained iron and a mixture of radionuclides and were larger than those in routine releases. The second group of episodic releases of radioactive particles occurred in 1950. The key radioactive constituents were ^{103}Ru and ^{106}Ru in large particles released from the REDOX reprocessing facility. A layer of radioactive contamination formed on the lining of the stack by deposition of volatile ruthenium tetroxide and ammonium nitrate. Large radioactive particles were released upon disturbance of the layer of contaminated ammonium nitrate. The Columbia River has received releases of radioactivity following "a large number of ruptures of irradiated fuel elements in the single-pass production reactors" (Voilleque et al. 2002). Furthermore, discrete ^{60}Co particles have been found along the shorelines downstream of the Hanford reactors (Nees and Corley 1973; Poston et al. 2007). Further information on physico-chemical forms of the radioactive contamination in the Columbia River is, however, scarce. Recently, PuO_{2+x} particles with phosphor incorporated in the oxide crystal have also been reported in Hanford crib Z-9 (Batuk et al. 2015).

B. Rocky Flats, USA The Rocky Flats Nuclear Weapon Plant operated from 1952 to 1989 as a major processor of weapon-grade Pu to build nuclear weapon triggers called “pits”. Recycling of Pu retrieved from decommissioned nuclear warheads took also place at Rocky Flats. The largest releases of Pu outside the Rocky Flats Plant boundaries were caused by two major events: a fire that occurred in the Pu processing building in 1957 (Mongan et al. 1996a) and windblown releases, mainly during 1968–1969, from an outdoor waste storage area called the 903 Area, located at the plant (Mongan et al. 1996b). The presence of Pu particles in the surrounding area has been reported (McDowell and Whicker 1978). However, no particle characteristics except for particle size (submicron to ~7 μm) appear available.

C. Los Alamos, USA The TA-21 waste disposal site at Los Alamos was created after the Manhattan Project. Batuk and co-workers identified Zn/U (Cu) particles, and particulate Pu was observed in association with Fe or as isolated PuO_{2+x} particles in waste buried in soils (Batuk et al. 2015).

D. Chalk River, Canada During the course of the operation of the NRX reactor at Chalk River Laboratories of Atomic Energy of Canada Ltd., small quantities of low-level radioactive particles were discharged to the Ottawa River through a process sewer discharge pipe. The particle characteristics vary, but some particles carry a mixture of radionuclides including U and metals (Lind et al. 2014).

3.3.2 Particles Released from Russian Sites

Productions of plutonium for the production of nuclear weapons were conducted at three main sites in the former Soviet Union: Mayak PA (Chelyabinsk-45 or Chelyabinsk-65), Krasnoyarsk Mining and Chemical Industrial Complex (Krasnoyarsk-26) and Siberian Chemical Combine (Tomsk-7). Relatively large routine releases occurred during the early years of operation of these facilities (UNSCEAR 1993), and accidents have contributed to radioactive contamination downstream and in the vicinity of the sites.

A. Mayak PA Releases from Mayak PA directly to the Techa River occurred during 1949–1951, to a 300-km trace in the NE to the site due to the East Ural Radioactive Trace accident (waste tank explosion) in 1957 and to the surrounding of the site due to a tornado spreading contaminated sand from the shore of Lake Karachay in 1967. Screening of contaminated soil and sediments from in and around the Mayak PA site using digital autoradiography indicated widespread presence of radioactive particles. EXAFS results for U particles (5–50 μm) isolated from Reservoir 17 sediments showed the presence of UO_2+ U_3O_8 and U(VI)-oxyhydroxide species (Batuk et al. 2015). However, no source identification beyond gamma spectrometry was attempted for these particles impeding a full interpretation of the data. Using nano-SIMS, Novikov and co-workers successfully characterised U- and Pu-containing radioactive colloids in a groundwater well drilled at a distance of 3.2 km from Lake Karachay (Novikov et al. 2006). Similarly, ^{60}Co colloids have previously been observed in these groundwaters (Salbu et al. unpublished). Radioactive, beta-emitting particles with a Sr matrix were present in reservoir sediments (Jnreg 2004; Salbu and Lind 2011).

B. Krasnoyarsk-26 Releases from Krasnoyarsk-26, including those resulting from three accidents, have contaminated the Yenisey River downstream of the site with highly radioactive U fuel particles and other forms of radioactive particles (Bolsunovsky and Tcherkezian 2001; Sukhrukov et al. 2004; Chuguevsii et al. 2010; Lind et al. 2011a). The isotopic compositions obtained from gamma spectrometry and mass spectrometry (ICP-MS and AMS) analysis vary substantially between particles and indicate several different source terms. However, a high burn-up fuel origin is indicated for all particles in contrast to the low $^{240}Pu/^{239}Pu$ weapon-grade signatures determined previously in bulk sediment samples from the same area (Lind et al. 2011a).

C. Tomsk-7 Releases from Tomsk-7 are attributed to direct releases to the downstream river, a tributary to the river Ob and nuclear events, such as the accidental explosion that occurred in the radiochemical plant at Tomsk-7 on April 6, 1993 (AMAP 2004). The snow-covered region close to the facility was contaminated, and a radioactive trace including radioactive particles was spread 20 km in a northeastern direction. Total γ-activity of some of the hottest particles reached 12 k Bq (Tcherkezian et al. 1995).

3.3.3 Particles Released from European Reprocessing Plants

A. Sellafield, UK Among the three major reprocessing plants in Europe (Sellafield and Dounreay, UK; La Hague, France), the Sellafield site has been the major contributor of radionuclide contamination to the north European seas since early 1950 (McCartney et al. 1994). Discharges of radionuclides to the environment include aerosols and particles in air emissions or as ions, colloids and particles via the effluent pipeline to the Irish Sea (Leonard et al. 1995; Salbu et al. 1993). During the years, releases from Sellafield have also contaminated the coastal zones, especially in Cumbria, UK. Hot particles, including a large number of highly active fuel fragments (Cresswell and Sanderson 2012), have been identified in the effluent and have been shown to persist in the marine environment close to Sellafield, for instance, in Esk and Ravenglass estuary intertidal sediments (Salbu and Lind 2011; Sajih and Livens 2010). Jernström and co-workers isolated radioactive particles with a U matrix containing about 2/3 U(IV) and 1/3 U(VI) from Irish Sea sediments (Jernstrom et al. 2004).

B. Dounreay, UK Highly radioactive particles and fragments have been recovered from the foreshore at the UK Atomic Energy Authority's (UKAEA) former reactor research establishment at Dounreay, Scotland, and from a neighbouring beach. Inadvertent releases of small pieces of fuel material to the marine environment are believed to have occurred during reprocessing operations involving irradiated fuel, which took place during 1960–1970 (Dennis et al. 2007; Maucec et al. 2004). The size of the particles and fragments varies widely, but is typically 0.2–2 mm. The radionuclide compositions are dominated by the fission products ^{137}Cs (ranging from 10^3 to 10^8 Bq) and $^{90}Sr/^{90}Y$, although they also contain some Pu and

^{241}Am (Darley et al. 2003). The DMTR (Dounreay Materials Testing Reactor) fragments contain an alloy (Al/U ~ 7) matrix of Al and highly enriched U (82.9 ± 0.8 ^{235}U) as well as Nd and Fe (Tamborini 2004). DFR (Dounreay Fast Reactor) particles contain U, Nb and Fe. In both DMTR and DFR particles, U is present as UO_2 (Salbu et al. unpublished).

C. La Hague Based on size fractionation of radionuclides in an effluent sample from La Hague reprocessing plant, all of ^{54}Mn, 90 % of ^{60}Co and 40 % of ^{106}Ru were associated with radioactive particles larger than 0.45 μm, while all of the ^{125}Sb and 80 % of ^{137}Cs were present as mobile low molecular mass species (Salbu et al. 2003). The colloidal fraction was of minor importance. Following the distribution of radionuclide species upon mixing with seawater, ^{60}Co and ^{106}Ru were mobilised and appeared as low molecular mass mobile species, while an increasing fraction of ^{137}Cs associated with colloids could be observed. Particles and colloids were present in the effluent. Electron-dense structures having diameters from few nm to several hundred nm, with most colloids in the 50–500 nm range, could be observed by transmission electron microscopy. The structures observed in the La Hague effluent were quite different from those observed in effluents from Sellafield (Salbu et al. 1993).

3.4 Particles Associated with Dumping of Waste

A. Novaya Zemlya, Russia During 1959–1991, radioactive waste including 6 reactors with fuel, 11 reactors without fuel, vessels, barges and more than 6000 containers were dumped in the Abrosimov, Stepovogo and Tsivolky Bays and in the Kara Sea trough (AMAP 1997). In addition, the fuel assembly from the Lenin reactor was dumped in the Tsivolky Bay. In the close vicinities of dumped objects, especially containers, enhanced levels of Pu isotopes and fission products in sediments have been observed (Salbu et al. 1997). Based on autoradiography, heterogeneities in both sediment samples and filter-feeding organisms collected from the top of the hull of the sunken K-27 submarine reflected the presence of particles (Gwynn et al. 2015). Using SEM, crud particles containing ^{60}Co were identified in sediments (Salbu et al. 1997).

B. Kola Bay, Russia Two types of radioactive particles have been identified in marine sediment and in lichen samples collected in the vicinity of nuclear fuel storage and radioactive waste sites at the Kola Bay, NW Russia (Pollanen et al. 2001). Large (~100 μm) greenish particles found in the sediment matrix, most probably pieces of paint, were associated with ^{137}Cs. The element composition was heterogeneous, but ^{137}Cs was found to be evenly distributed. ^{60}Co in the lichen matrix was associated with small (~1 μm) particles. Neither U nor transuranium elements were identified in either type of particles.

3.5 Nuclear Accidents Involving Satellites

Destruction of satellites powered by ^{238}Pu-based radioisotope thermoelectric generators (RTGs) or nuclear reactors upon re-entry to the earth's atmosphere has caused regional and global contamination of radioactive particles on at least three occasions.

A. SNAP9-A The US SNAP9-A (satellite nuclear auxiliary power unit), which contained 1 kg (629 TBq) of ^{238}Pu metal, was destructed upon re-entry to the earth's atmosphere in 1964 and thereby added to the global fallout of Pu. About 95 % of the Pu had been deposited by the end of 1970, most probably as finely dispersed particles (Krey 1967).

B. Cosmos 954 and 1402 Satellites The destructive re-entry into the atmosphere of the Soviet satellite Cosmos 954 in 1978 caused contamination of large areas (124,000 km^2) in Canada with radioactive debris from the fission reactor (50 kg of 90 % ^{235}U) (Amap 1997). The size distribution pattern varied from submicron to fragments, with ~25 % of the inventory estimated as mm-sized particles (Amap 1997; Krey et al. 1979). In 1983, a nuclear reactor from the Cosmos 1402 Soviet radar reconnaissance satellite disintegrated over the South Atlantic Ocean upon re-entering the earth's atmosphere (Leifer et al. 1987). Information appears to be scarce about the size distribution of debris.

3.6 Conventional Detonation of Nuclear Weapons

Apparently, four nuclear weapon accidents have been described in the open literature, i.e. the accidents which occurred on the McGuire Air Force Base, New Jersey, and Johnston Atoll, USA, and at Palomares, Spain, and Thule Air Base, Greenland. In all four cases, the US nuclear weapons involved were conventionally fragmented resulting in radioactive particle contamination (Fig. 4).

A. McGuire Air Force Base A Boeing Michigan Aeronautical Research Center (BOMARC) missile was destroyed on June 7, 1960 at the former US McGuire Air Force Base, New Jersey, when a high-pressure helium tank exploded and ruptured the fuel tank. A significant quantity of weapon-grade Pu particles with varying sizes (sub-micrometre-sized or single large particles) containing Pu and Am were inhomogeneously dispersed over a 7-acre area as a consequence of the ensuing fire (Drell and Peurifoy 1994; Lee and Clark 2005; Mian et al. 2001). It is, however, worth mentioning that the high explosives associated with the warhead did not detonate. Bowen and co-workers characterised a set of Pu- and U-containing particles that exhibited a smooth and crystalline structure different from that reported for Palomares or Thule particles. Apparently, the Pu/U ratio on BOMARC particle surfaces was higher than observed for Palomares (U and Pu about equal) and Thule (more U than Pu) particles (Bowen et al. 2013). Micro-beam EXAFS and

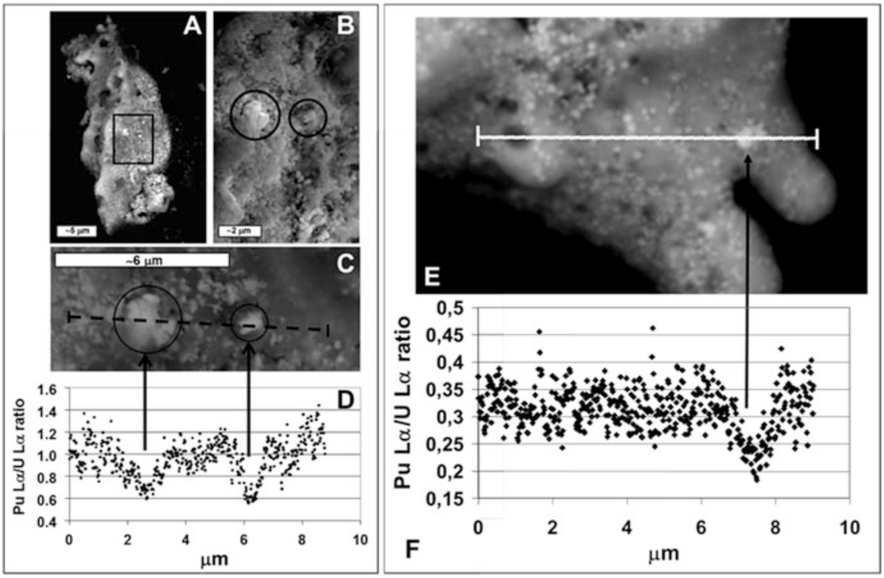

Fig. 4 ESEM line scan analysis of a Palomares particle compared to a Thule particle (Lind et al. 2007). (**A**) BEI image of the whole Palomares particle shows bright areas indicating high average atomic number area heterogeneities. (**B**) SEI image of the bright area highlighted in (**A**) (**B**) at higher magnification shows the agglomerated structure of the spots. (**C**) BEI image of the analysed area including the two bright spots in (**B**). The location of the scanned line is indicated. (**D**) Pu Lα/U Lα intensity ratios along a ~9-µm line scanned over the area in (**B**) and (**C**). (**E**) BEI image of the analysed area of a Thule particle including a bright spot indicating a high average atomic number area. The location of the scanned line is indicated. (**F**) Pu Lα/U Lα intensity ratios along a ~9-µm line scanned over the area indicated in (**E**). Resolution ~1 µm

XRD were used to demonstrate the presence of $Pu(U)O_{2+x}$ and UO_{2+x} in two McGuire AFB particles (Batuk et al. 2015). In the same work, one particle was described as a conglomerate of a Pu-rich and a U-rich particle in which U and Pu were not significantly mixed and in which small Fe and Ga spots were present. In a second particle, Pu and U were mixed. This is more in line with previous observations for a range of particles originating from nuclear weapon materials (Lind 2006; Lind et al. 2007; Wolf et al. 1997; Bowen et al. 2013; Eriksson et al. 2005).

B. Johnston Atoll In the late 1950s and early 1960s, Johnston Atoll was the launch site of atmospheric nuclear weapon tests (Wolf et al. 1997). In 1962, Pu- and U-containing particles were deposited throughout the atoll following the destruction of three nuclear warhead-carrying THOR missiles. The contamination was observed as discrete hot particles with actinide containing inclusions exhibiting widely varying U/Pu ratios and comprising >99 % of the total activity of the sample (Wolf et al. 1997).

C. Thule and Palomares Two quite similar accidents involving USAF B-52 bombers carrying four nuclear weapons and conventional explosions of the weapon material and subsequent fires occurred in 1966 in Palomares, Spain, and in 1968 in Thule, Greenland, respectively. The surrounding areas were contaminated with submicron to mm particles containing Pu and enriched U (Jimenez-Ramos et al. 2007; Lind et al. 2007; Eriksson et al. 2008). Based on synchrotron radiation X-ray micro-techniques, the Pu/U particles were oxidised (Lind et al. 2007). Considering their long residence times in very different environmental conditions (semi-desert area in Palomares and arctic marine environment in Thule), the characteristics of the U/Pu mixed oxide particles were remarkably similar, indicating that source term could be a more important factor influencing weathering than local environmental conditions (Lind et al. 2007).

3.7 Depleted Uranium Ammunitions

Due to high density, hardness and pyrophoric properties of U, large amounts of depleted uranium (DU), a waste product of the enrichment of U from reprocessing, have been applied as armour-piercing ammunition. DU weapons have been utilised in several countries, and contamination of DU has been reported in Kosovo (Danesi et al. 2003a, b; Salbu et al. 2003), in Serbia–Montenegro (McLaughlin et al. 2003), in Bosnia and Herzegovina (UNEP 2003), in Kuwait (Salbu et al. 2005) and in Iraq (Gerdes et al. 2004). DU ammunition has also been used at military proving grounds (Sowder et al. 1999) (Sowder et al. 1999). Within most contaminated sites, hot spots containing DU particles varying in size have been identified. Following impact with hard targets, DU will disperse and dispersed DU will ignite. Thus, DU particles ranging from submicron to several hundred micrometres have been observed in sand, in soils and in damaged vehicles. Using a combination of synchrotron radiation-based X-ray microscopic techniques (μ-XRF, μ-XANES, μ-XRD) on single particles, DU particles from corroded unspent penetrators varied with respect to particle size, and the oxidation state was predominantly +4 (Lind et al. 2009). DU particles released during impact with tanks varied also with respect to particle size, and cocrystalline phases such as U_{met}, UC, UO_2 and $UO_{2.34}$ (oxidation state 0 to +4) were identified (Fig. 3). DU particle releases during a fire in a DU ammunition storage facility were large, fragile, highly soluble and bright yellow. Crystalline phases such as schoepite ($UO_3 \cdot 2.25\ H_2O$), dehydrated schoepite ($UO_3 \cdot 0.75\ H_2O$) and metaschoepite ($UO_3 \cdot 2.0\ H_2O$) could be identified, and the oxidation state was +6. Although the source was similar (DU penetrators), the release scenario (detonation, fire, corrosion) influenced the characteristics of released particles.

3.8 Radioactive Particles of Naturally Occurring Radioactive Material Origin

Radioactive particles released from NORM (naturally occurring radioactive material) sources such as U mining and tailing areas have, with a few notable exceptions (Boehnke et al. 2005; Landa et al. 1994; Selchau-Hansen et al. 1999; Alsecz et al. 2007), been much less in focus than particles carrying anthropogenic radionuclides. Th, U and daughter nuclides such as $^{210}Po/^{210}Pb$ may be heterogeneously distributed in minerals (Landa et al. 1994; Alsecz et al. 2007), thus occurring as hot spots in U mining and tailing sites. Lind and co-workers utilised nano- and microanalytical techniques to identify radioactive particles (submicron to several hundred microns) and fragments containing U and a range of heavy metals in dust samples, in mineral grains and in mineral fragments from the abandoned former Soviet Union U mining sites Kurday, Kazakhstan; Kadji Sai, (Fig. 5) Kyrgyzstan; and Taboshar, Tajikistan (Lind et al. 2013a). Similarly, heterogeneities were observed in NORM samples from the Fen and Søve, Norway, as particles enriched in Th and as inclusions in rock fragments (Lind et al. 2011b).

4 Conclusion

A series of nuclear and radiological sources have contributed to radioactive contamination of the environment during the years. Following severe nuclear events, a major fraction of refractory radionuclides will be present as radioactive particles. Several years of research (IAEA 2011) demonstrate that the particle composition will depend on the specific source, reflecting the matrix and the refractory radionuclide composition (burn-up). The release scenarios (temperature, pressures and redox conditions) will, however, influence particle characteristics such as particle size distribution, crystallographic structures and oxidation states, being essential for the ecosystem behaviour. When refractory radionuclides are observed in a contaminated area, radioactive particles should be expected.

Particles can contain sufficient radioactivity (MBq) and represent a point source of biological relevance, as the contact dose can be substantial externally (skin dose) or internally (retained in GI tract or inhaled). As previously observed, particles can be retained in filtering organisms such as mussels and snails, as well as in grazing animals. Following deposition, soil and sediments can act as a transient sink for deposited particles. Due to particle weathering and remobilization, particle-contaminated soil and sediments may also act as a potential diffuse source in the future. Thus, within radioecology, there is a need of knowledge with respect to particle characteristics and processes influencing particle weathering and remobilization of associated radionuclides to assess long-term impact from radioactive particle contamination, as also addressed by the ongoing IAEA Coordinated

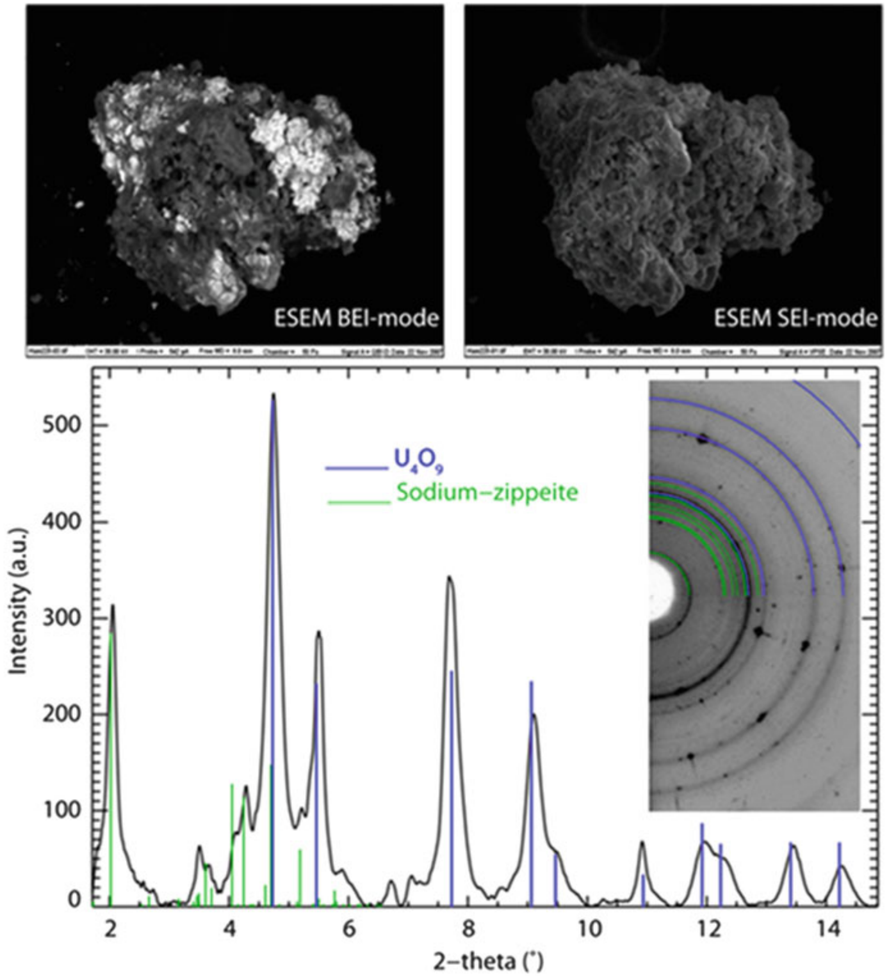

Fig. 5 Electron micrographs (backscattered electron imaging mode, *upper left*, and secondary electron imaging mode, *upper right*) of a TENORM particle from the former Kadji Sai U mining site in Kyrgyzstan (Lind et al. 2013b). Diffractogram (*bottom*) obtained from the same particle shows that uraninite (UO_2/U_4O_9) coexists with Na-zippeite ($Na_4(UO_2)_6[(OH)_{10}(SO_4)_3]\cdot 4H_2O$) within the particle. Darker pixels correspond to areas with a relatively higher concentration of the respective elements. Bar 50 µm

Research Project on "Environmental Behaviour and Potential Biological Impact of Radioactive Particles" and by the EC-funded COMET/RATE project.

To obtain information on radionuclide species such as colloids and particles, advanced analytical methods including nano- and microanalytical techniques are needed for identification, isolation and characterisation of radioactive particles. Measurements on radioactivity (Bq) will not be sufficient for understanding the underlying mechanisms of importance for ecosystem transfer, uptake and effects, and the combination of tools from other scientific fields such as materials science (e.g. the use of synchrotron X-ray micro- and nano-techniques) provides new opportunities in radioecology. For areas affected by particle contamination, the inclusion of radionuclide species including particles and description of their interactions and transfer will significantly reduce the overall uncertainties in impact and risk assessments.

Acknowledgement This work is supported by the Research Council of Norway through the CERAD Centre of Excellence funding scheme, project number 223268/F50.

References

Abe Y, Iizawa Y, Terada Y, Adachi K, Igarashi Y, Nakai I (2014) Detection of uranium and chemical state analysis of individual radioactive microparticles emitted from the Fukushima nuclear accident using Multiple Synchrotron Radiation X-ray analyses. Analyt Chem 86:8521–8525

Adachi K, Kajino M, Zaizen Y, Igarashi Y (2013) Emission of spherical cesium-bearing particles from an early stage of the Fukushima nuclear accident. Sci Rep 3:2554

Admon U (2009) Single particle handling and analysis. In: Oughton DH, Kasparov VA (eds) Radioactive particles in the environment. The NATO Science for Peace and Security program: Springer

Alsecz A, Osan J, Kurunczi S, Alfoldy B, Varhegyi A, Torok S (2007) Analytical performance of different X-ray spectroscopic techniques for the environmental monitoring of the recultivated uranium mine site. Spectrochim Acta B-Atom Spectrosc 62:769–776

AMAP (1997) Arctic pollution issues: Radioactive contamination. sterts: Norwegian Radiation Protection Authority

AMAP (2004) AMAP assessment 2002: radioactivity in the Arctic. Arctic Monitoring and Assessment Programme, Oslo, Norway, pp 1–100

Anspaugh LR, Church BW (1986) Historical estimates of external g exposure and collective external g exposure from testing at the Nevada Test Site. 1. Test series through Hardtack II, 1958. Health Phys 51:35–51

Appleby LJ, Luttrell SJ (1993) Case-studies of significant radioactive releases. In: Warner F, Harrison RM (eds) Radioecology after Chernobyl. Wiley, Chichester, UK

Arnold L (1992) The Windscale Fire 1957. Anatomy of a Nuclear Accident. Macmillan, London

Ault AP, Peters TM, Sawvel EJ, Casuccio GS, Willis RD, Norris GA, Grassian VH (2012) Single-particle SEM-EDX analysis of iron-containing coarse particulate matter in an urban environment: Sources and distribution of iron within Cleveland, Ohio. Environ Sci Technol 46:4331–4339

Baglan N, Cossonnet C, Pitet P, Cavadore D, Exmelin L, Berard P (2000) On the use of ICP-MS for measuring plutonium in urine. J Radioanalyt Nucl Chem 243:397–401

Baglan N, Hemet P, Pointurier F, Chiappini R (2004) Evaluation of a single collector, double focusing sector field inductively coupled plasma mass spectrometer for the determination of U and Pu concentrations and isotopic compositions at trace level. J Radioanalyt Nucl Chem 261:609–617

Batuk ON, Conradson SD, Aleksandrov ON, Boukhalfa H, Burakov BE, Clark DL, Czerwinski KR, Felmy AR, Lezama-Pacheco JS, Kalmykov SN, Moore DA, Myasoedov BF, Reed DT, Reilly DD, Roback RC, Vlasova IE, Webb SM, Wilkerson MP (2015) Multiscale speciation of

U and Pu at Chernobyl, Hanford, Los Alamos, McGuire AFB, Mayak, and Rocky Flats. Environ Sci Technol 49:6474–84

Boehnke A, Treutler HC, Freyer K, Schubert M, Holger W (2005) Localisation and identification of radioactive particles in solid samples by means of a nuclear track technique. Radiat Measure 40:650–653

Bolsunovsky AY, Tcherkezian VO (2001) Hot particles of the Yenisei River flood plain, Russia. J Environ Radioact 57:167–174

Boulyga SF, Becker JS (2001) Determination of uranium isotopic composition and U-236 content of soil samples and hot particles using inductively coupled plasma mass spectrometry. Fresenius J Anal Chem 370:612–617

Bowen J, Glover S, Spitz H (2013) Morphology of actinide-rich particles released from the BOMARC accident and collected from soil post remediation. J Radioanal Nucl Chem 296:853–857

Bunzl K (1997) Probability for detecting hot particles in environmental samples by sample splitting. Analyst 122:653–656

Bunzl K (1998) Detection of radioactive hot particles in environmental samples by repeated mixing. Appl Radiat Isot 49:1625–1631

Bunzl K, Tschiersch J (2001) Detection of radioactive hot particles in environmental samples using a Marinelli-beaker measuring geometry. Radiochim Acta 89:599–604

Burns PA, Cooper MB, Johnston PN, Martin LJ, Willims GA (1994) Determination of the ratios of Pu-239 and Pu-240 to Am-241 for nuclear-weapons test sites in Australia. Health Phys 67:226–232

Burns PA, Cooper MB, Lokan KH, Wilks MJ, Williams GA (1995) Characteristics of plutonium and americium contamination at the former UK atomic weapons test ranges at Maralinga and Emu. Appl Radiat Isotop 46:1099–1107

Chamberlain AC, Dunster HJ (1958) Deposition of radioactivity in North-West England from the accident at windscale. Nature 182:629–630

Chuguevsii AV, Sukhorukov FV, Mel'gunov MS, Makarova IV, Titov AT (2010) "Hot" particles of the Yenisei River: Radioisotope composition, structure, and behavior in natural conditions. Doklady Earth Sci 430:51–53

Conradson SD (2000) XAFS—A technique to probe local structure. Los Alamos Sci 26:422–435

Cooper MB, Burns PA, Tracy BL, Wilks MJ, Willams GA (1994) Characterization of plutonium contamination at the former nuclear-weapons testing range at Maralinga in South-Australia. J Radioanal Nucl Chem 177:161–184

Crean DE, Livens FR, Stennett MC, Grolimund D, Borca CN, Hyatt NC (2014) Microanalytical X-ray imaging of depleted uranium speciation in environmentally aged munitions residues. Environ Sci Technol 48:1467–1474

Cresswell AJ, Sanderson DCW (2012) Evaluating airborne and ground based gamma spectrometry methods for detecting particulate radioactivity in the environment: a case study of Irish Sea beaches. Sci Total Environ 437:285–296

Crocker GR, Oconnor JD, Freiling EC (1966) Physical and radiochemical properties of fallout particles. Health Phys 12:1099

Danesi PR (1998) Hot particles and the cold war. IAEA Bull Vienna

Danesi PR, Moreno J, Makarewicz M, Radecki Z (2002) Residual radioactivity in the terrestrial environment of the Mururoa and Fangataufa Atolls nuclear weapon test sites. J Radioanal Nucl Chem 253:53–65

Danesi PR, Bleise A, Burkart W, Cabianca T, Campbell MJ, Makarewicz M, Moreno J, Tuniz C, Hotchkis M (2003a) Isotopic composition and origin of uranium and plutonium in selected soil samples collected in Kosovo. J Environ Radioact 64:121–131

Danesi PR, Markowicz A, Chinea-Cano E, Burkart W, Salbu B, Donohue D, Ruedenauer F, Hedberg M, Vogt S, Zahradnik P, Ciurapinski A (2003b) Depleted uranium particles in selected Kosovo samples. J Environ Radioact 64:143–154

Darley PJ, Charles MW, Fell TP, Harrison JD (2003) Doses and risks from the ingestion of Dounreay fuel fragments. Radiat Prot Dosimet 105:49–54

De Nolf W, Jaroszewicz J, Terzano R, Lind OC, Salbu B, Vekemans B, Janssens K, Falkenberg G (2009) Possibilities and limitations of synchrotron X-ray powder diffraction with double crystal and double multilayer monochromators for microscopic speciation studies. Spectrochim Acta B: Atom Spectrosc 64:775–781

Denecke MA, Borchert M, Denning RG, De Nolf W, Falkenberg G, Honig S, Klinkenberg GM, Kvashnina K, Neumeier S, Patommel J, Petersmann T, Pruessmann T, Ritter S, Schroer CG, Stephan S, Villanova J, Vitova T, Wellenreuther G (2012) Highly resolved synchrotron-based investigations related to nuclear waste disposal. Act Nucl Energ Mat 1444:269–280

Dennis F, Morgan G, Henderson F (2007) Dounreay hot particles: the story so far. J Radiol Prot 27: A3–A11

Dobrovolsky E, Lyalko V (1995) Acidification of soils and radioactive hot particles behavior: a macrokinetic approach. Water Air Soil Pollut 85:767–772

Drell S, Peurifoy B (1994) Technical issues of a nuclear test ban. Annu Rev Nucl Part Sci 44:285–327

Eriksson M, Osan J, Jernstrom J, Wegrzynek D, Simon R, Chinea-Cano E, Markowicz A, Bamford S, Tamborini G, Torok S, Falkenberg G, Alsecz A, Dahlgaard H, Wobrauschek P, Streli C, Zoeger N, Betti M (2005) Source term identification of environmental radioactive Pu/U particles by their characterization with non-destructive spectrochemical analytical techniques. Spectrochim Acta Part B: Atom Spectrosc 60:455–469

Eriksson M, Lindhal P, Roos P, Dahlgaard H, Holm E (2008) U, Pu, and Am nuclear signatures of the Thule hydrogen bomb debris. Environ Sci Technol 42:4717–4722

Eroglu AE, Mcleod CW, Leonard KS, Mccubbin D (1998) Determination of plutonium in seawater using co-precipitation and inductively coupled plasma mass spectrometry with ultrasonic nebulisation. Spectrochim Acta Part B: Atom Spectrosc 53:1221–1233

Fifield LK (1999) Accelerator mass spectrometry and its applications. Rep Prog Phys 62:1223–1274

Fifield LK (2000) Advances in accelerator mass spectrometry. Nucl Instrum Method Phy Res Sec B-Beam Interact Mat Atom 172:134–143

Garland JA, Wakeford R (2007) Atmospheric emissions from the windscale accident of October 1957. Atmos Environ 41:3904–3920

Gerdes A, Weyer S, Brey G, Durakovic A, Zimmermann I (2004) Monitoring depleted Uranium contamination in the biosphere of Iraq using MC-ICP-MS. Geochim Cosmochim Acta 68: A506

Gruning C, Huber G, Klopp P, Kratz JV, Kunz P, Passler G, Trautmann N, Waldek A, Wendt K (2004) Resonance ionization mass spectrometry for ultratrace analysis of plutonium with a new solid state laser system. Int J Mass Spectrosc 235:171–178

Gwynn JP, Nikitin A, Shershakov V, Heldal HE, Lind B, Teien HC, Lind OC, Sidhu RS, Bakke G, Kazennov A, Grishin D, Fedorova A, Blinova O, Svaeren I, Lee Liebig P, Salbu B, Wendell CC, Stralberg E, Valetova N, Petrenko G, Katrich I, Logoyda I, Osvath I, Levy I, Bartocci J, Pham MK, Sam A, Nies H, Rudjord AL (2015) Main results of the 2012 joint Norwegian–-Russian expedition to the dumping sites of the nuclear submarine K-27 and solid radioactive waste in Stepovogo Fjord, Novaya Zemlya. J Environ Radioact. doi:10.1016/j.jenvrad.2015.02.003

Hamilton TF, Jernstroem J, Martinelli RE, Kehl SR, Eriksson M, Williams RW, Bieleski M, Rivers AN, Brown TA, Tumey SJ, Betti M (2009) Frequency distribution, isotopic composition and physical characterization of plutonium-bearing particles from the Fig-Quince zone on Runit Island, Enewetak Atoll. J Radioanal Nucl Chem 282:1019–1026

Heft RE (1970) Characterization of radioactive particles from nuclear weapons tests. Adv Chem Ser 254

IAEA (1998) Radiological conditions at the Semipalatinsk test site, Kazakhstan: preliminary assessment and recommendations for further studies. International Atomic Energy Agency, Vienna, pp 1–43

IAEA CRP (2011) Radioactive particles in the environment: sources, particle characteristics, and analytical techniques. IAEA-TECDOC Vienna

Jakeman D (1986) Notes of the level of radioactive contamination in the Sellafield area arising from discharges in the Early 1950s. Atomic Energy Establishment, Winfrith

Jernstrom J, Eriksson M, Osan J, Tamborini G, Torok S, Simon R, Falkenberg G, Alsecz A, Betti M (2004) Non-destructive characterisation of low radioactive particles from Irish Sea sediment by micro X-ray synchrotron radiation techniques: micro X-ray fluorescence (mu-XRF) and micro X-ray absorption near edge structure (mu-XANES) spectroscopy. J Analyt Atom Spectrosc 19:1428–1433

Jimenez-Ramos MC, Barros H, Garcia-Tenorio R, Garcia-Leon M, Vioque I, Manjon G (2007) On the presence of enriched uranium in hot-particles from the terrestrial area affected by the Palomares accident (Spain). Environ Pollut 145:391–394

JNREG (2004) Impacts on man and the environment in Northern areas from hypothetical accidents at "Mayak" PA, Urals, Russia, sterts, Joint Norwegian-Russian expert group for investigation of radioactive contamination in the Northern areas

Kashparov VA, Lundin SM, Zvarych SI, Yoshchenko VI, Levchuk SE, Khomutini YV, Maloshtan IM, Protsak VP (2003) Territory contamination with the radionuclides representing the fuel component of Chernobyl fallout. Sci Total Environ 317:105–119

Kasparov VA, Oughton DH, Protsak VP, Zvarisch SI, Levchuk SE (1999) Kinetics of fuel particle weathering and 90 Sr mobility in the Chernobyl 30 km exclusion zone. Health Phys 76:251–259

Kersting AB, Efurd DW, Finnegan DL, Rokop DJ, Smith DK, Thompson JL (1999) Migration of plutonium in ground water at the Nevada test site. Nature 397:56–59

Krey PW (1967) Plutonium-238 from Snap-9A Burnup 39. Trans Am Nucl Soc 10

Krey PW, Leifer R, Benson WK, Dietz LA, Coluzza JL, Hendrikson HC (1979) Atmospheric burnup of the Cosmos-954 reactor. Science 205:583–585

Landa ER, Stieff LR, Germani MS, Tanner AB, Evans JR (1994) Intense alpha-particle emitting crystallites in uranium mill wastes. Nucl Geophys 8:443–454

Lee MH, Clark SB (2005) Activities of Pu and Am isotopes and isotopic ratios in a soil contaminated by weapons-grade plutonium. Environ Sci Technol 39:5512–5516

Lehto J, Hou XL (2011) Chemistry and analysis of radionuclides. Wiley-VCH, Weinheim

Leifer R, Juzdan ZR, Kelly WR, Fassett JD, Eberhardt KR (1987) Detection of uranium from Cosmos-1402 in the stratosphere. Science 238:512–514

Leonard KS, McCubbin D, Lovett MB (1995) Physico-chemical characterisation of radionuclides discharged from a nuclear establishment. Sci Total Environ 175:9–24

Lind OC (2006) Characterisation of radioactive particles in the environment using advanced techniques. PhD Thesis, Norwegian University of Life Sciences, pp 1–191

Lind OC, Oughton D, Salbu B, Skipperud L, Sickel M, Brown JE, Fifield LK, Tims S (2006) Transport of low 240 Pu/ 239 Pu atom ratio plutonium-species in the Ob and Yenisey Rivers to the Kara Sea. Earth Planet Sci Lett 251:33–43

Lind OC, Salbu B, Janssens K, Proost K, Garcia-Leon M, Garcia-Tenorio R (2007) Characterization of U/Pu particles originating from the nuclear weapon accidents at Palomares, Spain, 1966 and Thule, Greenland, 1968. Sci Total Environ 376:294–305

Lind OC, Salbu B, Skipperud L, Janssens K, Jaroszewicz J, De Nolf W (2009) Solid state speciation and potential bioavailability of depleted uranium particles from Kosovo and Kuwait. J Environ Radioact 100:301–307

Lind OC, Oughton DH, De Nolf W, Janssens K, Stromman G, Bolsunovsky ALKF, Melgunov M, Salbu B (2011a) Characterisation of individual radioactive particles from Krasnoyarsk-26. In: Barescut JC (ed) International Conference on Radioecology and Environmental Radioactivity, Hamilton, Canada

Lind OC, Salbu B, Janssens K (2011b) Microanalytical characterisation of radioactive TENORM particles. In: Barescut JC (ed) International conference on radioecology and environmental radioactivity, Hamilton, Canada

Lind OC, De Nolf W, Janssens K, Salbu B (2013a) Micro-analytical characterisation of radioactive heterogeneities in samples from Central Asian TENORM sites. J Environ Radioact 123:63–70

Lind OC, Stegnar P, Tolonutov B, Rosseland BO, Stromman G, Uralbekov B, Usubalieva A, Solomatina A, Gwynn JP, Lespukh E, Salbu B (2013b) Environmental impact assessment of radionuclide and metal contamination at the former U site at Kadji Sai, Kyrgyzstan. J Environ Radioact 123:37–49
Lind OC, Cagno S, Falkenberg G, Janssens K, Jarszewicz J, Nuyts G, Priest N, Audet M, Vanmeert F, Salbu B (2014) Low-level radioactive river sediment particles originating from the Chalk River nuclear site carry a mixture of radionuclides and metals. International Conference on Radioecology and Environmental Radioactivity, Barcelona, Spain
Mamuro T, Fujita A, Yoshikawa K, Matsunami T (1962) Microscopic examination of highly radioactive fall-out particles. Nature 196:529–531
Mamuro T, Fujita A, Matsunam T (1965) Microscope examination of highly radioactive fallout particles from first Chinese nuclear test explosion. Health Phys 11:1097–1101
Mamuro T, Yoshikawa K, Matsunami T, Fujita A (1966) Radionuclide fractionation in debris from a land surface burst. Health Phys 12:757–763
Maucec A, De Meijer RJ, Rigollet C, Hendriks PHGM, Jones DG (2004) Detection of radioactive particles offshore by mu-ray spectrometry—Part I: Monte Carlo assessment of detection depth limits. Nucl Instrum Methods Phys Res A 525:593–609
McCartney M, Kershaw PJ, Woodhead DS, Denoon DC (1994) Artificial radionuclides in the surface sediments of the Irish Sea, 1968–1988. Sci Total Environ 141:103–138
McDowell LM, Whicker FW (1978) Size characteristics of plutonium particles in rocky flats soil. Health Phys 35:293–299
McLaughlin JP, Vintro LL, Smith KJ, Mitchell PI, Zunic ZS (2003) Actinide analysis of a depleted uranium penetrator from a 1999 target site in southern Serbia. J Environ Radioact 64:155–165
Mian Z, Ramana MV, Rajaraman R (2001) Plutonium dispersal and health hazards from nuclear weapon accidents. Curr Sci 80:1275–1284
Mongan TR, Ripple SR, Brorby GP, diTommaso DG (1996a) Plutonium releases from the 1957 fire at Rocky Flats. Health Phys 71:510–521
Mongan TR, Ripple SR, Winges KD (1996b) Plutonium release from the 903 pad at rocky flats. Health Phys 71:522–531
NCRPM (2009) Ionizing radiation exposure of the population of the United States. National Council on Radiation Protection Report. National Council on Radiation Protection and Measurements Bethesda, USA
Nees WL, Corley JP (1973) Environmental surveillance at Hanford for CY-1973. Pacific Northwest Laboratories, Richland, Washington
Novikov AP, Kalmykov SN, Utsunomiya S, Ewing RC, Horreard F, Merkulov A, Clark SB, Tkachev VV, Myasoedov BF (2006) Colloid transport of plutonium in the far-field of the Mayak Production Association, Russia. Science 314:638–641
Oughton DH, Salbu B, Brand TL, Day JP, Aarkrog A (1993) Under-determination of Sr-90 in soils containing particles of irradiated uranium oxide fuel. Analyst 118:1101–1105
Oughton DH, Fifield LK, Day JP, Cresswell RC, Skipperud L, Di Tada ML, Salbu B, Strand P, Drozcho E, Mokrov Y (2000) Plutonium from Mayak: measurement of isotope ratios and activities using accelerator mass spectrometry. Environ Sci Technol 34:1938–1945
Oughton DH, Skipperud L, Fieield LK, Cresswell RG, Salbu B, Day P (2004) Accelerator mass spectrometry measurement of Pu-240/Pu-239 isotope ratios in Novaya Zemlya and Kara Sea sediments. Appl Radiat Isotopes 61:249–253
Pointurier F, Barglan N, Hemet P (2004) Ultra low-level measurements of actinides by sector field ICP-MS. Appl Radiat Isotopes 60:561–566
Pollanen R, Klemola S, Ikaheimonen TK, Rissanen K, Juhanoja J, Paavolainen S, Likonen J (2001) Analysis of radioactive particles from the Kola Bay area. Analyst 126:724–730
Poston TM, Peterson RE, Cooper AT (2007) Past radioactive particle contamination in the Columbia River at the Hanford site, USA. J Radiol Prot 27:A45
Ranebo Y, Eriksson M, Tamborini G, Niagolova N, Bildstein O, Betti M (2007) The use of SIMS and SEM for the characterization of individual particles with a matrix originating from a nuclear weapon. Microsc Microanal 13:179–190

Sajih M, Livens FR (2010) Identification and characterisation of radioactive particles in salt marsh sediments. In: Rao L, Tobin JG, Shuh DK (eds) Actinides 2009. Iop Publishing Ltd., Bristol
Sakaguchi A, Steier P, Takahashi Y, Yamamoto M (2014) Isotopic compositions of U-236 and Pu Isotopes in "Black Substances" collected from roadsides in fukushima prefecture: Fallout from the Fukushima Dai-ichi Nuclear Power Plant Accident. Environ Sci Technol 48:3691–3697
Salbu B (2000a) Source-related characteristics of radioactive particles: a review. Radiat Protect Dosimetry 92:49–54
Salbu B (2000b) Speciation of radionuclides in the environment. In: Meyers RA (ed) Encyclopedia of analytical chemistry. Wiley, Chichester, UK
Salbu B (2001) Hot particles-a challenge within radioecology. J Environ Radioact 53:267–268
Salbu B (2009) Challenges in radioecology. J Environ Radioact 100:1086–1091
Salbu B, Kudo A (2001) Actinides associated with particles. Plutonium in the environment. Elsevier, Tokyo
Salbu B, Lind OC (2011) Radioactive particles released into the environment from nuclear events. In: Kalmykov SN, Denecke MA (eds) Actinide nanoparticle research. Springer, Berlin, Heidelberg
Salbu B, Von Philipborn H, Steinhuser F (1988) Radionuclides associated with colloids and particles in rainwaters, Oslo, Norway. Hot particles from the Chernobyl Fallout. Bergbau- und Industrimuseum, Theuern
Salbu B, Bjornstad HE, Svaren I, Prosser SL, Bulman RA, Harvey BR, Lovett MB (1993) Size distribution of radionuclides in nuclear-fuel reprocessing liquids after mixing with Seawater. Sci Total Environ 130:51–63
Salbu B, Krekling T, Oughton DH, Ostby G, Kashparov VA, Brand TL, Day JP (1994) Hot particles in accidental releases from Chernobyl and Windscale nuclear installations. Analyst 119:125–130
Salbu B, Nikitin AI, Strand P, Christensen GC, Chumichev VB, Lind B, Fjelldal H, Bergan TDS, Rudjord AL, Sickel M, Valetova NK, Foyn L (1997) Radioactive contamination from dumped nuclear waste in the Kara sea-results from the joint Russian-Norwegian expeditions in 1992–1994. Sci Total Environ 202:185–198
Salbu B, Janssens K, Krekling T, Siminovici A, Drakopoulos M, Raven C, Snigireva I, Snigirev A, Lind OC, Oughton DH, Adams F, Kashparov VA (2000) μ-X-ray absorption tomography and μ-XANES for characterisation of fuel particles. In: Cornuejols D, Admans G (eds) ESRF highlights 1999. European Synchrotron Radiation Facility
Salbu B, Krekling T, Lind OC, Oughton DH, Drakopoulos M, Simionovici A, Snigireva I, Snigireva A, Weitkamp T, Adams F, Janssens K, Kashparov V (2001a) High energy X-ray microscopy for characterisation of fuel particles. Nucl Instrum Methods Phys Res A 467:1249–1252
Salbu B, Lind OC, Borretzen P, Oughton D, Brechignac F, Howard B (2001b) Advanced speciation techniques for radionuclides associated with colloids and particles. Radioactive pollutants—impact on the environment. EDP Sciences, Les Ulis Cedex A
Salbu B, Skipperud L, Germain P, Guesueniat P, Strand P, Lind OC, Christensen G (2003) Radionuclide speciation in effluent from La Hague reprocessing plant in France. Health Phys 85:311–322
Salbu B, Lind OC, Skipperud L (2004) Radionuclide speciation and its relevance in environmental impact assessments. J Environ Radioact 74:233–242
Salbu B, Janssens K, Lind OC, Proost K, Gijsels L, Danesi PR (2005) Oxidation states of uranium in depleted uranium particles from Kuwait. J Environ Radioact 78:125–135
Schneider S, Walther C, Bister S, Schauer V, Christl M, Synal HA, Shozugava K, Steinhauser G (2013) Plutonium release from Fukushima Daiichi fosters the need for more detailed investigations. Sci Rep 3:2988
Selchau-Hansen K, Ghose R, Freyer K, Treutler C, Enge W (1999) Hot particles in industrial waste and mining tailings. Radiat Meas 31:451–454

Simon SL, Jenner T, Graham JC, Borchert A (1995) A Comparison of macroscopic and microscopic measurements of plutonium in contaminated soil from the Republic-Of-The-Marshall-Islands. J Radioanalyt Nucl Chem-Art 194:197–205
Sisefsky J (1961) Debris from tests of nuclear weapons—activities roughly proportional to volume are found in particles examined by autoradiography and microscopy. Science 133:735
Skipperud L, Oughton DH (2004) Use of AMS in the marine environment. Environ Int 30:815–825
Skipperud L, Oughton DH, Fifield LK, Lind OC, Tims S, Brown J, Sickel M (2004) Plutonium isotope ratios in the Yenisey and Ob estuaries. Appl Radiat Isot 60:589–593
Smith JN, Ellis KM, Polyak L, Ivanov G, Forman SL, Moran SB (2000) ^{239,240}Pu transport into the Arctic Ocean from underwater nuclear tests in Chernaya Bay, Novaya Zemlya 61. Continent Shelf Res 20:255–279
Solodukhin VP (2005) Nuclear-physical methods in macro- and microanalytical investigations of contamination with radionuclides at Semipalatinsk Nuclear test site. J Radioanalyt Nucl Chem 264:457–462
Sowder AG, Clark SB, Field RA (1999) The transformation of uranyl oxide hydrates: the effect of dehydration on synthetic metaschoepite and its alteration to becquerelite. Environ Sci Technol 33:3552–3557
Sturup S, Dahlgaard H, Nielsen SC (1998) High resolution inductively coupled plasma mass spectrometry for the trace determination of plutonium isotopes and isotope ratios in environmental samples 28. J Anal At Spectrom 13:1321–1326
Sukhrukov FV, Degermendzhi AG, Bolsunovsky A, Belolipetskii VM, Kosolapova LG (2004) Distribution and migration behaviours of radionuclides in the Yenisei River floodplain. SB RAS Publishers, Novosibirsk
Tamborini G (2004) SIMS analysis of uranium and actinides in microparticles of different origin. Microchim Acta 145:237–242
Tcherkezian V, Galushkin B, Goryachenkova T, Kashkarov L, Liul A, Roschina I, Rumiantsev O (1995) Forms of contamination of the environment by radionuclides after the tomsk accident (Russia, 1993). J Environ Radioact 27:133–139
UNSCEAR (1993) Sources and effects of ionizing radiation. United Nations, New York
UNSCEAR (2000) Sources and effects of ionizing radiation. United Nations, New York
Utsunomiya S, Jensen KA, Keeler GJ, Ewing RC (2002) Uraninite and fullerene in atmospheric particulates. Environ Sci Technol 36:4943–4947
Voilleque PG, Killough GG, Rope SK (2002) Methods for estimating radiation doses from short-lived gaseous radionuclides and radioactive particles released to the atmosphere during early Hanford Operations - FINAL REPORT. Centers for Disease Control and Prevention Department of Health and Human Services
Wendel CC, Fifield LK, Oughton DH, Lind OC, Skipperud L, Bartniki J, Tims SG, Hoibraten S, Salbu B (2013) Long-range tropospheric transport of uranium and plutonium weapons fallout from Semipalatinsk nuclear test site to Norway. Environ Int 59:92–102
Wolf SF, Bates JK, Buck EC, Dietz NL, Portner JA, Brown NR (1997) Physical and chemical characterization of actinides in soil from Johnston Atoll. Environ Sci Technol 31:467–471

Mobility and Bioavailability of Radionuclides in Soils

Andra-Rada Iurian, Marcelle Olufemi Phaneuf, and Lionel Mabit

Contents

A.-R. Iurian (✉)
Faculty of Environmental Science and Engineering, Babeş-Bolyai University, 30 Fântânele Street, 400294 Cluj-Napoca, Romania
e-mail: iurian.andra@ubbcluj.ro

M.O. Phaneuf
Terrestrial Environment Laboratory, IAEA Environment Laboratories, Department of Nuclear Sciences and Applications, International Atomic Energy Agency, Vienna International Centre, 1400 Vienna, Austria

L. Mabit
Soil and Water Management & Crop Nutrition Laboratory, Joint FAO/IAEA Division for Nuclear Techniques in Food and Agriculture, Vienna International Centre, 1400 Vienna, Austria

C. Walther, D.K. Gupta (eds.), *Radionuclides in the Environment*,
DOI 10.1007/978-3-319-22171-7_2

Abstract It is crucial to understand the behaviour of radionuclides in the environment, their potential mobility and bioavailability related to their long-term persistence and their radiological hazard and potential impact on human health. Such key information is used to support decision-making. The environmental behaviour of radionuclides depends on ecosystem characteristics. A given soil's capacity to immobilise radionuclides has proved to be the main factor responsible for their resulting activity concentrations in plants. The mobility and bioavailability of radionuclides in soils is complex, depending on clay-sized soil fraction, clay mineralogy, organic matter, cation exchange capacity, pH and quantities of competing cations. Moreover, various plant species have different behaviours regarding radionuclide absorption from soils.

This chapter is intended to provide comprehensive up-to-date background information concerning the mobility and bioavailability of selected key artificial and natural radionuclides (e.g. ^{137}Cs, ^{90}Sr, ^{239,240}Pu, ^{241}Am, ^{238}U, ^{226}Ra, ^{232}Th) in different soil types under various environmental conditions.

Keywords Radionuclide behaviour in soil • Radionuclide mobility • Radionuclide bioavailability • Soil physico-chemical characteristics

1 Introduction

1.1 Objective and Overview

The main objective of this chapter is to provide background information and comprehensive data on the behaviour and potential mobility of selected artificial and natural radionuclide in soils. Such information is particularly useful and/or necessary for (1) developing long-term remediation and management strategies for terrestrial ecosystems contaminated with artificial radionuclides or radionuclides originating from uranium mining legacy sites, with the goal of limiting the radionuclides' transfer into the biological food chain, and (2) the use of radionuclides as tracers of environmental processes in terrestrial ecosystems. Therefore, the authors have attempted to summarise the existing knowledge regarding the main factors controlling the mobility and geochemical behaviour of key targeted long-lived radionuclides in soils, with reference to a wide range of soil conditions. Significant research studies on the behaviour of radionuclides in soil were discussed and reported. However, this area of research is ongoing and knowledge is still evolving; therefore, the authors may not come to final conclusions in all cases.

Environmental contamination with artificial radionuclides (^{137}Cs, ^{90}Sr, ^{239,240}Pu, ^{241}Am) is a direct consequence of the following:

1. Atmospheric releases of radioactive particles from nuclear weapon tests (UNSCEAR 1969) that took place from the beginning of 1950s to the mid-1960s with a major peak release in 1963. These anthropogenic radionuclides were distributed globally, but the fallout patterns followed a clear latitudinal zoning, substantially greater in the Northern Hemisphere where most of the nuclear weapon tests were performed.
2. Accidental releases of artificial radionuclides into the environment such as occurred in Chernobyl in April 1986 (IAEA 2006) and Fukushima in March 2011 (ANS 2012). Other less well-known radioactive incidents and/or radionuclides potentially released into the environment from nuclear waste sites have only impacted local or regional communities and did not result in global dispersion.

Following deposition, long-lived artificial radionuclides are generally absorbed to the soil matrix, showing lower transport velocities in the unsaturated zone (about 1 cm y^{-1}) (Kirchner et al. 2009). Thus, a major fraction of the originally deposited activity may remain within the rooting zone for decades, having high potential to be introduced in the food chain. Most literature sources refer to ^{137}Cs from Chernobyl and from weapons fallout, while a limited number of studies have focused on other radionuclides.

Uranium mining legacy sites are of concern all over the world, due to the presence of radioactive waste materials in a range of activities that can potentially have an environmental health impact through the transfer into the food chain and human exposure to radiation (Carvalho 2011). Radionuclides, in particular radium, can be transferred from mine sites and mining wastes to underground and stream waters, from water to soil and from soil to vegetables and animals, thus entering the food chain.

The applications of environmental radionuclides in tracer studies in terrestrial ecosystems are facilitated by their natural distribution into the environment and are based on the basic principle of radioactive decay. There are two major groups of applications: (1) providing timescales of past and present processes and (2) tracing substances involved in terrestrial transport, exchange and mixing processes (Froehlich and Masarik 2009). It is commonly assumed that these radiotracers are strongly particle bound, being suitable for tracing soil and sediment processes. However, the use of artificial radiotracers is often limited to site-specific applications due to their possible nonhomogeneous deposition on the landscape, being also limited to a timeframe which starts at the contamination moment. Among the long-lived fission products employed as useful tracers of landscape processes, ^{137}Cs has been most widely studied, but ^{134}Cs, ^{239,240}Pu, as well as ^{241}Am were also used individually or in combination with ^{137}Cs.

1.2 Vertical Movement of Radionuclides in Undisturbed Soils

The mobility of radionuclides in soil follows basic processes including convective transport by flowing water, dispersion caused by spatial variations of convection velocities, diffusive movement within the fluid and physico-chemical interaction with the soil matrix (Kirchner et al. 2009). The diffusion is considered to be an active process over time, while the convection and dispersion are a direct result of fluid flow in the porous medium over a travel distance. The *effective diffusion coefficient, D,* is commonly used to describe the contaminant diffusion in porous media, accounting for the geometry of porous structure and for the contaminant interaction with the pore walls (Van Genuchten and Cleary 1979). An additional contribution to these natural physical processes might be (1) the soil fauna—such as earthworms, ants or termites (Matisoff and Whiting 2011)—acting more towards a dispersion-like translocation (Boudreau 1986), (2) bioturbation, (3) leaching, (4) preferential flow paths, (5) erosion and (6) ploughing.

Fallout radionuclides (e.g. ^{137}Cs, $^{239,240}Pu$) move downwards with time, from top soil to deeper soil horizons. The penetration depth is determined by the delivery rates, the radionuclide half-life (Bossew and Kirchner 2004), the fallout history and the land use. The processes involved in the transport of radionuclides into the soil column are very complex, and in order to understand them, it is necessary to predict their temporal behaviour. Transport models like the *convection–dispersion model* (Van Genuchten and Cleary 1979; Schuller et al. 1997), *the compartment model* (Kirchner 1998a) and other *statistical distribution function models* (Kirchner 1998b) have been initially employed for ^{137}Cs to describe its migration and diffusion process in undisturbed soil. These models were later extended to include other fallout radionuclides.

1.3 The Solid–Liquid Distribution Coefficient, K_d

The natural soil system, nonhomogeneous in granular and chemical composition, can be seen as a multifunctional absorbing media with three phases: solid phase (mineral soil), liquid phase (soil solution) and gaseous phase (soil atmosphere). The solid and liquid phases are of major importance in the radionuclide interaction with the soil. The result of this interaction is determined by the combined action of different factors, such as physico-chemical characteristics of the radionuclide, adsorption capacity, soil organic matter, soil water content, elemental concentration and composition of soil solution (e.g. Ca^{2+}, Mg^{2+}, K^+, H^+, NH_4^+, Cl^-, NO_3^-), pH of the soil and climatic conditions. These factors will be discussed in more detail in Sect. 3.2 of this chapter.

The migration ability of radionuclides is commonly investigated using different methods involving sequential chemical fractionation. Over a long time following deposition, the exchange and readily soluble forms of radionuclide in soil can change in proportion, thus affecting their movement through environmental media and uptake by vegetation. Specifically, the binding between a radionuclide and the mineral soil determines the content of radionuclide in solution, which is directly responsible for the fraction of radionuclide that may enter into organisms. Radionuclide–soil interaction and subsequent radionuclide transport in the soil column are investigated through the *solid–liquid distribution coefficient,* K_d *(Bq* kg^{-1} *soil or sediment per Bq* l^{-1} *water at equilibrium)*, one of the key parameters in environmental assessment research. This parameter is commonly determined as the ratio of the radionuclide activity concentration sorbed on a specified solid phase to the radionuclide activity concentration in a specified liquid phase (IAEA 2010), assuming that the radionuclide in the solid phase is in equilibrium with the radionuclide in solution and that exchange between these phases is reversible. As radionuclides are mobilised over time through weathering, the radionuclide distribution and hence the K_{d} will change (Salbu et al. 1998).

For a given radionuclide and soil type combination, K_{d} values obtained by researchers have varied by orders of magnitude as a result of different approaches, experimental conditions, radionuclide speciation and soil geochemistry. Various factors can influence the K_{d} values, from which the aqueous chemistry of the radionuclide of interest and the nature of the geological substratum are of major importance (Sheppard and Thibault 1990). Simplified models of radionuclide transport incorporate selected K_{d} values together with other hydrological and physico-chemical parameters for migration predictions. The main soil parameters influencing the K_{d} predictions should be measured and monitored to improve its determination.

The 'Handbook of parameter values for the prediction of radionuclide transfer in temperate environments', International Atomic Energy Agency (IAEA) Technical Reports Series (TRS) 364 (IAEA 1994), was the first attempt to establish a $\mathrm{K_d}$ database for soils and to provide ranges of values for specific radionuclides and soil conditions. The IAEA TRS 364 values were revised 15 years later to include additional key data from post-Chernobyl research and the various radioecological mechanisms that govern soil–radionuclide interaction. A new updated report, the IAEA TRS 472, i.e. 'Handbook of parameter values for the prediction of radionuclide transfer in terrestrial and freshwater environments', was published in 2010 (IAEA 2010), followed by the IAEA TRS 479 'Handbook of parameter values for the prediction of radionuclide transfer to wildlife' in 2014 (IAEA 2014a).

1.4 Radionuclide Bioavailability in Soils

In soil systems, each radionuclide follows dynamic processes being partially transported into the soil solution and available to be incorporated via the roots into plants, while another part of its concentration becomes strongly bound to the soil particles (Baeza et al. 1999). Different soil types and different plant species show distinct radionuclide uptake behaviour. For specific radionuclides, their uptake in plants is facilitated by their chemical similarity with other elements that the plant normally uses for its growth (e.g. similarity between Cs and K). Radionuclide uptake in plants is more controlled by soil–plant specific parameters rather than radionuclide concentrations in soils (Bunzl et al. 2000). The most important specific parameters are the following:

1. The radionuclide bioavailability in the soil solution (Sanchez et al. 2002)
2. The capacity of plant species to absorb bioavailable radionuclides
3. The availability of competing ions in the soil solution (Ehlken and Kirchner 2002)

Furthermore, soil parameters also have an important role in the radionuclide transfer to plants: pH and cation exchange capacity of soil, soil organic matter content and radionuclide interception parameter (RIP). In addition, Bundt et al. (2000) demonstrated that plant uptake is also affected by the heterogeneous radionuclide distribution in soil. The transfer factor (TF), also often referred to as concentration ratio (CR), is a commonly used parameter to express the proportion in which a specific radionuclide is transferred from soil to plants, when uptake by plant roots is the only process affecting transfer. The TF is determined as the ratio of the mass activity concentration of the plant to that of the soil. Range of updated TF values for different soil systems and environmental conditions are provided by the IAEA TRS 472 (IAEA 2010) and IAEA TRS 479 (IAEA 2014a).

2 Factors Controlling the Behaviour of Radionuclides in Soil

The behaviour of radionuclides in soil systems depends both on their elemental properties and on the physico-chemical characteristics of the soil, the complexity of the interaction increasing due to the multitude of processes that run simultaneously and their dependence on the environmental conditions. Different soil types and environmental conditions suggest different radionuclide behaviour between soils. Activities taken towards soil mapping, such as the GlobalSoilMap.net project (Sanchez et al. 2009), may be of real need to improve soil management and to predict the potential behaviour of radionuclides at regional scales based on the physico-chemical properties of the soil. On the other hand, it is also important to avoid generalisations on the basis of the work undertaken so far, and whenever possible, it is recommended to determine the specific characteristics of the studied soil. The role of the main factors controlling the mobility of radionuclides in soil and the relevance of these factors for their long-term behaviour in terrestrial environments are presented in this chapter.

2.1 Soil Organic Matter

There is high heterogeneity in the organic matter content of soils, being rapidly decomposed in arid environments and eroded soils, while its accumulation is a slow process influenced by climate, soil type, vegetation and soil organisms. Its composition consists of organic acids, lipids, lignin, fulvic and humic acids, making possible the existence of various possible reactions and interactions of radionuclides with these constituents. The formation of mineral–organic complexes and chelates is an important process of this interaction. The stability of these combinations depends on the bioclimatic condition, the soil pH, the cation concentration in the soil, the functional group and the degree of saturation of the potential sorption sites, while their mobility depends on the size and the water solubility of the ligands (Koch-Steindl and Pröhl 2001). Compounds with low molecular weight and water-soluble (e.g. polyphenol, carbon acids, fulvic acids and polysaccharides) form mobile complexes, while humic acids of high molecular weight form compounds of lower mobility (Goryachenkova et al. 2009). In specific cases, organic matter may increase or decrease the radionuclides mobility as discussed in Sect. 3.

2.2 Mineral Soil Components

Radionuclide mobility in various soil types is possible associated with specific minerals. Silt and clay soil fractions contain different adsorbing components of which the most important are minerals such as smectite, illite, vermiculite, chlorite, allophane and imogolite, as well as the oxides and hydroxides of silica, aluminium, iron and manganese (Korobova et al. 2014). The permanent negative charge at the surface of the clay minerals results in cations' adsorption ability, whereas their variable charge (which can be positive or negative) leads to the adsorption of cations or anions and is dependent on the degree of protonation of functional Si, Al, Fe or C groups and on the soil pH. Soils with a high content of illite, smectite, vermiculite or mica within the clay fraction adsorb large amounts of cations due to their intrinsic negative charge, while halloysite and imogolite components of clay minerals are important anion adsorbing constituents (Koch-Steindl and Pröhl 2001). Soils containing clays with of low exchange activity (such as kaolinite), despite having high clay content, exhibit a low exchange capacity. This can lead to an increase of the radionuclides' mobility in the soil column. The presence of organic matter reduces anion adsorption due to the formation of organic coatings on the surface anion adsorbing minerals.

2.3 Redox Potential (E_h) and the pH

The radionuclide oxidation status determines the chemical behaviour of radionuclides in soil. The pH value and the redox potential (E_{h}) of the soil are recognised as major factors controlling the radionuclide chemical speciation. All redox processes in soil occur in the presence of water. The redox potential and the pH value are negatively correlated, i.e. the pH will increase with the decrease of E_{h}. The oxygen supply controls the redox reactions in the soil and the radionuclide chemical speciation, thus establishing the E_{h}–pH conditions (Koch-Steindl and Pröhl 2001). The optimum pH value depends on soil composition and texture and on its organic matter content. Various factors can influence soil redox potential, such as the soil type, the presence of water-impermeable soil horizons and the biological activity. However, it should be highlighted that even under optimum soil conditions, the redox potential shows temporary fluctuations within the year.

2.4 Rainfall

Soil water content mainly controls gas exchange between the soil and the atmosphere, having a direct impact on redox potential and radionuclide speciation. The water flow along macropores can partially carry on chemically unchanged particles, whereas slow infiltration favours the chemical interaction of soil matrix and soil solution. Radionuclide migration to deeper soil layers may be enhanced by high intensity rainfalls. In addition, Thørring et al. (2014) indicated that precipitation composition may influence the mobility of radiocaesium in an early phase after deposition and presumably before significant time-dependent fixation has occurred. However, depth distribution of already present Chernobyl fallout ^{137}Cs was not significantly affected by the chemical composition and the pH of precipitation.

2.5 Soil Structure and Texture

In natural environmental conditions, silt (0.010 mm) to clay (0.001 mm) particle size fractions in soils appeared to be responsible for radionuclide adsorption. Soil ultrasonic treatment performed by Korobova et al. (2014) showed that radionuclide retention occurs due to natural water-resistant aggregation of fine particles. However, a soil layer with aggregated fine particles and a considerable content of coarse fractions might present a smoothing effect in the radionuclide distribution in the different mass fractions. It should be pointed out that the particle size and composition of the soils, which control radionuclide sorption, are known to exhibit spatial and in-soil depth specificity.

2.6 Climate Change and Soil Management

Past soil management and climate may differ from present conditions and direct changes in water balance and temperature or indirect modification of the growth conditions for plants and the activity of soil organisms may occur. Soil characteristics, such as redox potential, water content and temperature, may vary within days or weeks, while significant changes of land use and soil organic matter content and quality happen within years to decades. The higher turnover of organic matter can result in a mobilisation of incorporated radionuclides and in an increased biological availability. Under both humid and arid conditions, erosion potentially increases by water or wind and possibly causes a wider spatial distribution of radionuclides in contaminated soil. Shifting from farm to waste land would modify soil properties and increase soil degradation, favouring radionuclide mobility.

Higher temperature and increased precipitation amount affect the long-term behaviour of radionuclides in soil as well as all soil processes which are thereby accelerated. Increasing temperature combined with increasing aridity causes reduced decomposition of organic matter and slower weathering processes, thus decreasing the mobilisation of radionuclides. On the other hand, at low temperature and enhanced humidity, the degradation of organic matter is reduced, and radionuclide absorption to the organic soil fraction potentially increased. Also, radionuclide mobility in soil can increase with higher soil acidity (pH value tends to decrease) inducing more potential root uptake or a potential loss of radionuclides to deeper soil layers. Higher mobility and potential bioavailability of ^{137}Cs was found by Kovacheva et al. (2014a) in two different soil types (a luvisol and a cambisol) in soil drought and frozen experimental conditions. Kovacheva and Djingova (2014) showed that the freezing, following the radionuclide contamination of chernozem soil, causes an increase of the amount of potentially mobile forms of radiocobalt, radiocaesium, radium and thorium, having an insignificant impact on the fractionation of americium and uranium (Kovacheva et al. 2014b).

3 Behaviour of Key Specific Artificial Radionuclides in Soil

3.1 Caesium

^{137}Cs is an artificial radionuclide with long half-life ($T_{1/2} = 30.05$ years) (LNHB 2008), occurring in the natural environment predominantly as Cs(I). It was generated into atmosphere as a fission product after nuclear accidents (e.g. Chernobyl) and past nuclear weapon tests (IAEA 2006). Depending on latitude, the global release of ^{137}Cs from weapons' fallout ranged from 160 to 3200 Bq m^{-2} (UNSCEAR 1969). The total amount deposited on the European territory at the beginning of the 1980s was estimated at 20 PBq (De Cort et al. 1998). The release of ^{137}Cs following the Chernobyl accident is estimated to be 85 PBq, from which

70 PBq was deposited in the Northern Hemisphere (UNSCEAR 2000). The heterogeneity of the Chernobyl radionuclide fallout was mainly related to the presence or absence of rainfall during the radioactive cloud passage.

Caesium-137 is the most widely investigated artificial radionuclide, being the first radiotracer applied to study soil and sediment agro-environmental redistribution and related impacts (IAEA 2014b; Mabit et al. 2008; Ritchie and McHenry 1990). Several studies have been conducted to verify the adsorption pattern of ^{137}Cs by soil particles, not only with the aim of using caesium as radiotracer but also to investigate the nuclide's chemical properties and its impact on the food chain contamination following the accidental nuclear release (Cornell 1993; Voigt and Fesenko 2009). It has been demonstrated that ^{137}Cs sorption is related to soil physico-chemical characteristics such as clay content, pH, organic matter, redox potential and potassium availability (Schuller et al. 1988). After its initial fallout at the soil surface, ^{137}Cs is rapidly (Cornell 1993) and strongly adsorbed to soils with well-known cation exchange characteristics such as illite, montmorillonite and zeolites (Atun and Kilislioglu 2003; Matisoff and Whiting 2011). It has been demonstrated that ^{137}Cs sorption pattern is highly efficient for clay minerals and less so for sandy loam soils (Giannakopoulou et al. 2007; Livens and Loveland 1988). However, all mineral soils have the capacity to adsorb caesium, though in differing fractions (Livens and Baxter 1988). Korobova and Chizhikova (2007) showed that amorphous and labile iron forms have a significant role in the migration and fixation of ^{137}Cs in the secondarily contaminated horizons of some Russian alluvial soils.

The maximum sorption of caesium was found for pH 8 (Giannakopoulou et al. 2007). At low pH values, caesium sorption is relatively low for all soils, and thus, the acidification of soils can cause ^{137}Cs desorption and a greater mobility (Giannakopoulou et al. 2007). However, this situation is unlikely to occur for most agricultural soils. Several authors (Chibowski and Zygmunt 2002; Staunton et al. 2002) reported that organic matter has a low affinity for caesium retention, and thus adsorption issues can be related with organic soils.

Potassium and ammonium concentrations as well as stable Cs in soil can influence the sorption of ^{137}Cs (Shenber and Eriksson 1993). Carvalho et al. (2006) suggested a common accumulation mechanism for Cs and K ions, being in direct competition for the uptake of nutrients by plants. Moreover, redox conditions may promote the production of NH_4^+, competing ^{137}Cs for selective retention sites and thus leading to a release of ^{137}Cs in the environment (Dion et al. 2005). High concentrations of NH_4^+ under anaerobic redox conditions ($<$ -200 mV) can result in increases in water-soluble ^{137}Cs and increases in the activities of ^{137}Cs bound on nonselective clay sites (Pardue et al. 1989). Observations of anaerobic oxidation of methane (CH_4) in surface soils with fluctuating redox conditions are scarce, although a few independent studies have been conducted for surface peat lands as well as for forested soils.

Factors required to predict plant uptake of ^{137}Cs are soil clay content, exchangeable K status, pH, NH_4 concentration and organic matter content, as well as the effect of time on radiocaesium fixation (Absalom et al. 2001). Transfer of radiocaesium from soil to plants also depends to a large extent on its soil concentration at the plant root depth (Pietrzak-Flis et al. 1996). High uptake of Cs (i.e. 10–15 %) has been reported in soils where sands or kaolinites dominate the ion exchange complex (Cummings et al. 1969) as well as in organic soils (Van Bergeijk et al. 1992). Nutrient deficiency (e.g. K) and the predominance of kaolinite and gibbsite in the clay fraction also conducted to higher values of ^{137}Cs transfer factors (Wasserman et al. 2002). Moreover, the uptake of ^{137}Cs by plants was found to be negatively correlated with the soil organic matter content (Van Bergeijk et al. 1992), as the large cation exchange capacity of organic matter and the presence of organic substances around clay particles would prevent adsorption and subsequent fixation of ^{137}Cs on the clay minerals. The rate of ^{137}Cs uptake by plants appeared to be higher with fast-growing species (Broadley et al. 1999).

The strong adsorption characteristic of caesium is represented by the low rate of vertical migration for the most types of soils (Matisoff et al. 2002; Van der Perk et al. 2002). Transport velocities of about 1 cm y^{-1} indicate that a major fraction of the initially deposited fallout may remain within the rooting zone for a long time period. Bossew and Kirchner (2004) determined the parameters describing the radionuclide's mobility in soil after deposition (the transport velocities and diffusion coefficients of ^{137}Cs) for several soil profiles from Austria and grouped these coefficients with regard to soil types. They found that parameter variability had small variations within soil groups and highlighted that caesium mobility generally increased in the following order: humic soils < podzols < brown earths, chernozems.

Typical depth profiles of ^{137}Cs in undisturbed landscape present a sharp decline in caesium activity with increasing depth with more than 75 % of the total inventory located in the top 15 cm (Belyaev et al. 2005; Iurian et al. 2013; Mabit et al. 2010). A typical example of the vertical distributions of the ^{137}Cs in undisturbed soil is presented in Fig. 1. This specific shape of the depth profile fully supports the assumption of the adsorption and fixation of fallout caesium by most mineral soils. However, some studies have highlighted considerable changes of migration rates with time. Heavy rainfall during the deposition phase may result in initial migration rates with infiltrating water of 2 cm h^{-1} (Schimmack et al. 1989).

In tilled soils, the radionuclide depth profile exhibits relatively uniform concentration over the plough depth (Matisoff et al. 2002). Ploughing of agricultural soils will mix soils to depths of 10–30 cm, and the radionuclide depth profile will remain homogeneous in time within the soil profile, as ^{137}Cs has no current input.

3.2 *Plutonium and Americium*

Concern arises from the very long physical and biological half-lives and the high radiotoxicity values of transuranium elements in the environment. The behaviour of these radionuclides has been less studied in comparison with ^{137}Cs, even if ^{241}Am (decay product of ^{241}Pu) is becoming one of the major transuranium elements in the

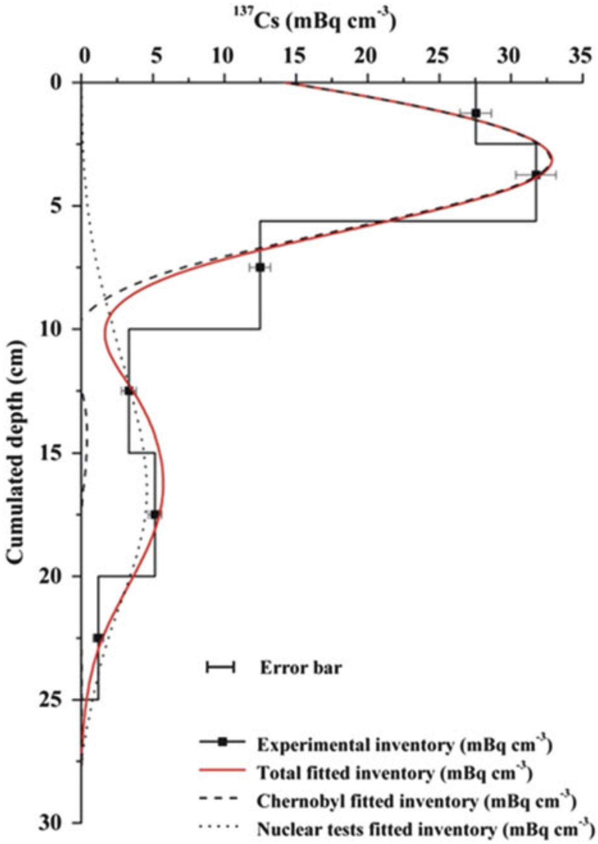

Fig. 1 Experimental depth distribution of ^{137}Cs in undisturbed site (Romania). Chernobyl and the nuclear tests fitting curves were obtained by applying the convection–diffusion equation (*error bars* represent the uncertainty of the gamma-ray spectrometric measurements at 2σ confidence limit) (Iurian et al. 2014; with permission from Elsevier)

areas affected by Chernobyl fallout. About 0.12 PBq of $^{239,240}Pu$ and 0.0028 PBq of ^{238}Pu have been produced and distributed globally (Hardy et al. 1973). Another 0.005 PBq of ^{238}Pu was released by the accidental burning of the satellite SNAP-9A (Hardy et al. 1973).

Plutonium can exist in four oxidation states, III, IV, V and VI, while americium can occur only as Am(III). The III and IV states of Pu may be present as simple hydrated cations, while V and VI form linear dioxo species (Choppin 1988). The redox speciation of plutonium is complicated by effects such as hydrolysis, complexation, disproportionation, solubility, redox interchange reactions and reduction by organic complexants (Choppin et al. 1997).

Sequential extractions showed that Pu has a high affinity for organic matter and metal oxides in soil, even if the organic matter content is low (Bunzl et al. 1995a, 1998; Lee and Lee 2000; Livens and Baxter 1988). Americium is also retained by organic matter, oxides and minerals in soil (Bunzl et al. 1995a) but to a lesser extent than Pu as more Am can be found in soluble and exchangeable form in soil (Bunzl et al. 1995a; Goryachenkova et al. 2009; Ibrahim and Salazar 2000). In general, transuranic elements form soluble complexes with high-molecular components of soil humus and with Fe, Al and Ca (Sokolik et al. 2001), thus resulting in a reduced content of their mobile forms in soil. Many authors reported high retention of Pu by the soil organic matter (Kim et al. 1998; Komosa 1999); a slow migration of Pu and Am in soils with high organic content attributed to complexation reactions with soil organic substances (Bunzl et al. 1995b). Moreover, owing to the large surface area of clay which allows Pu to bind strongly to the soil, Kim et al. (1998) presented a positive correlation between clay content and concentration of Pu in soil.

It is assumed that the specific behaviour of radionuclides in soil can be attributed to their low concentrations in the environment, insufficient for formation of their own phase and specific entrance forms (Pavlotskaya 2002). Humus and low molecular weight are significantly involved in the mobility of radionuclides. Pu and Am appear to be associated with low-mobile humates and fulvates of Ca, Fe and Al and poorly soluble humin (residue), Pu being more strongly bound to humates as compared to Am in chernozem and soddy–podzolic soil (Goryachenkova et al. 2009). Fujikawa et al. (1999) related that 5–10 % of Pu in the soil was associated with humic acid and 1 % with fulvic acid, whereas Livens and Singleton (1991) found that radionuclides concentrations are four to five times higher in the humic acid than in the fulvic acid fractions. Evidence has been also presented to suggest that Pu was less concentrated than Am in the lower molecular weight fractions.

Actinides show more affinity for the fine particle size fraction, being retained on the surface coating of soil (Eakins et al. 1990). Goryachenkova et al. (2009) found that in aqueous extracts, from 60 to 100 % of the radionuclides and organic carbon were associated with fine colloidal particles (<0.05 µm), Pu and Am being retained by particles of various sizes. Therefore, different rates and mechanisms of Pu and Am migration in soils could be expected. Higher Pu concentrations were found with decreasing soil particle sizes, while the values for Am seemed to be more scattered.

The number of anaerobic bacteria in soil might be another factor which affects the mobility of Pu in soil layers (Mahara and Kudo 1998). The mobility of actinides in soil systems can be influenced by microorganisms through redox reactions, pore water chemistry regulation and degrading organic ligands that can complex radionuclides and through biosorption (Panak and Nitsche 2001).

Similar to ^{137}Cs, Pu depth distribution in soil is limited to the first top layers. ^{239,240}Pu migration rates were found in a range from 0.29 cm y^{-1} in podzols to 0.58 cm y^{-1} in fluvisols in Lublin region (Poland), depending on soil type (Orzeł and Komosa 2014). The migration of nuclear test derived plutonium and Chernobyl-originated plutonium showed no significant difference in Russian soils (Pavlotskaya et al. 1991). In general, the upper 10 cm of soils contain the most Pu. While the Pu movement into the rooting zone of the soil column may increase its availability for plant uptake, its downward movement will reduce resuspension (Harley 1980). Several authors reported a greater vertical migration of Am in comparison with Pu (Bunzl et al. 1992; Jia et al. 1999; Sokolik et al. 2001). Moreover, Watters et al. (1983) showed that the main contamination pathway of vegetation is the direct atmospheric deposition of Pu, which contributes ten times more to the plant contamination than does the transfer from soil through roots.

3.3 Strontium

The long-lived radioactive isotope ^{90}Sr is one of the most hazardous pollutants for human beings, known as having high contribution to the internal exposure dose. Soil high exchange capacity, total amount of Ca and Mg, pH, mechanical makeup and organic carbon content are the main factors involved in the mobility behaviour of ^{90}Sr (Fedorkova et al. 2012). Similar mechanisms between Ca and ^{90}Sr for nutrient plant uptake and a deficiency in the Ca soil content can possibly lead to higher transfer factors of ^{90}Sr from soil to plants. Keeping in mind that 40–60 % of this radionuclide in a wide range of soil types has an exchangeable chemical form; its higher migration in soils was found to be associated with fulvic acids and other low-molecular-weight organic substances (Generalova and Onoshko 2006). Fulvic acids can absorb between 25 and 35 % of ^{90}Sr from soil. Fedorkova et al. (2012) found that only 18–24 % of radioactive strontium is associated with high molecular fraction ($M > 500$ g mol^{-1}) in chernozems, chestnut soil and peat soil. Around 33–34 % of ^{90}Sr was found in association with mineral compounds ($M < 180$ g mol^{-1}) in soddy–podzolic soil and light grey forest soil (Fedorkova et al. 2012).

A limited number of data are available on the vertical migration of radionuclides other than ^{137}Cs in soil. Herranz et al. (2011) determined the mean values of apparent convection velocity (i.e. 0.20 cm y^{-1}) and apparent diffusion coefficient (i.e. 3.67 cm^2 y^{-1}) for ^{90}Sr by using a convective–diffusive model for the vertical migration of the radionuclide in Spanish mainland soils. The comparison made by the authors between the migration behaviours of ^{90}Sr and ^{137}Cs showed that ^{137}Cs migrates around 57 % of the depth migrated by ^{90}Sr. In two Spanish Mediterranean pinewood ecosystems, Guillén et al. (2015) found similar migration velocities for ^{90}Sr and ^{239,240}Pu, both higher than that of ^{137}Cs. Moreover, sequential speciation procedures showed that ^{90}Sr is characterised by higher bioavailability than ^{239,240}Pu and ^{137}Cs, explaining the different velocities between ^{90}Sr and ^{137}Cs. Although limited number of experiments is related to the mobility of radionuclides and sorption in soils, data confirmed that the migration rates decrease in the following order: Sr > Cs > Pu, Am (Kirchner et al. 2009).

4 Natural Radionuclides

From the human health safety point of view, it is important to study and understand the behaviour of uranium series radionuclides in the environment. Enhanced radioactivity levels may be associated with residues of uranium mining and milling, uranium processing, phosphate mining, heavy metal mining, coal use, inappropriate radioactive waste disposal, uncontrolled nuclear weapon tests, oil and gas extraction/transport/storage, ashes from coal burning and slag from ore-smelting industries. However, it is important to bear in mind that while uranium is a radioactive element, it is also a heavy metal whose principal effect on human health is through chemotoxic action on the kidneys. Because of the low radiological risk relative to the chemotoxic risk, uranium is usually managed as a chemically toxic species.

4.1 Uranium

Most rocks and soils contain uranium in concentrations of 1–10 mg kg^{-1}, being mobilised by the weathering of uranium-bearing minerals like uraninite, coffinite, pitchblende, carnotite, etc. Oxidative dissolution of mineral to the soluble uranyl ion (UO_2^{2+}) can be produced by the action of water. Uranium occurs in valences of III, IV, V and VI, from which the valences IV and VI are the most common under soil conditions. The oxidation of organic matter or iron in the soil provides uranium IV valence state, strongly adsorbed by soil particles into stable complexes (e.g. hydroxides, hydrated fluorides and phosphates) immobile in soils (Ravi et al. 2014). U(IV) is rather insoluble, whereas U(VI) has a high solubility which can be complexed by fluoride, sulphate, carbonate as well as phosphate. U(IV) is predominant in soils with high water content at E_h <200 mV, while U (VI) dominates in sufficiently aerated soils.

There are only scarce investigations related to the speciation of uranium in soils. Available data shows that the mobility and bioavailability of uranium is influenced by the oxidation (oxygen content), carbonate content (organic material content, pH, parent material, weathering) and cation exchange capacity (texture, clay content, organic matter, pH). Sheppard and Evenden (1987) showed that the uranium retention in soils increases with higher soil cation exchange capacity, while the uranium mobility is increased by the presence of carbonate, through the formation of anionic U and CO_3 complexes. At low pH values ($pH < 3$), uranium has a low sorption by soils, while for pH ranging from 5 to 7, the sorption is maximum and decreases again at pH above 7, due to the increasing number of negatively charged binding sites available on mineral surfaces, such as iron oxides and aluminium oxides (EPA 1999). Under acidic conditions ($pH < 6$), U(VI) is complexed by carbonate increases favouring uranium mobility in soil (Elless and Lee 1998).

Different sorption reactions are involved in the dynamic of uranium in soil. The formation of organic complexes and colloids in the presence of organic matter will increase the uranium mobility in soils, while at the same time, a decrease in mobility is possible through sorption by exchange. In the absence of carbonates, the presence of iron oxides/hydroxides is associated with uranium adsorption (EPA 1999). There is competition between the sorption to Fe/Al oxides and hydroxides and the complexation of uranium (Koch-Steindl and Pröhl 2001). Considering all the factors involved in uranium behaviour in soils, the maximum uranium concentrations were found at alkaline pH, high inorganic carbon content and low cation exchange capacity, organic matter content, clay content, amorphous iron and phosphate levels Vandenhove et al. (2007). More detailed information can be found in the review of Mitchell et al. (2013).

Kovacheva et al. (2014a) discussed the influence of climatic impacts on the uranium behaviour in soils. The redistribution of U between the carbonates and organic matter, causing its immobilisation, appeared during prolonged soil drought conditions. Moreover, a sharp increase in the temperature favoured the increase of the potential mobility of uranium in frozen soil, while the redistribution of uranium between the soil phases of chernozem soil occurred during the warming and the enhanced humidity of the dry soil.

Soil microorganisms can influence uranium mobility through sorption or incorporation. Sulphate or iron-reducing bacteria may enzymatically reduce or precipitate U(VI) to U(IV) at $E_h < -100$ mV (Lovley and Philips 1992). This can happen in conditions of high soil moisture (e.g. after flooding or heavy rainfalls). An enhanced uranium mobility in the rooting zone may also occur in the presence of organic compounds able to complex iron (siderophores) (Marschner 1995), which may act as complexing agents for uranium as well (Braithwaite et al. 1997).

Uranium migration in soil is a long-term process (a few months) and has two possible pathways: upwards, in the case of water deficit, and downwards, as a result of leaching (Sheppard et al. 1984). Moreover, the same authors found that uranium migration was higher in sandy soils as compared to loamy soils, as evidence of the radionuclide affinity for fine particle size fraction of soil.

4.2 Thorium

Thorium exists only as Th(IV) valence state and it is known to be insoluble in water (EPA 1999). ^{232}Th represents more than 99 % of natural thorium. The mobility and bioavailability of thorium is highly dependent on soil properties (Guo et al. 2008). In acidic soil conditions, the exchangeable Th fraction is increasing due to the decomposition of resistant minerals favouring the enhancement of ThO_2 solubility (Langmuir and Herman 1980). Under strong alkaline conditions, the amount of thorium adsorbed by soil organic matter is released and then rapidly bound to carbonates (Guo et al. 2008). Thorium maximum absorption on clays, oxides and organic matter occurs at pH value of 6.5 (Syed 1999). However, an analysis performed by Sheppard et al. (2009) found only a weak correlation between thorium K_d values and pH.

The affinity to the adsorption sites of organic matter is higher for some thorium hydroxides, such as $Th(OH)_2{}^{2+}$ and $Th(OH)_3{}^{+}$ in a pH range from 2 to 5 (Guo et al. 2008). Moreover, organic matter appears to control the adsorption of reactive Th even at soil depths characterised by low content organic matter (0.8 %) (Ahmed et al. 2014). Thorium associated with humic acids is partially released to aqueous solution or coprecipitated with Fe/Mn hydroxides at pH above 3.5, owing that humic acids are soluble in these pH conditions (Chen and Wang 2007).

The K_d values reported in the existing literature for Th indicate that most soil types absorb and retain this radionuclide; currently, only scarce data are available regarding the study of thorium behaviour in soil and further investigations are still required. Vandenhove et al. (2009a) observed that geometric mean of K_d(Th) is low for sand and organic soils and higher for loam soils, while large variability (from 2 to 4 orders of magnitude) was registered within each soil group. The authors proposed that future K_d categorization to be performed on the pH basis.

Studying the particle size effect on Th availability for plant uptake, Vandenhove et al. (2009b) found the lowest TF results for organic soils, while no significant differences were registered for sand, loam and clay soils, though the TF values for Th were about tenfold lower in comparison with U, Ra and Pb.

4.3 Radium

Radium (Ra) is commonly present in naturally occurring radioactive materials (NORM), contributing to the human dose at longer timescales (Vandenhove and Van Hees 2007). It is an alkali earth element, and in its natural form, Ra is present as a divalent cation competing with other alkaline cations for sorption sites in soils (Vandenhove et al. 2009a). Its affinity with other elements for ion exchange has been established as following: $Ra^{2+} > Ba^{2+} > Sr^{2+} > Ca^{2+} > Mg^{2+}$ (EPA 2004). The low ability of Ca^{2+} and Mg^{2+} to replace Ra^{2+} is possibly caused by the differences in ionic size (Simon and Ibrahim 1990). Vandenhove and Van Hees (2007) found an increase in the radium K_d with increased soil sorption capacity (CEC) and a decrease with the concentration of competitive ions in the soil solution.

Organic matter and clays were showed to be the main factors contributing to the sorption of radium onto soil, although organic matter absorbs ten times more radium in comparison with clay (Simon and Ibrahim 1990). Similar conclusions were also drawn from the studies of Vandenhove and Van Hees (2007) and Sheppard et al. (2005), which suggested that radium sorption is highly correlated to the organic matter content, but yet not affected by soil granulometry. Thus, authors recommended that future classification of K_d for radium in soil should not be performed based on soil particle size distribution (Vandenhove and Van Hees 2007). However, they could not suggest a more suitable parameter (e.g. pH, CEC, OM) for classifying K_d values. Vandenhove et al. (2009a) indicated that a better soil characterisation is necessary in order to be able to fully understand the processes governing radium sorption and the main soil parameters involved in these processes. On the other hand, Blanco Rodríguez et al. (2008) observed a decrease in the activity concentration of radium as the particle size increased, with the greater content of the available fraction in the finest soil material.

In soil, published data (EPA 2004) show that at pH $\geq$ 7 radium is strongly absorbed to clays and mineral oxides. However, Vandenhove and Van Hees (2007) did not find a significant pH effect on Ra uptake. They concluded that radium mobility or transfer from soil to crops cannot be predicted using a single K_d or TF value for a certain soil group, as large variability of data has been reported in the existing studies.

5 Conclusions

There is an urgent need for an improved understanding of radionuclide mobility in a wide range of soils under various climatic conditions. Even if detailed information exist for specific radionuclides (e.g. caesium, uranium, plutonium) and progress has been made in the last decades to address this issue, it is expected that in the coming decade, the general knowledge will increase in order to include a wider number of radionuclides, especially after the Fukushima Daiichi nuclear power plant accidental releases in 2011.

Existing data show that by changing different soil properties and environmental conditions, radionuclides can be converted from a potential mobile form to an immobile one or vice versa, having a direct effect on plant uptake. The soil redox potential, the pH, the content and composition of the organic matter and the sorption to mineral soil constituents represent the main factors controlling the chemical form of radionuclides in soil. Thus, the collection of detailed information on the history of soil development, as well as on specific soil characteristics and land use in different climatic regions with various geological substrates, may be helpful to better characterise radionuclide behaviour in soil for efficient soil remediation strategies.

References

Absalom JP, Young SD, Crout NMJ, Sanchez A, Wright SM, Smolders E, Nisbet AF, Gillett AG (2001) Predicting the transfer of radiocaesium from organic soils to plants using soil characteristics. J Environ Radioact 52:31–43

Ahmed H, Young SD, Shaw G (2014) Factors affecting uranium and thorium fractionation and profile distribution in contrasting arable and woodland soils. J Geochem Explor 145:98–105

ANS (2012) Fukushima Daiichi: ANS committee report. American Nuclear Society, LaGrange Park, IL

Atun G, Kilislioglu AO (2003) Adsorption behavior of cesium on montmorillonite-type clay in the presence of potassium ions. J Radioanal Nucl Chem 258:605–611

Baeza A, Paniagua JM, Rufo M, Barandica J, Sterling A (1999) Dynamics of ^{90}Sr and ^{137}Cs in a soil-plant system of a Mediterranean ecosystem. Radiochim Acta 85:137–141

Belyaev VR, Wallbrink PJ, Golosov VN, Murray AS, Sidorchuk AY (2005) A comparison of methods for evaluating soil redistribution in the severely eroded Stavropol region, southern European Russia. Geomorphology 65:173–193

Blanco Rodríguez P, Vera Tomé F, Lozano JC, Pérez-Fernández MA (2008) Influence of soil texture on the distribution and availability of ^{238}U, ^{230}Th, and ^{226}Ra in soils. J Environ Radioact 99:1247–1254

Bossew P, Kirchner G (2004) Modelling the vertical distribution of radionuclides in soil. Part 1: the convection–dispersion equation revisited. J Environ Radioact 73:127–150

Boudreau P (1986) Mathematics of tracer mixing in sediments: I. Spatially dependent, diffusive mixing. Am J Sci 286:161–169

Braithwaite A, Livens FR, Richardson S, Howe MT, Goulding KWT (1997) Kinetically controlled release of uranium from soils. Eur J Soil Sci 48:661–673

Broadley MR, Willey NJ, Philippidis C, Dennis ER (1999) A comparison of caesium uptake kinetics in eight species of grass. J Environ Radioact 46:225–236

Bundt M, Albrecht A, Froidevaux P, Blaser P, Fluhler H (2000) Impact of preferential flow on radionuclide distribution in soil. Environ Sci Technol 34:3895–3899

Bunzl K, Kracke W, Schimmack W (1992) Vertical migration of plutonium-239+240, americium-241 and caesium-137 fallout in a forest soil under spruce. Analyst 112:469–474

Bunzl K, Flessa H, Kracke W, Schimmack W (1995a) Association of fallout $^{239+240}$Pu and ^{241}Am with various soil components in successive layers of a grassland soil. Environ Sci Technol 29:2513–2518

Bunzl K, Kracke W, Schimmack W, Auerswald K (1995b) Migration of fallout $^{239+240}$Pu, ^{241}Am and ^{137}Cs in the various horizons of a forest soil under pine. J Environ Radioact 28:17–34

Bunzl K, Kracke W, Schimmack W, Zelles L (1998) Forms of fallout ^{137}Cs and $^{239+240}$Pu in successive horizons of a forest soil. J Environ Radioact 39:56–68

Bunzl K, Schimmack W, Zelles L, Albers BP (2000) Spatial variability of the vertical migration of fallout ^{137}Cs in the soil of a pasture, and consequences for long-term predictions. Radiat Environ Biophys 39:197–205

Carvalho FP (2011) Environmental radioactive impact associated to uranium production. Am J Environ Sci 7:547–553

Carvalho C, Anjos RM, Mosquera B, Macario K, Veiga R (2006) Radiocesium contamination behavior and its effect on potassium absorption in tropical or subtropical plants. J Environ Radioact 86:241–250

Chen VL, Wang XK (2007) Influence of pH, soil humic/fulvic acid, ionic strength and foreign ions on sorption of thorium(IV) onto γ-Al2O3. Appl Geochem 22:436–445

Chibowski S, Zygmunt J (2002) The influence of the sorptive properties of organic soils on the migration rate of ^{137}Cs. J Environ Radioact 61:213–223

Choppin G (1988) Chemistry of actinides in the environment. Radiochim Acta 43:82–83

Choppin GR, Bond AH, Hromadka PM (1997) Redox speciation of plutonium. J Radioanal Nucl Chem 219:203–210

Cornell RM (1993) Adsorption of cesium on minerals: a review. J Radioanal Nucl Chem 171:483–500

Cummings SL, Bankert L, Garrett AR Jr, Regnier JE (1969) Cs uptake by Oat plants as related to the soil fixing capacity. Health Phys 171:145–148

De Cort M, Dubois G, Fridman SD, Germenchuk MG, Izrael YA, Janssens A, Jones AR, Kelly GN, Kvasnikova EV, Matveenko II, Nazarov IM, Pokumeiko YM, Sitak VA, Stukin ED, Tabachny LY, Tsaturov YS, Avdyshin SI (1998) Atlas of caesium deposition on Europe after the chernobyl accident. EUR Report 16733. EC, Office for Official Publications of the European Commission Communities, Luxembourg

Dion HM, Romanek CS, Hinton TG, Bertsch PM (2005) Cesium-137 in floodplain sediments of the lower three runs creek on the DOE Savannah River site. J Radioanal Nucl Chem 264:481–488

Eakins JD, Morgan A, Baston GMN, Pratley FW, Strange LP, Burton PJ (1990) Measurements of α-emitting plutonium and americium in the intertidal sands of west Cumbria, UK. J Environ Radioact 11:37–54

Ehlken S, Kirchner G (2002) Environmental processes affecting plant root uptake of radioactive trace elements and variability of transfer factor data: a review. J Environ Radioact 58:97–112

Elless MP, Lee SY (1998) Uranium solubility of carbonate rich uranium-contaminated soils. Water Air Soil Pollut 107:147–162

EPA-United States Environmental Protection Agency (1999) Understanding variation in partition coefficient K_d values Volume II: Review of geochemistry and available K_d values for cadmium, cesium, chromium, lead, plutonium, radon, strontium, thorium, tritium (^{3}H) and uranium. US Environmental Protection Agency, Report US EPA 402-R-99-004B, Washington DC

EPA-United States Environmental Protection Agency (2004) Understanding variation in partition coefficient K_d values Volume III: Review of geochemistry and available K_d values for americium, arsenic, curium, iodine, neptunium, radium, and technetium. US Environmental Protection Agency, Report US EPA 402-R-04-002C, Washington DC

Fedorkova MV, Pakhnenko EP, Sanzharov NI (2012) Chemical forms of radioactive strontium interaction with organic matter of different soil types. Moscow Univ Soil Sci Bull 67:133–136

Froehlich K, Masarik J (2009) Radionuclides as tracers and timers of processes in the continental environment—basic concepts and methodologies. In: Froehlich K (ed) Environmental radionuclides, vol 16. Elsevier, Amsterdam

Fujikawa Y, Zheng J, Cayer I, Sugahara M, Takigami H, Kudo A (1999) Strong association of fallout plutonium with humic and fulvic acid as compared to uranium and ^{137}Cs in Nishiyama soil from Nagasaki, Japan. J Radioanal Nucl Chem 240:69–74

Generalova VA, Onoshko MP (2006) Effect of humus acids on migration of radiostrontium and radiocesium in valley deposits of the Sozh River. Radiochemistry 48:99–104

Giannakopoulou F, Haidouti C, Chronopoulou A, Gasparatos D (2007) Sorption behavior of cesium on various soils under different pH levels. J Hazard Mater 149:553–556

Goryachenkova TA, Kazinskaya IE, Kuzovkina EV, Novikov AP, Myasoedov BF (2009) Association of radionuclides with colloids in soil solutions. Radiochemistry 51:201–210

Guillén J, Baeza A, Corbacho JA, Munoz-Munoz JG (2015) Migration of ^{137}Cs, ^{90}Sr, and $^{239+240}Pu$ in Mediterranean forests: influence of bioavailability and association with organic acids in soil. J Environ Radioact 144:96–102

Guo P, Duan T, Song X, Xu J, Chen H (2008) Effects of soil pH and organic matter on distribution of thorium fractions in soil contaminated by rare-earth industries. Talanta 77:624–627

Hardy EP, Krey PW, Volchock HL (1973) Global inventory and distribution of fallout plutonium. Nature 241:444–445

Harley JH (1980) Plutonium in the environment—a review. J Radiat Res 21:83–104

Herranz M, Romero LM, Idoeta R, Olondo C, Valiño F, Legarda F (2011) Inventory and vertical migration of ^{90}Sr fallout and $^{137}Cs/^{90}Sr$ ratio in Spanish mainland soils. J Environ Radioact 102:987–994

IAEA (1994) Handbook of parameter values for the prediction of radionuclide transfer in temperate environments. IAEA Technical Reports Series No. 364. Vienna, Austria

IAEA (2006) Environmental consequences of the chernobyl accident and their remediation: twenty years of experience. Report of the Chernobyl forum expert group 'Environment'. Assessment Reports Series, ISSN 1020–6566, Vienna, Austria

IAEA (2010) Handbook of parameter values for the prediction of radionuclide transfer in terrestrial and freshwater environments. IAEA Technical Reports Series No. 472. International Atomic Energy Agency, Vienna, Austria. http://www-pub.iaea.org/MTCD/publications/PDF/trs472_web.pdf. Accessed March 2015

IAEA (2014a) Handbook of parameter values for the prediction of radionuclide transfer to wildlife. IAEA Technical Reports Series No. 479. Vienna, Austria. http://www-pub.iaea.org/books/IAEABooks/10514/Handbook-of-Parameter-Values-for-the-Prediction-of-Radionuclide-Transfer-to-Wildlife. Accessed April 2015

IAEA (2014b) Guidelines for using Fallout radionuclides to assess erosion and effectiveness of soil conservation strategies. IAEA-TECDOC-1741. Vienna, Austria. http://www-pub.iaea.org/books/IAEABooks/10501/Guidelines-for-Using-Fallout-Radionuclides-to-Assess-Erosion-and-Effectiveness-of-Soil-Conservation-Strategies. Accessed April 2015

Ibrahim SA, Salazar WR (2000) Physicochemical speciation of americium in soils from Rocky Flats, Colorado, USA. J Radioanal Nucl Chem 243:347–351

Iurian AR, Mabit L, Begy R, Cosma C (2013) Comparative assessment of erosion and deposition rates on cultivated land in the Transylvanian Plain of Romania using ^{137}Cs and $^{210}Pb_{ex}$. J Environ Radioact 125:40–49

Iurian AR, Mabit L, Cosma C (2014) Uncertainty related to input parameters of ^{137}Cs soil redistribution model for undisturbed fields. J Environ Radioact 136:112–120

Jia G, Testa C, Desideri D, Guerra F, Meli MA, Roselli C, Belli ME (1999) Soil concentration, vertical distribution and inventory of plutonium, ^{241}Am, ^{90}Sr and ^{137}Cs in the Marche region of central Italy. Health Phys 77:52–61

Kim CS, Lee MH, Kim CK, Kim KH (1998) ^{90}Sr, ^{137}Cs, $^{239+240}Pu$, ^{238}Pu concentrations in surface soils of Korea. J Environ Radioact 40:75–88

Kirchner G (1998a) Applicability of compartmental models for simulating the transport of radionuclides in soil. J Environ Radioact 38:339–352

Kirchner G (1998b) Modelling the migration of fallout radionuclides in soil using a transfer function model. Health Phys 74:80–85

Kirchner G, Strebl F, Bossew P, Ehlken S, Gerzabek MH (2009) Vertical migration of radionuclides in undisturbed grassland soils. J Environ Radioact 100:716–720

Koch-Steindl H, Pröhl G (2001) Considerations on the behaviour of long-lived radionuclides in the soil. Radiat Environ Biophys 40:93–104

Komosa A (1999) Migration of plutonium isotopes in forest soil profiles in Lublin region (Eastern Poland). J Radioanal Nucl Chem 240:19–24

Korobova EM, Chizhikova NP (2007) Distribution and mobility of radiocesium in relation to the clay fraction mineralogy and soil properties in the Iput River floodplain. Euras Soil Sci 40:1062–1075

Korobova EM, Linnik VG, Chizhikova NP, Alekseeva TN, Shkinev VM, Brown J, Dinu MI (2014) Granulometric and mineralogic investigation for explanation of radionuclide accumulation in different size fractions of the Yenisey floodplain soils. J Geochem Explor 142:49–59

Kovacheva P, Djingova R (2014) Influence of freezing on physicochemical forms of natural and technogenic radionuclides in Chernozem soil. Chem Paper 68:714–718

Kovacheva P, Slaveikova M, Todorov B, Djingova R (2014a) Influence of temperature decrease and soil drought on the geochemical fractionation of ^{60}Co and ^{137}Cs in fluvisol and cambisol soils. Appl Geochem 50:74–81

Kovacheva P, Mitsiev S, Djingova R (2014b) Physicochemical fractionation of americium, thorium, and uranium in Chernozem soil after sharp temperature change and soil drought. Chem Paper 68:336–341

Langmuir D, Herman JS (1980) The mobility of thorium in natural waters at low temperatures. Geochim Cosmochim Acta 44:1753–1766

Lee MH, Lee CW (2000) Association of fallout-derived ^{137}Cs, ^{90}Sr and $^{239,240}Pu$ with natural organic substances in soils. J Environ Radioact 47:253–262

Livens FR, Baxter MS (1988) Chemical association of artificial radionuclides in Cumbrian soils. J Environ Radioact 7:75–86

Livens FR, Loveland PJ (1988) The influence of soil properties on the environmental mobility of cesium in Cumbria. Soil Use Manage 4:69–75

Livens FR, Singleton DL (1991) Plutonium and americium in soil organic matter. J Environ Radioact 13:323–339

LNHB (Laboratoire National Henri Becquerel) (2008) LARA Database, CEA-R-6201, ISSN 0429–3460, http://laraweb.free.fr/. (last accessed January 2015)

Lovley DR, Philips EJP (1992) Reduction of uranium by *Desulfovibrio desulfuricans*. Appl Environ Microbiol 58:850–856

Mabit L, Benmansour M, Walling DE (2008) Comparative advantages and limitations of Fallout radionuclides (^{137}Cs, ^{210}Pb and ^{7}Be) to assess soil erosion and sedimentation. J Environ Radioact 99:1799–1807

Mabit L, Martin P, Jankong P, Toloza A, Padilla-Alvarez R, Zupanc V (2010) Establishment of control site baseline data for erosion studies using radionuclides: a case study in East Slovenia. J Environ Radioact 101:854–863

Mahara Y, Kudo A (1998) Probability of production of mobile plutonium in environments of soil and sediment. Radiochim Acta 82:399–404

Marschner H (1995) Mineral nutrition of higher plants, 2nd edn. Academic, London

Matisoff G, Whiting PJ (2011) Measuring soil erosion rates using natural (^{7}Be, ^{210}Pb) and anthropogenic (^{137}Cs, ^{239,240}Pu) radionuclides. In: Baskaran M (ed) Handbook of environmental isotope geochemistry. Springer, Heidelberg, Germany

Matisoff G, Bonniwell EC, Whiting PJ (2002) Soil erosion and sediment sources in an Ohio watershed using Beryllium-7, Cesium-137, and Lead-210. J Environ Qual 31:54–61

Mitchell N, Pérez-Sánchez D, Thorne MC (2013) A review of the behaviour of U-238 series radionuclides in soils and plants. J Radiol Prot 33:R17–R48

Orzeł J, Komosa A (2014) Study on the rate of plutonium vertical migration in various soil types of Lublin region (Eastern Poland). J Radioanal Nucl Chem 299:643–649

Panak PJ, Nitsche H (2001) Interaction of aerobic bacteria with plutonium (VI). Radiochim Acta 89:499–504

Pardue JH, DeLaune RD, Patrick WH Jr, Whitcomb JH (1989) Effect of redox potential on fixation of ^{137}Cs in lake sediment. Health Phys 57:781–789

Pavlotskaya FI (2002) Specific behavior of microquantities of matter in natural processes: a case of artificial radionuclides. Geokhimiya 3:298–305

Pavlotskaya FI, Kazinskaya IY, Korobova EM, Myasoedov BF, Emelyanov VV (1991) Migration of Chernobyl plutonium in soils. J Radioanal Nucl Chem 147:159–164

Pietrzak-Flis Z, Radwan I, Rosiak L, Wirth E (1996) Migration of ^{137}Cs in soils and its transfer to mushrooms and vascular plants in mixed forest. Sci Total Environ 186:243–250

Ravi PM, Rout S, Kumar A, Tripathi RM (2014) A review of the studies on environmental transport and speciation analysis of radionuclides in India. J Radioanal Nucl Chem 300:169–175

Ritchie JC, McHenry JR (1990) Application of radioactive fallout Cesium-137 for measuring soil erosion and sediment accumulation rates and patterns: a review. J Environ Qual 19:215–233

Salbu B, Krekling T, Oughton DH (1998) Characterisation of radioactive particles in the environment. Analyst 123:843–849

Sanchez AL, Smolders E, Van den Brande K, Merckx R, Wright SM, Naylor C (2002) Predictions of in situ solid/liquid distribution of radiocaesium in soils. J Environ Radioact 63:35–47

Sanchez PA, Ahamed S, Carré F, Hartemink AE, Hempel J, Huising J, Lagacherie P, McBratney AB, McKenzie NJ, Mendonça-Santos ML, Minasny B, Montanarella L, Okoth P, Palm CA, Sachs JD, Shepherd KD, Vågen TG, Vanlauwe B, Walsh MG, Winowiecki LA, Zhang GL (2009) Digital soil map of the world. Science 325:680–681

Schimmack W, Bunzl K, Zelles L (1989) Initial rates of migration of radionuclides from the Chernobyl fallout in undisturbed soils. Geoderma 44:211–218

Schuller P, Handl J, Trumper RE (1988) Dependence of ^{137}Cs soil to plant transfer factor on soil parameters. Health Phys 55:575–577

Schuller P, Ellies A, Kirchner G (1997) Vertical migration of fallout ^{137}Cs in agricultural soils from southern Chile. Sci Total Environ 193:197–205

Shenber MA, Eriksson Å (1993) Sorption behaviour of caesium in various soils. J Environ Radioact 19:41–51

Sheppard S, Evenden W (1987) Review of effects of soil on radionuclide uptake by plants. Research report prepared for the Atomic Energy Control Board, Ottawa, Canada, March 31, INFO-0230

Sheppard MI, Thibault DH (1990) Default solid/liquid partition coefficients, K_ds, for four major soil types: a compendium. Health Phys 59:471–482

Sheppard MI, Sheppard SC, Thibault DH (1984) Uptake by plants and migration of uranium and chromium in field lysimeters. J Environ Qual 13:357–361

Sheppard MI, Tait JC, Sanipelli BL, Sheppard SC (2005) Recommended biosphere model values for radium and radon. Report No. 06819-REP-01200-10144-R00, Ontario Power generation, Toronto, Ontario

Sheppard S, Long J, Sanipelli B, Sohlenius G (2009) Solid/liquid partition coefficients (K_d) for selected soils and sediments at Forsmark and Laxemar-Simpevarp. SKB Report R-09–27

Simon SL, Ibrahim SA (1990) Biological uptake of radium by terrestrial plants. In: The Environmental Behaviour of Radium, vol. 1, IAEA. Technical Report Series, No. 310, pp. 545–599

Sokolik GA, Ivanova TG, Leinova SL, Ovsiannikova SV, Kimlenko IM (2001) Migration ability of radionuclides in soil-vegetation cover of Belarus after Chernobyl accident. Environ Int 26:183–187

Staunton S, Dumat C, Zsolnay A (2002) Possible role of organic matter in radiocaesium adsorption in soils. J Environ Radioact 58:163–173

Syed HS (1999) Comparison studies adsorption of thorium and uranium on pure clay minerals and local Malaysian soil sediments. J Radioanal Nucl Chem 241:11–4

Thørring H, Skuterud L, Steinnes E (2014) Influence of chemical composition of precipitation on migration of radioactive caesium in natural soils. J Environ Radioact 134:114–119

UNSCEAR (1969) Radioactive contamination of the environment by nuclear tests, Rep. Suppl. 13 (A/7163), United Nations Scientific Committee on the Effects of Atomic Radiation, General Assembly, 24th Session, United Nations, New York

UNSCEAR (2000) ANNEX J. Exposures and effects of the Chernobyl accident. United Nations Scientific Committee on the Effects of Atomic Radiation reports to the General Assembly of the United Nation with annexes. United Nations, New York, pp 453–566

Van Bergeijk KE, Noordijk H, Lembrechts J, Frissel MJ (1992) Influence of soil pH, soil type and soil organic matter content on soil-to-plant transfer of radiocesium and strontium as analysed by a nonparametric method. J Environ Radioact 15:265–276

Van der Perk M, Slávik O, Fulajtar E (2002) Assessment of spatial variation of cesium-137 in small catchments. J Environ Qual 31:1930–1939

Van Genuchten MT, Cleary RW (1979) Movement of solutes in soil: computer simulated and laboratory results. In: Bolt GH (ed) Soil chemistry, Part B. Physiochemical models. Elsevier, Amsterdam

Vandenhove H, Van Hees M (2007) Predicting radium availability and uptake from soil properties. Chemosphere 69:664–674

Vandenhove H, Van Hees M, Wouters K, Wannijn J (2007) Can we predict uranium bioavailability based on soil parameters? Part 1: effect of soil parameters on soil solution uranium concentration. Environ Pollut 145:587–595

Vandenhove H, Gil-García C, Rigol A, Vidal M (2009a) New best estimates for radionuclide solid–liquid distribution coefficients in soils. Part 2. Naturally occurring radionuclides. J Environ Radioact 100:697–703

Vandenhove H, Olyslaegers G, Sanzharova N, Shubina O, Reed E, Shang Z, Velasco H (2009b) Proposal for new best estimates of the soil-to-plant transfer factor of U, Th, Ra, Pb and Po. J Environ Radioact 100:721–732

Voigt G, Fesenko S (2009) Remediation of contaminated environments. Radioact Environ 14:1–477

Wasserman MA, Perez DV, Bourg ACM (2002) Behavior of cesium-137 in some Brazilian oxisols. Commun Soil Sci Plan 33:1335–1349

Watters RL, Hakonson TE, Lane LJ (1983) The behavior of actinides in the environments. Radiochim Acta 32:89–103

The Influence of Edaphic Factors on Spatial and Vertical Distribution of Radionuclides in Soil

Snežana Dragović, Jelena Petrović, Ranko Dragović, Milan Đorđević, Mrđan Đokić, and Boško Gajić

Contents

Abstract This chapter summarises the edaphic factors affecting radionuclide spatial and vertical distribution in different soil types, with special emphasis on typical soil types in Serbia. The correlations between radionuclide and stable element content in soil and soil characteristics (particle size fractions, pH, carbonate content, organic matter content, cation exchange capacity, saturated hydraulic conductivity, specific electrical conductivity) are presented. These results provide insight into the main factors that affect radionuclide migration in the soil, which contributes to knowledge about radionuclide behaviour in the environment and factors governing their mobility within terrestrial ecosystems.

S. Dragović (✉)
Vinča Institute of Nuclear Sciences, University of Belgrade, P.O. Box 522, 11001 Belgrade, Serbia
e-mail: sdragovic@vinca.rs

J. Petrović
Institute for the Application of Nuclear Energy, University of Belgrade, Banatska 31b, 11080 Belgrade, Serbia

R. Dragović • M. Đorđević • M. Đokić
Faculty of Science and Mathematics, Department of Geography, University of Niš, P.O. Box 224, 18000 Niš, Serbia

B. Gajić
Faculty of Agriculture, Institute of Land Management, University of Belgrade, Nemanjina 6, 11080 Belgrade, Serbia

C. Walther, D.K. Gupta (eds.), *Radionuclides in the Environment*,
DOI 10.1007/978-3-319-22171-7_3

Keywords Uranium • Radium • Thorium • Potassium • Caesium • Physicochemical characteristics

1 Introduction

Distribution of natural radionuclides in soil depends primarily on the geological and geographical conditions and is governed by weathering, sedimentation, leaching/sorption and precipitation from percolating groundwater or dilution with other materials of different compositions. Anthropogenic radionuclides are derived from the radioactive fallout of nuclear fission products during nuclear weapons tests and nuclear accidents.

Due to its relatively long half-life of 30.2 years and chemical behaviour similar to that of potassium, ^{137}Cs is one of the most significant radionuclides in the environment. Studies on fallout from Chernobyl nuclear accident in 1986 clearly indicated that soil is the main reservoir of ^{137}Cs (Nimis 1996; Rafferty et al. 2000; Ciuffo et al. 2002), but its migration behaviour and associated profile distribution are site-specific and depend on soil characteristics and environmental conditions. In addition to being the main source of continuous radiation exposure to mankind, soil acts as a migration medium for transfer of radionuclides to the biological systems, and hence, it is the basic indicator of radiological contamination in the environment. In the assessment of soil contamination by radionuclides and its impact on the environment, it is important to identify the factors influencing the distribution of radionuclides in soil and their mobility and bioavailability. In this chapter, edaphic factors governing radionuclide mobility in soil are discussed with presentation of results of selected studies in Serbia performed by authors.

2 Sources of Radionuclides in Soil

Soil is the main reservoir for long-lived radionuclides deposited on terrestrial ecosystems via different pathways: as a part of the Earth's original crust, produced and deposited by cosmic ray interactions, or as a result of anthropogenic activities (UNSCEAR 2010). Radionuclides in soil occur in minerals or are adsorbed onto soil components (organic matter, carbonates and iron and manganese oxides), and from an environmental point of view, processes acting on their transfer and bioavailability are an important issue. The main contribution to external exposure comes from gamma-emitting radionuclides present in trace amounts in the soil, mainly ^{40}K, ^{238}U and ^{232}Th decay series commonly associated in nature (UNSCEAR 2010; Ivanovich 1994). Numerous studies have been conducted to assess the radiation exposure due to these radionuclides, and the results obtained are exploited to enrich the world's data bank, greatly needed for evaluating worldwide average values of radiometric and dosimetric quantities. According to UNSCEAR (2010) world average soil concentrations of ^{40}K, ^{238}U, ^{226}Ra and ^{232}Th are 412, 33, 32 and 45 Bq kg^{-1}, respectively.

Activities related to exploitation of natural resources to meet the human needs can lead to enhanced levels of naturally occurring radioactive material in products, by-products and wastes. The availability for release into the biosphere of the naturally occurring radioactive material in products, by-products or residues can be enhanced through physicochemical changes or by method by which the residues are managed (IAEA 2003). Processes enhancing concentrations of naturally occurring radioactive material include oil and gas production, coal mining and combustion, geothermal energy production, drinking water and wastewater treatment, production of industrial minerals, use of phosphate fertilisers and irrigation.

Naturally occurring radionuclides encountered in the processes of oil and gas exploration and production originate from underground formations. They are brought to the surface with water produced during pumping operations. These waters may contain elevated levels of ^{226}Ra and ^{228}Ra (Landa 2007). The largest concern in terms of radionuclide activity concentrations in the oil and gas industry involves the hard scales which form on the inside of the downhole tubing (IAEA 2003). Under temperature and pressure changes during oil and gas production operations, ^{226}Ra and ^{228}Ra found in produced waters may coprecipitate with barium sulphate scale in well tubular and surface equipment. The scales tend to be relatively insoluble; thus, the radionuclides would only be released slowly into the environment (Raabe 1996). These radionuclides may also occur in sludge that accumulates in oil field pits and tanks which become sources of naturally occurring radioactive material waste in oil and gas (Jibiri and Amakom 2011). The average radium concentration in soils sampled at an oil field contaminated with naturally occurring radioactive material in eastern Kentucky, United States, was 32,560 Bq kg^{-1} (Rajaretnam and Spitz 2000).

The coal is the most used fuel for the electricity production worldwide. It contains trace amounts of naturally occurring radionuclides which are being released into the environment during combustion in coal-fired power plants by two pathways: the nonvolatile products form ash particles, some of which settle to the bottom of the boiler to form bottom ash, and volatile and semi-volatile products, commonly named 'fly ash', are carried out by the exhaust gases to the atmosphere. The concentration of naturally occurring radioactive material in ash and other residues depends on their occurrence in coal, the operational parameters, and air pollution control device deployment of the combustion boilers (Clarke 1993; Miller et al. 2002; Sahu et al. 2014). Papastefanou et al. (1988) reported enrichment of radium in soils around coal power plants in Greece (up to 971 Bq kg^{-1}). The elevated ^{226}Ra activity concentrations (up to 337 Bq kg^{-1}) in soils around lignite field basin in southern Greece have been found by Rouni et al. (2001). Considerably, elevated concentrations of ^{238}U (up to 944 Bq kg^{-1}) and ^{226}Ra (up to 883 Bq kg^{-1}) have been found in soil around coal-fired power plant in Hungary (Papp et al. 2002). In addition to coal-burning power plant emissions, particulate emissions from coal-based domestic heating systems and the potential for exposure can be considerable, in particular, in less developed countries (Clarke 1992).

Naturally occurring radioactive material is found in the solid residues generated by the exploration and development of geothermal systems and in the extraction of the Earth's geothermal energy for use in either producing electric power or supplying direct heat. The wastes associated with geothermal energy production are similar to those associated with oil and gas production: temperature changes lead to precipitation of solids from hot formation waters in piping, equipment and retention ponds at the surface. Residues produced contain significant concentrations of radium and its decay products (IAEA 2003).

Conventional water treatment processes designed to remove suspended solids and dissolved chemical contaminants from drinking water supplies also remove radionuclides. Examples of naturally occurring radioactive material containing residues from municipal water treatment are radioactive contaminated sludges and solids including filter sludges, spent ion exchange resins, spent granular activated carbon, as well as waters from filter backwash (IAEA 2003). Disposal of sludges in lagoons results in the accumulation of radium in the bottom sediments. Naturally occurring radioactive material containing sludge is also disposed in sanitary landfills, discharged to sewers, injected in deep wells or spread on agricultural soils as a fertiliser, while the decanted water is recycled. The soil contamination due to the spread of sludge depends on the radionuclide concentration in the sludge and on the thickness of the sludge layer on land (UNSCEAR 2010). The common practice of dispersing sewage sludges or incinerator ashes onto agricultural land can lead to the accumulation of radionuclides and heavy metals in the soils and their uptake by plants (UNSCEAR 2010).

Several industries, such as pulp and paper industries, are heavy users of process water. Owing to the substances involved, significant radionuclide concentrations can accumulate in various products, intermediates, and wastes (HPS 2000).

As with drinking water, surface and groundwater used for irrigation may contain naturally occurring radioactive material that may accumulate in certain soil fractions and eventually transfer to plants. An active leaching of uranium from marine shales has been observed in irrigated areas in Southeastern Colorado (USGS 1994).

Naturally occurring radioactive material containing residues is generated by the mining and processing of phosphate rock (phosphorite) that is processed to phosphoric acid or elemental phosphorus (IAEA 2003). Uranium may be incorporated in sedimentary phosphorite ores through ionic substitution into the carbonate-fluorapatite crystals or by adsorption. Igneous phosphorite contains less uranium, but more thorium. High phosphate contents usually correspond to high uranium contents. The significant enrichment of ^{238}U in soils (up to 984 Bq kg^{-1}) around old phosphate mine in Jordan has been reported by Al-Jundi (2002). The activity concentrations of ^{226}Ra up to 820 Bq kg^{-1} have been found in soils around phosphate mines in Syrian Arab Republic (Othman and Al-Masri 2007).

Releases of radioactivity associated with uranium mining and milling operations are considered to be a significant cause of environmental and radiological problems in and around mining facilities. Production of large amounts of solid (tailings) is integral part of milling operation. The composition of tailings depends on mineralogy of the ore, host rock and blending materials and chemical extraction process used to recover the metal from the ore. Improper disposal of mill tailings can lead to substantial contamination of soils, surface water and groundwater. In Texas, United States, ^{238}U activity concentrations in soil have been found to be significantly higher overall in the uranium mining and milling areas compared to the control sites (McConnel et al. 1998). The ^{238}U activity concentrations in sediments in a uranium-mineralised region of Spain where abandoned uranium mine is located have been found to be about 40 times higher than in sediments considered to give the background level (Lozano et al. 2002). The radioactive contamination of the area surrounding the abandoned uranium mine in Yunnan Province, China, has been reported by Xu et al. (2002). The mean activity concentrations of ^{238}U, ^{230}Th and ^{226}Ra have been found to be 10–30 times higher in area affected by uranium mining in the southwest of Spain than those in non-affected area (Blanco et al. 2005). The concentrations of ^{238}U and ^{232}Th in soil samples from the uranium mining area in western Namibia and the neighbouring area have been found to be much higher than the worldwide average values (Oyedele et al. 2010).

Major sources of man-made radionuclides in soil, and generally in the environment, are the production and testing of nuclear weapons, nuclear power plants, nuclear fuel reprocessing, repository of nuclear wastes and nuclear accidents. High-level waste liquid and sludge are generated from weapon production and reprocessing. Nuclear weapons testing began in New Mexico in 1945, and since then, over 2×10^8 TBq of radioactivity has been released into the atmosphere (Choppin 2003). In the United States, a total of 1054 nuclear tests had been conducted until 1992, taking place in the Pacific Ocean, at the Nevada Test Site, and on miscellaneous sites in the continental United States (US DOE/NV 1992). Testing at the Nevada Test Site contributed to the global fallout budget as well as produced a legacy of radioactivity on the surface and below ground. Very low ^{137}Cs/^{239,240}Pu ratios and high ^{239,240}Pu/^{238}Pu ratios, in addition to high activity concentrations of ^{239,240}Pu in soils around the Nevada Test Site, reported by Turner et al. (2003), have been attributed to nuclear weapons tests. During 1949–1989, the Soviet Union conducted a total of about 460 nuclear weapons tests in Semipalatinsk, including 133 atmospheric nuclear tests. Starting in 1961, more than 300 test explosions were conducted underground. Thirteen of the underground tests resulted in releases of radioactive gases to the atmosphere (IAEA 1998). In the late 1940s to early 1960s, about 350 atmospheric atomic bomb tests were conducted at different test sites in the northern hemisphere (Eikenberg et al. 2004). Between 1966 and 1996, France had conducted nuclear weapons tests in French Polynesia (Pfingsten et al. 2001), where particles containing plutonium and small amounts of americium resulting from safety trials are found in soils and sediments (Danesi et al. 2002).

As of 21 January 2015, in 31 countries 439 nuclear power plant units with an installed electric net capacity of about 377 GW are in operation, and 69 plants with an installed capacity of 66 GW are in 16 countries under construction (ENS 2015). Over 200 radionuclides are produced during the operation of a typical reactor; most of the radionuclides are relatively short-lived and decay to low levels within a few decades (Crowley 1997). Neutron activation products and, to a less extent, volatile fission products such as iodine isotopes may enter the surrounding environment through atmospheric and aquatic releases from the nuclear power plants.

Relatively large quantities of radioactive material are involved at nuclear fuel reprocessing stage. Some fission and activation products are volatile under the conditions of used fuel reprocessing, such as noble gases (particularly isotopes of Kr and Xe), ^{3}H, ^{14}C and ^{129}I. Extensive studies conducted in the area of Sellafield reprocessing plant have shown that discharged radionuclides accumulate on salt marshes through a range of natural geochemical processes such as mixing and tidal currents (Assinder et al. 1985; Livens et al. 1994) and on tide-washed pastures bordering the Irish Sea coast of England and Wales (Sanchez et al. 1998). A number of technologies have been developed, tested and applied in the last decades to control emission of volatile radionuclides from nuclear fuel reprocessing plants.

Nuclear wastes arise at various stages in the nuclear fuel cycle. They include low- and intermediate-level wastes, mainly from reactor operation, high-level waste from fuel reprocessing, and spent fuel for direct disposal (UNSCEAR 2010). The migration of radionuclides from waste repositories to the biosphere potentially leads to a contamination of soil. The radionuclides ^{36}Cl, ^{79}Se, ^{99}Tc, ^{129}I, ^{237}Np and ^{238}U have been identified to be of greatest importance in the context of biosphere modelling in the framework of safety studies of nuclear waste disposals (Watkins et al. 1999).

As a result of the accident of the Chernobyl nuclear power plant, the environment was contaminated with radioactive materials whose total activity amounted to approximately 12.5 EBq, including 6.5 EBq of noble gases, as of 26 April 1986 (IAEA 2001). The Chernobyl accident resulted in significant fallout of radionuclides such as ^{137}Cs and $^{239,240}Pu$ on surface soils throughout northern Europe.

The latest serious accident occurred on 12 March 2011 in the Fukushima Daiichi nuclear power plant in Japan as a consequence of an earthquake in the Pacific Ocean followed by a tsunami. Following the continuing air releases of radionuclides after the accident, several fission products were recorded in the air by a number of monitoring stations. High radioactive deposition in soil taken from locations near the power plant was detected soon after deposition occurred (Endo et al. 2012).

In Europe, the elevated concentrations of several fission products (^{131}I, ^{132}I, ^{132}Te, ^{134}Cs and ^{137}Cs) were detected along the Iberian Peninsula. The analysis of back trajectories of air masses demonstrated that detected radionuclides are derived in Fukushima accident (Lozano et al. 2011). Traces of short- and long-lived fallout isotopes (^{131}I, ^{134}Cs and ^{137}Cs) were found in environmental samples collected in northwest Germany (rain water, river sediment, soil, grass and cow milk) following the radioactivity releases after the nuclear accident in Fukushima (Pittauerová et al. 2011).

3 Environmental Geochemistry of Selected Radionuclides

The parent rock material, mode of formation of the minerals and recent physical and chemical events (i.e. chemical leaching, transport with water and precipitation/adsorption) can affect the final distribution of radionuclides in the soil (Kemski et al. 1992). The geochemistry of the radionuclides controls migration through the geosphere by determining solubility, speciation, sorption and the extent of transport by colloids. Therefore, it is of importance in evaluating the long-term radiological impacts to the environment.

Uranium is a ubiquitous element with 14 isotopes which are all radioactive. Natural uranium consists primarily of three isotopes: ^{234}U (0.0057 %), ^{235}U (0.71 %) and ^{238}U (99.3 %). Uranium-234 ($T_{1/2} = 2.5 \times 10^5$ years) decays through a series of radionuclides to the stable ^{206}Pb, simultaneously emitting alpha and beta particles and gamma rays. In the uranium decay chain, ^{222}Rn ($T_{1/2} = 3.8$ days) is one of the radionuclides of concern because it can easily enter the human lungs. Uranium-235 ($T_{1/2} = 7 \times 10^8$ years) and ^{238}U ($T_{1/2} = 4.5 \times 10^9$ years) decay to stable ^{207}Pb and ^{206}Pb, respectively, emitting alpha and beta particles and gamma rays. It can exist in the +3, +4, +5 and +6 oxidation states. In soil, the most common oxidation states are +4 and +6. The content of uranium in soils worldwide varies from 0.7 to 10.7 mg kg^{-1} (Kabata-Pendias and Pendias 1985). There are several factors that affect uranium in soil, the most important being pH, redox potential, temperature, soil texture, organic and inorganic compounds, moisture and microbial activity (Rivas 2005). Soluble forms can migrate with soil water, be uptaken by plants or aquatic organisms or be volatilised (Igwe et al. 2005). Uranium (+4) occurs in strongly reducing environments and is formed by the oxidation of organic matter or iron in the soil. It is rather insoluble and can be complexed in small amounts by inorganic ligands such as fluoride, chloride, sulphate and phosphate (Langmuir 1978). It forms hydroxides, hydrated fluorides and phosphates which are very immobile in soils. The uranium (+6) occurs in oxidising environments. It is much soluble and can be complexed by fluoride, sulphate, carbonate and phosphate.

Uranium interacts with all components of the soil matrix such as clay minerals, aluminium and iron oxides, organic matter and microorganisms (Koch-Steindl and Pröhl 2001). Its complex behaviour in soil has been a subject of numerous studies, including studies of uranium uptake by oxides and hydroxides (Hsi and Langmuir 1985; Waite et al. 1994), clay minerals and silica (Stamberg et al. 2003; Payne et al. 2004) and organic matter (Shanbag and Choppin 1981). The bacterial reduction of soluble U^{6+} to insoluble U^{4+} is an important process for uranium fixation in soil (Anderson et al. 1989; Klimkhanner and Palmer 1991). The investigations of potential of bacteria for bioaccumulation of uranium have been indicated its accumulation in the form of sparingly soluble phosphate compounds (Selenska-Pobell et al. 2002). The mobility of uranium in soil and its vertical transport to groundwater depend on soil properties such as pH, oxidation–reduction potential, concentration of complexing anions, porosity of the soil, soil particle size and sorption properties, as well as the amount of water available (Allard et al. 1982; Bibler and Marson 1992).

Radium (^{226}Ra) is the decay product of ^{238}U, with a half-life of 1600 years. Radium exists in the environment typically as a divalent cation. Compared with uranium, radium has a higher mobility in soils (Zhang et al. 2002). It readily adsorbs to clays and mineral oxides present in soil especially in neutral and alkaline conditions. The relative affinity for ion exchange on clay minerals comparing with other elements can be described as follows: $Ra^{2+} > Ba^{2+} > Sr^{2+} > Ca^{2+} > Mg^{2+}$ (USEPA 2004). The degree of sorption of radium onto soil constituents depends on several variables owing to the multiple modes of interaction between radium and the soil mineral matrix. The most important ones are the ionic strength of the solution and the particle surface area. High concentrations of sulphate ion, low calcium concentrations and low ionic forces of solutions restrain the migration of radium and favour its absorption in soils (Landa 1980). The Ra^{2+} ion is weakly incline to complexing, though there are citric anionic complexes stable in an acid medium (Bagnall 1957; Sedlet 1966). An increase of mineral surface charge, the increased stability of inorganic radium complexes in high ionic strength solutions and the formation of strong organic complexes decrease radium sorption (IAEA 2006). The biosorption experiments have shown that different biomass types, mainly fungi, accumulate large amounts of radium present in solution (Volesky 1990).

Thorium has several isotopes whose atomic masses range from 212 to 236, but only one naturally occurring isotope, ^{232}Th ($T_{1/2} = 1.4 \times 10^{10}$ years), decays through emission of an alpha particle. Six alpha and four beta decay steps occur before ^{232}Th becomes stable ^{208}Pb. Thorium occurs in only one oxidation state (+4) in nature. Hydroxides of Th^{4+} are the dominant species in soil, although carbonate complexes also form (Zhang et al. 2002). The global concentration of thorium in soil ranges from 3.4 to 10.5 mg kg^{-1}. Thorium in soil, like uranium, is governed by the formation of the hydrated cation Th^{4+}, which is responsible for its solubility over a wide range of soil pH. Organic acids increase the solubility of thorium in soil, but its mobility may be limited due to the formation of slightly soluble precipitates (phosphates, oxides) and by adsorption on clay minerals and organic matter. The humic substances are considered particularly important in the adsorption of thorium (Mitchell et al. 2013). The adsorption of thorium on clays, oxides and organic matter increases with increasing pH, reaching a maximum at a pH of 6.5 (Syed 1999). As reported by USEPA (1999), thorium organic complexes predominate over inorganic ones in organic-rich soils. Thorium has low mobility under all environmental conditions, mainly due to the high stability of the insoluble oxide ThO_2 and the strongly resistant nature of its carrier minerals such as monazite and zircon (USEPA 1999).

Among naturally occurring potassium isotopes, only ^{40}K ($T_{1/2} = 1.3 \times 10^9$ years) is unstable. It decays by beta particle emission to ^{40}Ca (89 %) and by electron capture to ^{40}Ar (11 %) and produces 1.46 MeV gamma rays after electron capture decay. Potassium-40 is present at 0.0117 % by mass in natural potassium. The overall mean content of potassium in soils worldwide is about 1.8 % (Bowen 1982).

The weathering behaviour of potassium-bearing minerals determines potassium content in soil. The potassium behaviour during weathering and pedogenesis is different from that of uranium and thorium. As potassium is highly soluble, its concentration decreases with increased weathering (Wilford 2008). Potassium can persist in soils in the form of muscovite or associated with large phenocrysts (Dickson and Scott 1997). It can also be associated indirectly with clays such as illite (Wilford 2008).

Caesium exists in the environment in the +1 oxidation state. Its concentrations in soil range between 0.3 and 25 mg kg^{-1} (Lindsay 1979). Caesium fission products include three main isotopes at significant concentrations: ^{134}Cs ($T_{1/2} = 2.05$ years), ^{135}Cs ($T_{1/2} = 3 \times 10^6$ years) and ^{137}Cs ($T_{1/2} = 30.2$ years). Caesium released by weathering of rocks and minerals is rapidly and strongly adsorbed by soil. Some micaceous minerals, such as illite and vermiculite, tend to take up caesium in their intrastructural layers (Cremers et al. 1988). The high retention of caesium in soil is determined by two different processes: structural fixation and reversible selective sorption (Konoplev et al. 2002). Reversible selective sorption occurs on frayed edge sites, located at the edges of micaceous clay particles (Cremers et al. 1988). The interlayer distance in certain micaceous minerals excludes diffusion of some major ions while permitting the Cs^+ ion to fit perfectly between the layers. The low hydration energy of Cs^+ ion is considered to be the major factor in its fixation (Sawhney 1972). Caesium may also adsorb onto iron oxides which complex caesium to sites whose abundance is pH dependent (USEPA 1999).

4 Edaphic Factors Influencing Radionuclide Distribution in Soil

The soil parameters which dominantly affect radionuclide mobility, according to Bunzl (1997), include: (1) the composition of the soil solution (pH, concentration of inorganic ions, redox potential, concentration of organic substances), (2) physical and chemical soil properties (species/characteristics and contents of clay minerals, oxides and organic matter, surface and charges of particles), (3) microorganisms and fungi (mycorrhiza) and (4) temperature (Bunzl 1997). Variations of background concentrations of radionuclides in soil depend on the soil type, moisture content, inhomogeneity of its permeability, formation, transport processes and geomorphology associated with meteorological conditions (El-Arabi 2005). Soil formation processes also influence the distribution patterns of uranium, thorium and their decay products (Karakelle et al. 2002). The vertical migration of radionuclides in soil is influenced by the site-specific water balance, i.e. the net infiltration of water into the soil which transports radionuclides down the soil profile (Strebl et al. 2007).

The cationic species UO_2^{2+}, Th^{4+} and $Th(OH)_2^{2+}$ are the dominant forms of uranium and thorium in soils and are strongly sorbed on soil solids, including organic matter (Sheppard and Evenden 1988). However, organic complexes and colloids can increase their mobility in mineral soils. Mortvedt (1994) noted that the plant uptake of thorium, uranium and radium was influenced by soil pH and that this may be related to indirect effects of competition from calcium and magnesium, particularly for radium, which belongs to the alkaline earth series. It has been shown that clay content is the most important determinant of background levels of ^{40}K, ^{226}Ra, and ^{232}Th in soils (Van den Bygaart et al. 1999). There is evidence of increased association of the three radionuclides with the clay fraction compared with the sand fraction of soils contaminated by uranium mine tailings. Soil organic matter appears to form strong complexes with thorium and to increase its mobility in soil (Sheppard 1980). Selenium, available potassium, carbonate, phosphorus and nitrates have been observed to influence plant uptake of uranium (Van Netten and Morley 1983).

Dragović et al. (2012) analysed the influence of edaphic factors and content of stable elements on vertical distribution of natural radionuclides (^{40}K, ^{226}Ra and ^{232}Th) and Chernobyl-derived ^{137}Cs in the soils representing the dominant soil types of Belgrade (capital and the largest city in Serbia). The activity concentrations of ^{40}K, ^{226}Ra and ^{232}Th were found to be influenced by soil type. They showed homogenous distribution down the soil profiles (up to 50 cm with 5 cm increments). The activity concentrations of ^{137}Cs were found to be maximal at 10–15-cm depth, which is in accordance with numerous studies showing that ^{137}Cs deposition is mostly contained within the surface soil layer (Pietrzak-Flis et al. 1996; Yoshida et al. 2004; Karadeniz and Yaprak 2008b). The correlation analysis identified associations of ^{40}K, ^{226}Ra and ^{137}Cs with fine-grained soil fractions (Table 1) which confirmed results obtained worldwide showing that the fine-grained soil fraction has a higher tendency for radionuclide adsorption than coarse-grained soils since the soil particle surface area is larger (Baeza et al. 1995b; Navas et al. 2002). Strong positive correlations ($p < 0.01$) were found between ^{226}Ra and ^{232}Th and Fe and Mn, which indicate association of these radionuclides with Fe and Mn oxides (assuming the secular equilibrium between ^{232}Th, ^{228}Ra and ^{228}Ac) or deposition of Fe and Mn oxides on the surfaces of ^{226}Ra and ^{232}Th minerals. This association is supported by strong positive correlations with Ni, Pb and Zn which also appear to be related to the above-mentioned oxides. Similar relationships have been found in other studies (Navas et al. 2005; Chao and Chuang 2011). The correlations observed between ^{40}K and Cr, Ni, Pb and Zn and also between ^{137}Cs and Cd, Cr, Pb and Zn could be attributed to their common affinity for clay minerals (Van der Graaf et al. 2007). The strength of these correlations may be influenced by variations in pH and/or organic substances.

The leading mechanism of radiocaesium fixation in soils is its exchangeable and non-exchangeable sorption and fixation (Korobova et al. 2007). It has been shown that ^{137}Cs sorption by soils is controlled by ion exchange mechanisms. The compensation of the negative charge of clay particles by positively charged caesium ions depends on the structure of the particular minerals, their selectivity with respect to caesium ions, the size of the mineral particles and the degree of their aggregation, the presence of competitive ions, the pH and ionic strength of the soil

Table 1 Pearson correlation coefficients between radionuclides and both soil properties and stable element content of the studied soils of Belgrade area

	^{40}K	^{226}Ra	^{232}Th	^{137}Cs
Sand	0.05	−0.49**	−0.24	0.01
Silt	0.33**	0.49**	−0.11	0.28*
Clay	0.34**	0.28**	0.20	0.29*
pH	0.10	−0.30*	−0.59**	−0.13
Organic matter	−0.18	−0.19	0.09	0.73**
Cation exchange capacity	−0.27	−0.27	−0.25	0.41**
Carbonates	0.08	−0.67**	−0.73**	−0.13
Bulk density	−0.05	0.05	0.50	−0.52**
Particle density	0.15	0.11	−0.07	−0.61**
Saturated hydraulic conductivity	−0.04	−0.03	−0.19	0.68**
Specific electrical conductivity	−0.09	−0.44**	−0.57**	0.61**
Al	0.19	0.13	−0.15	0.05
Ca	0.12	−0.57**	−0.75**	0.01
Cd	0.15	0.30*	0.11	0.41**
Co	0.18	0.32*	0.12	0.02
Cr	0.45**	−0.09	0.60**	0.68**
Cu	−0.06	−0.24	−0.16	0.06
Fe	0.31	0.48**	0.51**	−0.22
K	0.81**	−0.06	−0.16	−0.33*
Li	0.17	−0.04	−0.18	−0.26*
Mg	0.14	0.21	−0.28*	0.06
Mn	0.12	0.54**	0.37**	−0.16
Na	−0.01	0.17	−0.05	−0.21
Ni	0.35**	0.26*	0.54**	−0.14
Sr	−0.06	0.08	−0.13	−0.17
Pb	0.44**	0.36**	0.67**	0.56**
Zn	0.35**	0.60**	0.74**	0.48**
Ti	0.05	0.14	0.06	−0.16

Reproduced from Dragović et al. (2012)
**Correlation is significant at the 0.01 level. *Correlation is significant at the 0.05 level

solution and the caesium concentration in it. The vertical migration of radiocaesium in soils is related to the rate of infiltration of water together with colloidal and clay particles carrying the radionuclides. Elejalde et al. (1996) have shown that ^{137}Cs activity concentration in soil is significantly related to the formation of a complex with organic matter, substitution for K^+, H^+ or NH_4^+ and a competitive effect of ^{40}K for retention by soil with a small contribution due to soil texture. Bihari and Dezső (2008) noted that ^{137}Cs association is concentrated in the finest soil fractions but adsorbed almost entirely to clay minerals. Baeza et al. (1995a) reported significant correlation between ^{137}Cs activity concentrations in soil and organic matter content. The lateral and vertical distribution of ^{137}Cs is also influenced by soil management such as tillage, soil erosion and soil organic matter cycling. Dragović et al. (2012)

found significant positive correlations between ^{137}Cs activity concentration and both organic matter content and cation exchange capacity (Table 1). Elejalde et al. (1996) also observed that ^{137}Cs activity concentration was related to organic matter and cation exchange phenomena. Organic matter is a component of great importance because it tends to form soluble or insoluble complexes with radionuclides, which can migrate throughout the profile or be retained in the soil (Campbell 1978; Vega et al. 2004). Saturated hydraulic conductivity and specific electrical conductivity were also positively correlated with the activity concentration of ^{137}Cs.

The deposition of Chernobyl-derived radionuclides on the territory of Serbia led to a considerable radioactive contamination of soil, vegetation and other ecological compartments. Uneven rainfall on the Belgrade area during May 1986 resulted in variable local distribution of radioactivity (Popović and Spasić-Jokić 2006). Petrović et al. (2013) investigated the influence of pedogenic factors on the spatial and vertical distribution of ^{137}Cs in surface soils from the urban area of Belgrade. The activity concentration of ^{137}Cs in surface soil samples was found to be highly correlated with pH, cation exchange capacity and organic matter (Table 2). The negative correlation of soil pH with the ^{137}Cs activity concentration in surface soils agrees with the findings of Schimmack et al. (1991) and Kim et al. (1998) who found weak correlations between pH and ^{137}Cs activity concentrations. In soil profiles the ^{137}Cs activity concentration and organic matter content were also closely correlated, while the correlations with specific electrical conductivity and silt were less close (Table 3). The positive correlation between specific electrical conductivity and the ^{137}Cs activity concentration detected for the soil profiles agrees with the earlier findings of Dragović et al. (2012). Previous research has shown correlations between electrical conductivities with soil properties such as soil organic matter, cation exchange capacity and soil texture (Officer et al. 2004; Peralta et al. 2013).

The investigations of vertical distribution of ^{137}Cs in Banat Sands, southeastern sector of Pannonian Plain, Serbia (Table 4), showed that more than half of deposited ^{137}Cs is retained in the first 5 cm of the profile, which is in accordance with previous studies on caesium migration in soil (Al-Masri 2006; Fawaris and

Table 2 Pearson correlation coefficients between ^{137}Cs and properties of the analysed surface soils from Belgrade area

Parameter	^{137}Cs
pH	−0.37**
Specific electrical conductivity	−0.11
Cation exchange capacity	−0.33**
Organic matter	0.33**
Sand	−0.17
Silt	0.18
Clay	0.05
Carbonates	−0.15

Reproduced from Petrović et al. (2013)
**Correlation is significant at the 0.01 level. *Correlation is significant at the 0.05 level

Table 3 Pearson correlation coefficients between ^{137}Cs and properties of the analysed soil profiles from Belgrade area

Parameter	^{137}Cs
pH	−0.01
Specific electrical conductivity	0.25*
Cation exchange capacity	0.13
Organic matter	0.41**
Sand	−0.10
Silt	0.28*
Clay	−0.17
Carbonates	−0.22

Reproduced from Petrović et al. (2013)
**Correlation is significant at the 0.01 level. *Correlation is significant at the 0.05 level

Table 4 Pearson correlation between ^{137}Cs and properties of the analysed soil profiles from Banat Sands

Parameter	^{137}Cs
pH	−0.63**
Specific electrical conductivity	−0.01
Cation exchange capacity	−0.17
Organic matter	0.47**
Sand	−0.41**
Silt	0.41**
Clay	0.14
Carbonates	−0.07

**Correlation is significant at the 0.01 level. *Correlation is significant at the 0.05 level

Johanson 1994; Karadeniz and Yaprak 2008b). In analysed soils, positive correlation coefficient was found between ^{137}Cs activity concentration and organic matter content which was also reported in a number of studies (Lee et al. 1997; Kim et al. 1998; Dragović et al. 2012; Karadeniz and Yaprak 2008a). Due to large cation exchange capacity, the role of organic matter in the retaining and preventing downward migration of ^{137}Cs through soil profile is very important. In the organic horizons, soil microflora and microfauna can immobilise the ^{137}Cs. Brückmann and Wolters (1994) reported that the soil microflora strongly contributes to the immobilisation of ^{137}Cs in the organic layer of forest soils. Positive correlation coefficient was also found between ^{137}Cs activity concentration and silt content which agrees with the findings of Dragović et al. (2012) and Petrović et al. (2013).

In surface soils from a water-eroded area in southeastern part of Serbia (Pčinja and South Morava River Basins), positive correlations were found between ^{137}Cs activity concentration and specific electrical conductivity and organic matter (Table 5).

Numerous studies following Chernobyl accident have shown that radiocaesium interaction in soils occurs on cation exchange sites at several levels of specificity and reversibility. The soil phases responsible for radiocaesium adsorption are basically organic matter (mainly humic substances) and clays, although in mineral

Table 5 Pearson correlation between ^{137}Cs and properties of the analysed surface soils from Pčinja and South Morava River Basins area

Parameter	^{137}Cs
pH	−0.16
Specific electrical conductivity	0.47**
Cation exchange capacity	−0.12
Organic matter	0.31*
Sand	0.001
Silt	0.03
Clay	−0.12
Carbonates	0.16

**Correlation is significant at the 0.01 level. *Correlation is significant at the 0.05 level

soils it is widely accepted that radiocaesium adsorption is controlled by phyllosilicates, especially illite and vermiculite. However, adsorption experiments showed that the specific sites in clays control radiocaesium adsorption in organic soils and that organic compound has an indirect but significant effect (Rigol et al. 2002).

Soil biota play an important role in the movement of radionuclides through a soil system. Microbial diversity within soil is integral to soil ecosystem function (Torsvik and Øvreås 2007). The complex and dynamic nature of natural microbial communities has a profound effect on the soil medium and therefore to the geochemical behaviour of radionuclides in soil (Fomina et al. 2007). Prokaryotes can be considered especially important since they represent the largest phylogenetic diversity of any grouping on the Earth and are involved in all biogeochemical cycling (Torsvik and Øvreås 2007). Fungi impact upon the structural dynamics of soil, and any transport process that is affected by soil structure are also likely to be affected by the effect of fungi on soil architecture (Ritz 2006). Both bacteria and fungi immobilise and complex radionuclides by mechanisms such as volatilisation, extracellular complexing, intracellular accumulation and cell surface binding (Ragnarsdottir and Charlet 2000). Fungi accumulate radionuclides and are also able to form mycorrhizal links to vascular plants and thus enhance radionuclide uptake by vascular plant hosts (Haas et al. 1998). The long-term retention of radionuclides in organic layers of soils could be attributed to fungal and microbiological activities.

5 Conclusions

To assess the impact caused by radionuclides in soil, it is important to identify the factors that govern their mobility and availability. The interaction of radionuclides with the soil environment depends on both soil properties and environmental factors. The concentration of competitive elements present in the soil is of particular importance for determining radionuclide distribution between soil and soil solution. The study of the association of edaphic factors affecting radionuclide spatial and vertical distribution in soil is a step towards understanding radionuclide behaviour and estimating the hazards they may pose to the human and the environment.

Acknowledgement This work was supported by the Ministry of Education, Science and Technological Development of the Republic of Serbia (Project No. III43009).

References

Al-Jundi J (2002) Population doses from terrestrial gamma exposure in areas near to old phosphate mine, Russaifa, Jordan. Radiat Meas 35:23–28
Allard B, Olofsson U, Torstenfelt B, Kipatsi H (1982) Sorption of actinides in well-defined oxidation states on geologic media. Mater Res Soc Symp Proc 11:775–782
Al-Masri MS (2006) Vertical distribution and inventories of ^{137}Cs in the Syrian soils of the eastern Mediterranean region. J Environ Radioact 86:187–198
Anderson RF, Lehuray AP, Fleisher MQ, Murray JW (1989) Uranium deposition in Saanich Inlet sediments, Vancouver Island. Geochim Cosmochim Acta 53:2205–2213
Assinder DJ, Kelly M, Aston SR (1985) Tidal variations in dissolved and particulate phase radionuclide activities in the Esk estuary, England, and their distribution coefficients and particulate activity fractions. J Environ Radioact 2:1–22
Baeza A, Del Río M, Jiménez A, Miro C, Paniagua J (1995a) Relative sorption of Cs-137 and Sr-90 in soil—influence of particle-size, organic matter content and pH. Radiochim Acta 68:135–140
Baeza A, Del Río M, Jiménez A, Miro C, Paniagua J (1995b) Influence of geology and soil particle size on the surface-area/volume activity ratio for natural radionuclides. J Radioanal Nucl Chem 189:289–299
Bagnall KW (1957) Chemistry of the rare radioelements. Academic, New York
Bibler JP, Marson DB (1992) Behavior of mercury, lead, cesium, and uranyl ions on four SRS soils (U), Technical Report WSR-RP-92-326. Westinghouse Savannah River Company, Aiken, SC
Bihari Á, Dezső Z (2008) Examination of the effect of particle size on the radionuclide content of soils. J Environ Radioact 99:1083–1089
Blanco P, Vera Tomé F, Lozano JC (2005) Fractionation of natural radionuclides in soils from a uranium mineralized area in the south-west of Spain. J Environ Radioact 79:315–330
Bowen HJM (1982) Environmental chemistry, vol 2. Royal Society of Chemistry, London
Brückmann A, Wolters V (1994) Microbial immobilization and recycling of ^{137}Cs in the organic layers of forest ecosystems: relationship to environmental conditions, humification and invertebrate activity. Sci Total Environ 157:249–256
Bunzl K (1997) Radionuklide. In: Blume HP, Felix-Henningsen P, Fischer WR, Frede HG, Horn R, Stahr K (eds) Handbuch der Bodenkunde. Ecomed, Landberg/Lech, Germany
Campbell CA (1978) Soil organic carbon, nitrogen and fertility. In: Schnitzer M, Khan SV (eds) Soil organic matter (Developments in soil science), vol 8. Elsevier, Amsterdam
Chao JH, Chuang CY (2011) Accumulation of radium in relation to some chemical analogues in *Dicranopteris linearis*. Appl Radiat Isot 69:261–267
Choppin GR (2003) Actinide speciation in the environment. Radiochim Acta 91:645–649
Ciuffo LEC, Belli M, Pasquale A, Menegon S, Velasco HR (2002) ^{137}Cs and ^{40}K soil-to-plant relationship in a semi natural grassland of the Giulia Alps, Italy. Sci Total Environ 295:69–80
Clarke LB (1992) Applications for coal-use residues, IEA CR/50. IEA Coal Research, London

Clarke LB (1993) The fate of trace elements during coal combustion and gasification: an overview. Fuel 72:731–736

Cremers A, Elsen A, De Preter P, Maes A (1988) Quantitative analysis of radiocaesium retention in soils. Nature 335:247–249

Crowley KD (1997) Nuclear waste disposal: the technical challenges. Phys Today 50:32–39

Danesi PR, Moreno J, Makarewicz M, Radecki Z (2002) Residual radioactivity in the terrestrial environment of the Mururoa and Fangataufa Atolls nuclear weapon test sites. J Radioanal Nucl Chem 253:53–65

Dickson BL, Scott KM (1997) Interpretation of aerial gamma-ray surveys: adding the geochemical factors. AGSO J Aust Geol Geophys 17:187–210

Dragović S, Gajić B, Dragović R, Jankovic-Mandic L, Slavkovic Beskoski L, Mihalovic N, Momcilovic M, Cujic M (2012) Edaphic factors affecting the vertical distribution of radionuclides in the different soil types of Belgrade, Serbia. J Environ Monit 14:127–137

Eikenberg J, Beer H, Bajo S (2004) Anthropogenic radionuclide emissions into the environment. In: Gieré R, Stille P (eds) Energy, waste and the environment: a geochemical perspective, geological society special publication 236. The Geological Society, London

El-Arabi AM (2005) Waste and the environment: a geochemical perspective, geological society special publication 236. J Environ Radioact 81:11–19

Elejalde C, Herranz M, Romero F, Legarda F (1996) Correlations between soil parameters and radionuclide contents in samples from Biscay (Spain). Water Air Soil Pollut 89:23–31

Endo S, Kimura S, Takatsuji T, Nanasawa K, Imanaka T, Shizuma K (2012) Measurement of soil contamination by radionuclides due to the Fukushima Dai-ichi nuclear power plant accident and associated estimated cumulative external dose estimation. J Environ Radioact 111:18–27

ENS (2015) Nuclear power plants, world-wide. http://www.euronuclear.org/info/encyclopedia/n/nuclear-power-plant-world-wide.htm. Accessed 14 March 2015

Fawaris BH, Johanson KJ (1994) Radiocaesium in soil and plants in a forest in central Sweden. Sci Total Environ 157:133–138

Fomina M, Charnock JM, Hillier S, Alvarez R, Gadd GM (2007) Fungal transformations of uranium oxides. Environ Microbiol 9:1696–1710

Haas JR, Bailey EH, Purvis OW (1998) Bioaccumulation of metals by lichens; uptake of aqueous uranium by *Peltigera membranacea* as a function of time and pH. Am Mineral 83:1494–1502

HPS (2000) NORM deposition in the pulp and paper industry. Health Physics Society (HPS), MacLean

Hsi CK, Langmuir D (1985) Adsorption of uranyl onto ferric oxyhydroxides: application of the surface complexation site-binding model. Geochim Cosmochim Acta 49:1931–1941

IAEA (1998) Radiological conditions at the Semipalatinsk test site, Kazakhstan: preliminary assessment and recommendations for further study, Radiological Assessment Reports Series. Vienna

IAEA (2001) Present and future environmental impact of the Chernobyl accident, IAEA-TECDOC-1240. Vienna

IAEA (2003) Extent of environmental contamination by naturally occurring radioactive material (NORM) and technological options for mitigation, Technical Report Series No. 419. Vienna

IAEA (2006) Applicability of monitored natural attenuation at radioactively contaminated sites, Technical Report Series No. 445. Vienna

Igwe JC, Nnorom IC, Gbaruko BC (2005) Kinetics of radionuclides and heavy metals behavior in soils: implications for plant growth. Afr J Biotechnol 4:1541–1547

Ivanovich M (1994) Uranium series disequilibrium: concepts and applications. Radiochim Acta 64:81–94

Jibiri NN, Amakom CM (2011) Radiological assessment of radionuclide contents in soil waste streams from an oil production well of a petroleum development company in Warri, Niger Delta, Nigeria. Indoor Built Environ 20:246–252

Kabata-Pendias A, Pendias H (1985) Trace elements in soils and plants. CRC, Boca Raton, FL

Karadeniz Ö, Yaprak G (2008a) Geographical and vertical distribution of radiocesium levels in coniferous forest soils in Izmir. J Radioanal Nucl Chem 277:567–577

Karadeniz Ö, Yaprak G (2008b) Vertical distribution and gamma dose rates of ^{40}K, ^{232}Th, ^{238}U and ^{137}Cs in the selected forest soils in Izmir, Turkey. Radiat Prot Dosimetry 131:346–355

Karakelle B, Öztűrk N, Köse A, Varinlioglu A, Erkol AY, Yilmaz F (2002) Natural radioactivity in soil samples of Kocaeli basin, Turkey. J Radioanal Chem 254:649–651

Kemski J, Klingel R, Schneiders H, Siehl A, Wiegand J (1992) Geological structure and geochemistry controlling radon in soil gas. Radiat Prot Dosimetry 45:235–239

Kim CS, Lee MH, Kim CK, Kim KH (1998) ^{90}Sr, ^{137}Cs, $^{239+240}Pu$ and ^{238}Pu concentrations in surface soils of Korea. J Environ Radioact 40:75–88

Klimkhanner GP, Palmer MR (1991) Uranium in the oceans: where it goes and why? Geochim Cosmochim Acta 55:1799–1806

Koch-Steindl H, Pröhl G (2001) Considerations on the behavior of long-lived radionuclides in the soil. Radiat Environ Biophys 40:93–104

Konoplev A, Kaminski S, Klemt E, Konopleva I, Miller R, Zibold G (2002) Comparative study of ^{137}Cs partitioning between solid and liquid phases in Lakes Constance, Lugano and Vorsee. J Environ Radioact 58:1–11

Korobova E, Chizhikova NP, Linnik VG (2007) Distribution of ^{137}Cs in the particle-size fractions and in the profiles of alluvial soils on floodplains of the Iput and its tributary Buldynka Rivers (Bryansk oblast). Euras Soil Sci 40:367–379

Landa ER (1980) Isolation of uranium mill tailings and component radionuclides from the biosphere: some earth science perspectives. U.S. Government Printing Office, Washington, DC

Landa ER (2007) Naturally occurring radionuclides from industrial sources: characteristics and fate in the environment. In: Shaw G (ed) Radioactivity in the terrestrial environment. Elsevier, Amsterdam

Langmuir D (1978) Uranium solution-mineral equilibria at low temperatures with applications to sedimentary ore deposits. Geochim Cosmochim Acta 42:547–569

Lee MH, Lee CW, Boo BH (1997) Distribution and characteristics of $^{239,240}Pu$ and ^{137}Cs in the soil of Korea. J Environ Radioact 37:1–16

Lindsay WL (1979) Chemical equilibria in soils. Wiley, New York, NY

Livens FR, Horrill AD, Singleton DL (1994) Plutonium in estuarine sediments and the associated interstitial water. Estuar Coast Shelf Sci 38:479–489

Lozano JC, Blanco Rodríguez P, Vera Tomé F (2002) Plutonium in estuarine sediments and the associated interstitial water. J Environ Radioact 63:153–171

Lozano RL, Hernández-Ceballos MA, Adame JA, Casas-Ruiz M, Sorribas M, San Miquel EG, Bolivar JP (2011) Radioactive impact of Fukushima accident on the Iberian Peninsula: evolution and plume previous pathway. Environ Int 37:1259–1264

McConnel MA, Ramanujam VMS, Alcock NW, Gabehart GJ, Au WM (1998) Distribution of uranium-238 in environmental samples from a residential area impacted by mining and milling activities. Environ Toxicol Chem 17:841–850

Miller BB, Kandiyoti R, Dugwell DR (2002) Trace element emissions from combustion of secondary fuels with coal: a comparison of bench-scale experimental data with predictions of a thermodynamic equilibrium model. Energy Fuel 16:956–963

Mitchell N, Pérez-Sánchez D, Thorne MC (2013) A review of the behaviour of U-238 series radionuclides in soils and plants. J Radiol Prot 33:R17–R48

Mortvedt JJ (1994) Plant and soil relationships of uranium and thorium decay series radionuclides—a review. J Environ Qual 23:643–650

Navas A, Soto J, Machín J (2002) Distribution of uranium-238 in environmental samples from a residential area impacted by mining and milling activities. Appl Radiat Isot 57:579–589

Navas A, Machín J, Soto J (2005) Mobility of natural radionuclides and selected major and trace elements along a soil toposequence in the central Spanish Pyrenees. Soil Sci 170:743–757

Nimis PL (1996) Radiocesium in plants of forest ecosystems. Studia Geobot 15:3–49

Officer SJ, Kravchenko A, Bollero GA, Sudduth KA, Kitchen NR, Wiebold WJ, Palm HL, Bullock DG (2004) Relationships between soil bulk electrical conductivity and the principal component analysis of topography and soil fertility values. Plant Soil 258:269–280

Othman I, Al-Masri MS (2007) Relationships between soil bulk electrical conductivity and the principal component analysis of topography and soil fertility values. Appl Radiat Isotopes 65:131–141

Oyedele JA, Shimboyo S, Sitoka S, Gaoseb F (2010) Assessment of natural radioactivity in the soils of Rossing Uranium Mine and its satellite town in western Namibia, southern Africa. Nucl Instrum Meth Phys Res A 619:467–469

Papastefanou C, Manolopoulou M, Charalambous S (1988) Radioecological measurements in the coal power plant environment. Radiat Prot Dosimetry 24:439–443

Papp Z, Dezső Z, Daróczy S (2002) Significant radioactive contamination of soil around a coal-fired thermal power plant. J Environ Radioact 59:191–205

Payne TE, Davis JA, Lumpkin GR, Chisari R, Waite TD (2004) Surface complexation model of uranyl sorption on Georgia kaolinite. Appl Clay Sci 26:151–162

Peralta NR, Costa JL, Balzarini M, Angelini H (2013) Delineation of management zones with measurements of soil apparent electrical conductivity in the southeastern pampas. Can J Soil Sci 93:205–218

Petrović J, Ćujić M, Đorđević M, Dragovic R, Gajic B, Miljanic S, Dragovic S (2013) Spatial distribution and vertical migration of ^{137}Cs in soils of Belgrade (Serbia) 25 years after the Chernobyl accident. Environ Sci Process Impacts 15:1279–1289

Pfingsten W, Hadermann J, Perrochet P (2001) Radionuclide release and transport from nuclear underground tests performed at Mururoa and Fangataufa—predictions under uncertainty. J Contam Hydrol 47:349–363

Pietrzak-Flis Z, Radwan I, Rosiak L, Wirth E (1996) Migration of ^{137}Cs in soils and its transfer to mushrooms and vascular plants in mixed forests. Sci Total Environ 186:243–250

Pittauerová D, Hettwig B, Fischer HW (2011) Fukushima fallout in Northwest German environmental media. J Environ Radioact 102:877–880

Popović D, Spasić-Jokić V (2006) Naslov. Vojnosanit Pregl 63:481–487

Raabe OG (1996) Studies of the solubility of naturally-occurring radionuclides in petroleum scale, NORM/NARM: regulation and risk assessment. Health Physics Society, Scottsdale, AZ

Rafferty B, Brennan M, Dawson D, Dowding D (2000) Mechanisms of ^{137}Cs migration in coniferous forest soils. J Environ Radioact 48:131–143

Ragnarsdottir KV, Charlet L (2000) Uranium behavior in natural environments. In: Cotter-Howels KV, Batchelder JD, Campbell J, Valsami-Jones E (eds) Environmental mineralogy: microbial interactions, anthropogenic influences, contaminated land and waste management. Mineralogical Society of Great Britain and Ireland, London

Rajaretnam G, Spitz HB (2000) Effect of leachability on environmental risk assessment for naturally occurring radioactive materials in petroleum oil fields. Health Phys 78:191–198

Rigol A, Vidal M, Rauret G (2002) An overview of the effect of organic matter on soil-radiocaesium interaction: implications in root uptake. J Environ Radioact 58:191–216

Ritz K (2006) Fungal roles in transport processes in soils. In: Gadd GM (ed) Fungi in biogeochemical cycles. Cambridge University Press, Cambridge

Rivas MC (2005) Interactions between soil uranium contamination and fertilization with N, P and S on the uranium content and uptake of corn, sunflower and beans, and soil microbiological parameters (Special Issue). Landbauforschung Völkenrode–FAL Agricultural Research, Braunschweig

Rouni PK, Petropoulos NP, Anagnostakis MJ, Hinis EP, Simopoulos SE (2001) Radioenvironmental survey of the Megalopolis lignite field basin. Sci Total Environ 272:261–272

Sahu SK, Tiwari M, Bhangare RC, Pandit GC (2014) Enrichment and particle size dependence of polonium and other naturally occurring radionuclides in coal ash. J Environ Radioact 138:421–426

Sanchez AL, Horrill AD, Howard BJ, Singleton D (1998) Anthropogenic radionuclides in tide-washed pastures bordering the Irish Sea coast of England and Wales. Water Air Soil Pollut 106:403–424

Sawhney BL (1972) Selective sorption and fixation of cations by clay minerals: a review. Clay Clay Miner 20:93–100

Schimmack W, Bunzl K, Kreutzer K, Schierl R (1991) Effects of acid irrigation and liming on the migration of radiocesium in a forest soil as observed by field measurements. Sci Total Environ 101:181–189

Sedlet J (1966) Radon and radium. In: Kolthoff IM, Elving PJ (eds) Treatise on analytical chemistry. Wiley, New York

Selenska-Pobell S, Flemming K, Tzvetelina T, Raff J, Schnorpfeil M, Geissler A (2002) Bacterial communities in uranium mining waste piles and their interaction with heavy metals. In: Merkel B, Planer-Friedrich B, Wolkersdorfer C (eds) Uranium in the aquatic environment. Springer, Heidelberg, Germany

Shanbag P, Choppin GJ (1981) Binding of uranyl by humic acid. Inorg Nucl Chem 43:3369–3372

Sheppard MI (1980) The environmental behaviour of uranium and thorium, AECL-6795. Atomic Energy of Canada Ltd., Pinawa

Sheppard SC, Evenden WG (1988) Critical compilation and review of plant/soil concentration ratios for uranium, thorium and lead. J Environ Radioact 8:255–285

Stamberg K, Venkatesan K, Vasudeva Rau P (2003) Surface complexation modeling of uranyl ion sorption on mesoporous silica. Colloid Surf 221:149–162

Strebl F, Ehlken S, Gerzabek MH, Kirchner G (2007) Behaviour of radionuclides in soil/crop systems following contamination. In: Shaw G (ed) Radioactivity in the terrestrial environment. Elsevier, Amsterdam

Syed HS (1999) Comparison studies adsorption of thorium and uranium on pure clay minerals and local Malaysian soil sediments. J Radioanal Nucl Chem 241:11–14

Torsvik V, Øvreås L (2007) Microbial phylogeny and diversity in soil. In: Van Elsas J, Jansson JK, Trevors JT (eds) Modern soil microbiology. CRC, Baton Rouge, FL

Turner M, Rudin M, Cizdziel J, Hodge V (2003) Excess plutonium in soil near the Nevada Test Site, USA. Environ Pollut 125:193–203

UNSCEAR (2010) Sources and effects of ionizing radiation, UNSCEAR 2008 Report to the General Assembly with Scientific Annexes, Vol. I. New York

USDOE/NV (1992) United States Nuclear Tests, July 1945 through September 1992. United States Department of Energy, Nevada Operations Office (USDOE/NV), Las Vegas

USEPA (1999) Understanding variation in partition coefficients, K_d, values: review of geochemistry and available K_d values for cadmium, cesium, chromium, lead, plutonium, radon, strontium, thorium, tritium (^3H), and uranium, EPA 402-R-99-004B, vol II. Washington, DC

USEPA (2004) Understanding variation in partition coefficient K_d values, Volume III: review of geochemistry and available K_d values for americium, arsenic, curium, iodine, neptunium, radium, and technetium, EPA 402-R-04-002C. Washington, DC

USGS (1994) Natural radioactivity in the environment, USGS Factsheet. Denver, CO

Van den Bygaart AJ, Protz R, McCabe DC (1999) Distribution of natural radionuclides and ^{137}Cs in soils of southwestern Ontario. Can J Soil Sci 79:161–171

Van der Graaf ER, Koomans RL, Limburg J, De Vries K (2007) In situ radiometric mapping as a proxy of sediment contamination: assessment of the underlying geochemical and -physical principles. Appl Radiat Isot 65:619–633

Van Netten C, Morley DR (1983) Uptake of uranium, molybdenum, copper, and selenium by the radish from uranium-rich soils. Arch Environ Health 38:172–175

Vega FA, Covelo EF, Andrade ML, Marcet P (2004) Relationships between heavy metals content and soil properties in mine soil. Anal Chim Acta 524:141–150

Volesky B (1990) Biosorption of heavy metals. CRC, Boca Raton, FL

Waite TD, Davis JA, Payne TE, Waychunas GA, Xu N (1994) Uranium (VI) adsorption to ferrihydrite: application of a surface complexation model. Geochim Cosmochim Acta 58:5465–5478

Watkins BM, Smith GM, Little RH (1999) A biosphere modeling methodology for dose assessment of the potential Yucca mountain deep geological high level radioactive waste repository. Health Phys 76:355–368

Wilford J (2008) Remote sensing with gamma-ray spectrometry. In: McKenzie NJ, Grundy MJ, Webster R, Ringrose-Voase AJ (eds) Guidelines for surveying soil and land resources, 2nd edn. Csiro Publishing, Melbourne

Xu L, Wang Y, Lü J, Lu X, Liu Y, Liu XY (2002) Radioactive contamination of the environment as a result of uranium production: a case study at the abandoned Lincang uranium mine, Yunnan Province, China. Sci China B 45:11–19

Yoshida S, Muramatsu Y, Dvornik AM, Zhuchenko TA, Linkov I (2004) Equilibrium of radiocesium with stable cesium within the biological cycle of contaminated forest ecosystems. J Environ Radioact 75:301–313

Zhang PC, Krumhansl JL, Brady PV (2002) Introduction to properties, sources and characteristics of soil radionuclides. In: Zhang PC, Brady P (eds) Geochemistry of soil radionuclides. Soil Science Society of America, Madison, WI

Modelling Speciation and Distribution of Radionuclides in Agricultural Soils

Volker Hormann

Contents

Abstract The behaviour of radionuclides (and thus their plant availability) in cultivated soils principally depends on soil solution composition and the presence of adsorbing surfaces. Both properties vary with soil type, soil cultivation and climatic conditions. We give an overview of the relevant soil processes and the

---

V. Hormann (✉)
IUP—Institute of Environmental Physics, University of Bremen, D-28359 Bremen, Otto-Hahn-Allee 1, Germany
e-mail: vhormann@physik.uni-bremen.de

C. Walther, D.K. Gupta (eds.), *Radionuclides in the Environment*,
DOI 10.1007/978-3-319-22171-7_4

basic sorption modelling concepts with the emphasis on surface complexation on minerals and humic matter. For estimating speciation and distribution of radionuclides, geochemical codes can be employed. We show an example how modelling can be carried out by using the well-known code PHREEQC and introducing the reference soil concept. Using the example of the UNISECS model, we discuss issues of parametrisation and validation as well as the sources of uncertainty. For selected nuclides, we evaluate the dependence of the distribution coefficient (K_d) on the most important soil parameters.

Keywords Agricultural soils • Speciation • Soil parameters • Sorption • Modelling, PHREEQC • K_d

1 Introduction

Cultivated soils are key entry points for radionuclides into the food chain. Artificial radioisotopes may contaminate those soils by dry and wet deposition as a result of atomic bomb explosions, nuclear accidents (e.g. Chernobyl and Fukushima) or other accidental nuclear releases into the environment. They may also be released from nuclear waste repositories more or less far in the future, migrating through the surrounding rock and subsequently becoming dissolved in groundwater which is frequently used for irrigation and thus introduced into the soil. The groundwater itself may rise carrying the radionuclides to the root zone. Plants are able to incorporate and even accumulate ions and small molecules present in the soil solution via root uptake. Essentials for the amount of activity transferred to plants are not only plant type and activity concentration in the root zone, but also the physicochemical properties of the soil and speciation of the soil solution which play a crucial role because they are governing the bioavailability of the nuclide in question. Sorption and complexation of ions to soil minerals and organic matter are mechanisms which may decrease solution activity and can delay transport drastically. On the other hand, binding of radionuclides to dissolved organic matter (DOM) or colloids in soil solution may enhance their mobility (Tipping 2002; Appelo and Postma 2005).

A lot of these important parameters and processes taking place in soils and on mineral surfaces have already been identified, analysed and quantified. For instance, the solid–liquid distribution coefficient K_d has been experimentally determined (usually in batch experiments) for a variety of nuclides and soil types. The values from the respective publications have recently been compiled and categorised (IAEA 2010). K_d is also being used in risk assessment models like ECOLEGO (Avila et al. 2003) or AMBER (Punt et al. 2005), e.g. to estimate the radiation dose after radionuclide ingestion. Unfortunately, the K_d for a certain nuclide may vary over orders of magnitude even within a single soil category

(IAEA 2010). This could in principle be amended by correlating K_d values with soil parameters like pH or clay content as found experimentally (Gil-García et al. 2009a, b; Vandenhove et al. 2009) and using this correlation for a particular soil. However, this is not feasible if the compiled soil analysis data are not sufficient or only few experimental studies have been performed for a particular radionuclide. Correlations may also be rather poor if additional important soil parameters have not been identified. Moreover, bioavailability is not always well predicted by K_d, for instance, in cases where nuclide speciation is important for plant uptake (Vandenhove et al. 2007b).

In this view, modelling K_d and speciation using geochemical codes may be an attractive alternative to provide data that can be used for estimating plant uptake, thus giving a basis for risk assessment calculations.

2 Important Soil Parameters and Processes

For modelling, it is crucial to identify the soil parameters that largely affect radionuclide distribution and migration. Some parameters may be only relevant for a certain subgroup of nuclides, whereas others are generally important. Physical parameters like porosity or water content have more influence on the migration of the solute than on its solid–liquid distribution unless chemical reactions or surface interactions are taking place on a similar or even slower timescale compared to water flow (Degryse et al. 2009). Here, a short review of the most important parameters is given. Detailed information about soil chemistry and physics can be found in textbooks (Sposito 1989; McBride 1994; Sparks 1999; Scheffer and Schachtschabel 2010).

2.1 Chemical Parameters and Processes

Soils are heterogeneous media, largely composed of a mixture of inorganic minerals, organic matter, water and air.

The mineral composition varies from site to site and not only depends on the chemistry of the underlying bedrock but also on weathering processes and erosion. Minerals with large surface areas that are capable of sorbing or complexing ions are important for modelling, because in almost all cases the radionuclides will be present in free or complexed form. In this respect, the two most important mineral classes are (1) clay minerals and (2) transition metal (mainly iron) oxides, which make up most of the clay fraction (particle size <2 μm) of the soil.

Soil organic matter (SOM) is composed of the decay products of larger organic structures (plant leaves and roots) and is also called ‘humus’. It does not include living organisms like bacteria and fungi which may accumulate radionuclides in some cases (e.g. Parekh et al. 2008; Akai et al. 2013) and which will not be treated here. SOM is also able to complex cations (Tipping 2002) and can be present either as larger immobile particles, thus contributing to radionuclide retention or in solution as dissolved organic matter (DOM) contributing to nuclide mobility. Some nuclides like ^{131}I can also be bound covalently to organic matter, probably mediated by bacterial activity (Christiansen and Carlsen 1991). SOM can also interact with mineral surfaces, possibly blocking mineral binding sites.

The soil solution is the medium where chemical reactions take place, either at surfaces or in the bulk phase. It also carries ions and molecules that may compete with the binding of radionuclides to surfaces or act as complexants which keep them in solution. The composition of the solution is spatially (there may even be differences in samples from a few metres apart (Campbell et al. 1989)) as well as temporally variable (dilution by rainfall events, concentration effects by evaporation, seasonal variations caused by plant activity).

One of the key parameters is the pH value which largely affects solution chemistry as well as surface properties. The redox potential (pe) is important for the chemical state of certain radionuclides like Se (Ashworth et al. 2008) and U (Langmuir 1997). Changes of pe may lead to reactions involving electron transfer (e.g. $Fe^{3+} \rightarrow Fe^{2+} + e^{-}$) and to precipitation or dissolution reactions. For example, as a single (uncomplexed) ion, uranium is usually present in solution as $UO_2{}^{2+}$ under oxic conditions, while its chemical form is the insoluble U^{4+} if the solution is depleted of oxygen (Langmuir 1997) as it is in the case of flooded soils under stagnant ponding (Sposito 1989).

Generally, the soil pores are not totally filled with water because after a rainfall or irrigation event, the water will redistribute due to gravitational and capillary forces. At the soil surface, water may be also removed by evaporation. In any case, air will penetrate the pore system, leaving it unsaturated. Below the soil horizon, the air may be partly depleted of oxygen and enriched with carbon dioxide due to biological processes (Sposito 1989). This, in turn, will have an impact on the soil redox state and thus on soil solution chemistry.

Air present in small pores will have an effect on water transport due to capillarity effects. Some radionuclides (radon) can also be transported via soil air.

2.2 Physical Parameters and Processes

The migration of fallout radionuclides into the root zone is usually mediated by advective flow of water, as the soil solution is the carrier of radionuclides in dissolved or colloidal phase. The vertical water transport velocity depends on a number of physical parameters including soil texture (i.e. clay, silt and sand content), porosity, water content and bulk density. A key parameter is the hydraulic conductivity which can be connected to these parameters by the so-called pedotransfer functions, which have been determined experimentally for a great number of soils (Weynants et al. 2009). In transport calculations, dispersive and for some nuclides, e.g. ^{137}Cs (Kirchner et al. 2009) also diffusive or diffusion-like effects have to be taken into account. For further reading on soil hydrology, textbooks like Kutílek and Nielsen (1994) are recommended.

2.3 Influence of Agricultural Use

While the parameters and processes described in Sects. 2.1 and 2.2 apply to all soils (including undisturbed), the effects of soil management also have to be taken into account. Ploughing mixes the upper soil layer (usually ca. 15–30 cm) and dilutes the total concentration of slowly migrating radionuclides like Cs in this layer. It also aerates the soil and thus increases the degradation of organic matter. Another effect is that it makes the soil susceptible to erosive processes in certain high slope conditions and inappropriate cultivation practices.

Often, lime is applied to soils in order to increase pH, changing the soil solution chemistry. Fertilisers introduce large amounts of ions that may interact with surfaces, e.g. displacement of Cs^+ from clay surfaces by NH_4^+ (Hormann and Kirchner 2002) or act as complexants (PO_4^{3-} with U).

3 Sorption Modelling Concepts

The interactions of radionuclides with solid and/or particulate surfaces present in the soil strongly depend on the chemical and physical properties of its mineral and organic components. For the estimation of the solid–liquid distribution of these elements, models for element–surface interaction have to be applied.

3.1 Empirical Models

The distribution coefficient K_d is defined as the quotient of the radionuclide activity present in (or sorbed to the surface of) the solid phase S and the respective activity C in the soil solution. Its unit is usually given as $l\ kg^{-1}$ and can be determined experimentally (Hilton and Comans 2001). Taking K_d as a proportionality factor between S and C, one gets a curve which is called 'linear isotherm'. In this case, one assumes that adsorption depends exclusively and linearly on solution concentration neglecting all effects originating from surface and soil solution composition. While this may be true for trace concentrations of unionised, hydrophobic organic molecules (Goldberg et al. 2007), for most metal ions and anions (including radionuclides), K_d exhibits a strong dependency on soil parameters like pH or CO_2 partial pressure (IAEA 2010) and therefore varies spatially as well as temporally. Other relations like Freundlich and Langmuir isotherms (McBride 1994) introduce additional fitting parameters and may account for nonlinearity and saturation effects, but still are only applicable for constant chemical and physical conditions.

3.2 Ion Exchange

In general, soil particle surfaces are charged, and in most cases, there is a contribution by a permanent (usually negative) charge and a variable pH-dependent charge. The binding to permanently charged surfaces is called 'unspecific sorption' or 'ion exchange', while binding to variable charge surfaces is called 'specific sorption' or 'surface complexation'.

Cation exchange can be described by a simple exchange reaction between two ions A^{n+} and B^{m+}, where n and m are integers:

$$\frac{1}{n} \cdot A^{n+} + \frac{1}{m} \cdot B - X_m \leftrightarrow \frac{1}{n} \cdot A - X_n + \frac{1}{m} \cdot B^{m+} \tag{1}$$

Here, X is an arbitrary surface group that is capable of binding cations. Usually, the exchange selectivity for an ion A^{n+} is given as the exchange coefficient for sodium (Na):

$$K_{\mathrm{Na}/A} = \frac{[\mathrm{Na} - X][A^{n+}]^{1/n}}{[A - X_n]^{1/n}[\mathrm{Na}^+]} \tag{2}$$

This mechanism is the most important for alkaline and alkaline earth cations and may be relevant for certain trace metal ions like Ni^{2+}, Cd^{2+} and Pb^{2+} (Appelo and Postma 2005), as well as for certain actinides (e.g. Am^{3+} on planar illite sites, Bradbury and Baeyens 2009b). The capability for cation exchange is called 'cation exchange capacity (CEC)' and is expressed in meq kg^{-1} soil. Some soil minerals may also exchange anions, but the anion exchange capacity of soils is generally much lower (Scheffer and Schachtschabel 2010).

3.3 Mineral Surface Complexation Models

A way to account for variable charge surfaces is the use of surface complexation models, which include equations for the binding of ions to reactive surface functional groups like S–OH (where S stands for Fe, Al), present on hydrous oxides and clay minerals. Most models include thermodynamic parameters, namely, the surface potential Ψ and the temperature T. An example for such a thermodynamical equilibrium constant (here: protonation of an S–OH surface group) is given in Eq. (3):

$$K_{+} = \left(\frac{[\mathrm{SOH}_2^{+}]}{[\mathrm{SOH}]\{\mathrm{H}^{+}\}}\right) \exp\left(\frac{F\Psi}{RT}\right) \tag{3}$$

Here, F is the Faraday constant and R is the molar gas constant. $[SOH_2^+]$ and [SOH] are surface group concentrations and $\{H^+\}$ is the proton activity. Similar expressions exist for the deprotonation of an S–OH surface group and complexation reactions with cations or anions (called 'complexation constants'), depending on the model. To date, there are various surface complexation models (SCM) making different assumptions concerning the shape of the surface potential and the complexation reactions to be included. While the constant capacitance model (CCM) assumes a linear decrease of Ψ with distance from the mineral surface, other models like the diffuse layer (DLM) and triple layer (TLM) models include one (DLM) or two (TLM) surface layers and a layer of counter ions which is called 'diffuse layer'. These are so-called two-pK models including two protonation reactions. In the 'one-pK models' (e.g. CD–MUSIC by Hiemstra and van Riemsdijk (1996), where multiple surface sites are distinguished), only one protonation reaction is considered. Some of these models also allow for bi- or tridentate binding. For a more extensive discussion of surface complexation modelling, the review articles by Goldberg et al. (2007) and Groenenberg and Lofts (2014) are recommended. A concise treatment of the double layer calculation is given in Appelo and Postma (2005).

The well-known generalised two-layer model by Dzombak and Morel (1990) includes monodentate binding and two separate ('strong' and 'weak') kinds of sites with different complexation constants. It will be used in the soil model described in Sect. 4.

3.4 Ion Binding of Organic Matter

In many soils and other natural systems, organic matter (OM) plays a significant role for transport and retention of radionuclides. While SCMs for minerals usually include just two or three kinds of surface sites, modelling complexation to OM has to take into account the great complexity of the material. There are two basic approaches to this: (1) assuming a continuous distribution of binding strengths (the NICA–Donnan model by Benedetti et al. 1996) and (2) using an assemblage of discrete binding sites (the humic ion-binding (HIB) model VI (Tipping 1998)). In both cases, only cation binding is considered because the OM surfaces exhibit negative charge at all pH values (Tipping 2002).

While the NICA–Donnan model gives the amount of a bound species in a closed analytical form with fitted parameters, model VI assumes two site types A and B, where each type has a distribution of sites with complexation constants K given by

$$\log K(i) = \log K_{\mathrm{MA}} + \frac{2i-5}{6}\Delta LK_{A1} \tag{4}$$

with $i = 1...4$ for site type A (associated with carboxyl groups) and

$$\log K(i) = \log K_{\mathrm{MB}} + \frac{2i-13}{6}\Delta LK_{B1} \tag{5}$$

with $i = 5...8$ for site type B (associated with phenolic groups). K_{MA} and K_{MB} are intrinsic equilibrium constants different for each cation. ΔLK_{A1} and ΔLK_{B1} are fitting parameters, which were shown to be equal for all metals (Tipping 2002). These formulas only describe monodentate binding; for bi- and tridentate binding, additional expressions are given, introducing an additional metal-specific fitting parameter ΔLK_2. In total, there are 80 binding sites, each having its own abundance. Equilibrium constants and fitting parameters for a number of cations have been derived for binding to both fulvic and humic acids. Electrostatic interaction is accounted for by a factor $\exp(2PZ\ \log(I))$, where Z is the charge on the humic substance in eq g^{-1}, I is the ionic strength of the solution and P is an adjustable coefficient. For details, see Tipping (2002).

3.5 Model Parametrisation

In principle, the complexation constants for a model have to be determined experimentally for each mineral phase to be considered. This is done by fitting the amount of adsorbed activity to either pH or to the activity concentration in solution at constant pH. If there are no experimental data, complexation constants can often be estimated by so-called linear free energy relationships (LFER). For example, in the case of transition metal cation complexation described by the model by Dzombak and Morel (1990) (see above), linear relationships between surface complexation constants $\log K_{\mathrm{i}}$ and the ions' first hydrolysis constants $\log K_{\mathrm{OH}}$ (for the reaction $M^{n+} + OH^- \leftrightarrow MOH^{(n-1)+}$, where M^{n+} is the metal cation) have been found both for weak and strong sites. If $\log K_i$ has not been determined for a specific transition metal cation, it may be estimated by using the respective LFER if $\log K_{\mathrm{OH}}$ is known. For further information, see Appelo and Postma (2005) and Tipping (2002).

The density of surface sites is one of the most important modelling parameters. It can either be calculated by the use of crystal dimensions if a pure phase is modelled or be determined experimentally by a wide range of methods including tritium exchange, acid–base titration and analysis of sorption isotherms (Davis and Kent 1990). As an example, the estimation of site densities on montmorillonite surfaces is described in Baeyens and Bradbury (1997). Surface areas are usually determined by the Brunauer–Emmett–Teller N_2 adsorption method (McBride 1994).

3.6 Assemblage Models

For solid–liquid distribution modelling, it has to be considered that each soil has its own characteristic mineral and organic composition. There are two basic concepts to model assemblages: the *general composite* (GC) approach and the *component additive* (CA) approach.

The GC approach is the most useful for predictive purposes if a specific field (sampling) site has to be considered and a large set of experimental data (titration and adsorption curves for the relevant radionuclides) is present. In this case, one can define 'generic' surface groups which represent the average soil surface properties, and the chosen model can be parametrised. Within the range of chemical conditions where the experimental data have been taken, predictions should be valid. However, for other field sites and/or chemical conditions, they will be questionable.

Following the CA approach, one assumes that the behaviour of a soil can be described by the sum of its most active pure components. If models and sufficient thermodynamic databases for these pure components exist, it is technically possible to predict the behaviour of the total assemblage. This is most convenient in cases where it is not possible to do extensive experimental work or to make estimations for a broader range of soil types. The main disadvantage is that interactions between the components (e.g. binding of humic material to mineral surfaces, thus reducing the mineral's number of accessible binding sites) are not taken into account. Moreover, in many natural systems, one finds a broad variety of minerals that often have not been investigated yet. Even so, by taking well-characterised minerals and organic substances as proxies for the most important soil components, one may predict the K_d of radionuclides for a certain soil type under given conditions with much higher accuracy than those listed in documents such as IAEA (2010) for general soil types like sand or clay. In the next paragraph, it will be shown how this can be accomplished.

4 Constructing a CA Soil Model

To perform calculations for K_d estimations, three basic components have to be chosen and assembled:

- A physicochemical speciation code for solving the set of equilibrium speciation equations
- A suitable combination of model components
- An appropriate set of thermodynamical data

The components have to be then implemented in the code (the interface is usually given as an input file) and have to be properly parametrised to give an optimal representation for the system to be modelled. If a code (e.g. PHREEQC (Parkhurst and Appelo 2004)) allows for performing user defined calculations using simulation data, this is convenient for direct calculation of the distribution coefficient.

4.1 Speciation Code and Representative Soil Components

Assuming that it is neither intended to write the necessary codes 'from scratch' nor to do the experimental work for calibrating surface complexation models, one has to assemble the necessary tools from the literature. Before starting, it is not only important to get a clear picture of the model's intended use in the immediate future, but also to think of possible applications further ahead. In the case of the CA model developed by Hormann and Fischer (2012, 2013) on behalf of the German Federal Agency of Radiation Protection (henceforth called 'UNISECS[1] model'), two properties have been emphasised: (1) easy expandability for the inclusion of further nuclides and (2) options for doing transport calculations or for being coupled to hydrological transport codes. For these purposes, one starts by looking for a speciation code that includes (or is able to include) various thermodynamical databases that may be modified and expanded in order to perform the appropriate solution chemistry calculations. The code also has to be capable of including surface complexation and exchange models for doing solid–liquid distribution estimations. Some popular codes are FITEQL (Herbelin and Westall 1996), ECOSAT (Keizer and Van Riemsdijk 1998), Visual Minteq (Gustafsson 2010) and PHREEQC (Parkhurst and Appelo 2004).

Before choosing the speciation code, the key components of the model system and models that describe sorption on these components have to be determined. For the UNISECS model, four components, their representative materials and respective models (given in parentheses) have been identified:

- Soil clay (illite, Bradbury and Baeyens 2000, 2009a, b)
- Hydrous oxides (ferrihydrite, Dzombak and Morel 1990)
- Immobile organic matter (humic acid, Tipping 1998)
- Dissolved organic matter (fulvic acid, Tipping 1998)

Clay minerals and hydrous oxides are significant soil components and have both high sorption capacities and large specific surface areas. On the other hand, it is probable that larger particles like quartz grains make only minor contributions to the sorptive capacity of a soil. The required models for illite and ferrihydrite (two-pK non-electrostatic model and diffuse double layer model, respectively) are already implemented in the geochemical code PHREEQC and can be readily parametrised.

---

[1] Because it had originally been developed to estimate the distribution of the long-lived radionuclides ^{238}U, ^{63}Ni, ^{79}Se and ^{135}Cs in agricultural soils (Hormann and Fischer 2012).

Organic matter will be present in the immobile form (e.g. as coatings or attached to soil particles) or in solution (dissolved organic matter, DOM). As humic acids have a larger average molecular weight than fulvic acids, they will tend to accumulate in the immobile phase (e.g. by coagulation). Thus, it seems to be appropriate to phase-separate these two humic substances as a first approximation. The humic ion-binding model can be included in PHREEQC by using the diffuse double layer model implementation and by replacing the electrostatic interaction factor described above by the Boltzmann factor from Eq. (3) (Appelo and Postma 2005).

4.2 Thermodynamical Data

Geochemical speciation codes are usually equipped with a database containing the thermodynamical constants for reactions in solution and on surfaces. The quality of a database depends on careful selection of data from the literature and on a thorough check for chemical consistency. PHREEQC provides several databases from different sources, but the authors emphasise that these data have not been checked for consistency and consider them as preliminary (Parkhurst and Appelo 2004). Especially when modelling radionuclides, it is possible that not all relevant reactions for a certain radionuclide are included in the database. In this case, these data have to be taken from the literature and added to the input or database file.

For the UNISECS model, we chose the NAGRA/PSI database (Hummel et al. 2002), which was assembled to support the safety assessment of a nuclear waste repository and also includes, as the authors state, 'elements commonly found as major solutes in natural waters'. It contains a large amount of radionuclide data, has been checked for consistency and is supplied in a format compatible with PHREEQC.

4.3 Model Parameters

Once the thermodynamical data have been implemented, the physicochemical characteristics of the system have to be specified. The most important are:

- Number of surface binding sites
- Soil solution composition
- Redox state and oxygen content
- Solid phases
- CO_2 pressure

In most of the surface binding models, the surface density of binding sites (in sites per m^2) and the specific surface area (in $m^2\ g^{-1}$) are given for specific minerals. These values must be treated with caution because they usually have been determined in the laboratory using model substances which may not have the same properties like the respective minerals present in the soil. Moreover, the number of sites blocked by other soil components (humic substances on mineral surfaces) may not be negligible. If the geochemical code requires the number of surface sites n_{w} per kg soil solution, but only the number n_{d} per kg dry mass is known, one can calculate n_{w} with the help of the dry soil density ρ and the water-filled porosity ϕ:

$$n_w = n_d \cdot \frac{\rho}{\Phi} \tag{6}$$

If not known, ρ and ϕ may be calculated from soil texture data using the so-called pedotransfer functions (Rawls et al. 1982; Saxton et al. 1986).

When modelling with a geochemical code, the composition of the solution is highly important for the following reasons:

1. The surface charge in surface complexation models usually depends on the ionic strength and the pH of the solution.
2. Ions in solutions will compete for surface binding sites (thus binding constants for major ions such as Fe^{3+} on humic acid or $PO_4{}^{3-}$ on hydrous oxides should be available).
3. Some dissolved species may form complexes with the radionuclide in question that are not or only weakly bound to surfaces.

If the soil solution composition is not available, it can be estimated using values from the literature (Scheffer and Schachtschabel 2010). If a radioactive contamination is introduced, in many cases, the activity[2] is given in Bq kg^{-1} soil. As the geochemical code usually requires a mass or concentration as input, this has to be converted using the specific activity for the respective nuclide. The oxygen content and thus the redox state of the solution will have an influence on chemistry and oxidation state of many ions (see above) and therefore has to be specified. In PHREEQC, pe can be adjusted, for instance, by consumption of dissolved oxygen by organic matter (Appelo and Postma 2005).

For dynamical simulations (e.g. pe changes and/or transport), solid phases may have to be defined, because they may remove ions from solution by precipitation or introduce new ions by dissolution. Selenium in solution, for example, will be precipitated as elemental selenium or selenide when submitted to anoxic conditions (Ashworth et al. 2008, Masscheleyn et al. 1990). The definition of solid (non-sorptive) phases is also useful for determining the concentration of major ions (e.g. equilibration of the solution with gibbsite for estimating the aluminium concentration). Carbonate and hydroxycarbonate are important major ions that act as a buffer and form complexes with cations. The concentration of these ions varies with the CO_2 pressure which itself depends on biological activity.

[2] Not to be confused with the chemical activity.

4.4 Calculating the Distribution Coefficient

When all soil parameters have been adjusted, the simulation can in principle be started. Usually, one would first equilibrate the surface ensemble with the uncontaminated soil solution to create 'standard conditions' in the sense that a realistic equilibrium distribution of major ions on the surfaces is calculated. Then, depending on the scenario, the contamination is introduced and a new equilibrium calculation is performed. The distribution coefficient K_d can be calculated by

$$K_\mathrm{d} = \frac{\Phi}{\rho} \cdot \frac{\sum_i a_{i,\,\mathrm{solid}}}{\sum_j a_{j,\,\mathrm{solution}}}, \tag{7}$$

where Φ is the water-filled porosity and ρ is the dry soil density. $a_{i,\mathrm{solid}}$ and $a_{j,\mathrm{solution}}$ are the activities of the radionuclide in its chemical form i associated with the solid phase and j in solution, respectively. This definition is somewhat ambiguous as the term 'solid phase' is not clearly defined. If a fraction of the activity has been precipitated during the equilibration, it is generally not clear, whether it is present in particulate or colloid form in solution (and thus transportable) or bound to the soil solid. If K_d is experimentally determined, frequently the activity of the extracted soil solution is measured; thus, precipitates may be attributed to the liquid phase, leading to a different distribution coefficient. In the UNISECS model, all precipitates have been assigned to the solid phase.

Note that in this case, K_d is calculated for the state of equilibrium. In most cases, it is assumed that the kinetics of the sorption/complexation reactions is fast (meaning in the order of milliseconds or seconds), a condition that is usually met in soils (Scheffer and Schachtschabel 2010). Still, in some cases, the reaction may be slow and diffusion controlled, like the exchange of alkali ions on clay minerals, which is in the order of hours (Sparks 1999).

5 Verifying and Validating the Model

Once a model has been implemented, it has to be checked for consistency, and it has to be made sure that it meets all of its specifications. This procedure is called verification and it should be performed before the validation process. Typical verification procedures may involve summing the activity of all species used for calculation of the K_d (which should result in the added activity) or checking for charge balance, pH and redox state after the equilibration.

Validating the model includes testing its ability to reproduce experimental results achieved in the laboratory under controlled conditions. This means that preferably all input data for the simulation should be known. As this is not always the case (if it is not feasible to perform experiments by oneself), there are several possible levels of validation, depending on the number of unknown parameters. In the following subsections (5.1 and 5.2), two validation procedures performed for the UNISECS model will be presented. More information about these procedures including an additional test for cesium modelling can be found in Hormann and Fischer (2013).

5.1 Comparison of Simulations with Averages of Experimental K_d Values for Two Soil Types

In the IAEA Technical Reports Series No. 472 (IAEA 2010), the best estimates of solid–liquid distribution coefficients are given for a number of radionuclides. These values have been derived from field and laboratory studies and are given as the geometric mean for four generic soil types. In most cases, the ranges of the K_d values span one or two orders of magnitude. The validity of a model may be checked by finding the physicochemical properties of a 'typical' or 'representative' soil type, simulating the distribution under 'normal' conditions using a soil solution composition derived from average field values and comparing the result with the best estimate for the respective nuclide.

The Refesol (reference soil) concept (Kördel et al. 2009) developed for establishing a reference system for chemical testing of soil presents an attractive possibility of choosing soils which are taken as representative for some of the soil types used in the IAEA report. The Refesols are well characterised and provide all the input parameters necessary for simulation, except for the soil solution composition, which can be derived by average values given in Scheffer and Schachtschabel (2010).

Using these parameters and the database as well as the complexation constants discussed in the previous sections of this chapter, K_d values have been calculated for a typical loamy soil (Refesol No. 2) and a typical sandy soil (Refesol No. 4). In Fig. 1, these values are compared with the best K_d estimates and the corresponding experimental ranges given in IAEA (2010). The calculated values are close to the best estimates, the deviations being always considerably less than an order of magnitude. Considering the ranges of experimental values, the simulations are fitting remarkably well. This demonstrates the model's ability of performing meaningful equilibrium K_d estimations at least for the elements U, Ni, Se and Cs in two generic soil types.

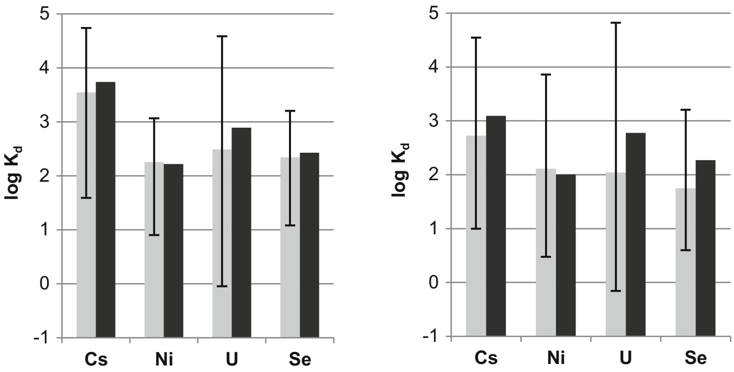

Fig. 1 Comparison of the IAEA best K_d estimates (*light grey*) and their ranges (*whiskers*) for Cs, Ni, U and Se with results calculated using the UNISECS model (*dark grey*) for a loamy soil (*left*) and a sandy soil (*right*) (Adapted from Hormann and Fischer 2013)

5.2 Simulating Experimental Uranium Distributions in Batch Experiments with Several Specified Soils

Having shown the general predictive capability of the UNISECS model, the next question is whether it is also able to estimate the solid–liquid activity distribution in specified soils. Uranium is an element that interacts with all model components, and the high variability of its distribution coefficient makes it particularly suitable for validating the model. Thus, a study has been chosen where 18 thoroughly characterised soils were used for determining the distribution of uranium after contamination of soil samples in batch experiments (Vandenhove et al. 2007a). These soils covered a wide range of soil parameters affecting K_d, such as pH, Fe and Al oxide and hydroxide content, clay content and organic carbon. The soil solutions had been extracted after 4 weeks of equilibration and subsequently analysed for uranium.

For each soil, the uranium concentration has been calculated by the UNISECS model using the soil component and soil solution data given in the experimental study. As shown in Fig. 2, the UNISECS estimations are quite close to the experimental results, and the largest deviation is by a factor of 2.4, which is again remarkable considering the fact that CO_2 pressure and dissolved organic matter content are not given in the experimental study and therefore have to be estimated.

5.3 Sources of Uncertainties

Even if validation efforts give promising results as shown above, a model still has to be used with caution. As soils are very complex systems, in many cases, their

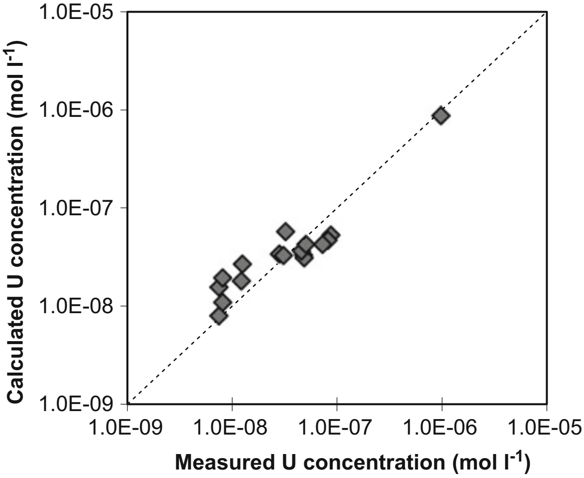

Fig. 2 Comparison of measured (Vandenhove et al. 2007a) U concentration in soil solution with results from simulations with the UNISECS model (Hormann and Fischer 2013, with permission from Elsevier)

chemical composition and behaviour may not be adequately taken into account, especially if unconsidered minerals are present in the soil that also have strong complexing abilities but different relative selectivities concerning the relevant nuclides. Considerations under which circumstances certain minerals will precipitate (e.g. oversaturation of gibbsite) may also be an issue.

Another source of uncertainty is the parametrisation of the model component. As an example, the number of surface sites is usually assumed to be constant. In real soils, the actual composition of the sorbent and thus its surface structure may be different. Moreover, a significant fraction of these sites may be blocked by other soil components (e.g. organic matter) and thus not be accessible for sorption. The surface sites themselves may be affected by the mineral's interior structure, allowing sorbed ions to diffuse into the crystallite, thus rendering the sorption partially irreversible as is the case with Cs on illite (Comans and Hockley 1992). However, these effects may only be significant after longer times (weeks or months).

Of course, the assumed soil composition is also a source of uncertainty, and thus, incorrect parametrisation with respect to soil parameters may cause misinterpretations of the simulation results. This is especially important if a parameter has to be estimated or if it is sensitive to climatic conditions. To give an overview, Table 1 qualitatively shows the most significant effects of parameter variation on the distribution coefficient.[3] Parameter ranges occurring in cultivated soils (Scheffer and Schachtschabel 2010) are compared to the calculated corresponding K_d variations for the Refesol 2 and the elements U, Ni, Se and Cs, respectively. Details are given in Hormann and Fischer (2013).

[3] Corresponding calculations were performed for clay, ferrihydrite, pCO_2, pH, DOM and organic matter.

Table 1 Simulated soil parameter ranges and corresponding K_d ranges

Element	Parameter and range	K_d range[a]	Correlation
U	pCO_2 (1.5–3.5)	80–5900	Positive
	pH (4–8)	30–1200	Non-monotonous[b]
Ni	pH (4–8)	35–1000	Positive
	Organic C (0–5 %)	50–500	Positive
	DOM (0–200 mg l^{-1})	400–1000	Negative
Se	Ferrihydrite (0–14 mg kg^{-1})	0–700	Positive
	pH (4–8)	15–950	Non-monotonous[c]
	pCO_2 (1.5–3.5)	100–600	Positive
Cs	Clay content (2–50 %)	550–19,000	Positive

[a]Values given in l kg^{-1}
[b]Maximum at pH = 6
[c]Minimum at pH = 4.5

It is obvious that the four elements exhibit different sensitivities toward the individual parameters reflecting the unique behaviour of each element in the pedosphere. If two or more parameters are varied, the effects may in some cases be potentiated, and in other cases, they may cancel each other out.

6 Conclusion

In summary, we have shown that it is possible to perform reasonable predictions of the solid–liquid distribution of radionuclides in agricultural soils, especially if generic soil types are considered. However, physicochemical parameters as well as thermodynamical data for these elements and for the most significant soil components must be available. The composite model should be extensively checked for consistency and validity. Still, one always has to be aware of the sources of uncertainty and their consequences for K_d estimation. For the simulation of individual soils and the interpretation of the results, even more caution is advised.

References

Akai J, Nomura N, Matsushita S, Kudo H, Fukuhara H, Matsuoka S, Matsumoto J (2013) Mineralogical and geomicrobial examination of soil contamination by radioactive Cs due to 2011 Fukushima Daiichi nuclear power plant accident. Phy Chem Earth, Parts A/B/C 58:57–67

Appelo CAJ, Postma D (2005) Geochemistry, groundwater and pollution, 2nd edn. CRC, Boca Raton, FL

Ashworth DJ, Moore J, Shaw G (2008) Effects of soil type, moisture content, redox potential and methyl bromide fumigation on K_d values of radio-selenium in soil. J Environ Radioact 99:1136–1142

Avila R, Broed R, Pereira A (2003) Ecolego—a Toolbox for radioecological risk assessments. In: International conference on protection of the environment from the effects of ionising radiation, 6–10 October 2003, Stockholm, Sweden

Baeyens B, Bradbury MH (1997) A mechanistic description of Ni and Zn sorption on Na-montmorillonite Part I: Titration and sorption measurements. J Contam Hydrol 27:199–222

Benedetti MF, van Riemsdijk WH, Koopal LK, Kinniburgh DG, Goody DC, Milne CJ (1996) Metal ion binding by natural organic matter: from the model to the field. Geochim Cosmochim Acta 60:2503–2513

Bradbury MH, Baeyens B (2000) A generalised sorption model for the concentration dependent uptake of caesium by argillaceous rocks. J Contam Hydrol 42:141–163

Bradbury MH, Baeyens B (2009a) Sorption modelling on illite Part I: titration measurements and the sorption of Ni, Co, Eu and Sn. Geochim Cosmochim Acta 73:99–1003

Bradbury MH, Baeyens B (2009b) Sorption modelling on illite. Part II: actinide sorption and linear free energy relationships. Geochim Cosmochim Acta 73:1004–1013

Campbell DJ, Kinniburgh DG, Beckett PHT (1989) The soil solution chemistry of some Oxfordshire soils: temporal and spatial variability. J Soil Sci 40:321–339

Christiansen JV, Carlsen L (1991) Enzymatically controlled iodination reactions in the terrestrial environment. Radiochim Acta 52–53:327–333

Comans RNJ, Hockley DE (1992) Kinetics of cesium sorption on illite. Geochim Cosmochim Acta 56:1157–1164

Davis JA, Kent DB (1990) Surface complexation modeling in aqueous geochemistry. Rev Miner Geochem 23:177–260

Degryse F, Smolders E, Parker DR (2009) Partitioning of metals (Cd, Co, Cu, Ni, Pb, Zn) in soils: concepts, methodologies, prediction and applications–a review. Eur J Soil Sci 60:590–612

Dzombak DA, Morel FMM (1990) Surface complexation modeling: hydrous ferric oxide. Wiley-Interscience, New York

Gil-García C, Rigol A, Vidal M (2009a) New best estimates for radionuclide solid–liquid distribution coefficients in soils. Part 1. Radiostrontium and radiocaesium. J Environ Radioact 100:690–696

Gil-García C, Tagami K, Uchida S, Rigol A, Vidal M (2009b) New best estimates for radionuclide solid–liquid distribution coefficients in soils. Part 3: miscellany of radionuclides (Cd, Co, Ni, Zn, I, Se, Sb, Pu, Am, and others). J Environ Radioact 100:704–715

Goldberg S, Criscenti LJ, Turner DR, Davis JA, Cantrell KJ (2007) Adsorption–desorption processes in subsurface reactive transport modeling. Vadose Zone J 6:407–435

Groenenberg JE, Lofts S (2014) The use of assemblage models to describe trace element partitioning, speciation, and fate: a review. Environ Toxicol Chem 33:2181–2196

Gustafsson PJ (2010) Visual MINTEQ (Version 3.0): an equilibrium speciation model that can be used to calculate equilibrium metal speciation. http://vminteq.lwr.kth.se/ Accessed 29 April 2015

Herbelin AL, Westall JC (1996) FITEQL: A computer program for determination of chemical equilibrium constants from experimental data. Department of Chemistry, Oregon State University, Corvallis, Oregon (1996) 97331

Hiemstra T, van Riemsdijk WH (1996) A surface structural approach to ion adsorption: the charge distribution (CD) model. J Colloid Interf Sci 179:488–508

Hilton J, Comans RNJ (2001) Chemical forms of radionuclides and their quantification in environmental samples. In: Van der Stricht E, Kirchmann R (eds) Radioecology, radioactivity and ecosystems. Fortemps, Liège

Hormann V, Fischer HW (2012) Bericht für das Vorhaben BfS 3609S50005. In: Fachliche Unterstützung des BfS bei der Erstellung von Referenzbiosphärenmodellen für den radiologischen Langzeitsicherheitsnachweis von Endlagern—Modellierung des Radionuklidtransports in Biosphärenobjekten. Universität Bremen. Endbericht des Teilprojekts Boden, Landesmessstelle für Radioaktivität (in German)

Hormann V, Fischer HW (2013) Estimating the distribution of radionuclides in agricultural soils—dependence on soil parameters. J Environ Radioact 124:278–286

Hormann V, Kirchner G (2002) Prediction of the effects of soil-based countermeasures on soil solution chemistry of soils contaminated with radiocesium using the hydrogeochemical code PHREEQC. Sci Total Environ 289:83–95

Hummel W, Berner U, Curti E, Pearson FJ, Thoenen T (2002) Nagra/PSI chemical thermodynamic data base 01/01, NAGRA Technical Report 02–16. Wettingen, Switzerland

IAEA (2010) Technical reports series No. 472: handbook of parameter values for the prediction of radionuclide transfer in terrestrial and freshwater environments. Vienna

Keizer MG, Van Riemsdijk WH (1998) ECOSAT. Technical Report. Department Soil Science and Plant Nutrition. Wageningen Agricultural University, Wageningen, The Netherlands

Kirchner G, Strebl F, Bossew P, Ehlken S, Gerzabek MH (2009) Vertical migration of radionuclides in undisturbed grassland soils. J Environ Radioact 100:716–720

Kördel W, Peijnenburg W, Klein CL, Kuhnt G, Bussian BM, Gawlik BM (2009) The reference-matrix concept applied to chemical testing of soils. Trends Analyt Chem 28:51–63

Kutílek M, Nielsen DR (1994) Soil hydrology. Catena, Cremlingen-Destedt

Langmuir D (1997) Aqueous environmental geochemistry. Prentice Hall, New Jersey

Masscheleyn PH, Delaune RD, Patrick WH Jr (1990) Transformations of selenium as affected by sediment oxidation-reduction potential and pH. Environ Sci Technol 24:91–96

McBride MB (1994) Environmental chemistry of soils. Oxford University Press, New York, Oxford

Parekh NR, Poskitt JM, Dodd BA, Potter ED, Sanchez A (2008) Soil microorganisms determine the sorption of radionuclides within organic soil systems. J Environ Radioact 99:841–852

Parkhurst DL, Appelo CAJ (2004) PHREEQC: a computer program for speciation, batch reaction, one dimensional transport, and inverse geochemical calculation. User Guide to PHREEQC. USGS Water-Resources Investigation Report 99–4259

Punt A, Smith G, Herben GM, Lloyd P (2005) AMBER: a flexible modelling system for environmental assessments, Proceedings of the Seventh International Symposium of the Society for Radiological Protection, Cardiff, 12–17 June 2005

Rawls WJ, Brakensiek DL, Saxton KE (1982) Estimation of soil water properties. Trans ASAE 25:1316–1320

Saxton KE, Rawls WJ, Romberger JS, Papendick RJ (1986) Estimating generalized soil-water characteristics from texture. Soil Sci Soc Am J 50:1031–1036

Scheffer F, Schachtschabel P (2010) Lehrbuch der Bodenkunde, 16th edn. Spektrum Akademischer Verlag, Heidelberg, Germany

Sparks DL (1999) Soil physical chemistry, 2nd edn. CRC, Boca Raton, FL

Sposito G (1989) The chemistry of soils. Oxford University Press, New York, Oxford

Tipping E (1998) Humic ion-binding model VI: an improved description of the interactions of protons and metal ions with humic substances. Aquat Geochem 4:3–47

Tipping E (2002) Cation binding by humic substances. Cambridge University Press, Cambridge, UK

Vandenhove H, Van Hees M, Wouters K, Wannijn J (2007a) Can we predict uranium bioavailability based on soil parameters? Part 1: effect of soil parameters on soil solution uranium concentration. Environ Pollut 145:587–595

Vandenhove H, Van Hees M, Wannijn J, Wouters K, Wang L (2007b) Can we predict uranium bioavailability based on soil parameters? Part 2: soil solution uranium concentration is not a good bioavailability index. Environ Pollut 145:577–586

Vandenhove H, Gil-García C, Rigol A, Vidal M (2009) New best estimates for radionuclide solid–liquid distribution coefficients in soils. Part 2. Naturally occurring radionuclides. J Environ Radioact 100:697–703

Weynants M, Vereecken H, Javaux M (2009) Revisiting Vereecken Pedotransfer functions: introducing a closed-form hydraulic model. Vadose Zone J 8:86–95

Radiotracers as a Tool to Elucidate Trace Element Behaviour in the Water–Sediment Interface

Katia N. Suzuki, Edimar C. Machado, Wilson Machado, Luis F. Bellido, Alfredo V.B. Bellido, and Ricardo T. Lopes

Contents

Abstract Behavioural trends of trace elements in the water–sediment interface of diverse aquatic systems have been elucidated by using radiotracer experiments. These experimental data have improved: (1) the comprehension on the biogeochemical mechanisms, (2) estimations of amounts and kinetics of the transfers across the interface and (3) the characterisation of the role of sediments as sinks for the studied elements. Many efforts have been found in the scientific literature through the use of radiotracers to evaluate the role of biological activity (mainly by bioturbation) in determining trace element behaviour, evidencing that this activity can be a major factor of influence on trace element exchanges across water–sediment interfaces. Moreover, biogeochemical studies with radiotracers definitely help in elucidating mechanisms, pathways, bioavailability and uptake by aquatic organisms. Furthermore, radiotracer percolation experiments within upper layers of

K.N. Suzuki (✉) • W. Machado • A.V.B. Bellido
Instituto de Química, Universidade Federal Fluminense, Niterói, RJ 24020-007, Brazil
e-mail: ksuzuki@id.uff.br

E.C. Machado
Instituto Federal de Educação, Ciência e Tecnologia do Rio de Janeiro, Nilópolis, RJ 26530-060, Brazil

L.F. Bellido
Instituto de Radioproteção e Dosimetria, CNEN, Rio de Janeiro, RJ 22783-127, Brazil

R.T. Lopes
Laboratório de Instrumentação Nuclear, COPPE, Universidade Federal do Rio de Janeiro, Rio de Janeiro, RJ 21945-970, Brazil

C. Walther, D.K. Gupta (eds.), *Radionuclides in the Environment*,
DOI 10.1007/978-3-319-22171-7_5

sediments are strongly recommended for intertidal ecosystems, since vertical tidal variability must be taken into account, besides conventional diffusion-based approach. Nevertheless, there is still a lack of data on the role of chemical speciation in such studies. Such behavioural aspects of chemical speciation deserve further attention in order to improve: predictions on environmental risk assessment for toxic elements, evaluations of the applicability and suitability of potential biological monitors for trace element contamination and predictions on trace element speciation and bioavailability sensitivity due to global environmental changes.

Keywords Radiotracer • Kinetics • Water–sediment interface • Aquatic systems

1 Introduction

Radiotracer techniques have been recognised as an effective tool for trace element biogeochemical studies in aquatic systems, providing to carry out experiments that can help in elucidating mechanisms, speciation, process reversibility and kinetics of trace element transfers and transformations (Hatje et al. 2003; Payne et al. 2004; Croot et al. 2011). In the study of reaction kinetics, it is necessary to follow the temporal concentration of a given chemical species, which can be affected by complex reactions with other constituents of the aquatic system. Conventional methods may imply in potential interferences on the evaluated process, limiting the reliability of kinetics evaluation along with experimental approaches. On the other hand, radiotracer techniques can improve such evaluations, as have been evidenced by a number of studies published in the last decades (Hall et al. 1989; Barros et al. 2004; Machado et al. 2008). These techniques can be useful tools, for example, in elucidating the behaviour of trace elements in the water–sediment interface, by using microcosm experiments.

As alternatives to classical experimental approaches, in which the interaction and spatial–temporal variability in physical, chemical and biological factors are difficult to be investigated, relatively simple and low-cost radiotracer experiments have been performed in order to elucidate these interactions and spatial–temporal variability that can influence the behaviour of trace elements in a wide range of aquatic systems, including freshwater (Ciffroy et al. 2001; IAEA 2010) and coastal and marine environments (Bradshaw et al. 2006; Cournane et al. 2010). In this book chapter, we describe some of our achievements to answer the following questions by using radiotracer experiments, such as: How do sediment physical, geochemical and physicochemical properties affect the behaviour of different trace elements? How do microbial, faunal and vegetation activities affect this behaviour? We do not provide here an extensive review on trace dynamics across the water–sediment interface. Rather, we examine integrated results of past studies on the processes possibly controlling the behaviour of trace elements of environmental concern in such interfaces, such as Ba, Cd, Co, Cr, Cs, Cu, Hg, Ni and Zn.

2 Experimental Studies on Sediment–Water Exchanges of Radiotracers

Most studies performed since the 1990s have employed experiments under laboratory conditions to evaluate radiotracer behaviour across and near the water–sediment interfaces (Petersen et al. 1998; Barros et al. 2004; Suzuki et al. 2014), while benthic chamber apparatus under field conditions were more applied until the late 1980s (Santschi et al. 1984; Sundby et al. 1986; Hall et al. 1989). These approaches have allowed the assessment of the bioavailability of toxic trace elements, such as ^{203}Hg and ^{109}Cd as tracers for metal contaminant behaviour (Schaanning et al. 1996), and ^{141}Ce nanoparticles (Zhang et al. 2012), which are information very important to improve predictions on the risk assessment of trace elements' deleterious effects in the aquatic ecosystems.

An experimental column apparatus employed for microcosm radiotracer studies with an obtained result for ^{65}Zn is shown in Fig. 1 (Machado et al. 2008). The results provided evidences for the effects of sediments under the influence of mangrove plants on ^{65}Zn removal from overlying water in comparison with data from bare sediments collected in the tidal channel that drains the studied mangrove forest. These data indicate that after the Zn flux into the sedimentary environments, mangrove forest sediments allowed a lower vertical mobility of Zn into subsurface

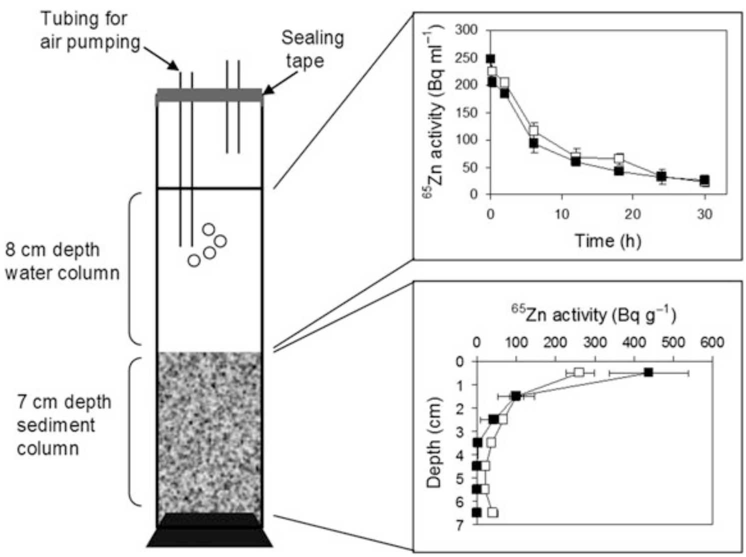

Fig. 1 Schematic diagram of experimental apparatus used to evaluate the ^{65}Zn removal from tidal water by coastal sediments, with insertions of results on the temporal variability of ^{65}Zn activities in overlying waters during 30 h experiments and depth variability of ^{65}Zn activities within sediments at the end of these experiments (means ± SE; $n = 3$). *Closed symbols* mangrove forest sediment cores. *Open symbols* tidal creek sediment cores. Figure reproduced from Machado et al. (2008)

layers (reaching 3 cm depth) than observed for creek sediments (reaching 7 cm depth), suggesting a more efficient retention of this metal by surface sediment layers of the mangrove forest. This effect is in agreement with theoretical assumptions on the large capacity of mangrove sediments to retain trace elements due to complexation with organic matter and association with metal sulphides, which may favour the role of sediments as trace element sinks (Lacerda et al. 1991; Machado et al. 2002; Alongi et al. 2003). On the other hand, a preferential retention of radiotracers within a thin surface layer has been observed in almost all radiotracer studies for most trace elements (Hall et al. 1989; Petersen et al. 1998; Machado et al. 2012), which may allow a greater exposure of the trace elements recently incorporated by these sediments to remobilisation by physical or biological disturbances of upper layers, affecting the net burial rate of the elements of interest.

3 Biological Effects

Results from the literature have evidenced that experimental radiotracer approaches are an important tool in evaluating the ability of aquatic sediments to remove and to retain trace metals transported by overlying waters. Besides the disturbances on the sediment floor due to bioturbation that would be not favourable to trace element retention within sediments, another important example of biological influence is that benthic fauna can promote sediment mixing and the construction holes and channels along with trace element diffusion into deeper layers may be enhanced (Santschi et al. 1984; Osaki et al. 1997; Bradshaw et al. 2006). This higher depth penetration may allow its accumulation under sedimentary conditions more stable. Such bioturbation effects have been observed from deep ocean (Santschi et al. 1984) to intertidal sedimentary environments (Osaki et al. 1997). Similar data for freshwater ecosystems was not found, to our knowledge.

A bioturbation-driven mechanism of ^{75}Se, ^{51}Cr and ^{60}Co diffusion was proposed by Suzuki et al. (2013) for mangrove sediments from southeastern Brazil. These authors considered that faunal bioturbation and mangrove plant rhizospheres develop an interaction that affects the net retention of trace element recently diffused into the sediments. According to this study, the influence of bioturbation extended the diffusion into depths in which mangrove rhizospheres can improve the trace elements retention (by stabilising physically the sediments and by providing organic and inorganic metal-binding compounds, as it was referenced above), suggesting increased net retention efficiency.

Figure 2 presents an X-ray microtomography illustrating a vertical cross section of mangrove sediment, showing density heterogeneity due to mineral and organic matter composition, which evidences the complex structure of this sediment, as well as the presence of bioturbation signs in upper sediment layers. It also presents a schematic diagram on the overall effect of the mechanistic interaction between biological factors affecting trace element accumulation within sediments, as proposed by Suzuki et al. (2013). This mechanistic interpretation of coupled influences

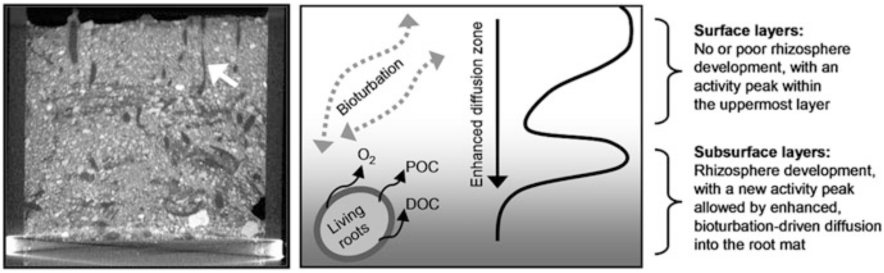

Fig. 2 *On the left* X-ray microtomography of mangrove sediments, with an *arrow* indicating a burrow structure. *On the right* schematic diagram illustrating the relative influence of bioturbation on the distribution of trace elements recently diffused into mangrove sediments. *Grey* shading indicates increasing rhizosphere influence in subsurface layers. Root-derived O_2, dissolved organic carbon (*DOC*) and particulate organic carbon (*POC*) are main factors affecting trace element trapping within rhizospheres. Figure reproduced from Suzuki et al. (2012)

between bioturbation and mangrove rhizosphere processes allowed by radiotracer experiments was previously unsuspected by conceptual models on trace element retention within mangrove environments (Clark et al. 1998; Marchand et al. 2006).

Despite the major role of microorganisms in controlling processes involved in trace element cycling, by driving redox processes, organic matter consumption and trace element speciation (Salomons and Förstner 1984; Harbison 1986; Bouchet et al. 2011), there was a lack of studies on this specific role in the research on radiotracer exchanges across water–sediment interfaces.

Studies on the effects of whole benthic organisms' activity (i.e. coupled faunal and microbial effects) on ^{58}Co, ^{51}Cr and ^{65}Zn diffusion into mangrove sediments were recently carried out by introducing the calculation of Benthic Activity Indices (BAI), as reported by Suzuki et al. (2013). BAI was calculated as the relative percent difference between data obtained for untreated sediments and data obtained for formaldehyde-treated sediments in relation to untreated sediment data. These data can be radiotracer activities per sediment mass (Bq g^{-1}) or inventories of radiotracer activities per sediment area (Bq cm^{-2}). Formaldehyde was chosen as the biocide substance for ceasing biological activity within the sediments after the considerations on advantages and limitations of other biocides (Tuominen et al. 1994; Neto et al. 2007). The relative enrichment of metals due to this activity (BAI) was calculated as follows:

$$\mathrm{BAI} = ((C_{\mathrm{untreated}} - C_{\mathrm{treated}})/C_{\mathrm{untreated}}) \times 100$$

where $C_{\mathrm{untreated}}$ is the data from untreated sediments and C_{treated} is the data observed in formaldehyde-treated sediments. Suzuki et al. (2013) estimated that biological activity was responsible for 32–44 % of total inventories of ^{58}Co, ^{51}Cr and ^{65}Zn within sediments. The chromate anion was the less affected radiotracer, while ^{65}Zn was the radiotracer most sensitive to biological activity inhibition. Benthic activity was quantitatively evidenced as a control on trace metal diffusion into the sediments, and it was also suggested that this influence can also affect the potential bioavailability of trace elements, considering that diffused elements can be more readily bioavailable.

Harbison (1986) provided evidences that benthic algae distribution along an intertidal area in Australia influenced the distribution of trace elements, such as Cd, Cr, Cu, Pb and Zn, in surface sediments. However, the possible role of trace elements uptake by benthic microalgae in the removal from water column is a potential additional factor of influence that has been not investigated in radiotracer studies in the water–sediment interface. The potential role of biological uptake is dependent on the radiotracers' chemical speciation that will determine their bioavailability in the water and sediments, considering that trace elements associated to solid-phase compounds are much less bioavailable than ionic dissolved forms, besides the importance of bioavailability to determine trace element toxicity to benthic organisms (Ankley et al. 1996; Chapman et al. 1998).

4 Water and Sediment Effects

Adsorption/desorption processes and kinetics of trace elements' associations to aquatic sediments are well known as influenced by the variability in water physicochemical conditions and sediment geochemical compositions (pH, redox-sensitive compounds of C, S, Fe and Mn) that contribute to determine the trace element binding to sediment's solid phase (Santschi 1988; Santschi et al. 1990). These responses can be strongly associated to chemical speciation changes experienced due to particular processes that affect certain elements, such as highly toxic chemical species of trace elements (e.g. methylated Hg; Bouchet et al. 2011). Generally there are few works on the role of chemical speciation using radiotracer experiments, mainly on trace elements' behaviour near the sediment–water interface, with some exceptions, such as those focused on chromium (Santschi 1988; Suzuki et al. 2014) and selenium (Santschi 1988).

Table 1 presents examples of chemical speciation responses to specific factors of influence. There is substantial evidence that behavioural differences found on multiple radiotracers studies are due to different degrees of elemental affinity to react with sediment particles surfaces, a behaviour called as "particle-reactive", which can involve diverse sorption/desorption processes.

Influences of different water quality conditions on different trace elements have been more scarcely compared by using radiotracer experiments. Particular interest has been dedicated to simulate different water oxygenation levels' effects. For example, Schaanning et al. (1996) demonstrated that ^{109}Cd bioaccumulation by aquatic organisms was affected by water column oxygen levels, while ^{203}Hg did not present this trend. Suzuki et al. (2014) evidenced that ^{58}Co removal from tidal water to underlying sediments was more sensitive to redox conditions in the tidal water column than observed for ^{65}Zn (that displays a behaviour more "particle-reactive" than ^{58}Co), as it was reflected by the depth distribution of these radiotracers within

Table 1 Examples of biogeochemical factors that determine the rates in which equilibrium distributions of some redox-sensitive trace element species are established (after the review by Santschi 1988)

Biogeochemical factor	Examples of affected trace elements and speciation responses	References
Particle surface reactions	Cr(III) ↔ Cr(VI)	Amdurer (1983)
Bacteria	Hg(II) ↔ Hg(0)	Wood and Wang (1985); Pan-Hou and Imoura (1982)
Complexation by humic and fulvic acids	Fe(II) ↔ Fe(III), Hg(II) ↔ Hg(0)	Theis and Singer (1974); Kerndorf and Schnitzer (1980); Buffle (1984)
Sorption/desorption by MnO_2	Co(II) ↔ Co(III)	Murray and Dillard (1979)

sediments at the end of experiments, with aerated water columns showing a trend of higher accumulation of both radiotracers within the uppermost sediment layer (Fig. 3).

Reversibility of processes that remove trace elements from water overlying aquatic sediments can also be an important aspect determining behavioural trends in the environment. Only the amounts of deposited, precipitated and diffused elements that escape from resuspension or re-solubilisation processes back to overlying water will be exposed to long-term sediment burial (besides possible uptake of part of these amounts by benthic organisms). Spatial and temporal variability in overlying water and sediment porewater physicochemical conditions can contribute to determine the efficiency in which trace elements will be preserved within bottom sediments (Cooper and Morse 1998), often resulting in a role of sediments as sources of, rather sinks for, these elements (Harbison 1986).

Hall et al. (1989) performed benthic chamber experiments in Gullmarsfjorden, Sweden, in which the evolution from high oxygen levels to high sulphide levels in overlying water resulted in a temporal sequence of first-order removal kinetics by bottom sediments, followed by events of return of radiotracers such as ^{54}Mn, ^{59}Fe and ^{65}Zn to the water column, characterising a redox-driven reversibility of the removal process.

Microcosm column experiments on the ^{65}Zn removal from tidal water by underlying sediment cores from a mangrove forest and a tidal creek that drains this forest in Sepetiba Bay, Brazil, indicated that ^{65}Zn mobility in the sediment pore water appears to be very limited under the mangrove plants influence, while a greater mobility was favoured within creek sediments. Table 2 presents the rates of ^{65}Zn exchanges between overlaying tidal water and bottom sediments for these environments, evidencing that only tidal creek sediments allowed a ^{65}Zn return back to tidal water column. A remarkable contrast between stations was found for the 12–18 h interval, with ^{65}Zn removal rates of 45 ± 4 kBq m^{-2} d^{-1} for mangrove sediment experiments and 8 ± 58 kBq m^{-2} d^{-1} for station tidal creek sediment experiments. This "^{65}Zn return" event was due to a negative flux found in one of the three replicates (-105 kBq m^{-2} d^{-1}; corresponding to a return of 17 % of the

Fig. 3 Temporal variability of ^{58}Co and ^{65}Zn activities in overlying waters during experiments under air and N_2 pumping into overlaying water and depth variability of these activities within sediments at the end of these experiments (means ± SE; $n = 3$). Figure reproduced from Suzuki et al. (2012)

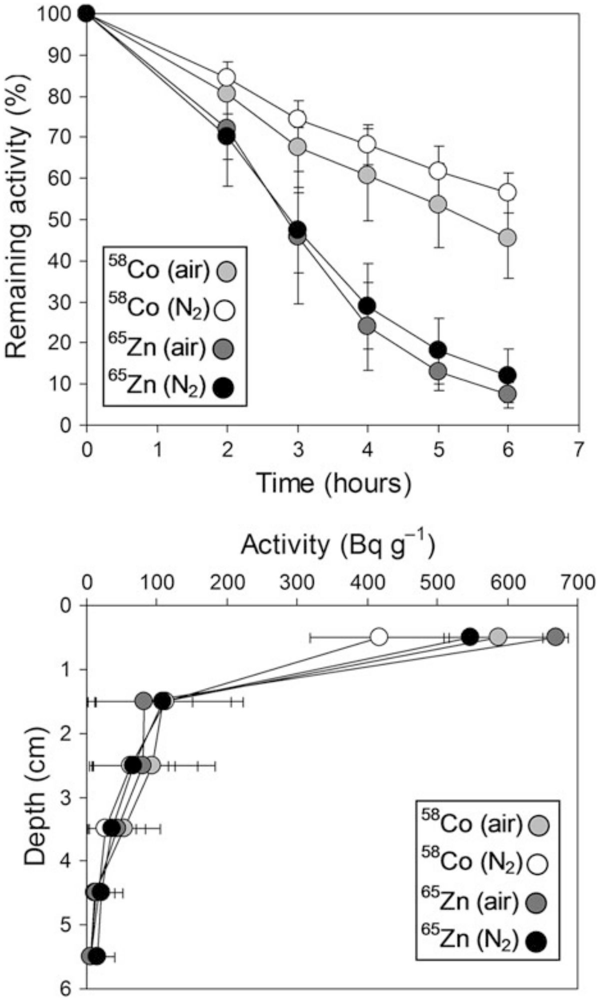

Table 2 Average ^{65}Zn removal rates ± SE (kBq m^{-2} d^{-1}) from waters overlaying sediments from the Itacuruçá mangrove forest (station F) and sediments from the tidal creek that drains this forest (station C), during 30-h experiments (after Machado et al. 2008)

Time (h)	Station F	Station C	Ratio (F:C)
0.00–0.25	2600 ± 655	1379 ± 169	1.89
0.25–2	198 ± 38	202 ± 42	0.99
2–6	358 ± 81	342 ± 40	1.05
6–12	88 ± 39	128 ± 11	0.68
12–18	45 ± 4	8 ± 58	5.63
18–24	29 ± 4	84 ± 48	0.34
24–30	15 ± 4	26 ± 10	0.60

initial ^{65}Zn activity in overlaying water). Differences in sediment physical and geochemical compositions (variability in metal-binding clay particles and in organic matter contents) are possible factors affecting such contrasting trends.

5 Transfer Kinetics from Overlying Water to Sediments

Most of the results from the scientific literature have evidenced that the experimental radiotracer half-removal rates from overlying water to sediments display a first-order kinetics, since the removal of radiotracers by bottom sediments has been generally characterised by a faster initial removal followed by slower and low-variable removal rates. This predominant trend has been observed for a large variety of sedimentary environments in relation to many radiotracers, such as ^{54}Mn, ^{59}Fe, ^{65}Zn, ^{203}Hg, ^{133}Ba, ^{137}Cs and ^{60}Co (Hall et al. 1989; Barros et al. 2004; Machado et al. 2008, 2012; Suzuki et al. 2014).

First-order half-removal times ($t_{1/2}$) observed even for the same radiotracer have been very variable, ranging from hours to days, depending on the experimental conditions, as is the case of Zn and Co (Fig. 3). In 7 h of experiment, the ^{58}Co $t_{1/2}$ values were 5.4 h under aerate condition and 7.3 h in nitrogen purged water column; both values were considerable higher than ^{65}Zn $t_{1/2}$ values (1.5 h and 1.9 h respectively), evidencing different behaviours due to different chemical forms (Suzuki et al. 2013).

However, while comparisons and correlations of kinetics data may be found within a particular radiotracer study, always be aware that due to variability in specific experimental conditions and chemical properties of the elements of interest, the extrapolation of the observed behavioural results to other sediments is speculative (Duursma and Eisma 1973). Further supports from additional analyses under the conditions of interest are, therefore, requested to allow generalisations on these behavioural trends for different environmental conditions.

6 Conclusions and Recommendations

The comprehension on biogeochemical mechanisms, transport kinetics across the interface and the role of sediments as sinks for the studied elements has been improved by using radiotracers. The role of biological activity has been generally focused on benthic fauna bioturbation, evidencing this activity as an important factor of influence on trace element transfer across water–sediment interfaces. These transfers may involve multiple processes, which may include the effects of deposition of particulate matter, adsorption onto organic and inorganic compounds of sediments and diffusion into the interstitial water. Possible effects of benthic algae uptake on the radiotracer transfer across the water–sediment interface remain to be elucidated. Potential losses of the tracers by adsorption onto the walls of the employed experimental apparatus should be taken into account.

Radiotracer techniques are able to contribute for the elucidation of the trace elements' biogeochemistry in complex environments, such as the water–sediment interfaces of mangrove ecosystems, as illustrated in Fig. 4. Plant–animal–microbial interactions with the sediments occur concurrently in these intertropical environments, affecting the cycling of trace elements, as it is also expected to occur in other plant-colonised aquatic ecosystems in tropical and temperate regions, such as salt marshes and sea grass meadows.

An increasing number of studies on intertidal sedimentary environments have been found in the literature, based on interpretations of radiotracer diffusion into the sediments. Unfortunately, radiotracer studies on these environments have not evaluated pore water vertical percolation effects on trace element behaviour. Water percolation effects may promote highly variable responses of different trace elements in relation to penetration into deeper sediment layers (Simpson et al. 2004), and this evaluation is strongly recommended for intertidal ecosystems, besides conventional diffusion-based approaches applied in radiotracer studies.

Behavioural differences due to chemical speciation variability deserve particular attention as future research needs. Further studies on this issue should be performed

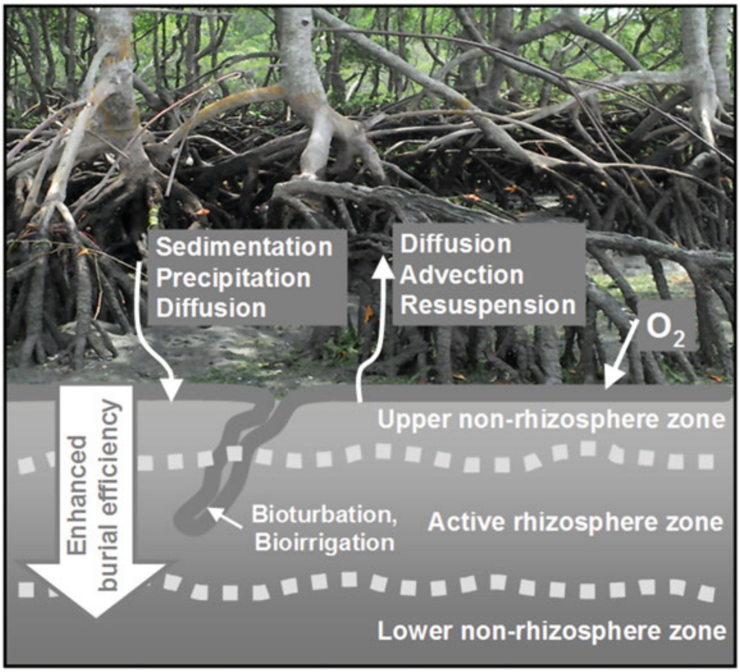

Fig. 4 Schematic diagram on major processes involved in determining the trace element transfers across the sediment–water interface and its accumulation within sediments from mangrove areas

in order to improve the comprehension and the prediction capacity on important aspects of environmental quality analysis, including the:

- Support to environmental risk assessment based on toxic trace element behaviour
- Evaluation of the suitability of potential biological monitors of trace element contamination
- Predictions on trace element speciation and bioavailability sensitivity to global environmental changes (e.g. due to water system acidification in response to atmospheric CO_2 rise and water system eutrophication)

Acknowledgements The authors are grateful to Dr. João A. Osso Jr. and IPEN-CNEN/SP for kindly providing radiotracers to this research and the Rio de Janeiro State Research Foundation for financial support (FAPERJ Proc. No. E-26/112.072/2012). K.N. Suzuki thanks the Brazilian Ministry of Education (CAPES) for her postdoctoral grant.

References

Alongi DM, Wattayakorn G, Boyle S, Tirendi F, Payn C, Dixon P (2003) Influence of roots and climate on mineral and trace element storage and flux in tropical mangrove soils. Biogeochemistry 69:105–123

Amdurer M (1983) Chemical speciation and cycling of trace elements in estuaries: Radiotracer studies in marine microcosms. Ph.D. thesis, Columbia University

Ankley GT, Di Toro DM, Hansen DJ, Berry WJ (1996) Technical basis and proposal for deriving sediment quality criteria for metals. Environ Toxicol Chem 15:2056–2066

Barros H, Laissaoui A, Abril JM (2004) Trends of radionuclide sorption by estuarine sediments. Experimental studies using ^{133}Ba as a tracer. Sci Total Environ 319:253–267

Bouchet S, Bridou R, Tessier E, Rodriguez-Gonzalez P, Monperrus M, Abril G, Amouroux D (2011) An experimental approach to investigate mercury species transformations under redox oscillations in coastal sediments. Mar Environ Res 71:1–9

Bradshaw C, Kumblad L, Fagrell A (2006) The use of tracers to evaluate the importance of bioturbation in remobilising contaminants in Baltic sediments. Estuar Coast Shelf Sci 66:123–134

Buffle J (1984) Natural organic matter and metal-organic interactions in aquatic systems. In: Siegel H (ed) Metal ions in biological systems, 18. Dekker, New York

Ciffroy P, Garnierb JM, Pham MK (2001) Kinetics of the adsorption and desorption of radionuclides of Co, Mn, Cs, Fe, Ag and Cd in freshwater systems: experimental and modelling approaches, J Environ Radioact 55:71–91

Chapman PM, Wang F, Janssen C, Persoone G, Allen HE (1998) Ecotoxicology of metals in aquatic sediments: binding and release, bioavailability, risk assessment, and remediation. Can J Fish Aquat Sci 55:2221–2243

Clark MW, McConchie DM, Lewis DW, Saenger P (1998) Redox stratification and heavy metal partitioning in Avicennia-dominated mangrove sediments: a geochemical model. Chem Geol 149:147–171

Cooper DC, Morse JW (1998) Biogeochemical controls on trace metal cycling in anoxic marine sediments. Environ Sci Technol 32:327–330

Cournane S, Vintró LL, Mitchell PI (2010) Modelling the reworking effects of bioturbation on the incorporation of radionuclides into the sediment column: implications for the fate of particle-reactive radionuclides in Irish Sea sediments. J Environ Radioact 101:985–991

Croot PL, Heller MI, Schlosser C, Wuttig K (2011) Utilizing radioisotopes for trace metal speciation measurements in seawater. In: Singh N (ed) Application in physical sciences. InTech, Rijeka, Croatia

Duursma EK, Eisma D (1973) Theoretical, experimental and field studies concerning reactions of radioisotopes with sediments and suspended particles of the sea part c: applications to field studies. Neth J Sea Res 6:265–324

Hall POJ, Anderson LG, Rutgers van der Loeff MM, Sundby B, Westerlund SFG (1989) Oxygen uptake kinetics in the benthic boundary layer. Limnol Oceanogr 34:734–746

Harbison P (1986) Mangrove muds—a sink and source for trace metals. Mar Pollut Bull 17:273–276

Hatje V, Payne TE, Hill DM et al (2003) Kinetics of trace element uptake and release by particles in estuarine waters: effects of pH, salinity, and particle loading. Environ Int 29:619–629

IAEA (2010) Handbook of parameter values for the prediction of radionuclide transfer in terrestrial and freshwater environments. International Atomic Energy Agency, Vienna

Kerndorf H, Schnitzer M (1980) Sorption of metals on humic acid. Geochim Cosmochim Acta 44:1701–1708

Lacerda LD, Rezende CE, Aragon GT, Ovalle AR (1991) Iron and chromium transport and accumulation in a mangrove ecosystem. Water Air Soil Pollut 57–58:513–520

Machado W, Moscatelli M, Rezende LG, Lacerda LD (2002) Mercury, zinc, and copper accumulation in mangrove sediments surrounding a large landfill in southeast Brazil. Environ Pollut 120:455–461

Machado EC, Machado W, Bellido LF, Patchineelam SR, Bellido AVB (2008) Removal of zinc from tidal water by sediments of a mangrove ecosystem: a radiotracer study. Water Air Soil Pollut 192:77–83

Machado EC, Machado W, Bellido AV, Bellido LF, Patchineelam SR (2012) Cesium, manganese and cobalt water–sediment transfer kinetics and diffusion into mangrove sediments inferred by radiotracer experiments. J Radioanalyt Nucl Chem 292:349–353

Marchand C, Lallier-Vergès E, Baltzer F, Alberic P, Cossa D, Baillif P (2006) Heavy metals distribution in mangrove sediments along the mobile coastline of French Guiana. Mar Chem 98:1–17

Murray JW, Dillard G (1979) The oxidation of cobalt(II) adsorbed on manganese dioxide. Geochim Cosmochim Acta 43:781–787

Neto M, Ohannessian A, Delolme C, Bedell JP (2007) Towards an optimized protocol for measuring global dehydrogenase activity in storm-water sediments. J Soil Sediments 7:101–110

Osaki S, Sugihara S, Momoshima N, Maeda Y (1997) Biodiffusion of ^{7}Be and ^{210}Pb in intertidal estuarine sediments. J Environ Radioact 37:55–71

Pan-Hou HS, Imoura N (1982) Involvement of mercury methylation in microbial detoxification. Arch Microbiol 131:176–177

Payne TE, Hatje V, Itakura T, McOrist GD, Russell R (2004) Radionuclide applications in laboratory studies of environmental surface reactions. J Environ Radioact 76:237–251

Petersen K, Kristensen E, Bjerregaard P (1998) Influence of bioturbating animals on flux of cadmium into estuarine sediments. Mar Environ Res 45:403–415

Salomons W, Förstner U (1984) Metals in the hydrocycle. Springer, Berlin

Santschi PH (1988) Factors controlling the biogeochemical cycles of trace elements in fresh and coastal marine waters as revealed by artificial radioisotopes. Limnol Oceanogr 33:848–866

Santschi PH, Nyffeler UP, O'Hara P, Buchholtz M, Broecker WS (1984) Radiotracer uptake on the sea floor: results from the MANOP chamber deployments in the eastern Pacific. Deep-Sea Res 31:451–468

Santschi PH, Höhener P, Benoit G, Brink MB (1990) Chemical processes at the sediment–water interface. Mar Chem 30:269–315

Schaanning MT, Hylland K, Eriksen DØ, Bergan TD, Gunnarson JS, Skei J (1996) Interactions between eutrophication and contaminants II Mobilization and bioaccumulation of Hg and Cd from marine sediments. Mar Pollut Bull 33:71–79

Simpson SL, Maher EJ, Jolley DF (2004) Processes controlling metal transport and retention as metal-contaminated groundwater efflux through estuarine sediments. Chemosphere 56:821–831

Sundby B, Anderson LG, Hall POJ, Iverfeldt A, Van der Loeff MMR, Westerlund SFG (1986) The effect of oxygen on release and uptake of iron, manganese, cobalt, and phosphate at the sediment-water interface. Geochim Cosmochim Acta 50:1281–1288

Suzuki KN, Machado EC, Machado W, Bellido AVB, Bellido LF, Osso JA Jr, Lopes RT (2012) Selenium, chromium and cobalt diffusion into Mangrove sediments: radiotracer experiment evidence of coupled effects of bioturbation and rhizosphere. Water Air Soil Pollut 223:3887–3892

Suzuki KN, Machado EC, Machado W, Bellido LF, Bellido AVB, Lopes RT (2013) Radiotracer estimates of benthic activity effects on trace metal diffusion into mangrove sediments. Mar Environ Res 83:96–100

Suzuki KN, Machado EC, Machado W, Bellido AVB, Bellido LF, Osso JA Jr, Lopes RT (2014) Kinetics of trace metal removal from tidal water by mangrove sediments under different redox conditions. Radiat Phys Chem 95:336–338

Theis TL, Singer PC (1974) Complexation of iron(II) by organic matter and its effect on iron (II) oxygenation. Environ Sci Technol 8:569–573

Tuominen L, Kairesalo T, Hartikainen H (1994) Comparison of methods for inhibiting bacterial activity in sediment. Appl Environ Microbiol 60:3454–3457

Wood JM, Wang HK (1985) Strategies for microbial resistance to heavy metals. In: Stumm W (ed) Chemical processes in Lakes. Wiley, New York

Zhang P, He X, Ma Y, Lu K, Zhao Y, Zhang Z (2012) Distribution and bioavailability of ceria nanoparticles in an aquatic ecosystem model. Chemosphere 89:530–535

Uptake and Retention of Simulated Fallout of Radiocaesium and Radiostrontium by Different Agriculture Crops

Stefan B. Bengtsson, Klas Rosén, and Mykhailo Vinichuk

Contents

Abstract The contamination level in potato, oilseed rape and wheat in terms of tubers, seeds and foliage has been investigated after the foliar application of wet-deposited ^{134}Cs and ^{85}Sr at different growth stages in a microscale field experiment conducted over consecutive years. The results indicate that the application of radionuclides in the beginning of the growth season resulted in low ^{134}Cs and ^{85}Sr activity in both seeds of wheat, oilseed rape and potato tubers across sampling occasions. In the middle of the growth season during radionuclide fallout, ^{134}Cs activity in potato tubers across sampling occasions was highest. The spraying of radionuclides at later stages resulted in even lower ^{134}Cs activity in potato tubers but increased activity in seeds of wheat and oilseed rape.

S.B. Bengtsson (✉)
Institute of Environmental Radioactivity, Fukushima University, 1 Kanayagawa, Fukushima 960-1206, Japan
e-mail: stefan.bengtsson@me.com

K. Rosén
Department of Soil & Environment, Swedish University of Agricultural Sciences, 7014, 75007 Uppsala, Sweden

M. Vinichuk
Department of Ecology, Zhytomyr State Technological University, 103 Chernyakhovsky Street, 10005 Zhytomyr, Ukraine

C. Walther, D.K. Gupta (eds.), *Radionuclides in the Environment*,
DOI 10.1007/978-3-319-22171-7_6

Keywords Radiocaesium • Potato • Wheat • Oilseed rape • Foliage • Tubers • Grains • Deposition

1 Introduction

Since nuclear power technology was introduced, a number of severe accidents have led to the release of radionuclides into the environment and threatened areas that were previously used for agricultural food productions. The Chernobyl nuclear power plant (NPP) accident in 1986 had a huge impact on the agricultural food production systems in the former western parts of the USSR (Smith and Beresford 2005) and in the Nordic countries (Åhman and Åhman 1994; Andersson et al. 2007). The Fukushima Dai-ichi NPP accident in 2011 had a large impact on the Japanese agricultural food production system, especially to the rice production. These two major and other NPP accidents have demonstrated that similar accidents resulting in contamination of large agricultural areas could occur in the near future. Moreover, the increasing construction, worldwide, of facilities that are producing or using radiation sources, such as spallation sources, together with NPP accidents, has highlighted the importance of understanding the behaviour of different types of radionuclides, especially in the agricultural ecosystem.

The agricultural production system in the Northern Hemisphere is cyclical and runs through the year with different phases in line with crop growth, from the rest in the winter to the vegetative development of the crops through the spring and the summer to the last ripening and harvest in the autumn. Transfer of radionuclides in food stuffs is affected if the crops are used directly from fresh, such as animal fodder or for the production of food stuffs in more refined forms. If radioactive fallout occurs during the vegetative development or at crop ripening, then the transport pathways of radionuclides may be short: being deposited and intercepted by foliar plant parts, it will be transferred directly to edible parts of the crop.

The most important radionuclides in the longer-term period after an NPP accidental release to the agricultural ecosystem are, e.g. radioiodine (^{131}I), radiocaesium (^{134,137}Cs) and radiostrontium (^{90}Sr). When deposited, these radionuclides can spread quickly within the agricultural ecosystem and reach humans via the food chain. Cereals, milk and oil crops, and to a lesser degree potatoes and vegetables, are among the main products which may be contaminated shortly after radionuclide fallout, thus contributing to the collective dose to humans (Middleton 1958; Lepicard and Dubreuil 2001; Madoz-Escande et al. 2004). Information about the level of contamination to the crops, in the case of radionuclide fallout, that could consequently affect the growth stage of the crop would be needed in order to predict whether the crops would be suitable for human consumption. This highlights the necessity for field studies, and the extended time periods can improve our understanding of the annual variations associated with agricultural crop production that can affect the transfer of radionuclides into agricultural crops.

Following the Chernobyl and Fukushima Daiichi NPP accidents, a large amount of data have been collected about the radionuclides' uptake from the soil into the plants (Rosén 1996). Still, there is a shortage of information about the effects of radioactive fallout on agricultural crops. However, there is a substantial amount of knowledge about the relationship between the concentration of radionuclides both in soils and in agricultural crops and how this relationship is controlled by different factors, and this is well known (IAEA 2010). This knowledge, on the relationship between soil and agricultural crops, is useful for predicting the uptake of radionuclides into agricultural crops after deposition on bare soil or on nonarable land and in the forthcoming years after a radionuclide fallout event has taken place. Nevertheless, this knowledge is not useful when radionuclides are directly deposited onto growing agricultural crops and redistributed to harvested agricultural products. Further knowledge about how different radionuclides are captured and redistributed to harvested products after deposition onto growing agricultural crops, in terms of the size and the time of deposition, is essential. To be able to suggest appropriate countermeasures for different scenarios, and to prevent further spread of radionuclides to foodstuffs, it is essential to collect data on the amount and time of deposition of radionuclides onto agricultural crops.

Several field experiments with artificial wet depositions of ^{134}Cs and ^{85}Sr during the growth period of agricultural crops have been carried out at the Swedish University of Agricultural Sciences (SLU) (Eriksson et al. 1998a, b; Bengtsson et al. 2012, 2013). The aim of these experiments was to get an understanding of the relative transfer of radionuclides to harvested products of agricultural crops after initial depositions of radionuclides at different times during the growth period. The reduction in transfer of radionuclides with time, from deposition to sampling, depends partly on the radionuclide dilution due to growth of the plant tissues and partly on fall-off to the ground. The data obtained in experiments can be used to extend our basic knowledge for prediction of the consequences after a fallout event of radionuclides at different time scenarios (Table 1).

2 Interception of Radionuclides by Agricultural Crops

In general, there are two types of deposition processes: *dry deposition* and *wet deposition*. In dry deposition, radioactive particles are deposited directly onto plant surfaces, and the transfer of radioactive particles to agricultural crops takes place through absorption, impaction and sedimentation in water (Smith 2001; IAEA 2010). In wet deposition, the radioactive particles are much smaller, and they are deposited when it hails, rains or snows (IAEA 2010). During wet deposition, radioactive particles are transported from the atmosphere at a higher rate than for dry deposition. The wet deposition of radioactive particles through rain takes place by two different processes: (1) *wash-out*, viz. the entrainment of radioactive particles by falling rain drops, and (2) *rainout*, viz. the condensation of air vapour into rain drops formed around radioactive particles.

Table 1 The percentage of ^{134}Cs and ^{85}Sr in different plant parts and stages of spring oilseed rape and spring wheat at harvest (September), after wet deposition occurred at different growth stages

Year/crop	Growth stage at deposition	^{134}Cs Seeds	Siliques (except seeds)	Straw	^{85}Sr Seeds	Siliques	Straw
2010/oilseed	13	20	8	72	14	14	72
	32	11	25	64	*	*	*
	61	14	34	52	3	57	40
	65	13	37	50	6	50	44
	80	8	39	53	4	51	45
2011/oilseed	15–19	21	15	64	13	31	56
	65	16	18	66	*	*	*
	69	23	32	45	9	79	12
	76	21	25	54	18	37	45
	82	17	44	39	19	49	32
		Grain	*Husk*	*Straw*	*Grain*	*Husk*	*Straw*
2010/wheat	21	49	18	33	*	*	*
	37	34	6	60	*	*	*
	65	34	4	62	7	6	87
	70	24	7	69	11	7	82
	89	11	16	73	10	15	75
2011/wheat	37	35	9	56	*	*	*
	65	68	16	16	36	28	36
	85	44	28	28	32	31	37
	89	35	35	30	31	33	36
	92	17	40	43	18	37	45

Means are from three replicates ($n = 3$), except where ‡ indicates $n = 2$. The percentage was not estimated due to activity concentration below minimum detectable limit is denoted by *, from Bengtsson et al. (2013).

In general, the interception of radiostrontium is higher than that of radiocaesium. This is due to the interception of radioactive particles in a process that is related to molecular mass and to valence (Oughton and Salbu 1994; Salbu et al. 2004; Pröhl 2009). The surface of plants is negatively charged and will act as a cation exchanger or exchange resin, causing a weaker retention of anions and monovalent ions on the plant's surface than for divalent and polyvalent cations (Kinnersley et al. 1997; Bréchignac et al. 2000; Vandecasteele et al. 2001; Pröhl 2009).

To be able to describe the level of interception of radioactive particles, different factors have been introduced. The first, and mostly used, is the interception fraction (f, Bq m^{-2}/Bq m^{-2}), and it is defined as the ratio between the activity concentration retained by the agricultural crop immediately after the deposition event and the total activity deposited (Pröhl 2009). However, this fraction does not account for the effects from the growth stage of agricultural crops. To be able to take into account these affects, the interception fraction has to be normalised to the standing plant biomass (B, kg m^{-2}, dry mass) (Pröhl 2009). By doing this, the mass interception fraction (f_B, = Bq kg^{-1} in crops/Bq m^{-2} deposited on ground = m^2 kg^{-1}) is introduced. Furthermore, as the surface area of the foliage of agricultural crops is in direct contact with the atmosphere, the interception fraction can also be normalised to the surface foliage area by using the leaf area index (LAI, m^2 m^{-2}) (Pröhl 2009).

It is well known that the interception of precipitation will increase linearly with LAI (Pröhl 2009), and this is related to the external water storage capacity on the foliage of agricultural crops; however, this is in turn dependent on the LAI. Furthermore, the interception will decrease as the amount of precipitation increases (Fig. 1), which results in the interception fraction being inversely proportional to the amount of precipitation (Kinnersley et al. 1997; Pröhl 2009).

The quantity of deposited radionuclides that can be intercepted by the standing agricultural crops is related to both the crops' biomass and the LAI (Fig. 2). The fraction of intercepted radionuclides is increasing in relation to the increasing biomass of the crop; strong relationships were found for cereals and grass crops (Vandecasteele et al. 2001; Bengtsson et al. 2013, 2014). However, for oil crops, e.g. oilseed rape, this relationship is much weaker and is explained by the fact that oil crops shed their leaves at the later growing stages, whereas the standing biomass still increases due to the rapid growth of siliques (Bengtsson et al. 2012). For the LAI, there is a relationship to the interception and the leaves' area, this is especially strong for cereals and grass crops; however, this relationship is somewhat weaker for oil crops, such as oilseed rape (Bengtsson et al. 2012).

The time elapsed since interception of radionuclides to harvest will have some effects on the radioactive concentration in the agricultural crops, and this

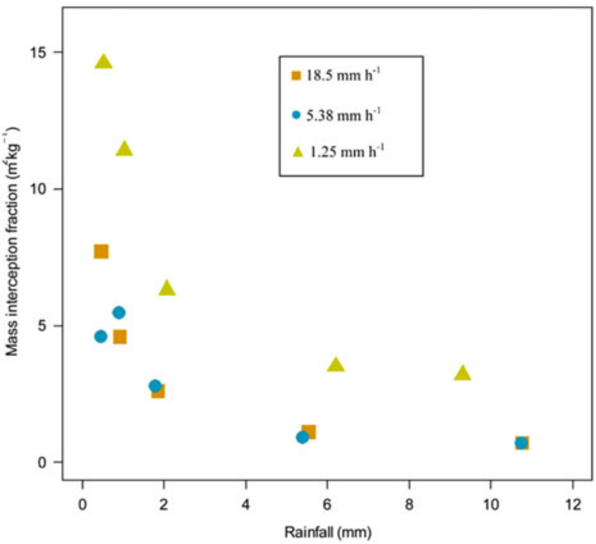

Fig. 1 Interception of ^{137}Cs by grass as a function of the amount of precipitation and precipitation intensity. Modelled after Kinnersley et al. (1997) and Bengtsson (2013)

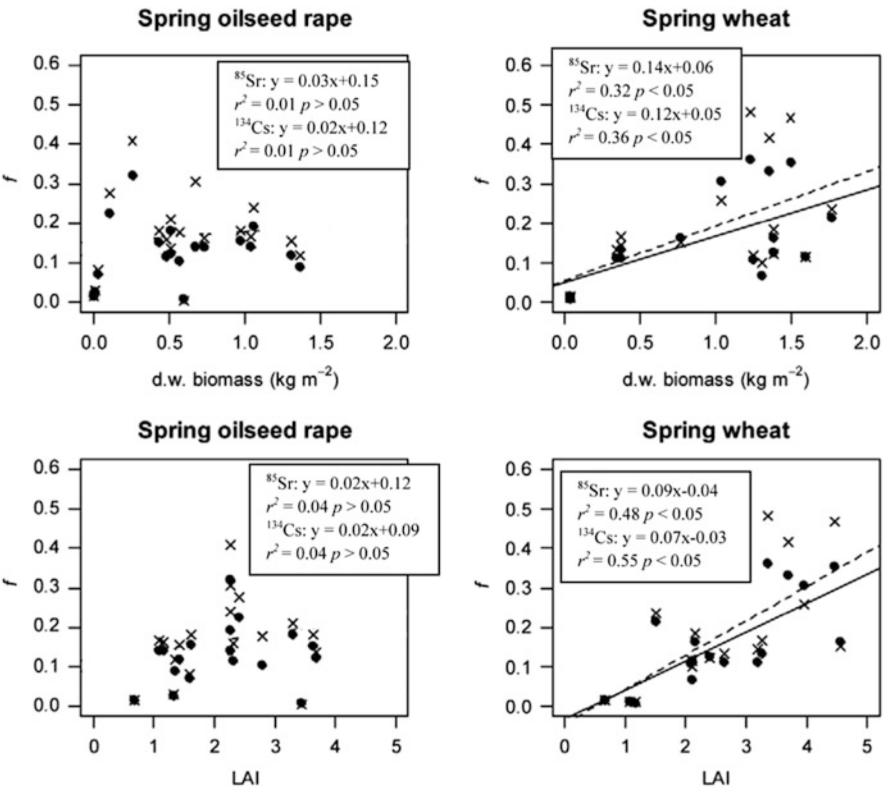

Fig. 2 Relationships between the interception fraction of ^{134}Cs (*filled circle*) and ^{85}Sr (*into mark*) deposited on spring oilseed rape and spring wheat as a function of standing biomass dry weight (DW) and LAI. Modified after Bengtsson et al. (2012)

depends on "field losses". Examples of these field losses can be wash-off effects (desquamation of the cuticle) and volatilisation (Chadwick and Chamberlain 1970; Madoz-Escande et al. 2004). The dilution of radionuclides, when the biomass increases at the growth of the crop until harvest, is of great importance.

However, it should be noted that when using the interception fraction for estimating the degree of radionuclide contamination of agricultural crops, it should be used with caution, as the estimation of interception requires a specific value for each agricultural crop, radionuclide, level of precipitation and radionuclide concentration in the precipitation (Hoffman et al. 1992; Kinnersley et al. 1997). Moreover, it has been found that the level of radionuclide interception is not directly related to the intensity of precipitation but rather indirectly related to the external water storage capacity of the plant and to the accumulation of radionuclides on the crop's surface (Kinnersley et al. 1997).

3 Activity Concentration of Radionuclides in Crops

The entrance of radioactive ions is not easily made through the cuticle layer of the epidermis of the leaves. However, the cuticle layer usually contains cracks and defects where radioactive ions can enter into the leaves (Fig. 3) (Tukey et al. 1961; Handley and Babcock 1972; Hossain and Ryu 2009). Moreover, radioactive ions can enter into the plant system through the stomata as well, but these pathways contribute only to a smaller fraction of the total uptake (Tukey et al. 1961; Eichert and Burkhardt 2001; Eichert et al. 2002). Once inside the cuticle layer, specialised epidermal cells (surface veins consisting of thin-walled parenchyma tissue) are easily penetrated by the radionuclides (Salisbury and Ross 1992). The radionuclides are then actively transported inside the plant cells through the symplastic partway (the inner side of the plasma membrane in which water can freely diffuse) and also by an exchange mechanism between phloem and xylem (vascular bundle system) through the vascular rays (Salisbury and Ross 1992; Sokołowska and Somiński 2013).

The uptake of radioactive ions is regulated by a number of different factors, e.g. the physical and chemical properties of the radioactive ions, the growth stage on the agricultural crop at the time of radionuclide contamination, the total amount of precipitation (Kinnersley et al. 1997), the intensity of the precipitation (IAEA 2010) and the ability of the agricultural crops to hold water. The concentration of radioactive ions in agricultural crops will be different depending on the growth

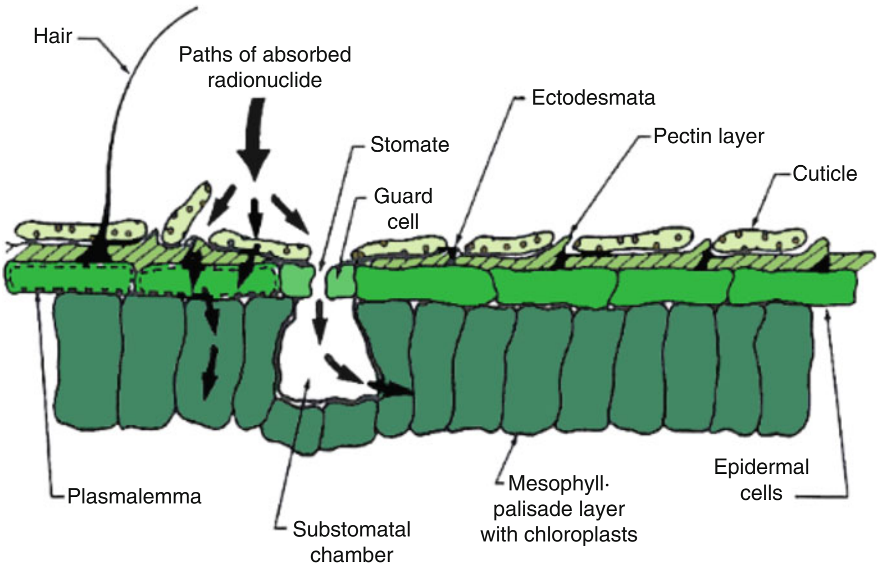

Fig. 3 A cross-sectional diagram of the leaves' surface, illustrating where the entrance of radionuclides to plants can take place. Illustration modified after Koranda and Robison (1978)

stage. Usually at a well-developed growth stage, the majority of deposited radionuclides will be taken up directly by the foliage (Andersson et al. 2002).

The proportion of radionuclides in the precipitation that can be held by an agricultural crop will quickly reach its contamination maximum when the external water storage capacity of the agricultural crop foliage reaches its maximum. However, the contamination of agricultural crops can still increase after the maximum external water storage capacity has been reached; this is related to the absorption of radioactive ions through the surface of the leaves. The degree of the continuous uptake is related to the chemical form of the radionuclides that are deposited (Kinnersley et al. 1997).

It has been found that during wet deposition of the radionuclides, radiocaesium and radiostrontium occur in the late growing season, which will lead to a higher activity concentration in the different plant parts of agricultural crops. The plant parts that generally have the highest activity concentration of radionuclides are the husks of cereals and in the siliques of oil crops (Bengtsson et al. 2013). It has been found that radiocaesium is relatively mobile inside plant tissues; however, its availability for root uptake from clay-rich soils is low (Absalom et al. 1995, 2001; Rosén 1996). This explains why direct contamination of agricultural crops, e.g. by radiocaesium, is an important pathway for the transfer of radionuclides from fallout to human food. For oil crops, the activity concentration of radiostrontium is generally higher than that for radiocaesium (Bengtsson et al. 2013).

The activity concentration of the radionuclides, radiocaesium and radiostrontium in seeds of cereals and oil crops will vary, depending on the timing of the deposition. There will be a lower activity concentration in seeds of cereals and oil crops when the deposition takes place at early growth stages, whereas there will be a higher activity concentration if the deposition takes place during the growth of the crops and at the flowering stage (Gerdung et al. 1999; Bengtsson et al. 2013). However, the highest activity concentration in seeds of cereals and oil crops will take place when the deposition of radionuclides occurs at the ripening phase (Eriksson et al. 1998b; Bengtsson et al. 2013). The increase in activity concentration in the seeds of cereals and oil crops in relation to growth is lower than in other plant parts, and this is due to dilution effects of radionuclides when the biomass increases due to growth (Coughtrey et al. 1983; Bengtsson et al. 2013).

In the case of the potato crop, the activity concentration of radiocaesium in potato tubers is generally controlled by two different factors: (1) the time of fallout and (2) the development stage of the crop. There will be a lower activity concentration in potato tubers when the deposition of radionuclides takes place at an early growth stage, whereas there will be a higher activity concentration of radionuclide if the deposition takes place during the later growth stages (Fig. 4). However, when deposition of radionuclides occurs in the middle of the growing season, i.e. growth stage III, the levels of ^{134}Cs activity concentration in tubers are highest (Fig. 4). Higher levels of ^{134}Cs activity concentration in potato tops at the later growth stages of the plant can be due to a smaller amount of radiocaesium, which is transferred to the potato tubers. Once the potato tubers have completed their development, less active substance transportation occurs within the crop. The activity concentration of

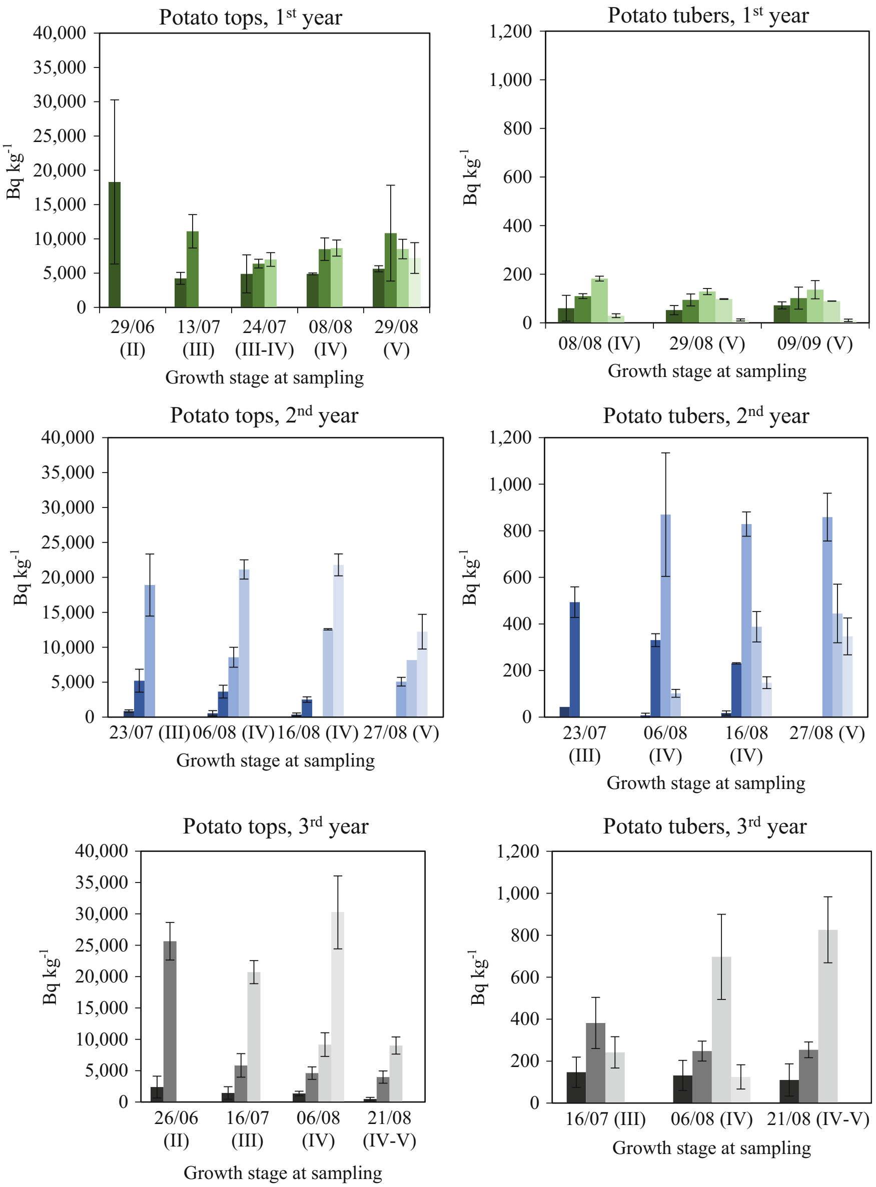

Fig. 4 The average activity concentration of ^{134}Cs (Bq kg^{-1}) at different sampling occasions after deposition at different growth stages in potato tops and potato tubers. Error bars indicate standard deviation. Modified after Rosén and Vinichuk (unpublished). Growth stages at deposition of ^{134}Cs, in 1st year ■ II ■ III ■ III–IV ■ IV ■ V, in 2nd year ■ II ■ II ■ III ■ IV ■ IV–V and in 3rd year ■ II ■ III ■ IV ■ IV–V

^{137}Cs in potato tubers is generally much lower than in other agricultural crops, e.g. in cereal grains (Tsukada and Nakamura 1999; Franic et al. 2007). If the fallout of radiocaesium occurs at later growth stages, then the content of radiocaesium in potato tubers becomes progressively lower with a shorter amount of time passing between the time of deposition and the time of harvest. There is a shortage of time for radiocaesium to be transferred from the potato tops to the potato tubers. Another reason for the lower levels of ^{134}Cs in the potato tubers can be due to the fact that potassium and caesium follow the same pathways inside the plant due to their similar chemical and physical forms; this relation is discussed further in Sect. 3.1. The potassium demand of the potato plant varies during the growing season, the need for potassium is highest during the intensive growth of the tops, and potassium demand decreases rapidly when the tops are fully developed (Harris 1992). When tuber formation starts, all photosynthetic products are transferred down to the potato tubers (Harris 1992; Bodin and Svensson 1996) and leaf growth is inhibited (Harris 1992). The highest concentration of radiocaesium in mature potato tubers if fallout occurred would be in the middle of the growing season, depending on the interception level by the potato tops. At this time, the interception of radioactive particles by potato tops is maximal, and consequently, the transfer of radionuclides to the potato tubers is highest.

3.1 Distribution of Radionuclides Between Plant Parts

It seems that plants do not distinguish between the transfer of the divalent cations of calcium (Ca^{2+}) and strontium (Sr^{2+}) to different plant parts (White 2001). However, these two divalent cations cannot be transferred through the plasma membranes after they have entered into the xylem systems of plants (White 2001), but like calcium, radiostrontium can be taken up through the roots (Veresoglou et al. 1996). Caesium is thought to follow the pathways of potassium (K^{+}) transportation. However, there may be differences in the transport of potassium and caesium (Gommers et al. 2000); these differences are suggested to be related to the caesium-potassium discrimination in the membrane transport system (Buysse et al. 1995). Moreover, the effective K^{+} transporters, which transport potassium efficiently, have only been found in root cells, so far, not in above ground plant parts (Zhu and Smolders 2000).

The biggest portion of radionuclides taken up by cereals and oil crops happens in the straw, whereas a smaller fraction goes into the seeds (Table 2). For potatoes, the biggest part that takes up radionuclides is the tops, whereas a smaller fraction is found in the tubers (Table 2). The concentration and distribution of radionuclides inside the crop and at harvest will be different depending on the time of deposition. Future uptake of radionuclides from soils to cereals and straw is relatively low the year after deposition of radionuclides (Rosén et al. 1996).

The redistribution rate of radiostrontium in the vascular bundle system is much lower than radiocaesium, due to its divalent form that makes it retain a much harder

Table 2 Percentage of ^{134}Cs in potato tops and tubers at harvest (August) after wet deposition at different growth stages

Year	Growth stage at deposition	Deposition (kBq m^{-2})	Potato tops	Potato tubers
2	II	19.6	0.2 ± 0.1	0.1 ± 0.1
	III	13.0	3 ± 1	3 ± 1
	IV	13.0	5 ± 2	12 ± 4
	IV–V	13.0	8 ± 4	3 ± 2
	V	13.0	17 ± 8	11 ± 5
3	II	19.6	1 ± 1	0.4 ± 0.2
	III	13.0	9 ± 2	1 ± 0.4
	IV	13.0	17 ± 1	4 ± 1
	V	13.0	51 ± 8	0.3 ± 0.1

Means are from four replicates ($n = 4$) with standard deviation. Modified after Rosén and Vinichuk (unpublished)

cuticle layer of the epidermis (Aarkrog 1969, 1975, 1983; Müller and Pröhl 1993; Bréchignac et al. 2000; Vandecasteele et al. 2001). Several studies have estimated that 25 % of the taken up radiostrontium in cereals is redistributed to other plant parts through the vascular bundle system, with between 5 and 10 % being redistributed to the grains, and as much as 50 % being redistributed to the roots (Coughtrey et al. 1983). However, at later growth stages, it has been found that radiostrontium can be washed-off, which is related to the desquamation of the cuticle (Chadwick and Chamberlain 1970; Madoz-Escande et al. 2004).

The redistribution of radiocaesium can vary by a factor of 100 during the growing season, and this big variation is related to the plant's physiological development. If the radiocaesium contamination occurs before the anthesis, then it will result in a low redistribution of radiocaesium from the leaves to the seeds; but if the contamination of radiocaesium takes place during the anthesis or after, then this will result in a large redistribution of radiocaesium to the seeds (Gerdung et al. 1999; Bengtsson et al. 2013). For potatoes, 3–12 % of the taken up radiocaesium is redistributed to the potato tubers (Table 2) (Rosén and Vinichuk (unpublished)). Although radionuclides are deposited at an early growth stage, i.e. growth stage I, the amount of ^{134}Cs intercepted and taken up will be negligible in potato tops and tubers.

As it is shown in Fig. 4, the activity concentration of ^{134}Cs in potato tops gradually decreased in the later growth stages, which is likely due to the loss of radionuclides from the surface of leaves, caused by wind and rain, as well due to radionuclide uptake and distribution within the crop. After fallout, parts of the intercepted radioactive fallout may be transported to the ground through wind and precipitation, thus reducing the radioactivity of the crop. ^{134}Cs activity concentration may be further reduced by plant debris and by dilution due to crop growth. However, there are some exceptions, e.g. radionuclide content was normally highest when potato tops were sampled on the following day or second day after the deposition event. In such a case, a high level of radionuclide activity in the potato tops is caused by the fact that radionuclides are intercepted by the potato tops and retained on the leaves' surface, as well as those which were intercepted and possibly taken up by the potato crop. According to Harris (1992) and Bodin and Svensson (1996), the beginning of tuber formation requires carbohydrates produced by photosynthesis, which is directly related to the leaves' area. Thus, radionuclide fallout at the well-developed leaves' stages resulted in higher ^{134}Cs activity concentration in potato tops due to radiocaesium interception, which is expected to be the more effective if the surface of the potato tops is larger.

4 Foliar Uptake of Radionuclides

It is assumed that activity concentration of radionuclides in agricultural crops is linearly related to the concentration in the root zone (Ehlken and Kirchner 2002). This relation is defined as the transfer factor (Ehlken and Kirchner 2002), which is used to describe the transfer of radionuclides from the environment to the agricultural crops in a specific situation (von Fircks et al. 2002).

To estimate the foliar uptake, the aggregated transfer factor (T_{ag}) can be used. The T_{ag} ($m^2\ kg^{-1}$) is defined as the activity concentration of radionuclides in edible plant parts based on the amount of deposition (Howard et al. 1996; Rosén et al. 1996; Ehlken and Kirchner 2002). However, the translocation factor (f_{tr}) can be used as well. The f_{tr} ($m^2\ kg^{-1}$) is defined as the activity concentration in edible plant parts to the amount intercepted (Thiessen et al. 1999; Vandecasteele et al. 2001). The T_{ag}-values, in agricultural crops, e.g. seeds, have the same trends as activity concentration of radionuclides. However, the f_{tr}-values have a lesser correlation to the deposited activity concentration, as f_{tr}-values are a function of the intercepted amount of radioactivity, which can vary between the different deposition occasions. Nevertheless, f_{tr}-values will have the same pattern as the T_{ag}-values have (Bengtsson et al. 2013).

At later growth stages, the T_{ag}-values will usually increase (Fig. 5), which is an indication that the interception of radionuclides is not the only thing happening and it is the explanation to the activity concentrations in seeds of cereals and oil crops. Other contributing factors can be, for example, dilution of radionuclide concentration due to growth of the biomass (Coughtrey et al. 1983), fall-off of radionuclides between the deposition events until harvest time (Eriksson et al. 1998b; Colle et al. 2009) and the decay rate of the radionuclides (Choi et al. 2002). Furthermore, the T_{ag}- and f_{tr}-values are influenced by the type of crop and the type of radionuclides.

The usefulness of T_{ag}- and f_{tr}-values for predicting possible contamination of food items in a real situation is somewhat insufficient, due to the uncertainty in these values (Bengtsson et al. 2013). Nevertheless, the T_{ag}- and f_{tr}-values are the best values that are currently available directly after an accidental deposition of radionuclides onto agricultural crops. Furthermore, the use of these factors should

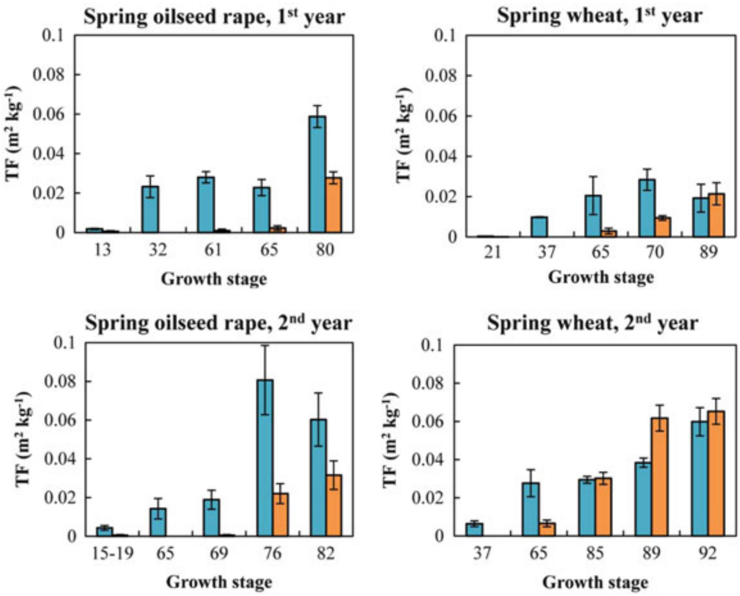

Fig. 5 The average transfer factors (T_{ag}, $m^2\ kg^{-1}$) of ^{134}Cs (*blue bars*) and ^{85}Sr (*orange bars*) for seeds after wet deposition at five different growth stages in spring oilseed rape and spring wheat. For all growing stages, the average number of observations was $n = 3$, except spring oilseed rape (2nd year), $n = 2$ at growth stage 65 for ^{134}Cs. *Error bars* indicate the standard error of the mean. Modified after Bengtsson et al. (2013)

be used with great caution, especially when used for mathematical ecosystem models (McGee et al. 1996). For that reason, preliminary assessment of activity concentrations in agricultural crops requires continuous sampling and monitoring. Nevertheless, the use of these transfer factors can be a rather quick tool to facilitate decision-making on countermeasures for reducing the distribution of radionuclides to foodstuffs (Howard et al. 1996; Kostiainen et al. 2002).

4.1 Radiocaesium Transfer, from Potato Tops to Tubers

Generally, the levels of ^{134}Cs T_{ag}-values for potato tops were found to be between one and two orders of magnitude higher than for potato tubers, depending on deposition and sampling time. ^{134}Cs T_{ag}-values for potatoes (tops and tubers) depend strongly on the date of radionuclide application and to a lesser degree on the date of sampling/harvest. Deposition of radionuclides at early growth stages of potatoes resulted in low levels of radionuclide transfer from deposition to the different plant parts. However, when the deposition of radionuclides occurred at later growth stages and at tuber bulking, this resulted in high levels of ^{134}Cs activity concentration in both potato tops and tubers (Rosén and Vinichuk (unpublished)). The reason for higher T_{ag}-values for potato tops at the later growth stages is interception of wet-deposited radiocaesium depending on the leaves' area (LAI), and this is likely to be more effective in the case of a larger surface on the potato tops. When deposition of radionuclides occurred in the second half of the growing season and at the senescence of potato tops, the transfer of ^{134}Cs from potato tops to potato tubers decreased (Fig. 6).

The level of ^{134}Cs T_{ag}-values in potatoes generally follows the same pattern as the levels of ^{134}Cs activity concentration. ^{134}Cs T_{ag}-values in potato tops generally decreased in the later growth stages, whereas ^{134}Cs activity concentrations in potato tubers slightly decreased or did not change. However, there were smaller parts of caesium transferred to the potato tubers (Fig. 4).

The ^{134}Cs T_{ag}-values were highest when deposition of radionuclide occurred at tuber initiation (growth stage III). Generally, deposition of radionuclide at the beginning of the growing season led to about 2.5 times lower ^{134}Cs transfer from deposition to potato tubers, compared to the situation if deposition occurred at tuber initiation (growth stage III). When deposition of radionuclides occurred at growth stage IV, ^{134}Cs transfer to potato tubers was found to be about four times lower compared with deposition occasion at growth stage III.

Although the effect of radionuclide deposition time on ^{134}Cs T_{ag}-values for potato tops when sampled/harvested in the period from August 6–29 for each year was less pronounced, it was still similar to that observed for potato tubers. Values of ^{134}Cs T_{ag} were found to be generally highest when deposition of radionuclide occurred at growth stage II, plant establishment. High ^{134}Cs T_{ag}-values were also measured when potato tops were sampled directly (on the next day) after deposition occurred and gradually decreased when sampling took place later on.

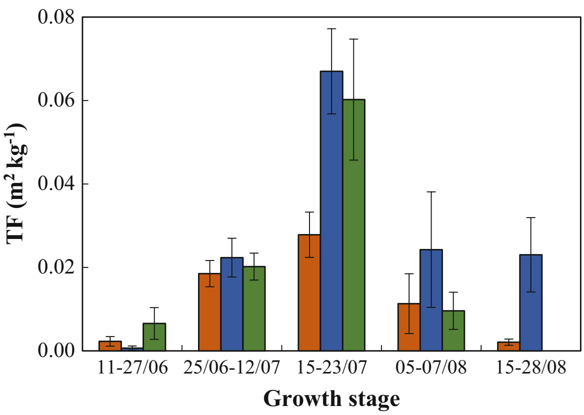

Fig. 6 The average transfer factors (T_{ag}, m^2 kg^{-1}) of ^{134}Cs for potato tubers after wet deposition at five different growth stages and 3 years in potatoes (*orange bars* year 1, *violet bars* year 2 and *green bars* year 3). Modified after Rosén and Vinichuk (unpublished)

5 Conclusions

The interception of deposited radionuclides on cereals and oil crops is highest at the ripening phase. The measurement of leaf area index (LAI) can be used, theoretically, to estimate the interception of radionuclides on agricultural crops.

The initial interception of radionuclides in the potato tops varies with the growth stage. At the early fallout, potato tops have a small interception rate, and the growth reduces the concentration of radiocaesium in potatoes during the growing season by dilution effect. Caesium activity concentrations in potato tops generally decrease in the later growth stages, whereas caesium activity concentrations in potato tubers slightly decrease or do not change, which indicates that only a relatively small part of caesium is transferred to the potato tubers.

The transfer of radionuclides to seeds of cereals and oil crops is highest when the deposition of radionuclides takes place close to the harvest time. Therefore, the highest risk of transfer of radionuclides into the human food chain is when deposition occurs at the end of the growing season for agricultural crops.

The biggest part of the radionuclides taken up by cereals and oil crops was found in the straw part, whereas a smaller part was found in the seeds. The amount of radionuclides between the different plant parts will not systematically vary at harvest and deposition occasions.

The timing of the deposition and growth stage controls the caesium content in mature potato tubers. Fallout during the first half of the growing season gives low levels in the potato tubers. At earlier deposition, lower levels of caesium are detected in mature potato tubers. The highest activity concentrations of radionuclides in the crops were detected if the deposition takes place in the middle of the growing season. After deposition in the second half of the growing season, the activity concentrations of caesium decreased, and if the deposition occurred closer to harvest, then a lower level of activity concentration of caesium would be detected.

References

Aarkrog A (1969) On direct contamination of rye, barley, wheat and oats with ^{85}Sr, ^{134}Cs, ^{54}Mn and ^{141}Ce. Radiat Bot 9:357–366

Aarkrog A (1975) Radionuclide levels in mature grain related to radiostrontium content and time of direct contamination. Health Phys 28:557–562

Aarkrog A (1983) Translocation of radionuclides in cereal crops. In: Coughtrey PJ, Bell JN, Roberts TM (eds) Ecological aspects of radionuclide release. Blackwell Scientific Publications, Oxford

Absalom JP, Young SD, Crout NMJ (1995) Radiocesium fixation dynamics—measurement in 6 cumbrian soils. Eur J Soil Sci 46:461–469

Absalom JP, Young SD, Crout NMJ, Sanchez A, Wright SM, Smolders E, Nisbet AF, Gillett AG (2001) Predicting the transfer of radiocaesium from organic soils to plants using soil characteristics. J Environ Radioact 52:31–43

Åhman B, Åhman G (1994) Radiocesium in Swedish reindeer after the chernobyl fallout—seasonal-variations and long-term decline. Health Phys 66:503–512

Andersson I, Bergman R, Enander A, Finck R, Johanson KJ, Nylén T, Preuthun J, Rosén K, Sandström B, Svensson K, Ulvsand T (2002) Livsmedelsproduktionen vid nedfall av radioaktiva ämnen. Jordbruksverket, Jönköping

Andersson P, Carlsson M, Falk R, Hubbard L, Leitz W, Mjönes L, Möre H, Nyblom L, Söderman AL, Yuen Larsson K, Åkerblom G, Öhlén E (2007) Strålmiljön i Svergie. Stockholm, Sweden

Bengtsson SB (2013) Interception and storage of wet deposited radionuclides in crops: Field experiments and modelling. Ph. D. thesis, Swedish University of Agricultural Sciences, Uppsala

Bengtsson SB, Eriksson J, Gärdenäs AI, Rosén K (2012) Influence of development stage of spring oilseed rape and spring wheat on interception of wet-deposited radiocaesium and radiostrontium. Atmos Environ 60:227–233

Bengtsson SB, Eriksson J, Gärdenäs AI, Vinichuk M, Rosén K (2013) Accumulation of wet-deposited radiocaesium and radiostrontium by spring oilseed rape (*Brássica napus* L.) and spring wheat (*Tríticum aestívum* L.). Environ Pollut 182C:335–342

Bengtsson SB, Gärdenäs AI, Eriksson J, Vinichuk M, Rosén K (2014) Interception and retention of wet-deposited radiocaesium and radiostrontium on a ley mixture of grass and clover. Sci Total Environ 497–498:412–419

Bodin B, Svensson B (1996) Potatis och potatisproduktion. Institutionen för växtodlingslära, SLU, Uppsala (In Swedish)

Bréchignac F, Vallejo R, Vandecasteele C, Shaw G, Forsberg S, Madoz-Escande C (2000) Improving the short and long term prediction ability of radiocontaminant behavior in agro-ecosystems. Rapport Scientifique et Technique IPSN e RST

Buysse J, Van den Brande K, Merckx R (1995) The distribution of radiocesium and potassium in spinach plants grown at different shoot temperatures. J Plant Physiol 146:263–267

Chadwick RC, Chamberlain AC (1970) Field loss of radionuclides from grass. Atmos Environ 4:51–56

Choi YH, Lim KM, Yu D, Park HG, Choi YG, Lee CM (2002) Transfer pathways of Mn-54, Co-57, Sr-85, Ru-103 and Cs-134 in rice and radish plants directly contaminated at different growth stages. Ann Nucl Energ 29:429–446

Colle C, Madoz-Escande C, Leclerc E (2009) Foliar transfer into the biosphere: review of translocation factors to cereal grains. J Environ Radioact 100:683–689

Coughtrey PJ, Jakson D, Thorne MC (1983) Radionuclide distribution and transport in terrestrial and aquatic ecosystems, vol 4, A critical review of data. CRC, Boca Raton, FL

Ehlken S, Kirchner G (2002) Environmental processes affecting plant root uptake of radioactive trace elements and variability of transfer factor data: a review. J Environ Radioact 58:97–112

Eichert T, Burkhardt J (2001) Quantification of stomatal uptake of ionic solutes using a new model system. J Exp Bot 52:771–781

Eichert T, Burkhardt J, Goldbach HE (2002) Some factors controlling stomatal uptake. Acta Hort (ISHS) 594:85–90

Eriksson Å, Rosén K, Haak E (1998a) Retention of simulated Fallout nuclides in agricultural crops, I. experiments on leys. SLU-REK-80. Institutionen för radioekologi, SLU, Uppsala

Eriksson Å, Rosén K, Haak E (1998b) Retention of simulated fallout nuclides in agricultural crops, II. deposition of Cs and Sr on grain crops. SLU-REK-81. Institutionen för radioekologi, SLU, Uppsala

Franic Z, Petrinec B, Marovic G, Franic Z (2007) Radiocaesium activity concentrations in potatoes in Croatia after the Chernobyl accident and dose assessment. J Environ Sci Health B 42:211–217

Gerdung S, Pollot M, Fischer P, Grillmaier RE, Müller P (1999) Contamination of wheat, rye, and potatoes by foliar application of Cs-134. J Radioanalyt Nucl Chem 240:451–454

Gommers A, Thiry Y, Vandenhove H, Vandecasteele CM, Smolders E, Merckx R (2000) Radiocesium uptake by one-year-old willows planted as short rotation coppice. J Environ Qual 29:1384–1390
Handley R, Babcock KL (1972) Translocation of ^{85}Sr, ^{137}Cs, and ^{106}Ru in crop plants. Radiat Bot 12:113–119
Harris PM (1992) The potato crop: the scientific basis for improvement (2nd edn). London: Chapman & Hall New York: Van Nostrand Reinhold, London: New York.
Hoffman FO, Thiessen KM, Frank ML, Blaylock BG (1992) Quantification of the interception and initial retention of radioactive contaminants deposited on pasture grass by simulated rain. Atmos Environ A 26:3313–3321
Hossain MB, Ryu KS (2009) Effect of foliar applied phosphatic fertilizer on absorption pathways, yield and quality of sweet persimmon. Scientia Horticult 122:626–632
Howard BJ, Johansson K, Linsley GS, Hove K, Pröhl G, Horyna J (1996) Transfer of radionuclides by terrestrial food products from semi-natural ecosystems to humans. In. Second report of the VAMP Terrestrial Working Group, International Atomic Energy Agency (IAEA) Bulletin, IAEA-TECDOC-857, Vienna
IAEA (2010) Handbook of parameter values for the prediction of radionuclide transfer in terrestrial and freshwater environments. Technical Reports Series 472, Vienna
Kinnersley RP, Goddard AJH, Minski MJ, Shaw G (1997) Interception of caesium-contaminated rain by vegetation. Atmos Environ 31:1137–1145
Koranda JJ, Robison WL (1978) Accumulation of radionuclides by plants as a monitor system. Environ Health Perspect 27:165–179
Kostiainen E, Hänninen R, Rosén K, Haak E, Eriksson A, Nielsen S, Keith-Roach M, Salbu B (2002) Transfer factors for nuclear emergency preparedness. Report from the NKS/BOK-1.4 project group countermeasures in agriculture and forestry, NKS-78, Roskilde, Denmark
Lepicard S, Dubreuil GH (2001) Practical improvement of the radiological quality of milk produced by peasant farmers in the territories of Belarus contaminated by the Chernobyl accident—The ETHOS project. J Environ Radioact 56:241–253
Madoz-Escande C, Henner P, Bonhomme T (2004) Foliar contamination of Phaseolus vulgaris with aerosols of Cs-137, Sr-85, Ba-133 and Te-123m: influence of plant development stage upon contamination and rain. J Environ Radioact 73:49–71
McGee EJ, Johanson KJ, Keatinge MJ, Synnott HJ, Colgan PA (1996) An evaluation of ratio systems in radioecological studies. Health Phys 70:215–221
Middleton LJ (1958) Absorption and translocation of strontium and caesium by plants from foliar sprays. Nature 181:1300–1303
Müller H, Pröhl G (1993) ECOSYS-87: a dynamic model for assessing radiological consequences of nuclear accidents. Health Phys 64:232–252
Oughton DH, Salbu B (1994) Influence of physico-chemical forms on transfer. Stud Environ Sci 62:165–184
Pröhl G (2009) Interception of dry and wet deposited radionuclides by vegetation. J Environ Radioact 100:675–682
Rosén K (1996) Transfer of radiocaesium in sensitive agricultural environments after the Chernobyl fallout in Sweden.2. Marginal and seminatural areas in the county of Jämtland. Sci Total Environ 182:135–145
Rosén K, Eriksson A, Haak E (1996) Transfer of radiocaesium in sensitive agricultural environments after the Chernobyl fallout in Sweden. 1. County of Gävleborg. Sci Total Environ 182:117–133
Salbu B, Lind OC, Skipperud L (2004) Radionuclide speciation and its relevance in environmental impact assessments. J Environ Radioact 74:233–242
Salisbury FB, Ross CW (1992) Plant physiology, 4th edn. Wadsworth Publishing Company, Belmont, CA

Smith FB (2001) Dispersion and transfer in the terrestrial environment. In: Van der Stricht E, Kirchmann R (eds) Radioecology radioactivity and ecosystems. Fortemps, Liège. ISBN 2-9600316-0-1

Smith FB, Beresford NA (2005) Chernobyl - Catastrophe and Consequences. Springer and Praxis Publishing.

Sokołowska K, Somiński P (2013) Symplastic transport in vascular plants. Springer, New York.

Thiessen KM, Thorne MC, Maul PR, Pröhl G, Wheater HS (1999) Modelling radionuclide distribution and transport in the environment. Environ Pollut 100:151–177

Tsukada H, Nakamura Y (1999) Transfer of Cs-137 and stable Cs from soil to potato in agricultural fields. Sci Total Environ 228:111–120

Tukey HB, Bukovac MJ, Wittwer SH (1961) Absorption of radionuclides by aboveground plant parts and movement within plant. J Agric Food Chem 9:106–113

Vandecasteele CM, Baker S, Forstel H, Muzinsky M, Millan R, Madoz-Escande C, Tormos J, Sauras T, Schulte E, Colle C (2001) Interception, retention and translocation under greenhouse conditions of radiocaesium and radiostrontium from a simulated accidental source. Sci Total Environ 278:199–214

Veresoglou DS, Barbayiannis N, Matsi T, Anagnostopoulos C, Zalidis GC (1996) Shoot Sr concentrations in relation to shoot Ca concentrations and to soil properties. Plant and Soil 178:95–100

von Fircks Y, Rosén K, Sennerby-Forsse L (2002) Uptake and distribution of Cs-137 and Sr-90 in Salix viminalis plants. J Environ Radioact 63:1–14

White PJ (2001) The pathways of calcium movement to the xylem. J Exp Bot 52:891–899

Zhu YG, Smolders E (2000) Plant uptake of radiocaesium: a review of mechanisms, regulation and application. J Exp Bot 51:1635–1645

Root Uptake/Foliar Uptake in a Natural Ecosystem

P.K. Manigandan, B. Chandar Shekar, and D. Khanna

Contents

Abstract The leaves of native tree species (sylva) and their associated soil samples were collected from Western Ghats, India, and analyzed to comprehend the mechanism of radionuclide uptake. For comparison, prominent tree species of the region, *Elaeocarpus oblongus* and *Michelia nilagirica* (tall trees), *Vaccinium neilgherrense* and *Viburnum hebanthum* (short trees), *Lasianthus coffeoiaes* and *Hedyotis stylosa* (bushes), and *Cymbidium aloifolium* (an orchid), were sampled, and the concentration of radionuclides in the plant and soil was measured using a gamma-ray spectrometer and an alpha counter selected for analysis. The activity concentration ratio (CR) of radionuclides in the plants from the underlying soil was calculated and found to vary widely within plants and between plants. CR values indicate the variation of radionuclide accumulation in various species, while *E. oblongus*,

P.K. Manigandan (✉)
Sai Nath University, Ranchi 834009, India
e-mail: pkmgs@yahoo.com

B.C. Shekar
Kongunadu Arts and Science College, Bharathiar University, Coimbatore, India

D. Khanna
Karunya University, Coimbatore, India

C. Walther, D.K. Gupta (eds.), *Radionuclides in the Environment*,
DOI 10.1007/978-3-319-22171-7_7

Evodia roxburghiana, and *C. aloifolium* exhibited preferential uptake of radionuclides. The dust particles trapped in the root system of *C. aloifolium* could be used as a bioindicator to monitor fallout radionuclides in the Western Ghats.

Keywords Radionuclides • Western Ghats • Concentration ratio • Bioindicator • Uptake mechanism

1 Introduction

The Nilgiri hill station is a part of the Western Ghats of India and is known to contain some of the significant distribution of monazite (Mishra 1993; Sunta et al. 2000). To determine the radiation exposure of the population, it is important to estimate the potential dose from naturally occurring and fallout radionuclides. The most common pathways for these radionuclides to reach humans usually involve direct ingestion and inhalation of contaminated dust particles. However, these radionuclides may also be transmitted through the food chain, and attendant doses are additive to those received from other pathways. When ingestion or inhalation of dust is minimized, because of a humid environment or continuous soil cover, the food chain contributing to the total doses will become predominant (Manigandan and ChandarShekar 2015). Thus, the behavior of these radionuclides is a major determinant of plant uptake.

Irrespective of biological necessity, plants have been observed to take up and absorb many cations present in their root region, with naturally occurring radionuclides being no exception. In the soil, each radioactive element follows complex dynamics, in which a part of the element is transported into the soil solution, while another part gradually becomes strongly bound to the soil particles. The portion of these radionuclides in the soil solution can be incorporated via the root into the plants. In some cases (U and Th), this process is facilitated by the chemical similarity of these radionuclides with other elements that the plant normally uses for its growth. It is important to study the dynamics of these radionuclides in soil and their transfer to plants, as these are the basic links in evaluating the transport of radionuclides along the food chain. To quantify the transfer of a radionuclide from the soil to the plant, one generally uses the corresponding transfer coefficient, which is the ratio between the activity concentrations of the radionuclides under consideration in the compartments.

In the food chain model in which the soil/plant relationship is depicted, plants can be viewed as a hydraulic conduit for the water stored in the soil to travel upward and evaporate from the leaves. This flow of water carries radionuclides, dissolved in the soil water to the roots. The flow of water is dependent on the retention of soil moisture and supply and is also linked to the size and growth rate of the plant. This relation is further complicated by the effects of weather, growth conditions, and multiple soil properties. Attempts to model all these processes in a mechanistic manner have not evolved to a broadly applicable level (Baldwin et al. 1973; Barber et al. 1984). Thus, root uptake is often treated at an empirical level, such as with the CR model.

Among the radionuclides of interest, the fallout radionuclide ^{210}Po is closely associated with atmospheric moisture and dust particles (Manigandan and ChandarShekar 2014). The epiphytic plants depend on atmospheric moisture and dust particles for their nutrients, resulting in a potentially higher absorption and accumulation of atmospheric ^{210}Po. The predominant tree species of the region, *Elaeocarpus oblongus* and *Michelia nilagirica* (tall tress), *Vaccinium neilgherrense* and *Viburnum hebanthum* (short tress), *Lasianthus coffeoiaes* and *Hedyotis stylosa* (bushes), and *Cymbidium aloifolium* (an orchid), were selected for analysis. Data on the naturally occurring radionuclide concentration in the plants of the Western Ghats region have not been reported previously, and the present study is the first systematic effort to obtain these data. Although the species selected for the present study are not directly involved in the human food chain, information on the activity concentration of radionuclides and their transfer factor is important because this information is useful in predicting the soil to plant transfer of the radionuclides. Prior to root uptake analysis, vertical distribution of radionuclides in the soil was analyzed so as to understand the availability of radionuclides at the root zones.

2 Materials and Methods

2.1 Study Area

The Nilgiris are a well-defined massif that forms the southern limit of the main Western Ghats system that stretches unbroken from Mumbai in the north to the Nilgiris in the south of India (Fig. 1). The altitude of this region varies from 1700 to 2400 M above mean sea level. This ecosystem is one of the oldest and most important in the Indian peninsula. The annual average rainfall is 1590 mm. The annual temperature variation ranges from approximately 4 to 24 °C. The total duration of the rainy season is approximately 5 months, from June to October. The soil in the study area is predominantly lateritic, dark brown, and loamy textured with fine medium grains.

2.2 Sample Collection and Processing

Various sylva plants were selected to study the transfer of these radionuclides to the plant from the forest soil. Different samples, such as leaves and bark of 2 kg each, were collected from these plants within the forests of long wood. Soil samples were also collected (20 cm depth) from four different places under the host trees

Fig. 1 Study area: Nilgiri's district

and mixed thoroughly; approximately 2 kg of composite sample was collected in a polythene bag. Similarly, *E. oblongus*, *M. nilagirica*, *V. neilgherrense*, *V. hebanthum*, *L. coffeoiaes*, and *H. stylosa* tree leaf samples of 2 kg each were collected, and soil samples were also collected at the same locations where the vegetation samples were collected. The *C. aloifolium* leaves were collected along with dust particles trapped in the root system. In order to study vertical migration of radionuclides in soil, 10 more soil samples were also collected at various depth profiles closed to the above said sampling points.

The vegetation samples were dried in an oven at 110 °C, and approximately 30 g samples were used for the wet ashing and subsequent analysis of ^{210}Po. The remaining samples were charred over a low flame and converted into uniform white ash using a muffle furnace at 400 °C; similarly, the soil samples were dried in an oven at 110 °C and used for analysis.

2.3 Activity Determination

The primordial radionuclide activities were measured using a γ-ray spectrometer, which consisted of a "3 × 3" NaI (Tl) detector coupled with a TNI PCA II Ortec model 8K multichannel analyzer. The "3 × 3" NaI (Tl) detector was protected from ambient radiation using adequate lead shielding, which reduced the background by a factor of 95. The efficiency for various gamma energies was determined using an International Atomic Energy Agency standard source with the required geometry. The system was calibrated both in terms of energy response and counting efficiency. The density of the sample used for the calibration was 1.3 g/cm^3, which was nearly the same as the average of the soil samples analyzed (1.24 g/cm^3). The soil samples were analyzed with a NaI (Tl) spectrometer for a 20,000 s counting time for each sample. The minimum detectable concentration (MDC) was 7 Bq kg^{-1} for the ^{232}Th series, 8.4 Bq kg^{-1} for the ^{238}U series, and 13.2 Bq kg^{-1} for ^{40}K at a 3σ confidence level. The concentrations of several radionuclides of interest were determined in each sample. The peaks corresponding to 1.46 Mev (^{40}K), 1.76 MeV (^{214}Bi), and 2.614 MeV (^{208}Tl) were used in the evaluation of the activity levels of ^{40}K, the ^{238}U series, and the ^{232}Th series, respectively. The resolution of the crystal detector was 6 % for ^{40}K, 4.4 % for ^{232}Th series, and 5.5 % for the ^{238}U series. The activity concentration of the radionuclides measured in the soil samples was calculated using dedicated software, and the selection of a reference was made such that the radionuclides were sufficiently discriminated.

To determine the concentration of ^{210}Po, approximately 30 g of dried samples was collected. The samples were first digested with a 4 N HNO_3 and then with an 8 N HNO_3 and with a mixture of concentrated HNO_3 and H_2O_2. The digested samples were brought to the chloride medium by adding a 0.5 N HCl solution. Then, ^{210}Po was deposited on a background count, brightly polished silver disk using the electrochemical exchange method (Martinez-Aquire et al. 1997; Timpereley et al. 1970). Then, the concentration of ^{210}Po was counted in a ZnS [Ag] alpha counter with a background of 0.2 cpm and an efficiency of 30 %. The ^{210}Po activity was estimated using standard methods (Iyengar et al. 1990; Anand and Rangarajan 1990).

3 Results and Discussion

3.1 Activity Concentration Radionuclides as a Function of Soil Depth

We collected soil samples from a forest ecosystem in the Western Ghats and studied the activity concentrations of radionuclides as a function of soil depth (Table 1). The results show that the activity concentrations of ^{238}U, ^{232}Th, ^{210}Po, and ^{40}K increased in the first two profiles, but activity concentrations were variable in most samples below these profiles (Fig. 2).

The increase of activity concentrations in the first two profiles may be explained by changes in the amounts of organic matter. In particular, ^{238}U and ^{232}Th series are immobile radionuclides, but ^{238}U can move through the soil due to the formation of

Table 1 Activity concentration of radionuclides in different soil profiles collected around the host plants

Locations	Different layers (cm)	Activity concentration [Bq kg^{-1}]			
		^{238}U	^{232}Th	^{40}K	^{210}Po
L-1 *Ilex wightiana*	0–10	15.12	39.17	198.79	20.12
	10–20	28.45	55.37	213.1	24.33
	20–30	30.27	51.36	200.11	19.23
L-2 *Eugenia arnottiana*	0–10	21.03	45.89	205.37	26.32
	10–20	24.22	49.64	224.8	30.62
	20–30	27.03	52.88	211.17	26.83
L-3 *Turpinia pomifera*	0–10	19.99	47.76	202.77	24.13
	10–20	29.76	55.45	210.73	29.48
	20–30	24.28	48.53	229.13	20.83
L-4 *Isonandra candolleana*	0–10	21.42	48.91	195.39	27.03
	10–20	28.79	49.55	217.89	33.73
	20–30	23.51	51.53	181.17	28.11
L-5 *Cinnamomum wightii*	0–10	20.19	53.55	209.67	24.42
	10–20	21.01	57.63	221.22	29.44
	20–30	26.95	54.42	227.28	22.36
L-6 *Evodia roxburghiana*	0–10	27.9	51.86	218.06	32.2
	10–20	31.23	52.65	232.26	37.02
	20–30	16.77	44.23	226.99	35.01
L-7 *Myrsine wightiana*	0–10	18.57	46.96	201.14	22.1
	10–20	19.2	49.97	233.97	26.77
	20–30	20.3	48.31	186.54	20
L-8 *Elaeocarpus oblongus*	0–10	24.38	48.67	148.89	29.89
	10–20	34.02	51.29	159.65	34.99
	20–30	15.17	48.54	169.16	32.9
L-9 *Michelia nilagirica*	0–10	18.56	44.414	211.19	22.81
	10–20	22.12	52.07	219.78	29.66
	20–30	33.68	48.72	178.88	23.07
L-10 *Glochidion neilgherrense*	0–10	19.99	46.5	127.54	23.72
	10–20	23.81	41.59	155.1	26.81
	20–30	25.34	46.83	154.28	21.92

(L-1 to L-10 denote the location where sylva plants were collected)

organic complexes with soil colloids. Thorium is strongly adsorbed by soil and becomes immobile. Thus, the increased activity concentration of ^{232}Th in the first two profiles is due to the presence of monazite sand, which is dispersed during igneous, sedimentary, and metamorphic cycles of geological evolution. Thus, the activity concentrations of ^{238}U, ^{232}Th, and ^{40}K in the soil varied slightly from the surface to a depth of 20 cm.

In a step advance, the increase in activity is attributed to two reasons: (1) Uranium is oxidized to 5^{+} and 6^{+} states in the near-surface environment. The 6^{+} oxidation state is the most soluble and forms soluble uranyl complex iron

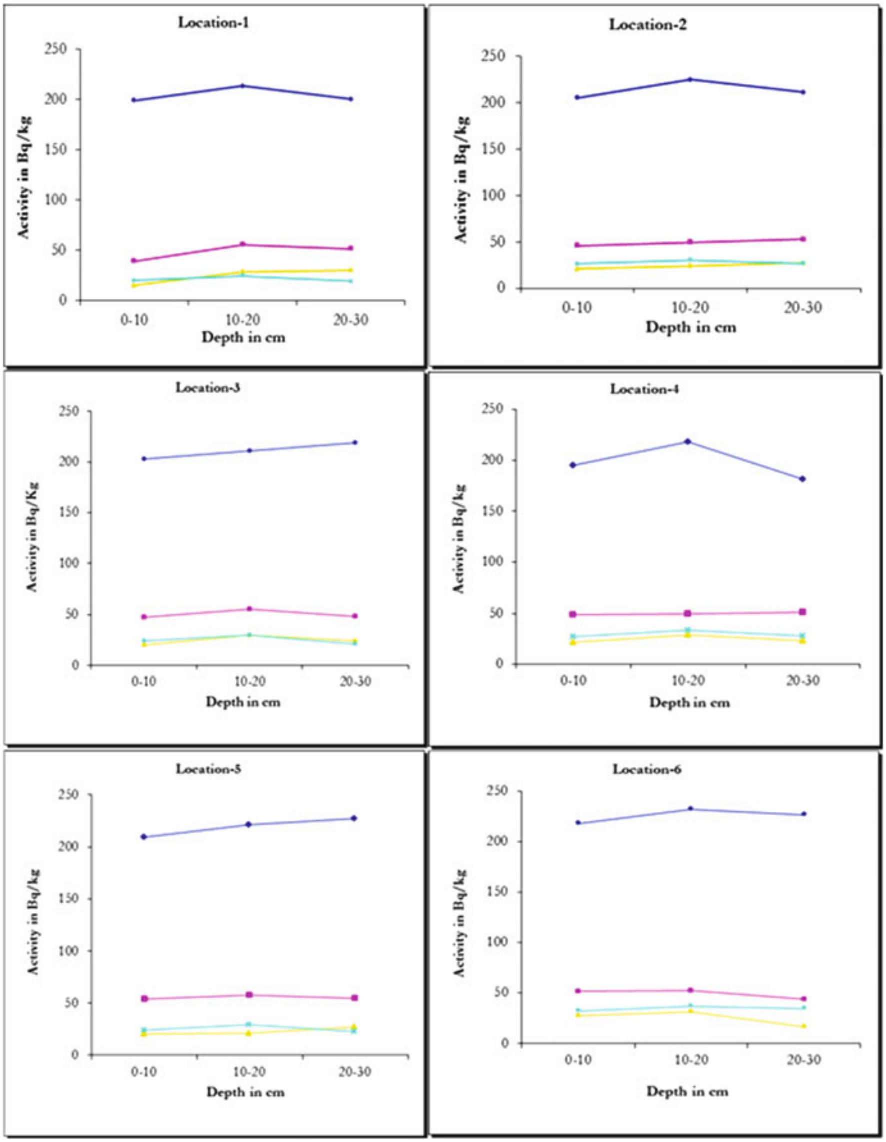

Fig. 2 Variation of activity concentration of different radionuclides at different depths of soil

[UO_2^{2+}], which plays the most important role in U transport (Gascoyne 1992). (2) Koczy (1954) stated that U has more mobility because uranyl ions are able to form complex compounds and U is generally soluble in nature. Similarly, ^{40}K in the form of K^+ is highly soluble in water and has higher mobility, leading to a variation of activity concentration in different layers in soil. The same was observed by Karunakara et al. (2001) and Shetty et al. (2006).

But the fallout radionuclide ^{210}Po strongly adsorbed in soil will move through soil under the influence of water, and salt solution tends to be available for plants. The presence of earthworms turns over the top soil which leads to the distribution of fallout radionuclides into the deep root soil. At the same time, a certain portion of ^{210}Po in the upper layer may get washed out due to heavy rain, and the deep soil keeps on accumulating without any movement. This is attributed to the increase of activity of ^{210}Po in the top two profiles.

3.2 Activity Concentration in Sylva Plant Species

In the soil, each radioactive element follows complex dynamics in which a part of its concentration is transported into the soil solution, while another part gradually becomes strongly bound to the particles of the soil. The portion of these radionuclides, which is in the soil solution, can be incorporated via the root into the plants. In some cases this is facilitated by their chemical similarity with other elements that the plant normally uses for its growth.

The same radionuclides were analyzed in a sample of different plant species, whose results are presented in Table 2. It is clear from the table that the activity concentrations of ^{238}U series and ^{232}Th series are below detectable limit, i.e., very low in most of the plants. According to CR principles, plant radionuclide concentration should reflect soil concentration. However, this may be not true because of sorption on soil, which may render radionuclides less available for uptake (Manigandan and ChandarShekar 2015). Furthermore, radionuclide belonging to physiologically regulated elements, or their analogues, may be selectively adsorbed, whereas others may be excluded. Root uptake of radionuclides is a complex phenomenon, especially for primordial nuclides. The low activity concentration of radionuclides in plants is clearly observed in most of the fast-growing plant species except *Evodia roxburghiana*, *Elaeocarpus oblongus*, and *Glochidion neilgherrense*. A significant difference in radioactivity concentration of these radionuclides between plant species is likely caused by physiological difference and related factors. The activity of ^{210}Po varies from 5.86 to 9.81 Bq kg^{-1} in the bark and 7.88–12.96 Bq kg^{-1} in the younger leaves. It's quite obvious that the concentration of ^{210}Po is higher in the younger leaves than in the bark where the requirement of nutrition is low for dead cell in bark than younger cells in leaves. And also the activity concentration of ^{210}Po is higher than that of ^{238}U in most of the samples. In general, the highest activity concentration in plants is found in those collected in areas with the highest radioactivity concentration in soil substrate.

In all results, the small amount of activity concentration of these radionuclides may result from (1) higher mobility of ^{210}Po within the plant absorbed from soil in colloidal form, (2) epiphytic plants that are growing in host tree which depend on the atmospheric moisture and dust particles for their nutrients, and (3) atmospheric deposition of dust into plants, from splash of soil into plants during rainfall and from dust created during food processing. Washing plant samples may be

Table 2 Activity concentration of radionuclides in the different fraction plants and host soil

Plant species	Type of sample	Activity concentration [Bq kg^{-1}]			
		^{238}U	^{232}Th	^{40}K	^{210}Po
Myrsine wightiana	Soil	22.53	55.17	219.27	26.83
	Bark	BDL	BDL	100.00	7.13
	Leaves	BDL	BDL	212.20	9.01
Evodia roxburghiana	Soil	33.53	68.12	203.90	37.71
	Bark	8.68	9.83	171.97	8.93
	Leaves	10.87	15.69	163.32	11.02
Isonandra candolleana	Soil	24.38	49.98	197.58	29.03
	Bark	BDL	BDL	78.32	6.83
	Leaves	BDL	BDL	162.85	8.92
Turpinia pomifera	Soil	24.35	50.47	213.93	28.54
	Bark	BDL	BDL	146.66	7.63
	Leaves	8.52	10.23	198.16	9.48
Cinnamomum wightii	Soil	19.34	48.40	206.29	24.98
	Bark	BDL	BDL	140.98	5.86
	Leaves	BDL	8.36	166.23	7.88
Michelia nilagirica	Soil	22.93	38.59	213.45	28.46
	Bark	BDL	BDL	105.05	8.03
	Leaves	BDL	BDL	145.10	9.46
Ilex wightiana	Soil	23.97	49.39	213.63	28.31
	Bark	BDL	BDL	19.53	8.13
	Leaves	BDL	BDL	121.26	9.02
Elaeocarpus oblongus	Soil	39.12	58.24	230.10	43.34
	Bark	9.32	10.88	165.25	9.81
	Leaves	11.86	16.20	203.43	12.96
Glochidion neilgherrense	Soil	24.00	48.20	202.49	30.46
	Bark	BDL	9.76	76.51	8.63
	Leaves	8.5	14.17	191.38	9.03
Eugenia arnottiana	Soil	24.45	49.43	225.69	29.71
	Bark	BDL	BDL	77.04	8.03
	Leaves	8.49	9.86	219.25	9.06

insufficient to remove all of the extraneous contamination as some of it may have been absorbed into plant.

Not unexpectedly, ^{40}K levels varied within and between plant species than others. It can be seen from the table that the activity concentration of ^{40}K in the bark varies from 19.53–171.97 Bq kg^{-1} and in younger leaves 121.26–219.25 Bq kg^{-1}. Thus, the concentration of K in the leaves depends significantly on their degree of maturity. So ^{40}K in the plant interior is actively mobilized toward the younger growing tissues. The uptake of potassium increased as the ^{40}K concentration in soil increased, but not linearly; this indicates that the availability of ^{40}K to plant is not directly proportional to the total of ^{40}K present in soil.

All the species seem to have similar requirement for ^{40}K, although there was a significant difference in ^{40}K levels. It is interesting to see that the uptake of all radionuclides is relatively higher in two plant species *Evodia roxburghiana* and *Elaeocarpus oblongus*.

3.3 Activity Concentration of Radionuclides in Physiologically Different Plants

Results of mean activity concentration of these radionuclides in different plants are presented in Table 3. All the species, except *Cymbidium aloifolium* (an orchid), have a similar growing habit and shed their leaves at the end of every growing season, i.e., during the last days of winter. Leaves start budding during the last day of summer. It is clear from the table that the activity concentration of ^{238}U series in the leaves is below detectable limit, i.e., very low in most of the plants, and the concentration of ^{232}Th series is quite significant in the all plants; this reveals the nature of soil presented in the study area (Manigandan and ChandarShekar 2014).

But the concentration of ^{40}K is greater in the leaves of the plant except *C. aloifolium*. This can be attributed to the fact that *C. aloifolium* being epiphytic plants depend mainly on atmospheric dust and on atmospheric moisture for its nutrients, whereas other plants take their nutrients directly from the soil in which ^{40}K concentration is higher compared to the dust trapped in the root dust of *C. aloifolium*. Also, the concentration of ^{210}Po is high compared to other radionuclides in all plant samples. This is because the partial diffusion of ^{222}Rn from the Earth's surface into atmosphere decays continuously to ^{210}Po through various other short-lived and long-lived radionuclides. Therefore, the concentration of ^{210}Po which returns to the biosphere and Earth's surface through dry and wet fallout will be continuous (Abe and Abe 1980). These results suggested that the dust trapped in the root system of *C. aloifolium* could be used conveniently as an indicator of fallout radionuclides from the natural origin.

In general, the highest activity concentration in plants was found in those collected from areas with the highest radioactivity concentration in soil substrate, but the activity concentration in the plants is not linearly related to the activity in soil. From the results of activity concentration of radionuclides in soil and plants, values of CR [CR = activity of radionuclide in plant (Bq kg^{-1} dry weight)/activity of radionuclides in soil (Bq kg^{-1}dry weight)] (Frissel 1997) have been calculated. The results are presented in Table 3 for the primordial and fallout radionuclides. CR values for ^{238}U series, ^{232}Th series, ^{40}K, and ^{210}Po were found to be in the range of BDL to 0.313, BDL to 0.341, 0.802–0.954, and 0.274–0.368, respectively. CR value for ^{210}Po and ^{40}K is considerably higher than that of other radionuclides, which suggests higher levels of uptake of these radionuclides. It is interesting to note that although all the tree species are grown in soils of similar physical–chemical characteristic and similar concentration of these radionuclides, the TF

Table 3 Activity concentration of radionuclides in physiologically different plants and its CR values

Plant species	Activity concentration in soil (Bq kg^{-1})				Activity concentration in plants (Bq kg^{-1})				CR			
	^{238}U	^{232}Th	^{40}K	^{210}Po	^{238}U	^{232}Th	^{40}K	^{210}Po	^{238}U	^{232}Th	^{40}K	^{210}Po
Michelia nilagirica	33.6	51.6	203.4	41.3	BDL	BDL	163.2	11.3	BDL	BDL	0.802	0.274
Elaeocarpus oblongus	36.1	59.9	216.3	45.6	11.3	18.4	206.4	16.8	0.313	0.341	0.954	0.368
Viburnum hebanthum	30.7	50.9	186.8	34.7	BDL	14.3	160.4	10.9	BDL	0.281	0.859	0.314
Vaccinium neilgherrense	38.5	64.6	213.8	44.1	9.6	16.9	187.4	13.5	0.249	0.262	0.877	0.306
Hedyotis stylosa	43.4	75.4	246.7	49.5	11.2	19.4	203.4	14.6	0.258	0.257	0.824	0.295
Lasianthus coffeoiaes	39.8	64.8	222.9	47.5	10.1	17.5	186.8	13.8	0.254	0.270	0.838	0.291
Cymbidium aloifolium					BDL	14.3	26.98	20.19	BDL	0.224	0.128	0.431
Root dust	14.3	16.7	19.84	56.31								
Surface soil	38.4	63.8	210.2	46.8								

values are different for different species. This indicates that the some plant species concentrate higher ^{210}Po and ^{40}K radionuclides than others. Karunakara et al. (2003) observed the same.

Root uptake of radionuclides is a complex phenomenon, especially for primordial nuclides. According to CR principles, plant radionuclide concentration should reflect soil concentration. However, this may not be true because of sorption on soil, which may render radionuclides less available for uptake. Furthermore, radionuclide belonging to physiologically regulated elements, or their analogues, may be selectively adsorbed, whereas others may be excluded. Thus, low activity concentration of radionuclides in plants were observed clearly in most of the plant species except *E. oblangus* and in the epiphytic plant, and also it's difficult to arrive at a conclusion that uptake of these radionuclides. The significant difference in radioactivity concentration of these radionuclides between plant species is likely caused by physiological difference and related factors.

The CR for orchid is low due to the fact that the orchids do not take their nutrients from soil but absorbs them directly from atmosphere (Parfenov 1974), and that is the reason why the CR value of fallout radionuclide Po is much higher in the plant of orchid. The value of CR reported by Zach et al. (1989) for ^{40}K varied in the range of 0.12–0.60, which is comparable with the present study. Figure 3 shows the correlation between CR values of different plants for different radionuclides ^{210}Po vs. ^{40}K and ^{232}Th vs. ^{40}K. A good correlation (Fig. 3a, $r = 0.946$) (Fig. 3b, $r = 0.701$) is observed between the CR values of these two radionuclides.

Also the higher concentration of fallout radionuclides in root dust must be due to the accumulation of atmospheric fallout over a long period of time through dry–wet deposition and due to strong adsorption of these nuclides to soil particles. The deposition fallout radionuclides on the upper layer of the Earth's crust may get washed out due to heavy rain. This leads to the movement of fallout nuclides along

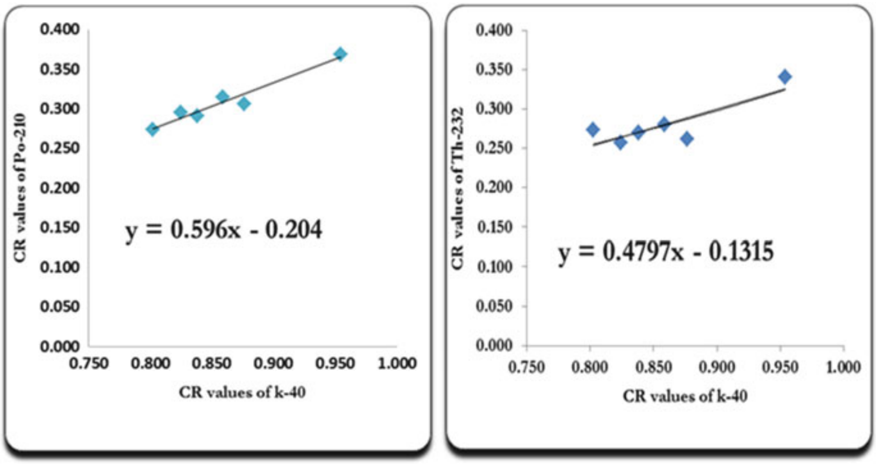

Fig. 3 Correlation between CR values of different radionuclides

with surface soil, whereas root dust keeps on accumulating without any movement (Cawse and Turner 1982).

CR values for different kinds of plant species like top story, second story, shrubs, and epiphytic were different. Thus, it is clear that the difference in physical characteristics in different plant species has a large effect on the accumulation of radionuclides in the plant (Cawse and Turner 1982). As discussed earlier, plants may take up potassium from soil as an essential element of metabolism, and other radionuclides may be taken as a homologue of an essential element (Sheppard and Evenden 1988).

4 Conclusions

The activity concentrations of surface samples were randomly distributed over space, but differed slightly with different soil depths. Also, the study has provided data on the activity of naturally occurring and natural fallout radionuclides in some of the predominant plant species of the Western Ghats region. From the fractional analysis of the plants, the younger leaves exhibit higher levels of activity of the aforementioned radionuclides than the bark. The uptake of the natural radionuclides of ^{238}U and ^{232}Th is low in all the wild plant species except for a few. All the plant species contain a significant concentration of ^{40}K and ^{210}Po; however, the level of ^{40}K is relatively higher than that of ^{210}Po. Physiologically different plants exhibited significant concentrations of ^{232}Th. The concentration of ^{40}K was higher in the leaves of *E. oblongus*, whereas the concentration of the natural fallout radionuclide ^{210}Po was higher in the epiphytic root dust of *C. aloifolium* (an orchid). The dust trapped in the root system of *C. aloifolium* could be used as bioindicator to monitor natural fallout radionuclides in the Western Ghats environment.

Acknowledgments The authors are thankful to Dr. A. Natarajan (Head, HASL, IGCAR), Dr. A.R. Lakshmanan (HASL, IGCAR), and Dr. A.R. Iyengar (Head, ESL, Kalpakkam, India) for their constant encouragement while this work was performed.

References

Abe M, Abe S (1980) Trends in the chemical state of Polonium-210 in the atmosphere. Proceeding International Symposium on Natural Radiation Environment, Houstan, USA 2: 430

Anand SJS, Rangarajan C (1990) Studies on the activity ratio of ^{210}Po to ^{210}Pb and their dry deposition velocities at Bombay in India. J Environ Radioact 11:235–250

Baldwin JP, Nye PH, Tinker PB (1973) Uptake of solutes by multiple root systems from soil. III-A model for calculating the solute uptake by a randomly dispersed root system developing in a finite volume of soil. Plant Soil 38:621–635

Barber SA, Bouldin DR, Karal DM, Hawkins SL (1984) Roots, nutrient and water influx, and plant growth. American Society of agronomy, Madison, WI

Cawse PA, Turner GS (1982) The uptake of radionuclides by plants. Environmental and Medical Sciences Division AERE, Harwell

Frissel MJ (1997) Protocol for the experimental determination of radionuclide transfer factors to be used in radiological assessment models. UIR News Lett 28:5–8

Gascoyne M (1992) Geochemistry of the actinides and their daughters. In: Ivanovich M, Harmon RS (eds) Uranium-series, disequilibrium: applications to earth, marine, and environmental sciences, 2nd edn. Clarendon, Oxford, England

Iyengar MAR, Ganapathy S, Kannan V, Rajan MP, Rajaram S (1990) Procedure manual. Workshop on Environmental Radioactivity, Kiga, India

Karunakara N, Avadhani DN, Somaseherappa HM, Narayana Y, Siddappa K (2001) ^{226}Ra, ^{232}Th and ^{40}K concentration in soil samples of Kaiga of south-west coast of India. Health Phys 80:470–476

Karunakara N, Avadhani DN, Somaseherappa HM, Narayana Y, Siddappa K (2003) ^{210}Po, ^{40}K and ^{7}Be activity concentrations in plant in the environment of Kaiga, India. J Environ Radioact 65:255–266

Koczy FF (1954) Geochemical balance in the hydrosphere. In: Henry F (ed) Nuclear geology. Wiley, New York

Manigandan PK, ChandarShekar B (2014) Measurement of radioactivity in an elevated radiation background area of Western Ghats. Nucl Technol Radiat Protect 29:128–134

Manigandan PK, ChandarShekar B (2015) Leaves of woody plants as bio-indicators of radionuclides in forest ecosystems. J Radioanalyt Nucl Chem 303:911–917

Martinez-Aquire A, Garcia-orellana l, Garcia-leon M (1997) Transfer of natural radionuclides from soils to plant in a marsh enhanced by the operation of non-nuclear industries. J Environ Radioact 35:149–171

Mishra UC (1993) Exposure due to the high natural radiation and radioactive springs around the world. Proceeding of the International Conference on High-level Radiation Areas (Ramsar) Iran-1990. IAEA Publication Series. IAEA, Vienna

Parfenov YD (1974) ^{210}Po in the environment and in the human organism. Atom Energy Rev 12:75–143

Sheppard SC, Evenden WG (1988) The assumption of linearity in soil and plant concentration ratio: an experimental evaluation. J Environ Radioact 7:221–247

Shetty PK, Narayana Y, Siddappa K (2006) Vertical profiles and enrichment pattern of natural radionuclides in monazite areas of coastal Kerala. J Environ Radioact 86:132–142

Sunta CM, David M, Abani MC, Basu AS, ManiKandan MK (2000) Natural radionuclide distribution in soils of Gudalore, India. Appl Radiat Isotop 52:209–306

Timpereley MH, Brooks RR, Peterson PI (1970) The significant of essential and non-essential trace elements in plants in relation to biogeochemical prospecting. J Appl Ecol 7:429–439

Zach R, Hawkin JL, Mayoh KR (1989) Transfer of fallout cesium and natural Potassium-40 in boreal environment. J Environ Radioact 10:19–45

Assessment of Radioactivity in Forest and Grassland Ecosystems

P.K. Manigandan, B. Chandar Shekar, and D. Khanna

Contents

Abstract Naturally occurring radionuclides were investigated in soil samples collected from a tropical rainforest in the Western Ghats, India. For comparison, a number of soil samples from nearby meadows (open grassland) were also studied using gamma-ray spectrometry. Average values of the activity concentration of radionuclides, outdoor gamma-ray dose rate, annual effective dose equivalent, and radiation hazard indices from soil activity were estimated. Significant differences were found between the soils from the forest and meadow sites: the meadow sites contained higher natural radionuclide concentrations than the forest sites. The activity concentration of ^{232}Th and average outdoor gamma-ray dose rates were found to be higher than the global average in both ecosystems, so high gamma radiation appears to affect the Western Ghats' environment in general. Therefore,

P.K. Manigandan (✉)
Sai Nath University, Ranchi 834009, Jharkhand, India
e-mail: pkmgs@yahoo.com

B.C. Shekar
Kongunadu Arts and Science College, Bharathiar University, Coimbatore, Tamil Nadu, India

D. Khanna
Karunya University, Coimbatore, Tamil Nadu, India

C. Walther, D.K. Gupta (eds.), *Radionuclides in the Environment*,
DOI 10.1007/978-3-319-22171-7_8

the radiological risks to the general population from ionizing radiation from the naturally occurring radionuclides in the soil are considered to be significant. However, other radiological hazard indices that were calculated were within acceptable limits.

Keywords Radionuclides • Western Ghats • Monazite • Radiological hazard • Cosmic radiation

1 Introduction

The natural radioactivity level can vary considerably between soil types, and it is usually determined from the ^{238}U, ^{232}Th, and ^{40}K activity concentrations in the soil (OECD 1979). Spatial variations in the external gamma-ray dose rate mean that it is essential to measure radionuclide concentrations in soil samples taken from around a particular site of interest rather than solely at the site itself. The external gamma-ray dose varies depending on the concentrations of the natural radionuclides ^{238}U and ^{232}Th, their daughter products, and ^{40}K in the soil, and these, in turn, depend on the local geology (Radhakrishnan et al. 1993; Quindos et al. 1994). Our study area, in the Western Ghats, India, is in a high background radiation zone, and exposure to external radiation in this area is caused by gamma rays emitted by radionuclides in monazite sands that originated in granites and gneisses. Monazite sands contain phosphates of a number of elements, including cerium and radioactive thorium.

Exposure to gamma radiation from radioactive materials in a forest ecosystem depends on the geological and geographical conditions, and will be different in different areas. Forest sites differ from meadow sites in several important ways, the main one being that meadow soils are periodically plowed and fertilized, whereas forest ecosystems, being relatively undisturbed, have relatively clear subdivisions between the upper (mainly organic) and lower (mineral) horizons. These horizons differ in several important characteristics, including pH, moisture content, nutrient status, and biological activity (Frissel et al. 1990). Meadows are often monocultures, whereas forest ecosystems are species rich. The cycling of radionuclides is, therefore, much more difficult to understand in forests than in simple meadows. In particular, the great variability found in radioactivity data for the soils, plants, and animals in forests makes it difficult for policy makers to formulate reliable analytical models.

In this study, we aimed to assess the environmental radiation levels in virgin (forest) and contaminated (Meadow) soils collected from the Western Ghats. We compared the results with local and global means. The results presented will be useful baseline data for natural radioactivity levels in the study area and surrounding region, and will be useful for assessing radiation doses received by the local population.

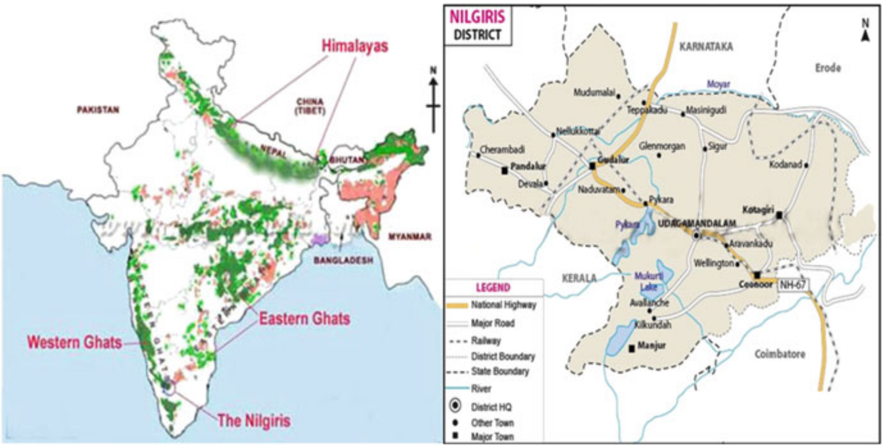

Fig. 1 Study area: Nilgiris District

2 Materials and Methods

2.1 *Study Area*

The soils analyzed were collected from elevations of between 2000 and 2400 m the Nilgiri Highlands, Tamil Nadu, South India, which are situated between 11° 00′ and 11° 30′ N and between 76° 00′ and 77° 30′ E. The Nilgiri massif is located at the junction between the Eastern and Western Ghats and is bounded by abrupt slopes. The study area is shown in Fig. 1. The vegetation above 2000 m in the highlands is a mosaic of high-elevation evergreen forests, called "shola" locally, and grasslands with different compositions of flora, including C4 grasses (C4 species often dominate full-sun conditions and northerly aspects) (Sukumar et al. 1995; Rajagopalan et al. 1997).

2.2 *Sample Collection and Processing*

The study area was divided into a 4-km grid and soil samples were collected from 25 sampling points in the natural, uncultivated, and grass-covered level areas within the grid, conforming to International Atomic Energy Agency recommendations (IAEA 1989). The 25 sampling points followed a zig-zag pattern. Five 20-cm-deep samples were collected at equal distances along a 1 m circle around the center of each sampling point. This sampling method was used to improve the representativeness of the samples. The position and elevation of each sampling point was determined using a global positioning system. For comparison, soil samples collected from 25 meadow sites in the Nilgiris District in the Western Ghats in 2003 and 2004 were also analyzed.

The soil samples were transported to the laboratory and plant roots and other unwanted materials were removed. The samples were then dried in an oven at 105 °C for 12–24 h, ground, and passed through a 2 mm sieve. About 400 g of dry sample was weighed into a plastic container, which was capped and sealed. The container was sealed to ensure that none of the daughter products of uranium and thorium that were produced, particularly radon and thoron, could escape. The prepared samples were stored for 1 month before counting to ensure that equilibrium had been established between radium and its short-lived daughters. Detailed gamma-ray spectrometry analysis was performed on the soil samples.

2.3 Activity Determination

The samples were analyzed using a NaI(Tl) spectrometer coupled with TNIPCAII Ortec model 8K multichannel analyzer. The ^{232}Th-series, ^{238}U-series, and ^{40}K activities were estimated, as were the amounts of these radionuclides that would enter the air from the soil. A 3 × 3 inch NaI(Tl) detector was used, with adequate lead shielding, which reduced the background by a factor of 95. The energies of interest were found using an International Atomic Energy Agency standard source and the appropriate geometry. The system was calibrated in terms of both the energy response and the counting efficiency. The density of the sample used for the calibration was 1.3 g/cm^3, which was the same as the mean density of the soil samples analyzed (1.24 g/cm^3), the detector was very well shielded, and the counting time was 20,000 s for each sample. The minimum detectable concentrations, defined as $3 \times \sigma$ (the standard deviation), were 7 Bq kg^{-1} for the ^{232}Th-series, 8.4 Bq kg^{-1} for the ^{238}U-series, and 13.2 Bq kg^{-1} for ^{40}K.

The concentrations of the radionuclides of interest were determined using the counting spectrum for each sample. The peaks corresponding to 1.46 MeV (^{40}K), 1.76 MeV (^{214}Bi), and 2.614 MeV (^{208}Tl) were considered when evaluating the ^{40}K, ^{238}U-series, and ^{232}Th-series activities, respectively. The crystal detector resolution was 6 % for ^{40}K, 4.4 % for the ^{232}Th-series, and 5.5 % for the ^{238}U-series. The gamma-ray spectrum activities for each soil sample were analyzed using dedicated software, and references were chosen to achieve sufficient discrimination.

In addition to the gamma-ray spectrometric analysis, a low-level survey environmental radiation dosimeter (type ER 705; Nucleonic System PVT Ltd., Hyderabad, India) was used to measure the ambient radiation levels in the study areas directly associated with radionuclide activity concentrations in the samples and cosmic rays. The dosimeter had a halogen quenched Geiger–Müller detector (Ind. lnc., USA) powered by a rechargeable battery, and was designed to read the exposure rate at two levels 0.1 μRh^{-1} and 1 μRh^{-1}. The dosimeter was calibrated using a standard source before the use. Outdoor terrestrial gamma dose rates were measured at 1 m above the ground by a portable digital ERD at all the sampling sites. A total of five readings were recorded at each spot and the average taken.

3 Results and Discussion

The ^{238}U, ^{232}Th, and ^{40}K activity concentrations were determined for the two soil sample types measured, and the mean activities, the standard deviations, and activity ranges are shown in Table 1.

It can be seen from Fig. 2 that the mean ^{232}Th activity concentration in the meadow samples was twice that in the forest samples, and that the ^{232}Th activity concentrations in both ecosystems were much higher than the global mean, 45 Bq kg^{-1} (UNSCEAR 2008).

The relatively high ^{232}Th activity concentrations at both sites were caused by the presence of monazite. However, the mean ^{238}U and ^{40}K activity concentrations were lower than the global means, 32 Bq kg^{-1} and 412 Bq kg^{-1}, respectively (UNSCEAR 2008).

There were no major differences in the activity concentrations in the virgin and agricultural soils in the study area. However, slightly higher activity concentrations were measured in the meadow samples, which would have been caused by agricultural activities redistributing the radionuclides in the soil profile.

3.1 Dose Calculations

3.1.1 Absorbed and Observed Dose Rates

The mean ^{238}U, ^{232}Th, and ^{40}K activity concentrations were converted into dose rates using conversion factors provided by UNSCEAR (2008), as shown in Eq. (1).

$$D = (0.462C_{\mathrm{U}} + 0.604C_{\mathrm{Th}} + 0.0417C_{\mathrm{K}})\mathrm{nGy\ h}^{-1} \quad (1)$$

where D is the absorbed dose rate (nGy/h) and C_{U}, C_{Th}, and C_{K} are the ^{238}U, ^{232}Th, and ^{40}K activity concentrations (Bq kg^{-1}) in the soil samples, respectively. It can be seen from Table 1 that the ^{232}Th-series contributed 71 % of the total gamma-ray dose in both ecosystems, whereas the ^{238}U-series and ^{40}K contributed 19 % and 10 % of the total gamma-ray dose. The thorium concentration in the Western Ghats region is slightly higher than the worldwide average, possibly because of the presence of monazite sand in this area. The forest site absorbed dose rates ranged between 38.9 nGy h^{-1} and 76.7 nGy h^{-1}, and the mean was 53.0 ± 11.4 nGy h^{-1}. The meadow site absorbed dose rates ranged between 39.11 nGy h^{-1} and 153.40 nGy h^{-1}, and the mean was 91.5 ± 34.0 nGy h^{-1}. The absorbed dose rate in both ecosystems exceeded the global mean of 56 nGy h^{-1} (UNSCEAR 2008).

The outdoor gamma-ray dose rates were measured 1 m above the ground at each of the sampling sites using a portable digital environmental radiation dosimeter. Five readings were made at each spot and the mean of the readings was used.

Table 1 Statistical summary of activity concentrations, dose rate, and hazard indices of two ecosystem

Ecosystem	Meadow sites								Forest sites							
	Soil activity			Dose rate			Hazard indices		Soil activity			Dose rate			Hazard indices	
Parameters	^{238}U ($Bq\ kg^{-1}$)	^{232}Th ($Bq\ kg^{-1}$)	^{40}K ($Bq\ kg^{-1}$)	Absorbed dose ($nGy\ h^{-1}$)	Observed dose ($nGy\ h^{-1}$)	Annual effective dose equivalent (μSv)	Ra_{eq} ($Bq\ kg^{-1}$)	$I_{\gamma r}$	^{238}U ($Bq\ kg^{-1}$)	^{232}Th ($Bq\ kg^{-1}$)	^{40}K ($Bq\ kg^{-1}$)	Absorbed dose ($nGy\ h^{-1}$)	Observed dose ($nGy\ h^{-1}$)	Annual effective dose equivalent (μSv)	Ra_{eq} ($Bq\ kg^{-1}$)	$I_{\gamma r}$
Mean ± σ	36.3 ± 17.3	107.8 ± 50.4	231.9 ± 84.3	133.3 ± 183.3	91.5 ± 34.0	112.3 ± 41.7	208.3 ± 79.4	1.47 ± 0.6	26.3 ± 9.1	53.6 ± 10.4	204.1 ± 30.4	97.0 ± 13.0	53.0 ± 11.4	65.0 ± 13.8	118.6 ± 25.3	0.85 ± 0.2
Standard error	3.5	10.1	15.9	36.6	6.8	8.3	15.9	0.11	2.3	2.7	7.8	3.4	2.9	3.6	6.5	0.05
Median	35.3	101.8	237.6	101.4	83.0	101.8	188.4	1.4	21.4	48.9	209.7	94.0	47.6	58.4	106.4	0.76
Range	12.4–85.8	30.3–204.1	83.1–411.6	20.7–92.7	39.1–53.4	48.0–203.8	86.93–379.22	0.61–2.69	15.1–4.2	39.2–76.1	127.5–248.1	83.0–123.8	38.9–76.7	47.8–94.1	86.44–172.08	0.63–1.22
Confidence level (95.0 %)	0.22	0.64	1.07	2.32	0.43	0.53	1.01	0.007	0.15	0.17	0.50	0.21	0.19	0.23	0.42	0.003

σ = Standard deviation

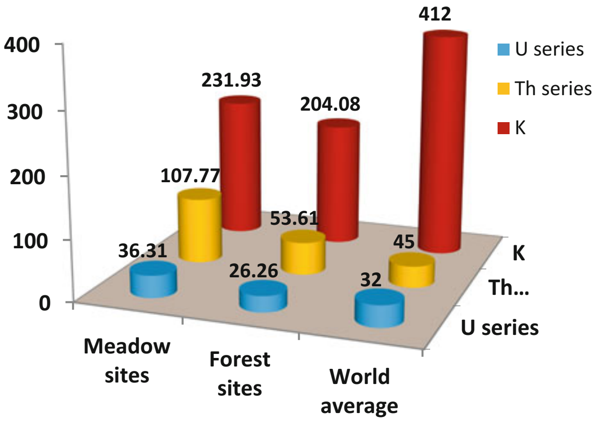

Fig. 2 Mean ^{238}U-series, ^{232}Th-series, and ^{40}K activity concentrations ($Bq\ kg^{-1}$) in the soil samples from the meadow and forest sites, and the global mean activity concentrations

The mean global outdoor gamma-ray dose rate has been found to be 60 nGy h^{-1} and the range has been found to be 10–200 nGy h^{-1} (Taskin et al. 2009). The mean gamma-ray dose rates in the study area were 97 nGy h^{-1} at the forest sites and 133.3 nGy h^{-1} at the meadow sites, which are both much higher than the global mean. The gamma radiation level is directly associated with the radionuclide activity concentrations in the samples and with cosmic rays (Taskin et al. 2009). The observed gamma-ray dose rate was more than 50 % of the dose calculated from the soil activities, and the difference would have been caused by the cosmic radiation contribution to the total dose in the Western Ghats environment, which is 2400 M above sea level.

3.1.2 Annual Effective Dose Equivalents

The absorbed dose to effective dose conversion coefficient (0.7 $SvGy^{-1}$) and an outdoor occupancy factor (0.2), which has been proposed by UNSCEAR (2008), were used to estimate the annual effective dose rates, as shown in Eq. (2).

$$\begin{aligned}&\text{Effective dose rate}(\text{Outdoor})\ \left(\mu\text{Sv y}^{-1}\right)\\&= D\left(\text{nGy h}^{-1}\right)\times 8760\text{h}\times 0.7\text{Sv Gy}^{-1}\times 0.2\times 10^{-3}\end{aligned} \tag{2}$$

The mean outdoor annual effective dose equivalents calculated for the samples are shown in Table 2. The mean outdoor annual effective dose equivalent for the forest sites was 65.0 ± 13.8 μSv, which is within the range of the global mean value of 70 μSv per year for outdoor (Orgun et al. 2007). However, the mean outdoor annual effective dose equivalent for the meadow sites was 112.3 ± 41.7 μSv, which is much higher than the global mean, and this may be attributed to the higher ^{232}Th activity concentrations found in the soil from the meadow sites. Even though the outdoor annual effective dose equivalents for the samples from the meadow sites

Table 2 Comparison of the activity concentrations with those found in similar studies

Country	Ecosystem	Activity (Bq kg^{-1})			Ra_{eq} (Bq kg^{-1})	$I_{\gamma r}$	References
		^{238}U	^{232}Th	^{40}K			
India	Virgin soil	26.26	53.61	231.93	118.6	1.47	This study
	Agri soil	36.31	107.7	231.93	208.28	0.85	
Algeria	Virgin soil	47.01	43	329	132	0.95	Wassila et al. (2011)
	Agri soil	53.2	50.03	311	154	1	
Brazil	Virgin soil	1.69	5.32	34.15	12	0.1	Becegato et al. (2008)
	Agri soil	10.22	7.27	54.75	24.8	0.2	
Egypt	Virgin soil	13.7	12.3	1233	126.2	1.04	Ahmed and El-Arabi (2005)
	Agri soil	366	66.7	4	461.7	3.1	
Pakistan	Virgin soil	27.39	31.16	602.77	142.71	1.02	Akhtar et al. (2005)
	Agri soil	51.96	42.48	847.22	233.04	1.75	

Agri Soil: Agricultural Soil

were much higher than the global mean value, this was not significant from the radiological hazard point of view.

3.2 Radiation Hazard Indices

A common radiological index, called the radium equivalent (Ra_{eq}) activity, has been introduced to represent the ^{238}U, ^{232}Th, and ^{40}K activities as a single quantity. Ra_{eq} is calculated using Eq. (3) (Beretka and Mathew 1985).

$$Ra_{eq}\left(\text{Bq kg}^{-1}\right) = (C_U + 1.43C_{Th} + 0.077C_K) \tag{3}$$

where C_U, C_{Th}, and C_K are defined as in Eq. (1) above.

Another radiation hazard index, called the representative level index, $I_{\gamma r}$, is defined using Eq. (4) (Ahmed and El-Arabi 2005).

$$I_{\gamma r} = \frac{1}{150\text{Bq kg}^{-1}}C_U + \frac{1}{100\text{Bq kg}^{-1}}C_{Th} + \frac{1}{1500\text{Bq kg}^{-1}}C_k \tag{4}$$

where C_U, C_{Th}, and C_K are defined as in Eq. (1).

The Ra_{eq} and $I_{\gamma r}$ values for the samples analyzed in this work are shown in Table 1. Based on the annual external dose of 1.5 mGy, activity limits in terms of Ra_{eq} and $I_{\gamma r}$ are 370 Bq kg^{-1} and 1, respectively, for the safe use of soil products. It has been observed that the Ra_{eq} values in the soils we analyzed were lower than the maximum value allowed, 370 Bq kg^{-1} (Beretka and Mathew 1985). The Ra_{eq} values were much higher for the meadow sites (208 Bq kg^{-1}) than for the forest sites (118 Bq kg^{-1}), mainly because of the use of fertilizers, which are rich in phosphates, on the meadow sites for agricultural purposes (Ahmed and El-Arabi

2005). Phosphate rocks contain significant concentrations of U, Th, Ra, and their decay products (Skorovarov et al. 1996).

The $I_{\gamma r}$ values for the samples analyzed in this study are shown in Table 1. The mean $I_{\gamma r}$ value for the meadow samples exceeded the upper limit (one), but the forest samples did not exceed the limit.

3.3 Comparison of the Activity Concentrations with Those Found in Similar Studies

The ^{238}U, ^{232}Th, and ^{40}K activity concentrations, Ra_{eq}, and $I_{\gamma r}$ for the samples from the forest and meadow were compared with the values found in similar investigation in other countries, and the results are summarized in Table 2. Table 2 shows a comparison of the ^{238}U, ^{232}Th, and ^{40}K activity concentrations, radium equivalent activities (Ra_{eq}s), and representative level indices ($I_{\gamma r}$s) found in soil and fertilizer samples in this and other studies.

According to UNSCEAR (2008), the global ^{232}Th activity concentration range is 7–50 Bq kg^{-1} (mean 45 Bq kg^{-1}). The measured ^{232}Th activity concentrations in the study area, for both forest and meadow soils, were between 1.5 and 2.5 times higher than the global mean.

The measured ^{238}U and ^{40}K concentrations in the soil samples from the forest and meadow sites were within the global range, but the soils from the meadow sites contained higher concentrations than the forest sites. As is shown in Table 2, the radioactivity found in forest and meadow soils varies from country to country. It is important to note that the values shown are not representative values for the countries mentioned, but only for the regions in which the samples were collected.

4 Conclusions

The radioactive concentrations in soil samples from forest and meadow sites in the Western Ghats, India, were measured using a gamma-ray spectrometry technique. The naturally occurring radionuclide activity concentrations in the soil samples were within usual global ranges (UNSCEAR 2008), but the ^{232}Th activity concentrations were at the higher end of the global range. The naturally occurring radionuclide concentrations were much higher in the meadow samples than in the soil samples. Variations in the activity levels in the forest soil samples were within the activity values measured around the world, but this was not the case for the meadow soil samples. The mean outdoor terrestrial gamma-ray dose rate was higher than the global mean, so the Western Ghats region should be classified as having above global average background radiation. It should also be noted that the calculated activity utilization index from meadow site was also found to exceed the recommended safe limit values. This implies that the inhabitants of the meadow sites are subjected to a radiation exposure significantly higher than the corresponding exposure levels reported in the other areas worldwide. Despite this, all of the other calculated radiological hazard indices were within acceptable limits, indicating that the soils in this area can be used safely.

Acknowledgments The authors are thankful to Dr. A. Natarajan (Head, HASL, IGCAR), Dr. A.R. Lakshmanan (HASL, IGCAR), and Dr. A.R. Iyengar (Head, ESL, Kalpakkam, India) for their constant encouragement while this work was performed.

References

Ahmed NK, El-Arabi AGM (2005) Natural radioactivity in farm soil and phosphate fertilizer and its environmental implications in Qena governorate, Upper Egypt. J Environ Radioact 84:51–64

Akhtar N, Tufail M, Ashraf M (2005) Natural environmental radioactivity and estimation of radiation exposure from saline soils. Int J Environ Sci Technol 1:279–285

Becegato VA, Ferreira FJ, Machado F (2008) Concentration of radioactivity elements derived from Phosphate fertilizers in cultivated soils. Braz Arch Biol Technol 51:1255–1266

Beretka J, Mathew PJ (1985) Natural radioactivity of Australian building materials, industrial wastes and by products. Health Phys 48:87–95

Frissel MJ, Noordijk KH, van Bergejik KE (1990) The impact of extreme environmental condition, as occurring in natural ecosystem's on the soil to plant transfer of radionuclides. In: Desmet G, Nasimbeni P, Belli M (eds) Transfer of Radionuclide in Natural and Semi-Natural Environments. Elsevier, London

IAEA (1989) Measurement of Radionuclides in Food and Environment. IAEA Technical Report Series No: 295, IAEA, Vienna

NEA-OECD (1979) Exposure to radiation from natural radioactivity in building materials. Report by NEA Group of Experts, Paris- France. http://www.oecd-nea.org/rp/reports/1979/exposure-to-radiation-1979.pdf

Orgun Y, Altinsoy N, Sahin SY, Gungor Y, Gultekin AH, Karaham G, Karaak Z (2007) Natural and anthropogenic radionuclides in rocks and beach sands from Ezine region (canakkale), Western Anatolia, Turkey. Appl Radiat Isotop 65:739–747

Quindos LS, Fernandez PI, Soto J, Rodenas C, Gomez J (1994) Natural radioactivity in Spanish soils. Health Phys 66:194–200

Radhakrishnan AP, Somashekarappa HM, Narayana Y, Siddappa KA (1993) New natural background radiation area on the south coast of India. Health Phys 65:390–395

Rajagopalan G, Sukumar R, Ramesh R, Pant RK (1997) Late quaternary vegetational and climatic changes from tropical peats in southern India—An extended record up to 40,000 years B.P. Curr Sci 73:60–63

Skorovarov JI, Rusin LI, Lomonsov AV, Chaforian H, Hashemi A, Novaseqhi H (1996) Development of uranium extraction technology from phosphoric acid solutions with extract. Proc Int Conf Uranium Extract Soil 217:106–113

Sukumar R, Suresh HS, Ramesh R (1995) Climate change and its impact on tropical montane ecosystems in southern India. J Biogeogra 22:533–536

Taskin H, Karavus M, Topuzoglu A, Hindiroglu S, Karahan G (2009) Radionuclide concentrations in soil and lifetime cancer risk due to the gamma radioactivity in Kirklareli, Turkey. J Environ Radioact 100:49–53

UNSCEAR (2008) Sources and biological effects of ionizing radiation. Report to general assembly with scientific annexes. United Nations, New York

Wassila B, Boucenna A (2011) The radioactivity measurements in soils and fertilizers using gamma spectrometry technique. J Environ Radioact 102:1–7

Terrestrial Environmental Dynamics of Radioactive Nuclides

Jun Furukawa

Contents

Abstract Dynamics of radioactive nuclides is the result of highly complex interaction between the radioactive nuclides and the environmental components. In this chapter, the simple outline of these interactions from the influx of radioactive nuclides into the terrestrial environment to the efflux to the next environmental systems is described. As important steps deciding the fate of radioactive nuclide behavior, the following four scenes are selected: deposition of radioactive nuclides from aerosol, its behaviors within soil, its circulation within forest ecosystem, and rediffusion from the system. Deposition of radioactive nuclides is affected by the environmental conditions and the chemical form when those are released and deposited, and those forms also regulate the behavior within the soil. The vegetation of land surface affects the deposition and the behavior of radioactive nuclides. The incorporation of radioactive nuclides into the forest ecosystem means the long retention period around the forest trees and the soil surface. And the rediffusion from the deposited site and system gradually occurs, even in the forest ecosystem. Not only the increase of understandings but the integration of a lot of findings from the measurement and the experiment is needed for the prediction of radioactive nuclide behavior in the environment.

J. Furukawa (✉)
Center for Research in Isotopes and Environmental Dynamics, University of Tsukuba, Tennodai 1-1-1, Tsukuba 305-8577, Japan
e-mail: furukawa.jun.fn@u.tsukuba.ac.jp

C. Walther, D.K. Gupta (eds.), *Radionuclides in the Environment*,
DOI 10.1007/978-3-319-22171-7_9

Keywords Radioactive nuclides • Deposition • Forest ecosystem • Material circulation • Rediffusion • Fukushima accident

1 Introduction

The radioactive nuclides transferred through the atmosphere as an aerosol are deposited on soil surface or forest area through dry or wet depositions. The behaviors of deposited radioactive nuclides within the terrestrial environment are drastically differed based on the deposition conditions and the materials which are bound to the radioactive nuclides. Radioactive nuclides deposited to the soil surface are mainly migrated with soil water as a soluble or a colloidal form interacting with soil components, such as soil organic matter and clay minerals (Kruyts and Delvaux 2002). In the forest area, radioactive nuclides deposited to the tree leaf, bark, or litters are incorporated into the forest ecosystem as one of the parts of material circulation. Either in soil or forest ecosystem, these radioactive nuclide behaviors are strongly affected by its adsorption/desorption characteristics with the clay minerals, plant and microbe activity, and feeding/evacuation by insects and animals. When the radioactive nuclides are tightly fixed with soil, especially clay minerals, in addition to above regulators, soil erosion induced by water or wind and resulting sedimentation to the depression contour, lake, and reservoir are also important in the environmental dynamics of such nuclides.

In this chapter, the terrestrial environmental dynamics of radioactive nuclides is described in the following four parts: deposition of radioactive nuclides from aerosol, its behaviors within soil, its circulation within forest ecosystem, and rediffusion from there. The understandings in the environmental dynamics of radioactive nuclides were mainly obtained by the investigation based on the radioactive fallout from nuclear tests in the atmosphere around 1950–1985 (Katsuragi 1983; Ritchie and McHenry 1990), nuclear power plant accidents at Chernobyl in 1986 (Fesenko et al. 1995; Realo et al. 1995; Lehto et al. 2008), and atomic bombs exploded at Hiroshima and Nagasaki in 1945. Here the factors related to the radioactive nuclide dynamics in terrestrial environment are outlined, and the results of the recent investigation after the Fukushima Daiichi nuclear power plant accident in 2011 will be introduced.

2 Deposition of Radioactive Nuclides in the Terrestrial Environment

As the maps of ^{137}Cs contamination for Chernobyl and Fukushima accidents indicate, the distribution of deposited nuclides is not constant (International atomic energy agency 2006; Kinoshita et al. 2011). The transfer of atmospheric radioactive nuclides is strongly affected by the wind direction and its velocity. The total amount contained in the plume is gradually decreased by the deposition through the rainfall or snowfall. After the Fukushima accident, it was reported that some cities passed by the plume which contained almost the same amount of radioactive nuclides had different levels of contamination depending on the weather conditions when the plume passed.

The amount of radioactive fallout through dry/wet deposition is drastically differed based on the wind condition and precipitation amount. Generally the radioactive nuclides in the atmosphere are mainly deposited with the raindrop (wet deposition), and the effect of dry deposition is minor in comparison with wet one. Sigurgeirsson et al. (2005) reported that the ^{137}Cs fallout in the soil was in proportion with the annual amount of precipitation in Iceland. However, in Canada, ^{137}Cs amount in soil was not related with the precipitation amount but was able to be explained by the summer storms which flush out the stratosphere ^{137}Cs (VandenBygaart et al. 1999). They also showed that the landscape and the vegetation were the factors for radioactive nuclide deposition from the atmosphere to the land surface. Considering these difficulties, the combination of the survey methods and the accumulation of monitoring data have high priority for understanding the land-surface contamination (Yoshida and Takahashi 2012).

The input of radioactive nuclide into the forest ecosystem occurs by the deposition of raindrop or fine particle which contains or attaches radioactive nuclides to soil, tree, and others. The surface area of tree is generally larger than that of crop; therefore, large amount of radioactive nuclides is deposited to the forest. However, tree deposition of radioactive nuclides was not constant, and the deposition pattern to the canopy was different between the tree species and radioactive nuclides (Kato et al. 2012). After the deposition, the nuclides absorbed are circulated among tree organs (Calmon et al. 2009).

In addition to these environmental factors at the deposition site, the chemical forms of released radioactive nuclides are also important and the details are described at chapters "Sources Contributing to Radionuclides in the Environment: With Focus on Radioactive Particles" and "Mobility and Bioavailability of Radionuclides in Soils." The relationship between chemical form and deposition is one of the focusing topics after Fukushima accident, because the aerosol samples obtained at several sites had different properties, for example, solubilization to the water (Kaneyasu et al. 2012; Adachi et al. 2013; Tanaka et al. 2013). As described by the following part, the solubility to the water is one of the most basic regulators for deciding the behavior of radioactive nuclides after the deposition. To elucidate the mechanisms of radioactive nuclide incorporation into the environment, the study based on the chemical form of deposited radioactive nuclides should have a high priority as the first interaction of those and the terrestrial environment.

3 Radioactive Nuclide Behavior Within Soil

The migration rate of radioactive nuclides in soil is defined as an average speed of downward movement of those after the deposition to the soil surface. The previous studies on vertical distribution of radioactive nuclides provide the ^{137}Cs migration rate in several soils (Zygmunt et al. 1998; Chibowski et al. 1999; Rosen et al. 1999), and the modeling method which separates the soil into several layers was also used for obtaining the migration rates (Bunzl et al. 1995; Holgye and Maly 2000; Chibowski and Zygmunt 2002). The migration rate is one of the most basic parameters for estimating the radioactive nuclide behavior in soil; however, to estimate the behavior of radioactive nuclides more in detail, the soil properties involving radioactive nuclide mobility should be focused. The chapters "Mobility and Bioavailability of Radionuclides in Soils," "The Influence of Edaphic Factors on Spatial and Vertical Distribution of Radionuclides in Soil," "Modelling Speciation and Distribution of Radionuclides in Agricultural Soils," and "Biotransformation of Radionuclides: Trends and Challenges" describe several factors related to the radioactive nuclide distribution in soil and the bioavailability.

The radioactive nuclides just deposited migrate within the soil more easily in comparison with the radioactive fallout deposited around 1950–1985, because newly deposited radioactive nuclides are changed to water-soluble form and gradually shifted to exchangeable form and then stored as fixed form (Roig et al. 2007). As a result of this transition, the mobility of deposited ^{137}Cs was decreased with time (Bossew and Kirchner 2004; Kirchner et al. 2009). The binding ability of radioactive cesium in soil is often indicated by the Radiocesium Interception Potential (RIP). RIP was proposed as the product of the selectivity coefficient of ^{137}Cs against potassium in the Frayed Edge Sites (FES), which has high binding ability to cesium, and the concentration of FES (Cremers et al. 1988). Vegetation of the land surface also affects the behavior of radioactive nuclides in soil, for example, plant root uptake of radioactive nuclides changes the retention time of those around the soil surface. Especially in the forest, material circulation between tree and soil is highly active and the radioactive nuclides do not penetrate into the deep layer. As for the material circulation of potassium, large amount of potassium yearly obtained by tree is derived from the decomposed litter (Schlesinger 1997). Based on the similarity of chemical property between potassium and cesium, ^{137}Cs contained in the litter is also reabsorbed through the root uptake. Microbe also affects the radioactive nuclide behavior in soil. As a reverse movement against the general downward migration, upward movement of radioactive nuclides induced by microbe was reported (Steiner et al. 2002; Fukuyama and Takenaka 2004; Fukuyama et al. 2005). The radioactive nuclides bound to the colloid are transferred in soil and groundwater (Kretzschmar et al. 1999). The colloid is mainly consisted of clay mineral and stabilized by the combination with humic substances (Ryan and Gschwend 1990). This complex is a potent candidate for the long-distance transfer of radioactive nuclides.

4 Radioactive Nuclide Dynamics Within Forest Ecosystem

Comparing to the farmland, radioactive nuclides are retained in the forest area for a much longer period (Shaw 2007). The radioactive nuclides contained in the aerosol are easily captured by forest trees, and, once those are integrated, the high activity of material circulation in the forest keeps the radioactive nuclides in the forest. The details of forest and grassland ecosystem are also described in the chapter "Assessment of Radioactivity in Forest and Grassland Ecosystems," and the topics related to the uptake of radioactive nuclides by plants are presented in chapters "Uptake and Retention of Simulated Fallout of Radiocaesium and Radiostrontium by Different Agriculture Crops," "Root Uptake/Foliar Uptake of Radionuclides in Natural Ecosystem," and "Methods for Decrease of Radionuclides Transfer from Soil to Agricultural Vegetation." In addition to those chapters, the factors affecting the ^{137}Cs uptake from the soil and surrounding topics were well summarized as a recent review (Yamaguchi et al. 2012).

The behavior of radioactive nuclides within the forest ecosystem is strongly affected by the material circulation, such as storage at the litter layer or soil surface, uptake through the plant root, transfer to tree organs, and re-influx through the litter fall. The diffusion of radioactive nuclides within the forest consists of two processes. Within the first several years, the radioactive nuclides deposited are rapidly diffused among forest ecosystem and then the relatively stable phase, in which the allocation of radioactive nuclides in the system is not drastically changed, is followed (Calmon et al. 2009). Immediately after the deposition, the main candidate of radioactive nuclide inlet into tree is the foliar and bark uptake (Calmon et al. 2009; Takata 2013). The radioactive nuclides after uptake into tree are transferred to each organ according to the similarities of chemical properties with essential elements in plant, for example, the behavior of ^{134}Cs and ^{137}Cs are followed by the potassium movement and ^{90}Sr is by the calcium. The migration of radioactive nuclides from tree to soil is mainly occurred by the litter fall and through fall. The migration rate of ^{137}Cs was estimated in the Irish pine forest, and the rates were the following: 65 Bqm^{-2} y^{-1} by through fall and 45 Bqm^{-2} y^{-1} by litter fall at 7–8 years after the Chernobyl accident (Rafferty et al. 2000). The radioactive nuclides fallen through these pathways are stored to the litter layer and the soil surface. In the litter layer, almost all ^{137}Cs existed in the well-decomposed mid- and lower layer in the pine forest (Rafferty et al. 2000). And in these layers, the sites holding radioactive nuclides have cation exchange ability and mainly belong to organic material-rich fraction. The radioactive cesium reached to the soil is absorbed by the tree with potassium through the root. The uptake activity is affected by the RIP value and the distribution ratio of radioactive cesium between solid and liquid phase of soil (Konopleva et al. 2009). In the common forest, the fertilization with potassium is not so familiar; therefore, the most trees are under the potassium starvation. That condition enhances potassium uptake mechanisms in trees, so the uptake of cesium should be also increased (White and Broadley 2000; Rigol et al. 2002).

The decomposition process induced by the microbe generates humic substances in the soil. Humic substance provides the electrically negative charge sites and covers the surface of clay minerals, resulting in the decrease of fixation ability of cesium (Rigol et al. 2002; Fan et al. 2014). In the material circulation in the soil, fungi also have an importance about the radioactive nuclide absorption and the re-influx of radioactive nuclides into the tree (Steiner et al. 2002). Fungi live in the organic layers and that layer contains relatively large amount of cesium in the exchangeable form. Both symbiotic mycorrhizal fungi which cohabits with trees and saprophytic fungi which decompose the litter are highly involved in the behavior and circulation of radioactive nuclides (Heinrich 1992; Sugiyama et al. 1993; Steiner et al. 2002). The forest area is generally under the poor nutrient condition, and the forest ecosystem adapts to that situation. Therefore, the material circulation is highly activated and the efflux of radioactive nuclide out of the forest ecosystem is considered to be limited.

5 Rediffusion of Radioactive Nuclides

Radioactive nuclides gradually flow away from the system once deposited over a long period of time. The main routes for the radioactive nuclide efflux from the system are the following: solubilization into the surface runoff water or percolating water, water- and wind-induced soil erosion, and its sedimentation.

The deposited radioactive nuclides, such as ^{137}Cs derived from radioactive fallout, are stabilized to the soil and stored at the soil surface for a long time. Therefore, ^{137}Cs in soil has been widely utilized as a tool for estimating the soil erosion (Ritchie and McHenry 1990). This method is based on the comparison of ^{137}Cs amount between the target site and the reference site. The reference site is considered as a place of no erosion and no sedimentation. However, there is difficulty in comparing the two sites because of the different rainfall, different vegetation, and different landscape (Parsons and Foster 2011). So, the additional measurement of ^{210}Pb, in which mobility is lower than ^{137}Cs within the soil, and the obtained ratio of ^{210}Pb to ^{137}Cs in each depth are utilized for the estimation more in detail (Wallbrink and Murray 1996).

In solubilization into the surface runoff water or percolating water, water- and wind-induced soil erosion and its sedimentation are the nonbiological factors affecting the ^{137}Cs amount in the soil. A part of radioactive nuclides deposited to the soil surface are solubilized into the surface runoff water and moved to the lower watershed and then accumulated at depression contour, river bed, reservoir, and sea. At the depression contour around the Chernobyl nuclear power plant, ^{137}Cs was penetrated to the soil 100 cm deep (Bixio et al. 2002). The solubilized radioactive nuclides are considered to be in the flow into the next system; however, the plant uptake of that water requires an attention (Nemoto and Abe 2013). The solubilized radioactive nuclides are easily absorbed by plant root and that means the re-influx of radioactive nuclides into the terrestrial environment. At the dry land, wind erosion is the important factor and the vegetation reduces its intensity. For the biological process in the efflux of radioactive nuclides, re-entrainment with the aerosol form is recently focused. The mechanism is not elucidated, but the increase of radioactive nuclide concentration in the atmosphere was frequently observed in the forest (Kita 2014). The wind velocity was poorly correlated with that increase; therefore, the potential of wind-induced re-entrainment is considered to be low. As a different pathway of deposited radioactive nuclide to the atmosphere, Kanasashi et al. (2015) reported the ^{137}Cs containing cedar pollen. The forests contaminated by the Fukushima accident are often consisted with cedar trees, and the dispersion of pollen is a well-known phenomenon in the Japanese springtime. The effect of these effluxes of radioactive nuclides should be investigated further.

6 Conclusion

The topics described in this chapter are summarized in Fig. 1. The flows indicate almost all components are under the control of both influx and efflux. These interactions are utilized for the model simulation of radioactive nuclide dynamics within the terrestrial environment. The observation about the radioactive nuclide amount in each component at the initial and present stage provides the upcoming

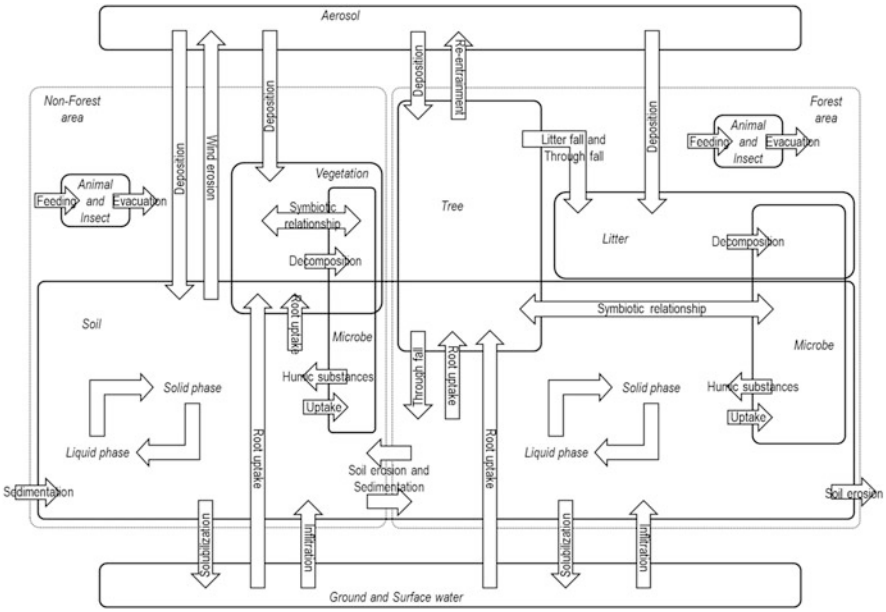

Fig. 1 Schematic flow of radioactive nuclides in the terrestrial environment. The environmental components are connected with *arrows*, which indicate the transfer of radioactive nuclides. Human-made process is eliminated from these relationships

distribution and the implication about which are the key components for recovering the environment. Of course, the prediction cannot be managed without the considerable contribution of detailed measurements and the analyses of transfer processes, but the results obtained will provide the new aspects for understanding the terrestrial environmental dynamics of radioactive nuclides.

References

Adachi K, Kajino M, Zaizen Y, Igarashi Y (2013) Emission of spherical cesium-bearing particles from an early stage of the Fukushima nuclear accident. Sci Rep 3:2554

Bixio AC, Gambolati G, Paniconi C, Putti M, Shestopalov VM, Bublias VN, Bohuslavsky AS, Kasteltseva NB, Rudenko YF (2002) Modeling groundwater-surface water interactions including effects of morphogenetic depressions in the Chernobyl exclusion zone. Environ Geol 42:162–177

Bossew P, Kirchner G (2004) Modelling the vertical distribution of radionuclides in soil. Part 1: the convection–dispersion equation revisited. J Environ Radioact 73:127–150

Bunzl K, Kracke W, Schimmack W, Auerswald K (1995) Migration of fallout $^{239+240}$Pu, ^{241}Am and ^{137}Cs in the various horizons of a forest soil under pine. J Environ Radioact 28:17–34

Calmon P, Thiry Y, Zibold G, Rantavaara A, Fesenko S (2009) Transfer parameter values in temperate forest ecosystems: a review. J Environ Radioact 100:757–766

Chibowski S, Zygmunt J (2002) The influence of the sorptive properties of organic soils on the migration rate of Cs-137. J Environ Radioact 61:213–223

Chibowski S, Zygmunt J, Klimowicz Z (1999) Investigation of adsorption and vertical migration of ^{137}Cs in three kinds of soil at Lublin vicinity. J Radioanal Nucl Chem 242:287–295

Cremers A, Elsen A, Depreter P, Maes A (1988) Quantitative-analysis of radiocesium retention in soils. Nature 335:247–249

Fan QH, Tanaka M, Tanaka K, Sakaguchi A, Takahashi Y (2014) An EXAFS study on the effects of natural organic matter and the expandability of clay minerals on cesium adsorption and mobility. Geochim Cosmochim Acta 135:49–65

Fesenko SV, Alexakhin RM, Spiridonov SI, Sanzharova NI (1995) Dynamics of ^{137}Cs concentration in agricultural products in areas of Russia contaminated as a result of the accident at the Chernobyl nuclear power plant. Radiat Prot Dosimetry 60:155–166

Fukuyama T, Takenaka C (2004) Upward mobilization of Cs-137 in surface soils of *Chamaecyparis obtusa* Sieb. et Zucc. (hinoki) plantation in Japan. Sci Total Environ 318:187–195

Fukuyama T, Takenaka C, Onda Y (2005) Cs-137 loss via soil erosion from a mountainous headwater catchment in central Japan. Sci Total Environ 350:238–247

Heinrich G (1992) Uptake and transfer factors of ^{137}Cs by mushrooms. Radiat Environ Biophys 31:39–49

Holgye Z, Maly M (2000) Sources, vertical distribution, and migration rates of ^{239,240}Pu, ^{238}Pu, and ^{137}Cs in grassland soil in three localities of central Bohemia. J Environ Radioact 47:135–147

International atomic energy agency (2006) Environmental consequences of the Chernobyl accident and their remediation: twenty years of experience. Radiological Assessment Report Series. IAEA, Vienna, pp 1–166

Kanasashi T, Sugiura Y, Takenaka C, Hijii N, Umemura M (2015) Radiocesium distribution in sugi (*Cryptomeria japonica*) in Eastern Japan: translocation from needles to pollen. J Environ Radioact 139:398–406

Kaneyasu N, Ohashi H, Suzuki F, Okuda T, Ikemori F (2012) Sulfate aerosol as a potential transport medium of radiocesium from the Fukushima nuclear accident. Environ Sci Technol 46:5720–5726

Kato H, Onda Y, Gomi T (2012) Interception of the Fukushima reactor accident-derived ^{137}Cs, ^{134}Cs, and ^{131}I by coniferous forest canopies. Geophy Res Lett 39. doi:10.1029/2012GL052928

Katsuragi Y (1983) A study of ^{90}Sr fallout in Japan. Papers Meteor Geophys 33:277–291

Kinoshita N, Sueki K, Sasa K, Kitagawa J, Ikarashi S, Nishimura T, Wong YS, Satou Y, Handa K, Takahashi T, Sato M, Yamagata T (2011) Assessment of individual radionuclide distributions from the Fukushima nuclear accident covering central-east Japan. Proc Natl Acad Sci USA 108:19526–19529

Kirchner G, Strebl F, Bossew P, Ehlken S, Gerzabek MH (2009) Vertical migration of radionuclides in undisturbed grassland soils. J Environ Radioact 100:716–720

Kita K (2014) Radioactivity measurement in the atmospheric aerosol and effect of re-entrainment from the land surface. In: Nakajima T, Ohara T, Uematsu M, Onda Y (eds) Radioactive environmental pollution from the Fukushima Daiichi nuclear power plant accident: earth science perspectives. University of Tokyo Press, Tokyo

Konopleva I, Klemt E, Konoplev A, Zibold G (2009) Migration and bioavailability of ^{137}Cs in forest soil of southern Germany. J Environ Radioact 100:315–321

Kretzschmar R, Borkovec M, Grolimund D, Elimelech M (1999) Mobile subsurface colloids and their role in contaminant transport. Adv Agron 66:121–193

Kruyts N, Delvaux B (2002) Soil organic horizons as a major source for radiocesium biorecycling in forest ecosystems. J Environ Radioact 58:175–190

Lehto J, Paatero J, Pehrman R, Kulmala S, Suksi J, Koivula T, Jaakkola T (2008) Deposition of gamma emitters from Chernobyl accident and their transfer in lichen, Äìsoil columns. J Environ Radioact 99:1656–1664

Nemoto K, Abe J (2013) Radiocesium absorption by rice in paddy field ecosystems. In: Nakanishi TM, Tanoi K (eds) Agricultural implications of the Fukushima nuclear accident. Springer, Tokyo

Parsons AJ, Foster IDL (2011) What can we learn about soil erosion from the use of ^{137}Cs. Earth Sci Rev 108:101–113

Rafferty B, Brennan M, Dawson D, Dowding D (2000) Mechanisms of ^{137}Cs migration in coniferous forest soils. J Environ Radioact 48:131–143

Realo E, Jõgi J, Koch R, Realo K (1995) Studies on radiocaesium in Estonian soils. J Environ Radioact 29:111–119

Rigol A, Vidal M, Rauret G (2002) An overview of the effect of organic matter on soil-radiocaesium interaction: implications in root uptake. J Environ Radioact 58:191–216

Ritchie JC, McHenry JR (1990) Application of radioactive fallout Cs-137 for measuring soil-erosion and sediment accumulation rates and pattern—a review. J Environ Qual 19:215–233

Roig M, Vidal M, Rauret G, Rigol A (2007) Prediction of radionuclide aging in soils from the Chernobyl and Mediterranean areas. J Environ Qual 36:943–952

Rosen K, Oborn I, Lonsjo H (1999) Migration of radiocaesium in Sweden soil profiles after the Chernobyl accident. J Environ Radioact 46:45–66

Ryan JN, Gschwend PM (1990) Colloid mobilization in 2 Atlantic coastal-plain aquifers-field studies. Water Resour Res 26:307–322

Schlesinger WH (1997) The biosphere: biogeochemical cycling on land. In: Schlesinger WH, Bernhardt E (eds) Biogeochemistry. An analysis of global change. Academic, San Diego, CA

Shaw G (2007) Radionuclides in forest ecosystems. In: Baxter MS (ed) Radioactivity in the environment, vol 10. Elsevier, Amsterdam

Sigurgeirsson MA, Arnalds O, Palsson SE, Howard B, Gudnason K (2005) Radiocesium fallout behavior in volcanic soils in Iceland. J Environ Radioact 79:39–53

Steiner M, Linkov I, Yoshida S (2002) The role of fungi in the transfer and cycling of radionuclides in forest ecosystems. J Environ Radioact 58:217–241

Sugiyama H, Terada H, Isomura K, Tsukada H, Shibata H (1993) Radiocesium uptake mechanisms in wild and culture mushrooms. Radioisotopes 42:683–690

Takata D (2013) Distribution of radiocesium from the radioactive fallout in fruit trees. In: Nakanishi TM, Tanoi K (eds) Agricultural implications of the Fukushima nuclear accident. Springer, Tokyo

Tanaka K, Sakaguchi A, Kanai Y, Tsuruta H, Shinohara A, Takahashi Y (2013) Heterogeneous distribution of radiocesium in aerosols, soil and particulate matters emitted by the Fukushima Daiichi Nuclear power plant accident: retention of micro-scale heterogeneity during the migration of radiocesium from the air into ground and river systems. J Radioanal Nucl Chem 295:1927–1937

VandenBygaart AJ, Protz R, Mccabe DC (1999) Distribution of natural radionuclides and Cs-137 in soils of southwestern Ontario. Can J Soil Sci 79:161–171

Wallbrink PJ, Murray AS (1996) Determining soil loss using the inventory ratio of excess lead-210 to cesium-137. Soil Sci Soc Am J 60:1201–1208

White PJ, Broadley MR (2000) Mechanisms of caesium uptake by plants. New Phytol 147:241–256

Yamaguchi N, Takata Y, Hayashi K, Ishikawa S, Kuramata M, Eguchi S, Yoshikawa S, Sakaguchi A, Asada K, Wagai R, Makino T, Akahane I, Hiradate S (2012) Behavior of radiocaesium in soil-plant systems and its controlling factor: a review. Bull Natl Inst Agro Environ Sci 31:75–129

Yoshida N, Takahashi Y (2012) Land-surface contamination by radionuclides from the Fukushima Daiichi nuclear power plant accident. Elements 8:201–206

Zygmunt J, Chibowski S, Klimowicz Z (1998) The effect of sorption properties of soil minerals on the vertical migration rate of cesium in soil. J Radioanal Nucl Chem 231:57–62

Biotransformation of Radionuclides: Trends and Challenges

Tania Jabbar and Gabriele Wallner

Contents

Abstract Radioactive contamination poses risks to environment and human health. The microbial-mediated transformation presents opportunity for the remediation of radionuclide contamination of the environment by immobilizing them or accelerating their removal. This chapter aims to interpret the mechanisms by which microbes interact with their surroundings to eliminate radionuclides of concern from the environment and how they influence the behavior and transport of radionuclides. Recent advances in microbial ecology have provided molecular strategies for the modeling of microbial process in order to increase the effectiveness and reliability of bioremediation and natural attenuation of polluted sites.

T. Jabbar (✉) • G. Wallner
Department of Inorganic Chemistry, University of Vienna, Währingerstr. 42, 1090 Vienna, Austria
e-mail: tania.jabbar@univie.ac.at

C. Walther, D.K. Gupta (eds.), *Radionuclides in the Environment*,
DOI 10.1007/978-3-319-22171-7_10

Keywords Microbes • Radionuclides • Mechanism of biotransformation • Future prospects

1 Introduction

The release of radioactive materials into the environment as a consequence of ongoing nuclear activities and through accidents (most recently Fukushima) has led to the accumulation of radioactive waste with tremendous environmental impact (Kazy et al. 2009). The major burden of anthropogenic radioactivity are, however, actinides (U, Pu, and Np) released from nuclear fuel processing plants and the fission products I, Cs, Sr, and Tc (Geissler et al. 2010). The radionuclides released may be in various chemical forms and may eventually transform in the environment to oxide, coprecipitates, and ionic, inorganic, and organic complexes (Francis and Dodge 2009).

Many remediation technologies exist to treat these contaminants to reduce risk to humans and the environment. The removal of radionuclides is mostly achieved by their reduction using physiochemical methods, such as the pump method, permeable reactive barriers (PRBs), ligand coupling, selective ion exchange separation, and complex formation with organic acids. However, environmental friendly methods are in demand due to high cost, low sustainability, and potential hazards linked with chemicals (Mohapatra et al. 2010). A lot of efforts have been made to understand the bioremediation of radionuclides as a potential remediation strategy. The main emphasis is to develop lower-cost techniques with minimal environmental disruption for removal of radionuclide contaminants.

Bioremediation technology uses microorganisms (prokaryotes and eukaryotes) to reduce, eliminate, or contain contaminants present in the environment (McCullough et al. 1999). The use of microbes for the remediation is determined largely by their ability to survive and catalyze the desired function under high radiation stress (Brim et al. 2000). The remediation strategy may be adopted by using techniques designed to extract or segregate the contaminated fraction from the rest of the soil, either in situ or ex situ. Ex situ bioremediation involves excavating the contaminated material and its treatment in aboveground facilities located on-site or off-site, whereas in situ remediation is undertaken at the site of contamination. In situ remediation technologies have several advantages over ex situ methods as they are cheaper and less disruptive because no excavation is required; however, they may require longer treatment time frames than the ex situ techniques (Francis and Nancharaiah 2015). Microbial activity could change the concentrations of radionuclides and their bioavailability in environment by changing chemical nature such as speciation, solubility, and sorption properties (Francis

2007). Microorganisms are ubiquitous in soil, sediments, and subsurface environment although their population sizes and respiratory metabolic activities can vary considerably depending on energy and nutrient inputs. They have developed very effective protection mechanism against radionuclides based on their ability for enzymatic/reductive precipitation, solubilization, biosorption, bioaccumulation, etc. (Merroun and Pobell 2008). Theoretically both immobilization and mobilization present opportunities for bioremediation. Although mobilization can be a better long-term strategy, the risk involved to immobilize the toxic contaminant in the capture zone makes it unsuitable to deploy in field studies (Cao et al. 2010). Among the several microbial processes that determine the environmental fate of radionuclides, biotransformation has been emerging as a potential technique achieved by either direct enzymatic reduction or by their end products (Mohapatra et al. 2010).

This chapter documented the existing fundamental information about critical redox reactions that lead to immobilization, understanding of key microbial metabolic processes during biotransformation, and the evaluation of results on microbial metabolic processes. Further aspects and new developments in genetic engineering are examined.

1.1 Uranium

Uranium exists in several oxidation states. U(IV) and U(VI) are the predominant states found in the environment (Francis 2002). Uranium exhibits higher solubility in oxidized form as uranyl ion (UO_2^{2+}). When uranyl ions encounter a reducing agent such as organic matter and microorganisms, it is precipitated into considerably less soluble lower oxidation state as the oxide mineral uraninite (UO_2) (McCullough et al. 1999; Marshall et al. 2010). Both aerobic and anaerobic microorganisms have been reported to involve directly or indirectly in redox transformation of various chemical forms of uranium in the environment (Francis 2012):

$$\mathrm{U(VI)} \xrightarrow{\text{dissimilatory metal reducers, fermenters, sulfate reducers}} \mathrm{U(IV)}$$

Immobilization of U has been potentially achieved by a diverse range of bacteria and archaea; however, the most identified are dissimilatory Fe(III) or sulfate-reducing bacteria (DIRB and DSRB), γ and δ Proteobacteria, and Firmicutes in the presence of suitable electron donors leading to bioreduction and bioprecipitation (Loughlin et al. 2011). At low pH, uranium adsorption onto cell surface of *Bacillus subtilis* (Lloyd et al. 2002) and cell wall of fungus *Rhizopus arrhizus* involving coordination of amine N of chitin (Gadd 2002) has been reported. The precipitation of uranium by *Citrobacter* sp. has also been demonstrated with enzymatically liberated inorganic phosphate (Macaskie et al. 1992). Thus, uranyl phosphate accumulates as polycrystalline HUO_2PO_4, at the cell's surface. Recently, Rui et al. (2013) have reported reduction of this biogenic mineral to U(IV) by metal-reducing bacteria, namely, *Geobacter sulfurreducens* strain PCA, *Anaeromyxobacter dehalogenans* strain K, and *Shewanella putrefaciens* strain CN-32.

Similar to *Citrobacter*, in *Halomonas* sp., U(VI) was not only bound to the cell surface but also accumulated intracellularly as electron-dense granules. EXAFS analysis of halophilic and non-halophilic bacterial cells demonstrated that U (VI) existed predominantly as uranyl hydrogen phosphate and complex forms of phosphate such as hydroxophosphate or polyphosphate as well as other ligands such as carboxyl species (Francis et al. 2004).

Direct enzymatic reduction depending on the hydrogen or organic compounds like acetate, ethanol, lactate, etc. on the surface of *Shewanella putrefaciens*, *Desulfovibrio vulgaris*, and *Desulfovibrio desulfuricans* in the presence of c-type cytochrome was reported as

$$UO_2{}^{2+}{}_{(soluble)} + H_2 \rightarrow UO_{2(insoluble)} + 2H^+$$
$$2UO_2{}^{2+}{}_{(soluble)} + CH_2O + 2H_2O \rightarrow 2UO_{2(insoluble)} + CO_2 + 2H^+$$

However, effective electron donor is selected on site-specific basis, e.g., ethanol was recommended for the Oak Ridge site, while acetate for US DOE Shiprock and Old Rifle, UMTRA site, Colorado (Finneran et al. 2002; Hazen and Tabak 2005; Luo et al. 2007). These electron donors stimulate nitrate reduction that can cause a rise in pH hence promoting removal of uranium either via hydrolysis and precipitation (Shelobolina et al. 2007) or bioreduction where uranium is being utilized as electron acceptor (Istok et al. 2004).

Indirect reduction by Fe(III)-reducing bacterium *Geobacter sulfurreducens* in the presence of homologous cytochrome (PpcA) and a triheme periplasmic cytochrome c7, anaerobic spore-forming fermentative bacteria *Clostridium* sp., mesophilic sulfate-reducing bacteria, hyperthermophilic archaea, thermophilic bacteria, and acid-tolerant bacteria has also been reported (Merroun and Pobell 2008; Francis and Dodge 2009; Anderson and Lovely 2002; Prakash et al. 2013).

1.2 Technetium

Technetium can exist in multiple oxidation states (0, +3, +4, +5, +6, +7). Tc(VII) has attracted considerable recent interest due to its mobility as soluble pertechnetate ion $TcO_4{}^-$ under oxic conditions and weak ligand-complexing capabilities like Np (V) (Lloyd et al. 2005; Francis 2007). Under reducing conditions, it can form insoluble and strongly sorbing hydrous phase Tc(IV)O_2 (Newsome et al. 2014).

Chemolithotrophic, haloalkaliphilic, aerobic, facultative, and anaerobic bacteria have been identified to reduce Tc(VII) catalyzed by the hydrogen component of the formate hydrogenlyase complex (FHL) or c-type cytochrome. The dissimilatory reduction of Tc is favored in neutral, acidic, and alkaline environment depending on the type of microbial activity (Mohapatra et al. 2010) coupled to oxidation of H_2 or certain organic compounds as an electron donor.

$$TcO^{4-}{}_{(soluble)} + 3e^- + 4H^+ \rightarrow TcO_2.nH_2O_{(insoluble)} + (2-n)H_2O$$

A Halomonas strain isolated from a seawater removed Tc(VII) by aerobically reducing it to Tc(IV). The predominate reduced species include TcO_2, Tc(OH), and TcS_2. The reduction of Tc(VII) by indirect microbial processes such as biomineralization via biogenic sulfide and Fe(II) has also proved to be efficient and useful mechanism for remediation by *Geobacter*, *Anaeromyxobacter*, and *Shewanella* (Plymale et al. 2011). However, limited ingrowth of Fe(II) at high concentration of nitrate in Oak Ridge, Tennessee, USA, has been explored suggesting strong inhibition of metal reduction (Geissler et al. 2010).

1.3 Plutonium

Plutonium has complex redox chemistry. At neutral pH, Pu can exist in multiple oxidation states, but small changes in pH and redox conditions can lead to changes in speciation. Plutonium can coexist as Pu(IV), Pu(V), and Pu(VI) in oxic environment. With a slight increase in microbial activity, Pu (VI) and Pu(V) can be reduced to Pu(IV) due to very small difference in reduction potential as shown below (Francis 2007). Therefore, the Pu(IV) is the dominant oxidation state under most environments and forms highly insoluble $Pu(OH)_4$.

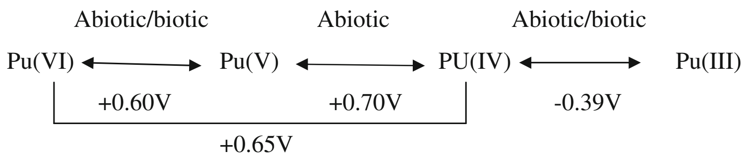

Fe(III)-reducing bacteria like *Shewanella oneidensis*, *S. putrefaciens*, and *Geobacter metallireducens* have been reported for the enzymatic reduction of Pu (VI)/(V) to Pu(IV), while Pu(III) has very little production. But the presence of complexing ligands has been found to facilitate Pu(IV) to Pu(III) reduction. However, anaerobic bacteria *Bacillus* sp., *Bacillus mycoides*, *Serratia marcescens* (Luksiene et al. 2012), and *Clostridium* sp. have shown tendency for reductive dissolution of Pu(IV)–Pu(III) (Francis 2007; Francis and Dodge 2009). *Shewanella* alga can reduce $Pu(V)O_2{}^+$ to amorphous $Pu(III)PO_4$ (Reed et al. 2007; Deo et al. 2011). Lichen *Parmotrema tinctorum* has been observed to play an important role in the elimination of Pu(VI) and U(VI). The accumulation of Pu and U(VI) has been identified on the upper and lower surfaces and in cortical and medullary layers, respectively. UV/vis absorption spectroscopy showing microbial activity can further reduce Pu(VI) to Pu(V) in solution and to Pu(IV) as Pu(IV) hydroxide by releasing organic substances, while the oxidation state of U(VI) remains unchanged (Ohnuki et al. 2004).

1.4 Neptunium

Neptunium predominantly exists as the neptunyl cation $Np(V)O_2^+$ in aerobic environment that has low ligand-complexing ability. It is highly mobile, is non-sorptive, and can be removed via combined bioreduction–biomineralization under anaerobic conditions. In situ bioremediation of Np(V) supplied with hydrogen or pyruvate is shown as (Rittmann et al. 2002; Mohapatra et al. 2010)

$$NpO^{2+}{}_{(soluble)} + e^- + 4H^+ \rightarrow Np^{4+}{}_{(insoluble)} + 2H_2O$$

Anaerobic microbial reduction of aqueous Np(V) citrate by *G. metallireducens* and *S. oneidensis* and reduction of un-chelated Np(V) by *S. oneidensis*, by *S. putrefaciens* MR-1, and by sulfate-reducing bacteria *Desulfovibrio desulfuricans* have been reported (Icopini et al. 2007). Contrary to reduction of UO_2^{2+} by first transferring an electron to an actinyl ion and then generation of U(IV) by disproportionation, it has been investigated that *G. sulfurreducens* cannot transfer an electron to NpO_2^+ (Renshaw et al. 2007).

The reduced Np(IV) can be precipitated with phosphate liberated by phosphatase activity of *Serratia* and *Citrobacter* sp. (Lloyd et al. 2000). Abiotic reduction has also been suggested in microbial active sediment system when provided with electron donor acetate or lactate (Newsome et al. 2014).

1.5 Strontium and Cesium

Since strontium and cesium are both redox inactive, their removal from the environment is mostly influenced by indirect microbial interactions such as bioaccumulation, sorption, and precipitation. Many active metabolizing microorganisms including *Pseudomonas fluorescens*, epilithic cyanobacteria, *Halomonas*, and *Sporosarcina pasteurii* have demonstrated ability to remove strontium as crystalline $SrCO_3$ (Newsome et al. 2014). In most cases, this occurs through microbially induced calcium carbonate precipitation (MICP) (Fujita et al. 2010) that can be implemented using reduction of sulfate, bacterial ureolysis, fermentation of fatty acids, and denitrification process (Francis and Nancharaiah 2015).

- Microbially catalyzed hydrolysis of urea produces ammonia and bicarbonate and increases the pH. Bicarbonate promotes the precipitation of $CaCO_3$, whereas ammonium ions promote the exchange of sorbed Sr (Fujita et al. 2000, 2004).

$$\begin{array}{l} NH_2(CO)NH_2 + 3H_2O \xrightarrow{\text{Urease}} 2NH_4{}^+ + HCO_3{}^- + OH \\ \text{Solid - }Sr^{2+} + 2NH_4{}^+ \leftrightarrow \text{Solid - }(NH_4{}^+) + Sr^{2+} \end{array}$$

- Denitrification involves the reduction of $NO_3{}^-$ to N_2 in the presence of an electron donor (i.e., acetate) (Wu et al. 2011).

$$\begin{array}{l} 8/5\,NO_3{}^- + CH_3COO^- \xrightarrow{\text{Denitrifiers}} 4/5\,N_2 + 2\,CO_2 + 13/5\,OH^- + 1/5\,H_2O \\ CO_2 + H_2O \leftrightarrow HCO_3{}^- + H^+ \\ Sr^{2+} + HCO_3{}^- + OH^- \leftrightarrow SrCO_3(s) + H_2O \end{array}$$

- Fermentation of fatty acids like citric acid (Anderson and Appanna 1994) due to the production of CO_2 from citrate metabolism.

In all abovementioned reactions, strontium is integrated into the calcite structure by substituting for calcium, thus forming strontium carbonate minerals of very low solubility (Fujita et al. 2008).

Alternative techniques proposed for strontium include sequestration as (Ba,Sr) SO_4 by desmid green algae (Krejci et al. 2011), incorporation into biogenic hydroxyapatite produced by a *Serratia* sp. (Handley-Sidhu et al. 2011a, b), and co-treatment with Tc(VII) and high ammonium and nitrate levels via microbially induced increased in pH and alkalinity and during bioreduction of Fe(III) and nitrate (Thorpe et al. 2012).

The mechanism of cesium removal by cesium-accumulating bacteria (strains *Rhodococcus erythropolis* CS98 and *Rhodococcus* sp. strain CS402) isolated from soil cannot be modeled as simple adsorption as they display the rod–coccus growth cycle and contain meso-diaminopimelic acid, mycolic acids, and tuberculostearic acids (Tomioka et al. 1992). Since the same metabolic transport systems are involved in K+ and Cs+ absorption due to the chemical similarity of the cations, the presence of potassium inhibited Cs accumulation by these strains (Tomioka et al. 1994).

Recently, adsorption of cesium by unicellular green algae and heterocystous blue green algae has been reported (Shimura et al. 2012). The terrestrial cyanobacterium Nostoc (N) was found to form jelly-like clumps of polysaccharides that absorbed high levels of radioactive cesium (Sasaki et al. 2013). It was monitored that in Nihonmatsu City, Fukushima Prefecture, *N. commune* accumulated 415,000 of ^{134}Cs and 607,000 Bq kg^{-1} of ^{137}Cs dry weight, respectively (Fujita et al. 2013). Very high radiocesium activities have been observed in the fruiting bodies of several fungal species since the Chernobyl accident (Dighton and Horrill 1998). The bonding of Cs with the cells (extra- or intracellular) remains unclear, as does the long-term fate of bio-associated Cs. However, in sediment systems, the Cs is fixed at interlayer sites and frayed edge sites of phyllosilicate minerals where Cs can form inner sphere complexes. Indirect microbial impacts such as the release of competing ammonium ions or changes in mineral stability may play a role in controlling Cs mobility (Brookshaw et al. 2012).

1.6 Iodine

Microbial processes can significantly influence the mobility of iodine in the environment through volatilization in the form of organic iodine compounds (i.e., CH_3I), the oxidation of iodide (I–) to iodine (I_2), the bioreduction of iodate (IO_3^-) to iodide (I^-), and via bioaccumulation (Amachi 2008; Jabbar et al. 2013).

Pure cultures of bacteria and fungi have shown tendency to incorporate radioiodine in the presence of organic substances or biomass via irreversible sorption process (Bors and Martens 1992). Positively charged single sites were recognized to be responsible for iodide sorption on to cell wall of Gram-positive soil bacterium *Bacillus subtilis*. However, the uptake and accumulation of iodide in washed cell suspensions of marine bacteria was accelerated by the addition of glucose without exhibiting any effect on iodate deposition (Amachi et al. 2005). Recently, the adsorption of iodine by unicellular green algae has been reported (Shimura et al. 2012).

D. desulfuricans was able to enzymatically reduce iodate to iodide in bicarbonate and HEPES buffers, while *S. putrefaciens* was only able to perform this transformation in HEPES (Councell et al. 1997). As Fe(II), sulfide, and FeS were shown to abiotically reduce iodate to iodide, it is inferred that Fe(III)- and sulfate-reducing bacteria are able to mediate iodate reduction both directly and indirectly (Hu et al. 2005). This study was further illustrated by sorption of 54 % of iodine and 75 % of ^{129}I from waters at near-neutral pH in in situ bacteriogenic Fe(III) oxides at Chalk River, Canada (Kennedy et al. 2011).

2 Mechanisms of Bioimmobilization of Radionuclides

The role of microbes in determining the environmental fate of radionuclides and understanding microbe–radionuclide interactions is of great importance for developing effective methods of bioremediation. In this section we discussed the principles and key factors affecting the processes of microbial transformations of radionuclides. The immobilization is achieved by direct or indirect reduction, biosorption onto the cells, precipitation by organic complexing ligands released by the cells, and bioaccumulation (Fig. 1) (Cao et al. 2010) depending on the form of the metal, the availability of electron donors and acceptors, nutrients, and

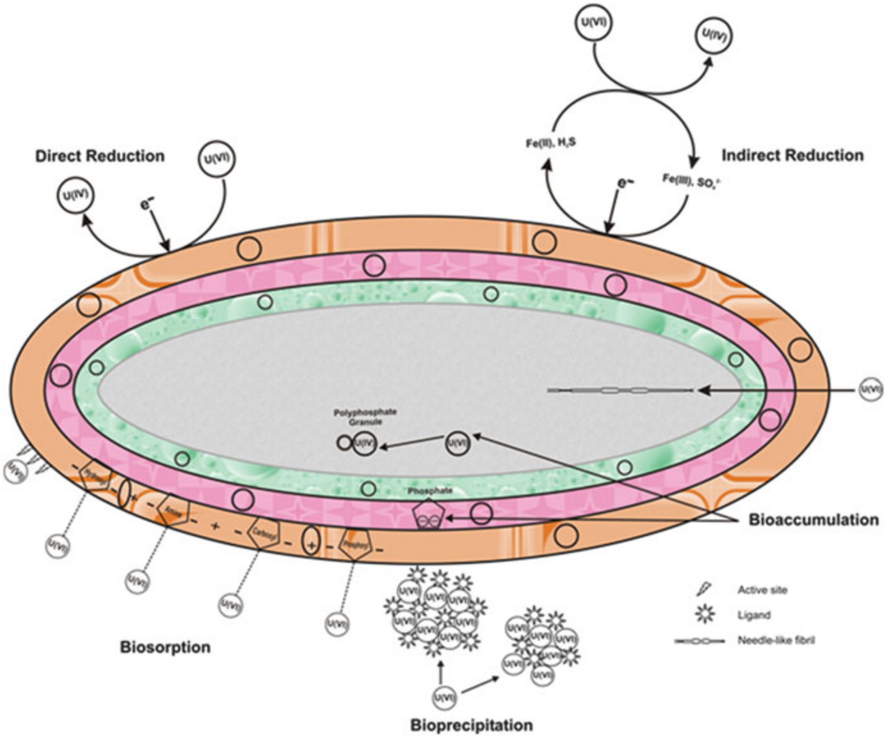

Fig. 1 Mechanisms of microbe–uranium interactions

environmental factors including moisture, temperature, pH, and Eh (Francis and Nancharaiah 2015).

2.1 Biosorption

Biosorption describes the passive uptake of radionuclide species to the surface of living or dead microbial cells by metabolism independent of physicochemical mechanisms. Metal cations either adsorb on cell wall possessing electronegative charges or may bind through chemical sorption by ligands such as carboxyl, amine, hydroxyl, phosphate, etc. The process is species specific and is affected by the chemical speciation of metal, pH of medium, physiological state of the cells, as well as the presence of exopolymers (Merroun and Pobell 2008). Biosorption is perhaps best suited to remove radionuclides of low concentration from effluents because it is faster than bioaccumulation and the biosorbent is easy to regenerate.

However, limitations included desorption due to competition with other cations for binding sites and saturation preventing further sorption leading to an inadequate long-term solution for bioremediation.

2.2 Bioaccumulation

Bacteria, fungi, and algae have been identified to have ability to accumulate radionuclides extra- or intracellularly independent of metabolism due to similarities with some essential elements needed for cell functioning. The accumulation mechanism may involve either chelation by polyphosphate granules or formation of needle-like crystals supported by enhanced cell membrane permeability resulting from the toxic effects of radionuclides (Cao et al. 2010; Francis and Nancharaiah 2015). However, metabolism-dependent transport process via siderophore-mediated Fe(III) transport system has been reported.

2.3 Biomineralization/Bioprecipitation

Radionuclide precipitation through microbial generation of ligands and biogenic mineral formation play an important role in retention of contaminant. The enzymatically produced highly localized ligand concentration around the cells provides the nucleation site for precipitation, e.g., phosphate precipitation. Contrary to direct precipitation, biogenic mineral method involves precipitation of a metal biomineral by microbial cells which then act as a trap for the subsequent deposition of radionuclide of interest.

2.4 Bioreduction

Microbes offer great potential for controlling mobility of target radionuclides in contaminated environment through reduction of radionuclides that are redox active and less soluble when reduced. Since microbial life is based on chemical energy driven by metabolic process that requires a reduced electron donor and an oxidized electron acceptor (Pedersen 2005), the reduction can be carried out directly by microbes or indirectly through electron transfer by dissimilatory metal-reducing bacteria (DMRB). Different mechanisms may exist for electron transfer from donor to acceptor among different species. It may or may not involve direct contact. Although U(VI) is significantly soluble to have direct contact with a cell, bacteria must have mechanisms of transferring electron extracellular to acceptor Fe(III) or sorbed U(VI). These include the use of electron-carrier protein such as cytochrome exposed to the outside of the cytoplasmic membrane, within the periplasm, and/or in the outer membrane or through release of chelators/electron shuttle like flavins and through conductive cell surface appendages such as pili (nanowires) (Lovley et al. 2004; Nielsen et al. 2010; Pfeffer et al. 2012).

Some DMRB can be beneficial by conserving energy for anaerobic growth via radionuclide reduction as in case of Fe(III)-reducing bacteria, but few are unable to conserve the energy like sulfate-reducing bacteria and clostridium species. The lower standard redox potential of Fe^{+2} than Pu(V)/Pu(IV), Np(V)/Np(IV), and U (VI)/U(IV) promotes the reduction of aforementioned radionuclide pair by Fe(III)-reducing bacteria either enzymatically or via Fe(II) produced from reduction of Fe (III) oxides by single-electron reduction and formation of cation more amenable to precipitation. Thus reduced natural organic matters NOM, Fe(II), and S(II) have proved to be potential reductants under typical suboxic and anoxic environments (Loughlin et al. 2011).

The most critical issue for all biotransformation is how stable the transformation is. The stability of reduced species for the success of remediation has been studied in terms of the long-term biocycling behavior of radionuclides in natural and engineered environments. For example, complexing agents such as ethylenediaminetetraacetate (EDTA), diethylenetriaminepentaacetic acid (DTPA), oxalate, citrate, humic acid, and fulvic acids promote dissolution of Tc(IV) oxides with the exposure to oxygen or changes in pH. Similarly, reoxidation of U(IV) in sediments with natural microbial communities present in Fe(III) minerals (Sani et al. 2005; Ginder-Vogel et al. 2006; Spycher et al. 2011); manganese oxides (Fredrickson et al. 2002; Wang et al. 2013); organic ligands such as citrate and EDTA, under anaerobic conditions (Luo and Gu 2011); and microbially generated bicarbonate, even under bioreducing conditions (Wan et al. 2005, 2008). Nitrate-reducing bacteria appear to be particularly important in mediating the reoxidation of U(IV) by nitrate (Wilkins et al. 2007).

3 Prospects and Challenges

Remediation of radionuclides through microbial treatment has numerous advantages including being eco-friendly, specificity, adaptability, recyclability of bio-products, etc. Major drawback to this method is slow speed of process and difficulty to control, which accelerates the accumulation of pollutants in the environment with time that can be potentially hazardous. Additionally long-term sustainability of microbial remediation is a question of great importance. With rapid radionuclide accumulation, upgradation of existing bioremediation processes to commercial level by making it faster, recyclable, and controlled is a major challenge.

Polluted environment often contains more than one metal as in the radioactive waste. Therefore, modification in the outer membrane proteins of bacteria with potential bioremediation properties for improving metal binding capacity of microbes may be needed. To large-scale remediation, even complex and combinatorial approaches have been developed to manipulate bacterial genetics in order to design multi-metal resistant bacteria strains. Genetically engineered microorganism

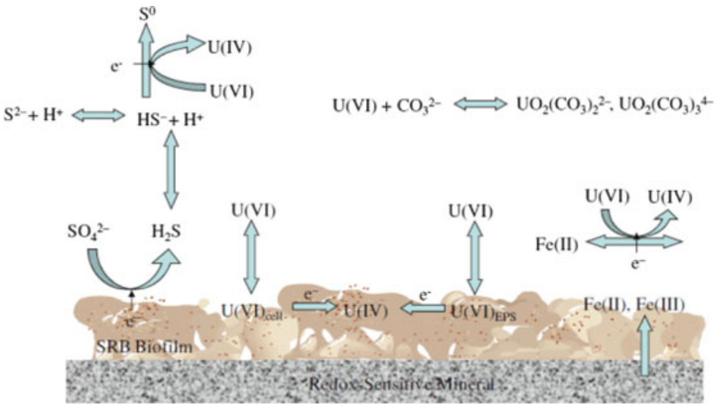

U(VI)cell: U(VI) adsorbed or intake by cells; U(VI)EPS: U(VI) accumulated in EPS

Fig. 2 Possible mechanisms of U immobilization and remobilization using SRB biofilms grown on iron-bearing surface. Reprinted (adapted) with permission from Marsili et al. (2007), American Chemical Society

is the term used to develop organisms with altered genetic material using recombinant DNA technology. This process is helpful to generate a character-specific efficient strain for biotransformation so that it can be used under various complex environmental conditions. For instance, the gene designated phoK responsible for alkaline phosphatase activity was extracted from *Sphingomonas* sp. strain BSAR-1. Later it was cloned and overexpressed in *Escherichia coli* strain BL21(DE3) (Nilgiriwala et al. 2008) and in the radio-resistant bacterium *Deinococcus radiodurans* (Kulkarni et al. 2013), respectively. The precipitation of >90 % of input uranium has been achieved by recombinant strain in less than 2 h from alkaline waste solutions. Deino-PhoK cell was even not affected by the presence of Cs and Sr. However, for utilizing GEM, sustaining the recombinant bacteria population under various environmental conditions and competition from native bacterial populations are major obstacles reported (Dixit et al. 2015).

Another approach is formation and development of biofilm synthetically. Biofilm is an agglomeration of microbial cells whose thickness is extremely variable ranging from single-cell monolayer to thick mucus microcolonies of microbes held together by extracellular polymeric substances (EPS). The bEPS from *Shewanella* sp. (Cao et al. 2011) and *Desulfovibrio desulfuricans* G20 (Beyenal et al. 2004) have been successfully utilized for immobilization of uranium (Fig. 2).

References

Amachi S (2008) Microbial contribution to global iodine cycling: volatilization, accumulation, reduction, oxidation and sorption of iodine. Microbes Environ 23:269–276

Amachi S, Fuji T, Shinoyama H, Muramatsu Y (2005) Microbial influences on the mobility and transformation of radioactive iodine in the environment. J Nucl Radiochem Sci 6:21–24

Anderson RT, Lovley DR (2002) Microbial redox interactions with uranium: an environmental perspective. In: Keith-Roach MJ, Francis RL (eds) Interactions of microorganisms with radionuclides. Elsevier, Amsterdam

Anderson S, Appanna V (1994) Microbial formation of crystalline strontium carbonate. FEMS Microbiol Lett 116:43–48

Beyenal H, Sani RK, Peyton BM, Dohnalkova AC, Amonette JE, Lewandowski Z (2004) Uranium immobilization by sulfate-reducing biofilms. Environ Sci Technol 38:2067–2074

Bors J, Martens R (1992) The contribution of microbial biomass to the adsorption of radioiodine in soils. J Environ Radioact 15:35–49

Brim H, McFarlan SC, Fredrickson JK, Minton KW, Zhai M, Wackett LP, Daly MJ (2000) Engineering *Deinococcus radiodurans* for metal remediation in radioactive mixed waste environments. Nat Biotechnol 18:85–90

Brookshaw DR, Pattrick RAD, Lloyd JR, Vaughan DJ (2012) Microbial effects on mineral–radionuclide interactions and radionuclide solid-phase capture processes. Mineral Mag 76:777–806

Cao B, Ahmed B, Beyenal H (2010) Immobilization of uranium in ground water using biofilms. In: Shah V (ed) Emerging environmental technologies, vol 2. Springer, Berlin

Cao B, Ahmed B, Kennedy DW, Wang Z, Shi L, Marshall MJ, Fredrickson JK, Isern NG, Majors PD, Beyenal H (2011) Contribution of extracellular polymeric substances from *Shewanella* sp. HRCR-1 biofilms to U(VI) immobilization. Environ Sci Technol 45:5483–5490

Councell T, Landa E, Lovely D (1997) Microbial reduction of iodate. Water Air Soil Pollut 100:99–106

Deo RP, Rittmann BE, Reed DT (2011) Bacterial Pu(V) reduction in the absence and presence of Fe(III)-NTA: modeling and experimental approach. Biodegradation 22:921–929

Dighton J, Horrill AD (1998) Radiocaesium accumulation in the mycorrhizal fungi *Lactarius rufus* and *Inocybe longicystis* in upland Britain. Trans Br Mycol Soc 91:335–337

Dixit R, Wasiullah MD, Pandiyan K, Singh UB, Sahu A, Shukla R, Singh BP, Rai JP, Sharma PK, Lade H, Paul D (2015) Bioremediation of heavy metals from soil and aquatic environment: an overview of principles and criteria of fundamental processes. Sustainability 7:2189–2212

Finneran KT, Anderson RT, Nevin KP, Lovley DR (2002) Potential for bioremediation of uranium-contaminated aquifers with microbial U(VI) reduction. Soil Sedim Contam 11:339–357

Fredrickson JK, Zachara JM, Kennedy DW, Liu CX, Duff MC, Hunter DB, Dehnalkova A (2002) Influence of Mn Oxides on the reduction of Uranium (VI) by the metal reducing bacterium *Shewanella putrefaciens*. Geochim Cosmochim Acta 66:3247–3262

Francis AJ (2002) Microbial transformation of uranium complexed with organic and inorganic ligands. In: Merkel BJ, Planer-Friedrich B, Wolkerdorfer C (eds) Uranium in the aquatic environment. Springer, Berlin

Francis AJ (2007) Microbial transformation of radionuclides released from nuclear fuel reprocessing plants. Brookhaven National Laboratory, BNL-79721-2007-CP

Francis AJ (2012) Impact of microorganism on radionuclides in contaminated environments and waste materials. In: Merkel BJ (ed) Radionuclide behavior in the natural environment. Woodhead Publishing Limited, BNL-98706-2012-BC

Francis AJ, Dodge CJ (2009) Microbial transformation of actinides and other radionuclides. Brookhaven National Laboratory, BNL-82098-2009-CP

Francis AJ, Nancharaiah YV (2015) In situ and ex situ bioremediation of radionuclides contaminated soils at nuclear and NORM sites. In: Velzen VL (ed) Environmental remediation and restoration of contaminated nuclear and NORM sites. Elsevier, Amsterdam

Francis AJ, Gillow JB, Dodge CJ, Harris R, Beveridge TJ, Papenguth HW (2004) Association of uranium with halophilic and nonhalophilic bacteria and archaea. Radiochim Acta 92:481–488

Fujita Y, Ferris FG, Lawson RD, Colwell FS, Smith RW (2000) Calcium carbonate precipitation by ureolytic subsurface bacteria. Geomicrobiology J 17:305–318

Fujita Y, Redden GD, Ingram JC, Cortez MM, Ferris GF, Smith RW (2004) Strontium incorporation into calcite generated by bacterial ureolysis. Geochim Cosmochim Acta 68:3261–3270

Fujita Y, Taylor JL, Gresham TLT, Delwiche ME, Colwell FS, McLing TL, Petzke LM, Smith RW (2008) Stimulation of microbial urea hydrolysis in groundwater to enhance calcite precipitation. Environ Sci Technol 42:3025–3032

Fujita Y, Taylor JL, Wendt LM, Reed DW, Smith RW (2010) Evaluating the potential of native ureolytic microbes to remediate a ^{90}Sr contaminated environment. Environ Sci Technol 44:7652–7658

Fujita T, Wang LP, Yabui K, Dodbiba G, Okaya K, Matsuo S, Nomura K (2013) Adsorption of cesium ion on various clay minerals and remediation of cesium contaminated soil in Japan. Resour Process 60:13–17

Gadd GM (2002) Microbial interactions with metals/radionuclides: the basis of bioremediation. In: Keith-Roach MJ, Francis RL (eds) Interactions of microorganisms with radionuclides. Elsevier, Oxford

Geissler A, Pobell SS, Morris K, Burke IT, Livens FR, Lloyd J (2010) The microbial ecology of land and water contaminated with radioactive waste: towards the development of bioremediation options for the nuclear industry. In: Batty LC, Hallberg KB (eds) Ecology of industrial pollution. Cambridge University Press, Cambridge

Ginder-Vogel M, Criddle CS, Fendorf S (2006) Thermodynamic constraints on the oxidation of biogenic UO2 by Fe(III) (hydr)oxides. Environ Sci Technol 40:3544–3550

Handley-Sidhu S, Renshaw JC, Moriyama S, Stolpe B, Mennan C, Bagheriasl S, Yong P, Stamboulis A, Paterson-Beedle M, Sasaki K, Pattrick RAD, Lead JR, Macaskie LE (2011a) Uptake of Sr^{2+} and Co^{2+} into biogenic hydroxyapatite: implications for biomineral ion exchange synthesis. Environ Sci Technol 45:6985–6990

Handley-Sidhu S, Renshaw JC, Yong P, Kerley R, Macaskie LE (2011b) Nanocrystalline hydroxyapatite bio-mineral for the treatment of strontium from aqueous solutions. Biotechnol Lett 33:79–87

Hazen TC, Tabak HH (2005) Developments in bioremediation of soils and sediments polluted with metals and radionuclides: 2. Field research on bioremediation of metals and radionuclides. Rev Environ Sci Biotechnol 4:157–183

Hu Q, Zhao P, Moran JE, Seaman JC (2005) Sorption and transport of iodine species in sediments from the Savannah River and Hanford sites. J Contam Hydrol 78:185–205

Icopini GA, Boukhalfa H, Neu MP (2007) Biological reduction of Np(V) and Np(V) citrate by metal reducing bacteria. Environ Sci Technol 41:2764–2769

Istok JD, Senko JM, Krumholz LR (2004) In situ bioreduction of technetium and uranium in a nitrate-contaminated aquifer. Environ Sci Technol 38:468–475

Jabbar T, Wallner G, Steier P (2013) A review on ^{129}I analysis in air. J Environ Radioact 126:45–54

Kazy SK, D'Souza SF, Sar P (2009) Uranium and thorium sequestration by a *Pseudomonas* sp.: mechanism and chemical characterization. J Hazard Mater 163:65–72

Kennedy CB, Gault AG, Fortin D, Clark ID, Ferris FG (2011) Retention of iodide by bacteriogenic iron oxides. Geomicrobiology J 28:387–395

Krejci MR, Wasserman B, Finney L, McNulty I, Legnini D, Vogt S, Joester D (2011) Selectivity in biomineralization of barium and strontium. J Struct Biol 176:192–202

Kulkarni S, Ballal A, Apte SK (2013) Bioprecipitation of uranium from alkaline waste solutions using recombinant *Deinococcus radiodurans*. J Hazard Mat 15:853–861

Lloyd JR, Yong P, Macaskie LE (2000) Biological reduction and removal of Np(V) by two microorganisms. Environ Sci Technol 34:1297–1301

Lloyd JR, Chesnes J, Glasauer S, Bunker DJ, Livens FR, Lovley DR (2002) Reduction of actinides and fission products by Fe(III) reducing bacteria. Geomicro J 19:103–120

Lloyd JR, Renshaw JC, May I, Livens FR, Burke IT, Mortimerc RJG, Morris K (2005) Biotransformation of radioactive waste: microbial reduction of actinides and fission products. J Nucl Radiochem Sci 6:17–20

Loughlin EJ, Boyanov MI, Antonopoulos DA, Kemmer KM (2011) Redox processes affecting the speciation of technetium, uranium, neptunium and plutonium in aquatic and terrestrial environments. In: Aquatic redox chemistry, ACS symposium series, American Chemical Society, Washington

Lovley DR, Holmes DE, Nevin KP (2004) Dissimilatory Fe(III) and Mn(IV) reduction. In: Poole RK (ed) Advances in microbial physiology, vol 49. Elsevier, London

Luo W, Gu B (2011) Dissolution of uranium-bearing minerals and mobilization of uranium organic ligands in a biologically reduced sediment. Environ Sci Technol 45:2994–2999

Luo WS, Wu WM, Yan TF, Criddle CS, Jardine PM, Zhou JZ, Gu BH (2007) Influence of bicarbonate, sulfate, and electron donors on biological reduction of uranium and microbial community composition. Appl Microbiol Biotechnol 77:713–721

Macaskie LE, Empson RM, Cheetham AK, Grey CP, Skarnulis AJ (1992) Uranium bioaccumulation by citrobacter sp. As a result of enzymatically-mediated growth of polycrystalline HUO_2PO_4. Science 257:782–784

Marshall MJ, Beliaev AS, Fredrickson JK (2010) Microbial transformations of radionuclides in the subsurface. In: Mitchell R, Gu DJ (eds) Environmental microbiology, 2nd edn. Wiley, Hoboken, NJ

Marsili E, Beyenal H, Palma L, Merli C, Dohnalkova A, Amonette J, Lewandowski Z (2007) Uranium immobilization by sulfate-reducing biofilms grown on hematite, dolomite, and calcite. Environ Sci Technol 41:8349–8354

McCullough J, Hazen T, Sally B (1999) Bioremediation of metals and radionuclides: what it is and how it works. Lawrence Berkeley National Laboratory, LBNL-42595

Merroun ML, Pobell SS (2008) Bacterial interactions with uranium: an environmental perspective. J Contam Hydrol 102:285–295

Mohapatra BR, Dinardo O, Gould WD, Koren DW (2010) Biochemical and genomic facets on the dissimilatory reduction of radionuclides by microorganisms—a review. Miner Eng 23:591–599

Newsome L, Morris K, Lloyd JR (2014) The biogeochemistry and bioremediation of uranium and other priority radionuclides. Chem Geol 363:164–184

Nielsen LP, Risgaard-Petersen N, Fossing H, Christensen PB, Sayama M (2010) Electric currents couple spatially separated biogeochemical processes in marine sediment. Nature 463:1071–1074

Nilgiriwala KS, Alahari A, Rao AS, Apte SK (2008) Cloning and overexpression of alkaline phosphatase PhoK from *Sphingomonas* sp. strain BSAR-1 for bioprecipitation of uranium from alkaline solutions. Appl Environ Microbiol 74:5516–5523

Ohnuki T, Aoyagi H, Kitatsuji Y, Samadfam M, Kimura Y, Purvis OW (2004) Plutonium (VI) accumulation and reduction by lichen biomass: correlation with U(VI). J Environ Radioact 77:339–35

Pedersen K (2005) Microorganisms and their influence on radionuclides migration in igneous rock environments. J Nucl Radiochem Sci 6:11–15

Pfeffer C, Larsen S, Song J, Dong M, Besenbacher F, Meyer RL, Kjeldsen KU, Schreiber L, Gorby YA, El-Naggar MY, Leung KM, Schramm A, Risgaard-Petersen N, Nielsen LP (2012) Filamentous bacteria transport electrons over centimetre distances. Nature 491:218–221

Plymale AE, Fredrickson JK, Zachara JM, Dohnalkova AC, Heald SM, Moore DA, Kennedy DW, Marshall MJ, Wang CM, Resch CT, Nachimuthu P (2011) Competitive reduction of pertechnetate ((TcO4 −)-Tc-99) by dissimilatory metal reducing bacteria and biogenic Fe(II). Environ Sci Technol 45:951–957

Prakash D, Gabani P, Chandel AK, Ronen Z, Singh OV (2013) Bioremediation: a genuine technology to remediate radionuclides from the environment. Microb Biotechnol 6:349–360

Reed DT, Pepper SE, Richmann MK, Smith G, Deo R, Rittmann BE (2007) Subsurface bio-mediated reduction of higher-valent uranium and plutonium. J Alloys Compd 444–445:376–382

Renshaw JC, Lloyd JR, Livens FR (2007) Microbial interactions with actinides and long-lived fission products. Comp Rendus Chimi 10:1067–1077

Rittmann B, Banaszak J, Reed D (2002) Reduction of Np(V) and precipitation of Np(IV) by anaerobic microbial consortium. Biodegradation 13:329–342

Rui KMJ, Loughlin EJ, Cheatham SD, Fein JB, Bunker B, Kemner KM, Boyanov MI (2013) Bioreduction of hydrogen uranyl phosphate: mechanism and U(IV) products. Environ Sci Technol 47:5668–5678

Sani RK, Peyton BM, Dohnalkova A, Amonette JE (2005) Reoxidation of reduced uranium with iron(III) (hydr)oxides under sulfate-reducing conditions. Environ Sci Technol 39:2059–2066

Sasaki H, Shirato S, Tahara T, Sato K, Takenaka H (2013) Accumulation of radioactive cesium released from Fukushima Daiichi nuclear power plant in terrestrial cyanobacteria *Nostoc commune*. Microbes Environ 28:466–469

Shelobolina ES, Coppi MV, Korenevsky AA (2007) Importance of *c*-type cytochromes for U (VI) reduction by *Geobacter sulfurreducens*. BMC Microbiol 7:16

Shimura H, Itoh K, Sugiyama A, Ichijo S, Ichijo M, Furuya F, Nakamura Y, Kitahara K, Kobayashi K, Yukawa Y, Kobayashi T (2012) Absorption of radionuclides from the Fukushima nuclear accident by a novel algal strain. PLoS One 7, e44200

Spycher NF, Issarangkun M, Stewart BD, Sevinç Şengör S, Belding E, Ginn TR, Peyton BM, Sani RK (2011) Biogenic uraninite precipitation and its reoxidation by iron(III) (hydr)oxides: a reaction modeling approach. Geochim Cosmochim Acta 75:4426–4440

Thorpe CL, Lloyd JR, Law GTW, Burke IT, Shaw S, Bryan ND, Morris K (2012) Strontium sorption and precipitation behavior during bioreduction of nitrate impacted sediments. Chem Geol 306–307:114–122

Tomioka N, Uchiyama H, Yagi O (1992) Isolation and characterization of cesium accumulating bacteria. Appl Environ Microbiol 58:1019–1023

Tomioka N, Uchiyama H, Yagi O (1994) Cesium accumulation and growth characteristics of *Rhodococcus erythropolis* CS98 and *Rhodococcus* sp. Strain CS402. Appl Environ Microbiol 60:2227–2231

Wan J, Tokunaga TK, Brodie E, Wang Z, Zheng Z, Herman D, Hazen TC, Firestone MK, Sutton SR (2005) Reoxidation of bioreduced uranium under reducing conditions. Environ Sci Technol 39:6162–6169

Wan J, Tokunaga TK, Kim Y, Brodie E, Daly R, Hazen TC, Firestone MK (2008) Effects of organic carbon supply rates on uranium mobility in a previously bioreduced contaminated sediment. Environ Sci Technol 42:7573–7579

Wang ZM, Lee SWW, Kapoor P, Tebo BM, Giammar DE (2013) Uraninite oxidation and dissolution induced by manganese oxide: a redox reaction between two insoluble minerals. Geochim Cosmochim Acta 100:24–40

Wilkins MJ, Livens FR, Vaughan DJ, Beadle I, Lloyd JR (2007) The influence of microbial redox cycling on radionuclide mobility in the subsurface at a low-level radioactive waste storage site. Geobiology 5:293–301

Wu Y, Ajo-Franklin JB, Spycher N, Hubbard SS, Zhang G, Williams KH, Taylor J, Fujita Y, Smith R (2011) Geophysical monitoring and reactive transport modeling of ureolytically-driven calcium carbonate precipitation. Geochem Trans 12:7–26

Methods for Decrease of Radionuclides Transfer from Soil to Agricultural Vegetation

A.V. Voronina, V.S. Semenishchev, M.O. Blinova, and P.Ju. Sanin

Contents

Abstract Characteristics of radioactive contamination of soils as a result of radiation accidents at Chernobyl nuclear power plant (USSR/Ukraine), Fukushima dai-ichi nuclear power plant (Japan), and Mayak PA (USSR/Russia) are considered. The evaluation of the efficiency methods for returning radioactively contaminated lands to farming use is given. It is shown that after a radiation accident, the major part of radionuclides is fixed in the upper 5–7 cm layer of a soil; further slow migration of a radionuclide to deeper layers of a soil occurs. Over 36 years after radiation accident, ^{137}Cs and ^{90}Sr radionuclides are located in a plowing horizon (0–25 cm); therefore, they are available for roots. The effectiveness of rehabilitation activities depends on physicochemical characteristics of a soil, radionuclides speciation in a soil solution, and a species of growing plant. The most efficient methods suggested for decrease of ^{137}Cs and ^{90}Sr radionuclides transfer from a soil

A.V. Voronina (✉) • V.S. Semenishchev • M.O. Blinova • P.J. Sanin
Radiochemistry and Applied Ecology Chair, Physical Technology Institute, Ural Federal University, Mira str., 19, Ekaterinburg, Russia
e-mail: av.voronina@mail.ru

C. Walther, D.K. Gupta (eds.), *Radionuclides in the Environment*,
DOI 10.1007/978-3-319-22171-7_11

to agricultural plants are transfer of the upper layer of radioactively contaminated soil to a depth of 80 cm and deeper (radionuclides transfer decreases up to a factor of 50) and addition of ferrocyanide sorbents based on natural aluminosilicates (up to a factor of 20). Addition of various ameliorators results in decrease of radionuclides transfer by up to 5 times independently of ameliorator type.

Keywords Radiation accident • Radioactively contaminated lands • Rehabilitation • Cesium and Strontium • Sorbents • Radionuclides in vegetation

1 Introduction

Radiation accidents happening at nuclear fuel cycle enterprises may lead to radioactive contamination of extended areas. In accordance with the International Nuclear Event Scale (INES), Chernobyl disaster (USSR/Ukraine), Fukushima dai-ichi accident (Japan), and the explosion of waste tank at Mayak PA (USSR/Russia) are examples of major accidents (INES 7) and serious accident (INES 6). Returning contaminated soils to farming use is one of the purposes of rehabilitation of radioactively contaminated lands. Activity of a soil and vertical distribution of a radionuclide, depending on the rate of its migration in soil, are important for choosing a method of returning radioactively contaminated lands to farming use. Natural systems consist of many components; therefore, a great number of factors exert influence on radionuclides distribution in these systems. Among these factors are particle-size distribution, mineral and elemental composition of soil, cation exchange capacity, organic compounds content, the hydrological regime (quantity of precipitation and groundwater flow rate), speciation of a radionuclide in a soil solution, the proportion between rates of a radionuclide uptake by soil and leaching from soil, and rate and mechanism of a radionuclide uptake by plants. Many of these processes are not finally studied yet.

The research activity in the field of rehabilitation of radioactively contaminated lands isn't constant; sometimes it decreases, but then it dramatically increases after another serious radiation accident. There is no common conventional approach to the solution of the rehabilitation because of a high complexity of this task. Therefore, new researches in development of rehabilitation technologies are necessary. In this chapter, the review of proven methods for decrease of cesium and strontium radionuclides transfer from radioactively contaminated soil to an agricultural vegetation as well as new researches in this field is presented.

2 Characteristics of Radioactive Contamination of Soils

2.1 *The Accident at Mayak PA, 1957*

In 1957, at the Mayak PA (USSR/Russia), a tank containing 250 m^3 of high-level liquid radioactive waste exploded because of a trouble in cooling system (Nikipelov et al. 1989). This accident is mostly known as "Kyshtym disaster" named after Kyshtym town located near the Mayak PA. As a result of this accident, 7.4×10^{16} Bq of radioactive fission products were emitted into the atmosphere (Sakharov 2006). The major part of radionuclides released (approximately 90 %) was located at the territory of the radiochemical plant; fine particles containing the rest 10 % of the radioactivity rose to a height of up to 1000 m and transferred to the North-East (Batorshin and Mokrov 2013). Radioactive materials deposition from the cloud occurred during the first 11 h after the explosion along the 300 km trace resulting in the radioactive contamination of an extended area with more than 2×10^4 km^2 (Volobuev et al. 2000). The radioactive contamination was conditioned by the following radionuclides: $^{144}Ce + {}^{144}Pr$ (66 %), $^{95}Zr + {}^{95}Nb$ (25 %), $^{90}Sr + {}^{90}Y$ (5.4 %), $^{106}Ru + {}^{106}Rh$ (3.7 %) и ^{137}Cs (0.35 %), and plutonium isotopes (0.0043 %) (Batorshin and Mokrov 2013). During the first year after the accident, ^{144}Ce and ^{144}Pr radionuclides were the major cause of radioactivity of soils and biota, whereas ^{90}Sr plays a leading role in current contamination of the environment at the East-Urals Radioactive Track (EURT).

The 700 km^2 area had a ^{90}Sr contamination level as high as 74–148 GBq km^{-2}. A number of researches deal with the modeling of radionuclides migration in soils (Arutyunyan et al. 1993; Kudryashov and Serebryakova 1993). Radionuclides slowly migrate to deeper layers of a soil during further years after the accident (Prokhorov 1981; Martyushov et al. 1996; Baturin 1997). The analysis of experimental data on radionuclides migration in various types of soils (sod-podzol, gray forest soil, and leached chernozem) has shown that migration rates of ^{90}Sr and ^{137}Cs radionuclides in these soils are as low as 0.23–0.17 cm per year and 0.11–0.09 cm per year, respectively. During the first 5 years after the accident, almost all radionuclides are located in the upper 0–5 cm layer of a soil; over further 30 years 50 % of deposited radionuclides migrate down out of this layer; however, 85–90 % of activity remains in the upper 0–20 cm layer of a soil, being available for roots (Baturin 1997). The rate of ^{90}Sr migration depends on the humidity of a soil. The highest migration rate is observed for peaty paludal soils, whereas the lowest rate is typical for gray forest soils and chernozem. For example, the migration rate in peaty paludal soils reaches 0.45–0.75 cm per year (Martyushov et al. 1996).

Speciation of ^{90}Sr in soils is studied under dynamic conditions at the territory of EURT. During the first several years after the accident, the contribution of exchangeable forms of ^{90}Sr to overall radiostrontium activity in a soil reached 70–90 % for all studied types of soils. The part of fixed forms of radiostrontium was different for various soils varying within the range of 3.0–5.0 % for chernozems, 5.0–8.1 % for gray forest soils, and 10.0–12.6 % for sod-podzol and paludal soils.

During further decades (10–36 years after the accident), a tendency to decrease of exchangeable forms of ^{90}Sr down to 40.8–49.9 % with respective increase of its fixed forms is exhibited in soils with increased humidity (Martyushov et al. 1996). It is also shown that ^{90}Sr may be redistributed from exchangeable forms to unexchangeable fixed forms. The aging of strontium radiocolloids in a soil with following increase of their size may be one of the causes of this process (Alexakhin and Naryshkin 1977). Mobility of ^{90}Sr in soils with normal moistening type (dark gray soils and chernozems) increases on a timescale of decades. Thus, the parts of exchangeable forms of ^{90}Sr in these soils are, respectively, 44.2 and 41.1 % over 10 years and also 56 and 48.8 % over 36 years after the accident (Martyushov et al. 1996).

The following activities against consequences of the accident were held at the radioactively contaminated area: limitation of a part of contaminated lands use in farming industry, deactivation of farming lands, reorganization of farming and forest industry, and monitoring of an agricultural production. 170 km^2 of the most contaminated area is still not suitable for living or for agricultural activity. This area is considered to be a radioecological wildlife area that is used for scientific researches.

2.2 *Chernobyl Disaster, 1986*

The destruction of fourth reactor at Chernobyl nuclear power plant (USSR/Ukraine) resulted in the emission of following activities of radionuclides into the atmosphere (PBq): radioisotopes of noble gases (Ar, Kr, Xe) = 24,000, $^{131}I = 2600$, $^{90}Sr = 38$, $^{106}Ru = 84$, $^{134}Cs = 120$, $^{137}Cs = 83$, $^{144}Ce = 14$, $^{241}Pu = 1.7$, $^{95}Zr + ^{95}Nb = 30$ (Sapozhnikov et al. 2006). 0.3–0.5 % of emitted radionuclides deposited immediately near the power plant, another 1.5–2 % deposited within 20 km from the power plant, and the rest was dispersed over the world (Sapozhnikov et al. 2006). The most contaminated area is 2.5×10^4 km^2 (Zubets et al. 2011).

The distribution of fallouts at radioactively contaminated areas was very anisotropic, looking like stains. The zone of 30 km around the Chernobyl NPP is the most contaminated area. Deposition of macroparticles released during the first 5 days was prevalent in this zone. The level of ^{137}Cs activity in the 30-km zone was more than 1500 kBq m^{-2} (Sapozhnikov et al. 2006). The main stains at the territory of former USSR had contamination levels higher than 560 kBq m^{-2}. For example, the Bryansk-Belorussian stain (200 km to the north-north-east from Chernobyl NPP) had the contamination level as high as 5000 kBq m^{-2} (Warner and Harrison 1993). Extended areas of Ukraine and Belarus had contamination levels higher than 40 kBq m^{-2}.

Concerning fallouts outside the former USSR, on the first day, the radioactive cloud at a height of 4–10 km has been divided. One part of this cloud was transferred to Scandinavia and Central Europe; another one spread to the east, to Japan, northern side of Pacific Ocean and North America. This resulted in wet fallouts (more than 100 kBq m^{-2}) in central Scandinavia (Warner and Harrison 1993). Among areas located relatively far from the accident area, the highest concentrations of radionuclides (more than 30 radioisotopes generated by Chernobyl reactor) in the air were found in Finland.

Data of the long-term radioecological monitoring (1987–2007) of soils and grass at the territory of Ukraine contaminated as a result of the Chernobyl disaster have shown that radionuclides transfer from a soil to a vegetation is a time function, depending also on a soil type and a plant species. The highest concentration ratios (F_V) of ^{137}Cs in plants are typical for peaty paludal soils; these values in the initial period after the accident were 223 m^2 kg^{-1} for a natural grass and 95 m^2 kg^{-1} for agricultural cereals. The lowest values are obtained for agricultural cereals growing on chernozems −3.3 m^2 kg^{-1} (Zubets et al. 2011). After the Chernobyl disaster, the average period of decrease of cesium activity in a grass at different soils varies as peaty paludal soils (by a factor of 2 for 2–4 years) > sod-podzol soil (by a factor of 10 for 4 years) > chernozem (by a factor of 10 for 12 years) (Zubets et al. 2011). These data show the high rate of cesium sorption by soils containing high organic compound concentrations as well as further slow decrease of cesium bioavailability (on a timescale of 12 years). Humic acids presenting in a soil solution play an important role in cesium distribution. Monovalent cations interact with humic acids due to ion exchange mechanism, forming simple salts with carboxylic groups (Stevenson 1994). Cesium uptake by humic acids occurs rapidly; the maximal sorption is reached in 60 min (Helal et al. 2007). However, sorption by humic acids is reversible; therefore, cesium can slowly migrate down, reaching mineral particles of a soil.

The affinity of sod-podzol soils for ^{137}Cs increases with the increase of humates concentration (Ivashkevich and Bondar 2008). Cesium uptake is conditioned by a non-hydrolyzable part of a soil. This part consists of humic compounds strongly bounded with a mineral part of a soil that cannot be dissolved in alkaline solutions as well as of insoluble organic compounds and even remains of vegetables and animals with anatomic structure. In contrast to cesium, the affinity of sod-podzol soils for ^{90}Sr decreases with the increase of humates concentration, and ^{90}Sr presents as exchangeable forms (Ivashkevich and Bondar 2008).

Over 25 years after the Chernobyl disaster, the major part of ^{137}Cs (90 %) and ^{90}Sr (75 %) presents in the plowing horizon (0–25 cm); these radionuclides are available for roots and may be included in the biological cycle (Bogdevich and Podolyak 2006).

2.3 Fukushima Dai-Ichi Nuclear Power Plant Accident, 2011

Radioisotopes of Kr, Xe, I, Cs, Sr, Ru, Ce, etc., were released into the atmosphere as a result of the accident at Fukushima Dai-ichi Nuclear Power Plant, Japan (Chino et al. 2011; Hirano et al. 2012; Kaneyasu et al. 2012; Yamaguchi et al. 2012). After the accident, radioactive trail was spread in the lower layer of the troposphere at a height of approximately 1000 m, resulting in radioactive contamination of more than 13,000 km^2 in eight prefectures of Japan, including water bodies and farming lands. Also, volatile radionuclides were distributed into the northern part of the atmosphere.

In accordance with the assessment of the Japan Atomic Energy Agency (JAEA) and the Nuclear Safety Commission of Japan, 1.1×10^{16} Bq of ^{137}Cs and ^{134}Cs were released into the atmosphere. Approximately 22 % of the emitted ^{137}Cs have been deposited on the land surface in regions located between 60 and 400 km from the Fukushima dai-ichi nuclear power plant (Katsumi 2012; Nakano and Yong 2013). The density of deposition of ^{134}Cs and ^{137}Cs in the most polluted regions of Japan varied from 10 to 1×10^4 kBq m^{-2} (Endo et al. 2012). The activity of soils was 0.1–380 kBq kg^{-1} (Endo et al. 2012), whereas that of sampled vegetation was 68–968 kBq kg^{-1} (Kato et al. 2012).

Recent studies have shown that approximately 80 % of deposited ^{137}Cs and ^{134}Cs were distributed in the upper 5 cm of soil during the initial period after the accident (Endo et al. 2012; Kato et al. 2012).

Thus, the analysis of radioactive contamination of soils as a result of the greatest three radiation accidents has shown that the long-term soil contamination is conditioned by fission products such as ^{137}Cs and, in a less degree, ^{90}Sr. During the first years after the accident, the major part of radionuclides is located in upper 5–7 cm of a soil. A slow vertical migration of radionuclides to a deeper layer of a soil occurs over decades after an accident; however, even over 36 years after contamination, the major part of ^{137}Cs and ^{90}Sr is located in a plowing horizon (0–25 cm), being available for plants.. For the majority of soil types, radionuclides bioavailability for plants decreases by a factor of 2–10 during 10 years. However, the bioavailability may increase in soils containing high level of organic compounds (chernozems, sod-podzol soils with high humus content, etc.). Thus, rehabilitation activities remain necessary for radioactively contaminated lands, since bioavailability of ^{137}Cs and ^{90}Sr will be high and radionuclides migration to a soil solution and groundwaters will be possible even over 30 years after the accident.

3 Methods for Decrease of Cesium and Strontium Radionuclides from Radioactively Contaminated Soil to Agricultural Vegetation

The principle of differential use should be on the basis of ideology of returning lands to farming use. The experience of rehabilitation activities at lands of EURT has shown that the differential use of radioactively contaminated lands allows decrease of radioactive contamination of agricultural products. In 1961, lands with density of contamination lower than 8 Ci km^{-2} were permitted for farming use (Teplyakov et al. 1997). There were no limitations of farming industry on the lands with ^{90}Sr activities in soils lower than 0.5 Ci km^{-2}. It was advised to grow forage for beef cattle on the lands with density of pollution at 0.2–2 Ci km^{-2} and to grow bread-corn as seeds on the lands with density of pollution at 2–8 Ci km^{-2}. After accumulation of information on the efficiency of various agrotechnical activities, the lands with density of contamination at up to 25 Ci km^{-2} were recommended for farming use in 1962–1964; those up to Ci km^{-2} were recommended for farming use in 1978 (Teplyakov et al. 1997).

Various rehabilitation methods are necessary, depending on radionuclide composition and density of pollution of a soil. The efficiency of rehabilitation activities should be evaluated experimentally.

Transfer of radionuclides from a soil to vegetation occurs through the soil water. Various agrotechnical methods were developed and tested in order to decrease radionuclides mobility in a soil and their accumulation in agricultural vegetation.

3.1 Removal or Plowing of Contaminated Soil Layer

The method of contaminated soil layer (approximately upper 5 cm) removal with further utilization may be used for rehabilitation of lands with dangerous density of contamination. This method was used for rehabilitation of industrial site of Mayak PA in immediate proximity to the tank explosion. Thus, 329,000 m^3 of upper layer of contaminated soil were removed and deposited in abandoned mines and ditches at Mayak PA (Batorshin and Mokrov 2013). The similar approach is suggested in the work (Nakano and Yong 2013) for rehabilitation of lands radioactively contaminated as a result of the Fukushima accident. When this approach is realized, it is necessary to take into the account factors such as characteristics of the contamination, density of pollution, the availability of a free area for deposition of removed soil, or necessity of development of a method for soil treatment. However, after the procedure of removal of contaminated layer will be done, we cannot ignore the residual cesium in the rest soil, since it may be enough to affect quality and safety of human health in this area. Further rehabilitation of such areas as well as of lower contaminated lands may be done using other methods that are more reasonable from ecological and economical points of view.

The method of transfer of the upper layer into sub-plowing horizons to a depth mainly unavailable for roots may be an effective way of rehabilitation of lands with high density of pollution (more than 2 Ci km^{-2}). For example, transfer of the contaminated layer (5–10 cm) into sub-plowing horizons to a depth of 80–100 cm without destruction of the soil layer and decrease of soil fertility was used as a method for decrease of radionuclides transfer to agricultural vegetation at the territory of EURT (Teplyakov et al. 1997). Since contact of the plowed contaminated layer with surface and groundwaters remains possible resulting in horizontal and vertical migration, transport of radionuclides to rivers, ocean, and sources of drinking water is not excluded after realizing of this method. Deep plowing to

35–40 cm was used on the lands radioactively contaminated as a result of the Chernobyl disaster (Zubets et al. 2011). However, deep plowing to 35–40 cm leads to disruption of a soil structure and decrease of its fertility; the method of transfer of the upper layer (5 cm) to a depth of 100 cm has none of these shortcomings. Described method allows decrease of radiocesium transfer to agricultural products by a factor of 8–12 on mineral soils and of 10–16 on organic soils; for strontium, this value is only 2.0–3.0 (Zubets et al. 2011).

3.2 Use of Mineral Fertilizers

Mineral fertilizers may be used for decrease of transfer of both radiocesium and radiostrontium to agricultural products (Sanzharova et al. 2005; Panov et al. 2009; Zubets et al. 2011).

Concentration of unbounded potassium in a soil is an important factor that affects ^{137}Cs uptake by roots. Potassium is an important element for plant nutrition; it is included in the mineral part of soils. Cesium and sodium possess similar chemical characteristics; therefore, cesium is consumed by plants due to the same mechanisms as potassium. Both elements may be transferred together (Hampton et al. 2005). Increase of mobile potassium in a soil leads to decrease of cesium accumulation in vegetation. This regularity is not linear, depending on both cesium/potassium ratio in a soil and a plant's necessity in potassium (Ehlken and Kirchner 2002; Staunton et al. 2003). A method of potassium fertilizers addition for decrease of ^{137}Cs transfer to agricultural products is based on antagonism of potassium and cesium. Biological characteristics of a plant significantly affect ^{137}Cs accumulation in a phytomass. As it is established by a number of scientists in lab conditions, potassium is mostly accumulated in herbage in contrast to cesium being accumulated in roots (Shov and Bell 1989; Ehlken and Kirchner 2002; Staunton et al. 2003). Different cesium distribution between herbage and roots for various types of plants indicates complex mechanisms of cesium translocation and transfer inside a plant. Addition of potassium fertilizers allows decreasing ^{137}Cs accumulation in plants by a factor of 1.5–2 (Sanzharova et al. 2005). Also, potassium fertilizers usually do not immediately affect ^{90}Sr uptake by plants. However, high potassium concentration in a soil solution may suppress Ca^{2+} and Mg^{2+} sorption by a soil resulting in decrease of ^{90}Sr uptake by plans.

Use of elevated doses of nitrogen fertilizers is not recommended on radioactively contaminated lands. Addition of NH_4^+ may result in increase of ^{137}Cs accumulation in plants. Ionic radius of NH_4^+ is very similar to that of Cs^+; therefore, ammonium affects cesium sorption by the mineral part of a soil. Effective diameters of hydrated alkaline ions are $Cs^+ = 0.25$ nm, $NH_4^+ = 0.25$ nm, $K^+ = 0.3$ nm, and $Na^+ = (0.4 \div 0.45)$ nm (Zolotov 1999). Thus, NH_4^+ ion competes with Cs^+ for sorption sites of clayey minerals suppressing cesium sorption by a soil.

Elevated doses of nitrogen fertilizers inhibit the positive effect of potassium fertilizers, when both types of fertilizers are used together (Moiseev et al. 1988;

Sanzharova et al. 1998). The effect depends on the dose of nitrogen fertilizers, soil type, plant species, and some other factors (Belli et al. 1995). Combined addition of both nitrogen and potassium fertilizers results in decrease of the negative nitrogen effect and allows obtaining radiologically pure agricultural products, when potassium/nitrogen ratio is 1.5:1. This approach results in decrease of radiocesium accumulation in plants by a factor of up to 2.8; however, it is advised to use this method only on the lands with pollution density higher than 25 Ci km^{-2} in case of growing species with high cesium uptake (Belous et al. 2009).

The influence of phosphate fertilizers on ^{137}Cs redistribution in "soil–groundwater–plant" systems is the least studied. Mechanisms of phosphate effect are still not finally studied. According to experimental data (Kuznetsov et al. 2001), phosphate fertilizers may result in either increase of cesium accumulation in farming products by a factor of 1.5–3.0, or decrease it by a factor of 2.0–2.5 depending on the soil type. Combined addition of both phosphate and potassium fertilizers results in decrease of ^{137}Cs transfer to plants by a factor of 2.4 (Belous et al. 2009).

3.3 Use of Organic Fertilizers

The influence of organic fertilizers on radionuclides transfer to vegetation is studied in following works (Prister et al. 1991; Sanzharova et al. 2005; Belous et al. 2009; Zubets et al. 2011). Peat, dung, and sapropels were used as organic fertilizers. Increase of humus concentration in a soil due to organic fertilizers addition has an ambiguous influence on radionuclides accumulation, different for various soils. Organic compounds may either stimulate radionuclides mobility in soils or suppress it.

Cs^+ ions are efficiently adsorbed by the mineral part of a soil and form weakly stable complexes with humates. Thus, increase of radiocesium accumulation by plants should be expected, when organic fertilizers are added to soils rich in the mineral fraction. Rate of cesium uptake by humic acids is usually higher than this by clayey minerals; therefore, cesium mostly interacts with humates, which are available for plants. Also, humates can envelop mineral particles of a soil, blocking their sorption sites. Humic acids are able to provide desorption of radionuclides from minerals (Polyakov et al. 2015). In addition, weakly decomposed fractions of a peat may acidify groundwater resulting in suppression of sorption ability of clayey minerals.

Addition of organic fertilizers into light soils results in decrease of ^{137}Cs accumulation in plants by a factor of 1.5–3.0 (Alexakhin et al. 1992). Humates bound with strontium more effectively than cesium. A positive effect of organic fertilizers addition is observed for soils with low organic content. Factors of decrease of ^{90}Sr transfer to vegetation varied from 4.6 to 5.6 depending on plant species (Yudintseva and Gulyakin 1968).

3.4 Liming

$CaCO_3$, dolomitic lime, calc-tuff, and peat tuff are used for soils liming. Soils liming results in the change of soil pH and increase of calcium concentration in groundwater.

Radioactive isotopes presenting in a soil are transferred to roots of plants due to the same mechanisms as stable isotopes. Plants are not able to discern chemically similar elements. The results of experiments on plants growing on simple inorganic solutions containing calcium and strontium have shown that there was no discrimination effect. Calcium is a chemical analogue of strontium; therefore, it affects strontium (and ^{90}Sr too) uptake by plants (Eizenbad 1967). Sr^{2+} is consumed by a plant through the same transport systems as Ca^{2+}. An analogue element with higher concentration in a soil solution will be accumulated in plants more intensively. That's why increase of Ca^{2+} concentration in a soil solution results in decrease of the transfer of ^{90}Sr to vegetation (Sanzharova et al. 2005). Formation of sparingly soluble compounds of strontium at elevated pH is another factor affecting ^{90}Sr accumulation by plants (Alexakhin et al. 1992).

Liming leads to suppression of K^+ ions mobility (Grinchenko et al. 1985). This effect is conditioned by increase of pH value resulting in increase of cation exchange capacity of a soil. Additional sorption sites of clayey minerals in a soil are filled by calcium. Decrease of potassium concentration leads to less competition of potassium and cesium for sorption sites. Cesium is adsorbed by frayed edge sites (FES), as opposed to calcium that is adsorbed by regular exchange sites (RES). The efficiency and strength of cesium sorption by a soil become higher. Uptake of ^{137}Cs by plants also depends on concentration of Ca^{2+} and Mg^{2+} bivalent cations in a soil solution (Smolders et al. 1997). Liming decreases the transfer of cesium radionuclides to vegetation by a factor of 1.5–3.0 and transfer of strontium radionuclides by a factor of 1.5–2.6 (Alexakhin et al. 1992; Ageets 2001; Zubets et al. 2011).

3.5 Phytoremediation

Such methods for rehabilitation of radioactively territories, as radionuclides elimination via contaminated turf removal or combined uptake suppression with turf removal, are based on the affinity of some plants to radionuclides. Realizing of the second method begins from a temporal cesium and strontium fixation due to addition of derivatives of polyacrylic or carboxymethylcellulose. Then clover or a grass forming the turf is sown. The turf uptakes the major part of radionuclides; at the same time, it may be easily removed using simple farm implements. Low degrees of deactivation because of a changeable grass composition on the turf as well as limitation of its use on the lands with high density of pollution are the main disadvantages of this method.

Use species of plants, which are able to accumulate ^{137}Cs, in phytoremediation techniques is mentioned in a number of publications (Lasat et al. 1998; Dushenkov et al. 1999; Kang et al. 2012). For example, a method for soils deactivation described by Vozzhenikov et al. (1997) consists of plants growing on a radioactively contaminated soil, resulting in ^{137}Cs and ^{90}Sr uptake by a plant through root system, and further removal and utilization of the grass. Suggested measures on the grass growing and utilization may be assumed repeatedly, including several times within the same vegetation season, until radioactive contamination becomes allowable according to normative documents. After phytoremediation, the soil should be suitable for farming. Sunflower, rape, calendula, alfalfa, and clover are recommended as plants for Cs^{137} accumulation; for ^{90}Sr, recommended plants are alfalfa, clover, pea, and fenugreek. In case of phytoremediation of a soil containing both ^{137}Cs and ^{90}Sr, ryegrass, alfalfa, and clover are advised (Vozzhenikov et al. 1997).

3.6 Addition of Sorbents

Decrease of radiocesium and radiostrontium transfer to a vegetation can be obtained as a result of addition of sorption-active materials (such as zeolites and clayey minerals) (Ovchinnikov and Bezdenezhnykh 1996; Campbell and Davies 1997; Bondar 1998; Katsnelson et al. 1983; Misaelides 2011), or composite sorbents (Budarkov et al. 1994) to a soil. The effectiveness of addition of clayey minerals is comparable to that of other agromeliorators (mineral and organic fertilizers, chalky materials) (Sanzharova et al. 2005; Zubets et al. 2011); this results in a decrease of radionuclide transfer to vegetation by a factor of 1.5–3.0, but only on light soils; a decrease has not been observed on other types of soil including organics (Sanzharova et al. 2005; Zubets et al. 2011).

Competitive uptake of a radionuclide from groundwater by a soil, a sorbent, and a plant occurs, when sorbents are used for soil rehabilitation. Humidity and grain composition of the soil, quantity and chemical composition of both organic and mineral parts of the soil, concentration of analogue ions in the groundwater, and physicochemical characteristics of the sorbent and the plant species affect the radionuclide distribution. Radionuclides accumulation in plants will depend on specificity and selectivity of the sorbent, its kinetic characteristics, and reversibility of the radionuclide sorption. The sorbent should possess optimal combination of characteristics in order to be effective for rehabilitation. The low effectiveness of natural aluminosilicates use for rehabilitation of radioactively contaminated lands may be conditioned by sorbents' relatively low selectivity as well as reversibility of radionuclides sorption (Voronina et al. 2013).

As it was shown by Petrova et al. (2008), strontium was almost completely eluted from a clayey mineral (montmorillonite). Radionuclide leaching from natural minerals under the conditions of their use for soil rehabilitation depends on chemical composition of sediments, soil solutions, and groundwater (Voronina et al. 2015). Addition of sorbents may become a prospective method for rehabilitation of radioactively contaminated lands; however, it requires the developing of new eco-friendly sorption materials with high selectivity for radionuclides, exchange capacity, stability, and affinity to environmental systems. Study of regularities and mechanisms of radionuclides competitive uptake in multicomponent natural systems in the presence of sorbents is also necessary for developing this method.

Ferrocyanide sorbents based on natural aluminosilicates are suggested by Voronina et al. (2013, 2015) to use for lands rehabilitation. Comparative study of selectivity of natural aluminosilicates and ferrocyanide sorbents based on them are described in the work (Voronina et al. 2013); the experimental comparison of their static exchange capacity and robustness against leaching of radionuclides is presented in the work (Voronina et al. 2015). The results obtained have sown that surface modification of aluminosilicates by ferrocyanides increases the selectivity of synthesized sorbents to cesium by a factor of 100–1000. High sorption capacity (allows for effective cesium separation for solution rich in analogue ions) and irreversibility of cesium sorption is the main advantages of modified aluminosilicates, being important characteristics for soil rehabilitation. At the same time, the surface modification of natural aluminosilicates does not impair their sorption characteristics for strontium: strontium distribution coefficients remain approximately the same, whereas exchange capacity for strontium becomes higher.

Some practical aspects of use of natural and modified aluminosilicates for rehabilitation of lands contaminated by radiocesium, such as working pH ranges and cesium transfer decrease factors for various soil/sorbent ratios, are presented below in this chapter.

3.6.1 Materials and Methods

Glauconite from the Karinskoye deposit (Chelyabinsk region, Russia) and clinoptilolite from the Shivertooyskoe deposit (Chita region, Russia) as well as mixed nickel–potassium ferrocyanides based on them were used in experiments. The degree of cesium sorption related to pH was studied for all sorbents, since pH values of groundwater may vary significantly for different types of soils. A series of solutions with volume $V = 50$ mL were prepared with a stable cesium concentration of 0.1 mg L^{-1} and ^{137}Cs activity of 6×10^4 Bq L^{-1}. The pH values of the solutions were adjusted by the addition of HCl or NaOH solutions, and then 20 mg of a sorbent was added to the solution. After 7 days of contact, the final solution was sampled and measured on a semiconductor α-β counter system (UMF-2000, Dosa, Russia). The degree of cesium sorption s (dimensionless value) was calculated in accordance with Eq. (1):

Table 1 Chemical composition of Knop mixture

Salt	Chemical compound	Concentration in g L^{-1}
Calcium nitrate	$Ca(NO_3)_2$	1.0
Potassium hydrophosphate	KH_2PO_4	0.25
Potassium chloride	KCl	0.125
Magnesium sulfate	$MgSO_4$	0.25

$$s = \frac{I_{\text{in}} - I_{\text{end}}}{I_{\text{in}} - I_{\text{b}}} \tag{1}$$

where I_{in}, I_{end}—initial and final count rate of the solution, cpm.

I_{b}—background count rate, cpm.

The distribution coefficients K_{d} (L kg^{-1}) were calculated in accordance with Eq. (2):

$$K_{\text{d}} = \frac{s}{1-s} \cdot \frac{V}{m} \tag{2}$$

where s is degree of sorption, dimensionless;

V is volume of the solution, L;

m is weight of the sorbent, kg^{-1}.

The effect of sorbents addition on ^{137}Cs transfer from a radioactively contaminated solution (on hydroponics system) and soils to an agricultural vegetation was studied in order to test the developed sorbents under the conditions similar to those of soil rehabilitation. Feed solutions for hydroponics contained the Knop mixture (see Table 1) and 10^4 Bq L^{-1} of ^{137}Cs.

Sorbents (natural or modified aluminosilicates) were added to the feed solution; then oats seeds were sowed. Oats vegetation was harvested during the tillering period in 21 days after seeds sowing. Vegetation samples were dried at 100 °C; cesium activity was measured by gamma spectrometry using scintillation NaI(Tl) - gamma-spectrometer Atomtech AT-1315 (Belarus). Oats vegetation grown on solutions without sorbents under the same conditions was used as control samples. Dimensionless values of concentration ratio (F_{V}) of cesium in plants and cesium transfer decrease factor ($K_{\text{tr. dec}}$) from soil to plants in the presence of sorbents were calculated according to Eqs. (3 and 4) using experimental data obtained:

$$F_{\text{V}} = \frac{A_{\text{v}}}{A_{\text{s}}} \tag{3}$$

where A_{v} is the activity concentration of radiocesium in the vegetation, Bq g^{-1},

A_{s} is the activity concentration of radiocesium in the soil, Bq g^{-1}.

$$K_{\text{tr.dec}} = \frac{A_{\text{control}}}{A_{\text{v}}} \tag{4}$$

where $A_{control}$ was activity of radiocesium in plants from control group of plants, grown in soil, contaminated by ^{137}Cs, without addition of sorbents, Bq g^{-1}.

In the experiments on oats growing on soils contaminated by radiocesium, the soil type similar to usual Japanese soils was chosen. Approximately 70 % of land in Japan consists of andosols (Takeda et al. 2013). These soils contain high quantities of crystalline fragments of volcanic rocks and amorphous aluminosilicates (collyrites) with high humus content. The basic physicochemical characteristics of the soil sample were determined; these were cation exchange capacity, organic carbon content, pH of salty and water extracts, and concentrations of K, Fe, and Ca. The cation exchange capacity (CEC) of studied soils was determined by a modified Bobko–Askinazi–Aleshin method, developed in the Central Institute of Agrochemical Service of Farming Industry (Russian State Standard 17.4.4.01.84 1984). Organic carbon content was determined by the wet ashing method (Russian State Standard 262113-91 1991); the pH of salty and distilled water leachates was determined at a soil/solution ratio of 1/2.5 (Mineeva 1989). Elemental composition of soils was determined using X-ray fluorescent spectrometer ARL Quant'X (Termo Fisher scientific, Austria).

The activity of ^{137}Cs in contaminated soil was 30 kBq kg^{-1} that corresponds to the contamination level of soils in some regions of Japan as a result of the Fukushima accident (Endo et al. 2012). In the experiment, 100 g of soil in flowerpots was contaminated using 20 mL of tap water spiked with ^{137}Cs. Contaminated soil was kept for 7 days in order to allow natural processes of radionuclide redistribution in soil to occur for simulation of contamination conditions in the immediate period after the accident. Then sorbents were added to the soil (excluding the control soil sample), after these oat seeds were sowed in the soil. The soil was regularly watered until the end of the experiment. Biomass harvesting, samples pretreatment, and measurements were done by the same ways as in hydroponics experiments.

3.6.2 Results and Discussion

The pH dependences of cesium distribution coefficients by natural clinoptilolite and glauconite and mixed nickel–potassium ferrocyanides based on them are presented in Fig. 1.

The results have shown that cesium sorption by natural clinoptilolite and glauconite strongly depends on the pH of the solution. In acidic media at pH < 5, H^+ ions compete with cesium for sorption sites; therefore, cesium sorption was suppressed at lower pH. In the pH range of 5–10, degree of cesium sorption remains stable for both sorbents reaching (0.70 ± 0.08) for natural clinoptilolite and (0.80 ± 0.04) for natural glauconite. Calculated cesium distribution coefficients (K_d) reach $(7.5 \pm 1.5) \times 10^3$ L kg^{-1} for clinoptilolite and $(8.8 \pm 1.3) \times 10^3$ L kg^{-1} for glauconite.

In the case of modified clinoptilolite and glauconite, cesium sorption remains constant over the pH range 2–8. The degrees of cesium sorption were (0.98 ± 0.08)

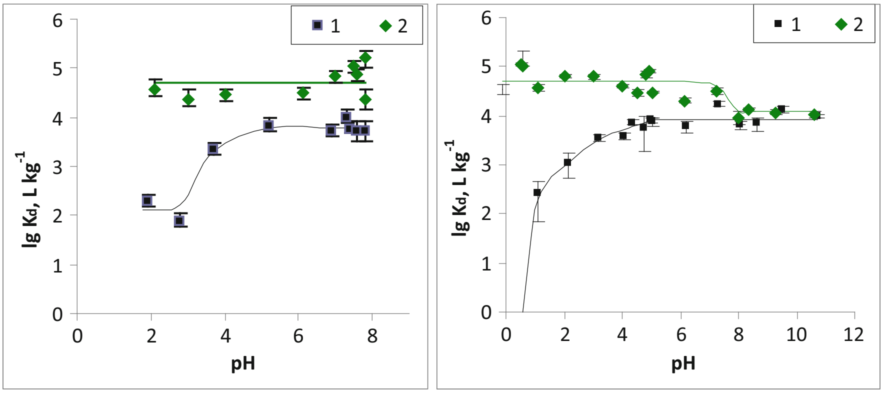

Fig. 1 Dependences of cesium distribution coefficients on pH: (**a**) natural clinoptilolite (1) and mixed nickel–potassium ferrocyanide based on clinoptilolite (2); (**b**) natural glauconite (1) and mixed nickel–potassium ferrocyanide based on glauconite (2)

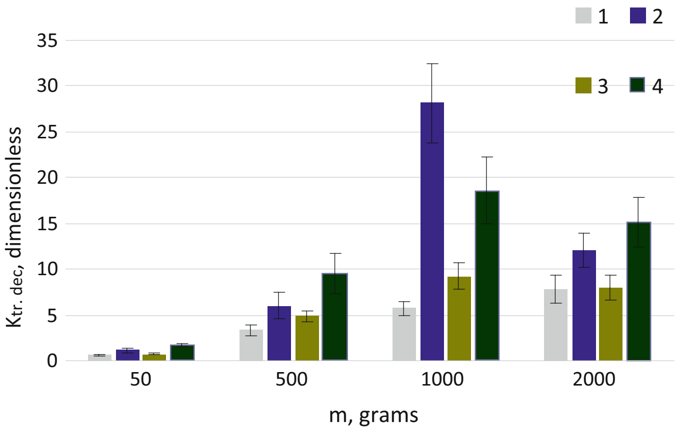

Fig. 2 The dependences of cesium transfer decrease factors on weights of sorbents for the oats grown on a hydroponics system: (1) natural clinoptilolite, (2) mixed nickel–potassium ferrocyanide based on clinoptilolite, (3) natural glauconite, (4) mixed nickel–potassium ferrocyanide based on glauconite

and (0.97 ± 0.05), respectively. Calculated cesium K_d was $(1.0 \pm 0.3) \times 10^5$ L kg^{-1} for both mixed nickel–potassium ferrocyanides. Thus, surface modification of aluminosilicates by ferrocyanides gives both increased cesium distribution coefficients and expansion of the effective pH range. Therefore, it could be expected that these sorbents should effectively separate cesium from a wide spectrum of soil types.

Cesium transfer decrease factors for the oats (*Avéna satíva*) vegetation from hydroponics solutions with various weights of sorbents are shown in Fig. 2.

Table 2 Physicochemical characteristics of the soil sample (for dry weight)

Soil type	Organic compounds content, g kg^{-1} of the soil	pH (H_2O)	pH (KCl)	CEC, cmol kg^{-1}	Metal concentration, g kg^{-1} of the soil		
					Ca	Fe	K
Clay	59.9	5.2	4.9	54.5	26.2 ± 0.2	40.5 ± 0.2	10.9 ± 0.2

Fig. 3 Photo of oats (*Avéna satíva*) vegetation during the tillering period

According to data mentioned above, the effectiveness of natural aluminosilicates is quite low. Cesium transfer decrease factors do not exceed 8, being slightly higher for the natural glauconite. The maximal ^{137}Cs transfer decrease factor obtained for 1 % wt. of mixed nickel–potassium ferrocyanide based on glauconite was 28 ± 4. Addition of more than 1 % wt of sorbents results in the increase of concentration ratio of ^{137}Cs in the oats.

A series of experiments on the oats growing on a soil was also executed in order to confirm the adequacy of the results on hydroponics experiments. The main physicochemical characteristics of the soil sample are given in Table 2.

The soil has high values of cation exchange capacity (54.5 cmol kg^{-1}) and concentration of organic compounds (59.9 g kg^{-1} of the soil). Also, it contains a high quantity of cations that can be leached to a soil solution, interfering cesium uptake. The pH value of the aqueous extract from the soil is very similar to that for the hydroponics feed solution.

Photo of oats (*Avéna satíva*) vegetation during the tillering period is presented in Fig. 3. Values of concentration ratio (F_V) of cesium in the oats vegetation and cesium transfer decrease factor ($K_{tr.\ dec}$) from soil to the oats in the presence of sorbents are given in Table 3.

The results obtained have shown that high values of cesium concentration ratio in control samples of oats biomass are typical for this type of soil. These results agree well with literature data on organic compounds of soils effect on ^{137}Cs

Table 3 Characteristics of ^{137}Cs accumulation in oats biomass in the presence of natural aluminosilicates and modified sorbents based on them

Sorbent sample added to a soil	% wt. of a sorbent added to the soil	F_V	$K_{tr.\ dec}$
Control	0	0.26	–
Natural glauconite	0.1	0.35	0.87
Mixed nickel–potassium ferrocyanide based on glauconite	0.1	0.15	1.98
Natural clinoptilolite	0.1	0.25	1.05
Mixed nickel–potassium ferrocyanide based on clinoptilolite	0.1	0.16	1.65
Control	0	0.53	–
Natural glauconite	3	0.22	2.39
Mixed nickel–potassium ferrocyanide based on glauconite	3	0.03	21.24

mobility. The presence of humates in the soil results in increased mobility of ^{137}Cs in the soil; this promotes an increased cesium accumulation in plants: the values of cesium concentration ratio in control samples vary from 0.26 to 0.53. In a soil rich in organics, cesium forms complexes with carboxylic groups of a humic acid (Helal et al. 2007). However, stability constants of these humate complexes are low because of low charge and a large ionic radius of Cs^+. The effect of organic compounds on increased mobility of ^{137}Cs in the soil is mentioned in a number of publications (Odintsov et al. 2004, 2005; Nakamaru et al. 2007; Helal et al. 2007). An extended variations range of the values of cesium concentration ratio in control samples is conditioned by the fact that these experiments were done under the natural conditions of growing other than climate cell. Temperature of the air, soil humidity, and illuminance seasonably varied during the experiments, affecting the regularities of radiocesium accumulation in the oats. Therefore, control samples were grown in each experiment in order to get an adequate evaluation of sorbents' effects on cesium transfer decrease factors.

It's obvious that the effectiveness of natural aluminosilicates (glauconite and clinoptilolite) use for soil rehabilitation with the aim of their returning to farming industry is rather lower than the effectiveness of modified ferrocyanide sorbents. Radiocesium transfer decrease factors are comparable within the error range for both natural glauconite and clinoptilolite. The maximal cesium transfer decrease factor was obtained for the case of addition of 3 % wt. of the mixed nickel–potassium ferrocyanide based on glauconite to the soil; this value was 21.6.

Different cation exchange capacities and selectivity for cations sorption are typical for various types of natural aluminosilicates. As it is known from the literature, clinoptilolite is a tectosilicate, whereas glauconite is a schistose silicate. The cation exchange capacity of aluminosilicates was provided by selective sorption sites, located in tetrahedral spaces of the aluminosilicate crystal lattice (exchanging ions are Na^+, K^+, Ca^{2+}, Mg^{2+}). These selective sorption sites are able to uptake only cations with a diameter similar to that of the tetrahedral space size;

hydrated cesium cation has the most appropriate ionic diameter. Other groups of selective sorption sites are wedge-shaped lateral locations on lateral cleavages of microcrystals (Popov et al. 2011). In addition, sorption sites on basal faces of schistose silicates show relatively high affinity to cesium ions. This affinity is connected with a steric effect: commensurability of cesium ionic radius and size of interstices (bitrigonal cells) in the interlayer space of the mineral (Kobets et al. 2014). Nonselective sorption sites are locations on lateral faces of tetrahedrons such as hydroxyl groups, whose dissociation is increased with increasing pH. Approximately 1–3 % of overall cation exchange capacity in schistose silicates is provided by selective sorption sites (Kornilovich et al. 2000); 30–50 % is provided by nonselective sites on lateral faces (Kobets et al. 2014). Therefore, competitive sorption of Na^+, K^+, NH_4^+ containing in natural waters and soil solutions greatly affects cesium sorption by natural aluminosilicates. The cation exchange capacity of clinoptilolite is higher than that of glauconite (Voronina et al. 2015); the capacity of selective sites in clinoptilolite is also higher than in schistose silicate (illite) (Popov et al. 2011). Therefore, clinoptilolite is a more selective sorbent for cesium with higher affinity than glauconite in various aqueous solutions (Voronina et al. 2015). However, there was no difference in the effectiveness of glauconite and clinoptilolite use for soil rehabilitation. This effect is probably conditioned by a relatively high concentration of analogue ions in the soil solution, being outside the scope of selectivity of sorbents, as well as by humates influence on sorption characteristics of natural aluminosilicates.

The results of experiments have also shown that cesium transfer decrease factors obtained for 0.05–0.1 % wt. of sorbents were comparable within the error range for both hydroponics and soil studies. The maximal values of cesium transfer decrease factors were comparable for both media too, but these values were obtained for different sorbents concentrations: 1 and 3 % wt. in cases of hydroponics and the soil, respectively. A higher sorbent concentration in the experiment resulted in an increased error of a value of cesium transfer decrease factor.

Mixtures for hydroponics are traditionally used for study processes of radionuclides accumulation in plants. This method is suitable for the determination of common tendencies of a radionuclide accumulation and mechanisms of a radionuclide transfer to a plant; however, it may give misrepresented quantitative characteristics of these processes. In hydroponics feed solution, the total ^{137}Cs presents in a form available for both sorbents and plants. An influence of organic compounds and soil sorption characteristics on these processes is absent under the described conditions. Therefore, overestimated values of cesium transfer decrease factors should be obtained, when the Knop mixture is used in hydroponics experiments; however, common tendencies are correct. Humates presenting in a soil affect radiocesium speciation in a soil solution, its bioavailability, and sorption characteristics of sorbents. In the case of soils with a high content of organic compounds, this regularity will become apparent. Thus, either experiments on plants growing on a radioactively contaminated soil or humates addition to the feed solution for hydroponics is necessary in order to develop practical recommendations on the quantity of sorbent to add to a soil as well as to evaluate cesium transfer decrease

Table 4 The effectiveness of decrease of radionuclides transfer to agricultural plants

Method	A radionuclide transfer decrease factor	
	^{137}Cs	^{90}Sr
Removal of the contaminated layer	No data	No data
Deep plowing 35–40 cm	8–12 (soils with low organics) 10–16 (soils with high organics)	2.0–3.0 (for soils with low organics only)
Transfer of the upper layer into sub-plowing horizons to a depth of:		
20–45 cm	No data	1.5–3.0
80 cm	No data	Up to 50.0
Addition of mineral fertilizers:		
Potassium	1.2–5.0	No influence
Potassium-phosphate	1.5–2.4	2.0–4.0
Addition of organic fertilizers	1.5–3.0 (for light soils only) increase of accumulation is possible as a result of peat addition	4.6–5.6 (for soils with low humus content only)
Liming	1.5–4.0	1.5–4.0
Phytoremediation	Only concentration ratios for vegetation are shown	Only concentration ratios for vegetation are shown
Addition of natural sorption materials (zeolites, clayey minerals)	1.5–3.0 (for light soils only)	1.5–1.8
Addition of ferrocyanide sorbents based on natural aluminosilicates	2.0–21.6	No data

factors expected as a result of this rehabilitation method. Use of the Knop mixture with humates addition allows developing specific recommendations for soils with various concentrations of organic compounds. The chosen soil type and conditions of experiments on the oats growing on radioactively contaminated soil as well as ^{137}Cs transfer decrease factors obtained may be considered to be an adequate and reliable evaluation of an effect of rehabilitation of soils contaminated as a result of the Fukushima accident.

The comparison of effectiveness of various methods for the decrease of cesium and strontium radionuclides transfer to agricultural plants is given in Table 4 in order to summarize the material of this chapter. Minimal and maximal values of a radionuclide transfer decrease factors are given among literature data on various soil types. The effect of soil type and plant species on the effectiveness of rehabilitation activities should be taken into account, when a rehabilitation method is used.

4 Conclusions

Decrease of ^{137}Cs and ^{90}Sr mobility and transfer to agricultural vegetation is the most important purpose of rehabilitation of radioactively contaminated lands. Among methods described in the literature for decrease of ^{137}Cs and ^{90}Sr from soils to agricultural plants, the most efficient ones are transfer of the contaminated layer (5–10 cm) into sub-plowing horizons to a depth of 80–100 cm (allows decreasing radionuclides transfer by a factor of up to 50) and addition of ferrocyanide sorbents based on natural aluminosilicates (up to 20). Addition of various ameliorators (mineral and organic fertilizer, clayey minerals, and lime materials) results in decrease of radionuclides transfer by a factor of up to 5 independently of ameliorator type. It is also necessary to take into account that the efficiency of rehabilitation activities is affected by physicochemical characteristics of a soil, radionuclides speciation and partitioning in a soil solution, and type of plants to grow.

The method of contaminated soil layer removal, suggested in a number of publications, is quite labor-intensive and difficult. Therefore, in practice this method was used only at very limited areas for decontamination of local stains with very high contamination levels, mostly at zones within the industrial site of an enterprise, where a radiation accident has occurred.

The results of experimental use of ferrocyanide sorbents based on glauconite and clinoptilolite presented in this chapter may be considered as reliable evaluation of the possibility of rehabilitation lands contaminated as a result of the Fukushima Dai-ichi NPP accident in Japan.

References

Ageets VY (2001) System of radioecological countermeasures in the agrosphere of Belarus, vol 4–6. Institute of Radiology Republican Research and Development Unitary Enterprise, Gomel, p 157–189

Alexakhin RM, Naryshkin MA (1977) Migration of radionuclides in forest ecosystems. Nauka, Moscow

Alexakhin RM, Vasilev AV, Dikarev VG, Egorova VA (1992) Agricultural radioecology. Ecologia, Moscow

Arutyunyan RV, Bol'shov LA, Zenich TS, Reshetin VP (1993) Mathematical simulation of vertical migration of ^{137}Cs and ^{134}Cs in soil. Atom Energy 74:206–211

Batorshin GS, Mokrov YG (2013) The experience of elimination of consequences of the accident at Mayak PA in 1957. Rad Saf Quest 1:13–20

Baturin VA (1997) Vertical migration of radionuclides in the soil of the East-Ural track and its effect on the intensity of the outgoing radiation. Atom Energy 82:44–48

Belli M, Sansone U, Ardiani R, Feoli E, Scimone M, Menegon S, Parente G (1995) The effect of fertilizer application on ^{137} Cs up take by different plant specials and vegetation types. J Environ Radioact 27:75–89

Belous NM, Malyavko GP, Shapovalov VF, Talyzin VV, Prudnikov PV (2009) The influence of long-term use of fertilizers and agrotechnical actions on ^{137} Cs accumulation in a harvest of agricultural plants during a distant period after the Chernobyl accident. Prob Agrochem Ecol 31:25–31

Bogdevich IM, Podolyak AG (2006) Accumulation of ^{137}Cs and ^{90}Sr in a herbage of basic types of grasslands in Belarusian Polesye as a dependence on parameters of vertical migration and radionuclides speciation in soils. Pedol Agrochem 1:233–246

Bondar PF (1998) About the assessment of efficiency of sorbents as means of radionuclides retention in soils. Radiat Biol Radioecol 2:267–272

Budarkov VA, Mayakov EA, Torubarova AA, Kalinin NF, Gelis VM, Milyutin VV, Penzin RA (1994) Method of caesium radionuclides transfer decreasing from soil to vegetation. Russian Federation Patent № 2013913 from 15.06.1994

Campbell LS, Davies BE (1997) Experimental investigation of plant uptake of caesium from soils amended with clinoptilolite and calcium carbonate. Plant Soil 189:65–74

Chino M, Nakayama H, Nagai H, Terada H, Katata G, Yamazawa H (2011) Preliminary estimation of release amounts of ^{131}I and ^{137}Cs accidentally discharged from the Fukushima Dai-ichi nuclear power plant into the atmosphere. J Nucl Sci Technol 48:1129–1134

Dushenkov S, Mikheev A, Prokhnevsky A, Ruchko M, Sorochisky B (1999) Phytoremediation of radiocaesium contaminated soil in the vicinity of Chernobyl, Ukraine. Environ Sci Technol 33:469–475

Ehlken S, Kirchner G (2002) Environmental processes affecting plant root uptake of radioactive trace elements and variability of transfer factor data: a review. J Environ Radioact 58:97–112

Eizenbad M (1967) Radioactivity of the environment. Atomizdat, Moscow

Endo S, Kimura S, Takatsuji T, Nanasawa K, Imanaka T, Shizuma K (2012) Measurement of soil contamination by radionuclides due to the Fukushima Dai-ichi nuclear power plant accident and associated estimated cumulative external dose estimation. J Environ Radioact 111:18–27

Grinchenko TA, Daragin YV, Alexeychik NN (1985) Activity of ions and buffer ability of sod-podzol soils of Belarussian SSR with respect to potassium. Agrochemistry 3:39–43

Hampton CR, Broadley MR, White PJ (2005) Short review: the mechanisms of radiocaesium uptake by Arabidopsis roots. Nukleonica 50:83–88

Helal AA, Arida HA, Rizk HE, Khalifa SM (2007) Interaction of cesium with humic materials: a comparative study of radioactivity and ISE measurements. Radiochemistry 49:523–529

Hirano M, Yonomoto T, Ishigaki M, Watanabe N, Maruyama Y, Sibamoto Y, Watanabe T, Moriyama K (2012) Insights from review and analysis of the Fukushima Dai-ichi accident. J Nucl Sci Technol 49:1–17

Ivashkevich LS, Bondar YI (2008) Effect of basic chemical characteristics of soils on mobility of radionuclides in them. Radiochemistry 50:98–102

Kaneyasu N, Ohashi H, Suzuki F, Okuda T, Ikemori F (2012) Sulfate aerosol as a potential transport medium of radiocesium from the Fukushima nuclear accident. Environ Sci Technol 46:5720–5726

Kang DJ, Seo YJ, Saito T, Suzuki H, Ishii Y (2012) Uptake and translocation of cesium-133 in napier grass (*Pennisetum purpureum* Schum.) under hydroponic conditions. Ecotoxicol Environ Saf 82:122–126

Kato H, Onda Y, Teramage M (2012) Depth distribution of ^{137}Cs, ^{134}Cs, and ^{131}I in soil profile after Fukushima Dai-ichi nuclear power plant accident. J Environ Radioact 111:59–64

Katsnelson YY, Sklyarova ES, Likhachyov VA, Zelenshchikov GV, Kapustyan AS (1983) Using of natural sorbents from Rostov region deposits for ecological remediation of lands being under high anthropogenic impact. Radiochemistry 2:111–121

Katsumi H (2012) 2011 Fukushima Dai-ichi nuclear power plant accident: summary of regional radioactive deposition monitoring results. J Environ Radioact 111:13–17

Kobets SA, Fedorova VM, Pshinko GN, Kosorukov AA, Demchenko VY (2014) Effect of humic acids and iron hydroxides deposited on the surface of clay minerals on the ^{137}Cs immobilization. Radiochemistry 56:325–331

Kornilovich BY, Pshinko GN, Spasenova LN (2000) Influence of humic compounds on caesium-137 sorption by mineral components of soils. Radiochemistry 42:92–96

Kudryashov NA, Serebryakova IE (1993) Mathematical modeling of the migration of long-lived radionuclides in soil as a result of radioactive fallout. Atom Energy 74:225–228

Kuznetsov VK, Sanzharova NI, Alexakhin RM, Anisimov VS, Abramova OB (2001) The influence of phosphate fertilizers on ^{137}Cs uptake by agricultural plants. Agrochemistry 9:47

Lasat MM, Ebbs SD, Kochian LV (1998) Phytoremediation of a radiocaesium-contaminated soil: evaluation of caesium-137 bioaccumulation in shoots of three plant species. J Environ Qual 27:165–169

Martyushov VV, Spirin DA, Romanov GN, Bazylev VV, Martyushov VZ (1996) Dynamics of speciation and migration of strontium-90 in soils of the East-Ural radioactive track. Quest Rad Saf 3:28–38

Mineeva VG (1989) Practical works on agrochemistry. MSU, Moscow

Misaelides P (2011) Application of natural zeolites in environmental remediation: a short review. Microporous Mesoporous Mater 144:15–18

Moiseev IT, Tikhomirov FA, Martyushov VS (1988) On the assessment of influence of mineral fertilizers on the dynamics of exchangeable ^{137}Cs in soils and on its bioavailability for vegetables. Agrochemistry 5:86–92

Nakamaru Y, Ishikawa N, Tagami K, Uchida S (2007) Role of soil organic compounds in the mobility of radiocesium in agricultural soils common in Japan. Colloids Surf A 306:111–117

Nakano M, Yong RN (2013) Overview of rehabilitation schemes for farmlands contaminated with radioactive cesium released from Fukushima power plant. Eng Geol 155:87–93

Nikipelov BV, Romanov GN, Buldakov LA, Babaev NS, Kholina YB, Mikerin EI (1989) A radiation accident in the southern Urals in 1957. Sov Atom Energy 67:569–576

Odintsov AA, Sazhenyuk AD, Satsyuk VA (2004) Association of ^{90x}Sr, ^{137}Cs, ^{239,240}Pu, ^{241}Am, and ^{244}Cm with soil absorbing complex in soils typical of the vicinity of the Chernobyl NPP. Radiochemistry 46:95–101

Odintsov AA, Pazukhin EM, Sazhenyuk AD (2005) Distribution of ^{137}Cs, ^{90}Sr, $^{239+240}$Pu, ^{241}Am, and ^{244}Cm among components of organic compounds of soils in near exclusion zone of the Chernobyl NPP. Radiochemistry 47:96–101

Ovchinnikov NA, Bezdenezhnykh VS (1996) Method of soils rehabilitation. Russian Federation Patent № 2064748 from 10.08.1996

Panov AV, Alexakhin RM, Prudnikov PV, Novikov AA, Muzalevskaya AA (2009) Influence of protective activity on ^{137}Cs accumulation by farming plants from soil after Chernobyl accident. Pedology J 4:484–497

Petrova MA, Flowers AG, Krip IM, Shimchuk TV, Petrushka IM (2008) Sorption of Sr on clay minerals modified with ferrocyanides and hydroxides of transition metals. Radiochemistry 50:502–507

Polyakov EV, Volkov IV, Khelbnikov NA (2015) Competitive sorption of cesium and other microelements onto iron (III) hexacyanoferrate(II) in the presence of humic acids. Radiochemistry 57:161–171

Popov VE, Il'icheva NS, Stepina IA, Maslova KM (2011) Influence of the potassium and ammonium ion concentrations on the selective sorption of ^{137}Cs by illite and clinoptilolite. Radiochemistry 53:97–102

Prister BS, Perepelyatnikova LV, Perepelyatnikov GP (1991) Problems of agricultural radioecology. Naukova Dumka, Kiev

Prokhorov VM (1981) Migration of radioactive pollutants in soils. Energoatomizdat, Moscow

Russian State Standard 17.4.4.01-84 (1984) Soils. Determination of cation exchange capacity by modified Bobko-Askinazi-Aleshin method, developed in Central Institute of Agrochemical Service of Farming Industry. Moscow

Russian State Standard 262113-91 (1991) Soils. Method of determination of organic carbon content. Moscow

Sakharov VK (2006) Radioecology. Lan, Saint Petersburg

Sanzharova NI, Kuznetsov VK, Brovkin VI, Kozhik ZA (1998) The assessment of efficiency of protective measures on soils contaminated by radionuclides. Agrochem Bull 4:22–26

Sanzharova NI, Sysoeva AA, Isamov NN, Alexakhin RM, Kuznetsov VK, Zhigareva TL (2005) Chemistry role in remediation farming land being under radioactive pollution. Russ Chem J 49:26–34

Sapozhnikov JA, Aliev RA, Kalmykov SN (2006) Radioactivity of the environment. Binom, Moscow

Shov G, Bell JNB (1989) The kinetics of caesium absorbtion by roots of winter Wheat and the possible consequences for the derivation of soil-to-plant transfer factor for radiocaesium. J Environ Radioact 10:213–231

Smolders E, Van den Brande K, Merckx R (1997) Concentrations of ^{137}Cs and K in soil solution predict the plant availability of ^{137}Cs in soils. Environ Sci Technol 31:3432–3438

Staunton S, Hinsinger P, Guivarch A, Brechignac F (2003) Root uptake and translocation of radiocaesium from agricultural soils bu various plant species. Plant Soil 254:443–445

Stevenson FJ (1994) Humus chemistry: genesis, composition, reaction. Willey, New York

Takeda A, Tskada H, Nakao A, Takaky Y, Hisamatsu S (2013) Time-dependent changes of phytoavailability of Cs added to allophanic andosols in laboratory cultivations and extraction tests. J Environ Radioact 122:29–36

Teplyakov IG, Romanov GN, Spirin DA (1997) Returning of lands in East-Ural radioactive trace to farming use. Rad Saf Quest 3:33–41

Volobuev PV, Chukanov VN, Shtinov AA, Alexeenko NN (2000) East-Urals radioactive track. Problems of rehabilitation of population and territory of Sverdlovsk region. Publisher of UrB RAS, Yekaterinburg

Voronina AV, Semenishchev VS, Savchenko MO, Bykov AA, Kutergin AS, Nedobuh TA (2013) Approaches to rehabilitation of radioactive contaminated territories. J Chem Technol Biotechnol 88:1606–1611

Voronina AV, Blinova MO, Semenishchev VS, Gupta DK (2015) Returning land contaminated as a result of radiation accidents to farming use. J Environ Radioact 144:103–112

Vozzhenikov GS, Alexandrova ZN, Vozzhenikov EG (1997) The method for soils deactivation. Russian Federation Patent № 2077749

Warner F, Harrison RM (1993) Radioecology after Chernobyl–biogeochemical pathways of artificial radionuclides. SCOPE 50. Wiley, Chichester

Yamaguchi N, Eguchi S, Fujiwara H, Hayashi K, Tsukada H (2012) Radiocesium and radioiodine in soil particles agitated by agricultural particles: field observation after the Fukushima nuclear accident. Sci Total Environ 425:128–134

Yudintseva EV, Gulyakin IV (1968) Agrochemistry of radioactive isotopes of caesium and strontium. Atomizdat, Moscow

Zolotov YA (1999) Basis of analytical chemistry. Part I. Common questions, separation methods. High School, Moscow

Zubets MV, Prister BS, Alexakhin RM, Bogdevich IM, Kashparov VA (2011) Urgent problems and tasks of scientific support of farming in radioactively contaminated zone of Chernobyl NPP. Agroecol J 1:5–20

Bacterial Diversity in Clay and Actinide Interactions with Bacterial Isolates in Relation to Nuclear Waste Disposal

Henry Moll, Laura Lütke, and Andrea Cherkouk

Contents

Abstract One potential source of actinides (An) in the environment could be the accidental release from nuclear waste disposal sites. Hence, the long-term safety of nuclear waste in a deep geologic repository is an important issue in our society. Microorganisms indigenous to potential host rocks are able to influence the speciation and therefore the mobility of An and their retardation both by direct and indirect pathways. They can as well affect the conditions in a geologic repository (e.g., by gas generation or canister corrosion). The focus of this chapter lies on the influence of indigenous microbes on the speciation of An. Therefore, for the safety assessment of such a repository, it is necessary to know which microorganisms are present in the potential host rocks (clay and salt) and if these microorganisms can influence the speciation of released An. Hence, dominant bacterial strains from potential host rocks for future nuclear waste depositions have to be investigated regarding their interaction mechanisms with soluble An ions. This chapter will cover the following research areas. Gained knowledge concerning the bacterial diversity in, e.g., Mont Terri Opalinus clay by applying direct molecular culture-

H. Moll (✉) • A. Cherkouk
Helmholtz-Zentrum Dresden-Rossendorf, Institute of Resource Ecology, Bautzner Landstraße 400, 01328 Dresden, Germany
e-mail: h.moll@hzdr.de

L. Lütke
Institut für Radioökologie und Strahlenschutz (IRS), Leibniz Universität Hannover, 30419 Hannover, Germany

C. Walther, D.K. Gupta (eds.), *Radionuclides in the Environment*,
DOI 10.1007/978-3-319-22171-7_12

independent retrievals and cultivation experiments will be presented. Their influence on the geochemical behavior of selected An (uranium and curium) will be highlighted. These investigations contribute to a better understanding of microbial interactions of An on a molecular level for an improved prediction of the safety of a planned nuclear waste repository.

Keywords Bacterial diversity • Bacteria • Complexation • Uranium • Curium • *Sporomusa* sp. • *Paenibacillus* sp. • TRLFS • Potentiometry

1 Introduction

Besides the prominent processes influencing the migration of An in the environment, e.g., sorption onto mineral surfaces, there is growing attention to the influence of indigenous microorganisms on their speciation. The comprehensive concept of geological disposal comprises a detailed knowledge concerning potential host rock formations. One of such formations is the Opalinus clay formations of the Mont Terri underground rock laboratory (URL), Switzerland, which is under investigation to test their suitability as host rock for future disposal of radioactive waste (Thury and Bossart 1999). Enriched bacteria indigenous to such subterranean soil environments can affect the speciation and hence the mobility of released An (Lovley et al. 1991; Kalinowski et al. 2004; Merroun and Selenska-Pobell 2008; Lloyd and Gadd 2011; Anderson et al. 2011; Brookshaw et al. 2012; Lütke et al. 2013; Moll et al. 2014). Therefore, it is of importance to identify relevant interaction processes occurring with dominant bacterial strains isolated from mentioned sites destined for the safe disposal of nuclear waste and to assess the resulting actinide speciation. Bacteria belong to the most widely spread organisms in nature. Besides archaea, these organisms represent the only form of life which can inhabit hostile environments of, e.g., high salinity (Oren 2002), temperature (Takai et al. 2008), and radiation (Makarova et al. 2001), like in designated nuclear waste disposal sites.

In general, the versatile interactions between microbes and An can be classified into two major categories: the direct and indirect interaction mechanisms. Direct interactions include the processes bioaccumulation, biosorption, biomineralization, and biotransformation (Fig. 1). Bioaccumulation means the incorporation of the An inside the cell (Brockmann et al. 2014; Günther et al. 2014; Merroun and Selenska-Pobell 2008; Suzuki and Banfield 2004). Biosorption describes a pure binding of the An to surface functional groups of the respective cell envelope (Reitz et al. 2014; Günther et al. 2014; Moll et al. 2014; Lütke et al. 2012, 2013; Markai et al. 2003; Texier et al. 2000; Fowle et al. 2000). Biomineralization refers to the cellular liberation of inorganic ligands leading to the formation of a precipitate, e.g., meta-autunite (Merroun and Selenska-Pobell 2008; Krawczyk-Bärsch et al. 2015;

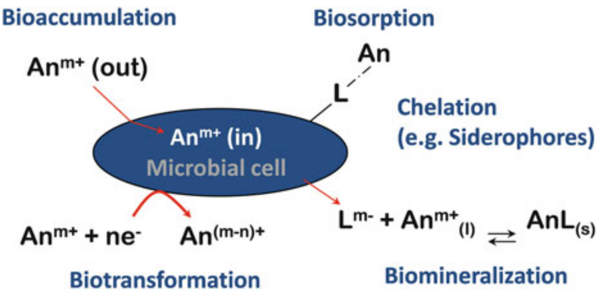

Fig. 1 Interaction mechanisms between microbes and actinides (An)

Reitz et al. 2014). Biotransformation is a very general term referring to a microbe-mediated conversion of the oxidation state (oxidation or reduction) of the respective An (Lovley et al. 1991; Panak and Nitsche 2001; Moll et al. 2006; Merroun and Selenska-Pobell 2008; Zhengji 2010; Kelly et al. 2010; Bernier-Latmani et al. 2010). Indirect interaction, for instance, by chelation, refers to the release of cellular ligands which bind to the An in solution. A prominent example is the release of siderophores of the pyoverdin type by *Pseudomonas fluorescens* which have shown to possess great binding potential toward U(VI), Cm(III), and Np (V) (Moll et al. 2008a, b, 2010). Our study is focused to broaden the knowledge concerning the bacterial diversity in Mont Terri Opalinus clay. After cultivation and characterization of dominant bacterial populations, we investigated their influence on the geochemical behavior of uranium and curium (Moll et al. 2013a).

2 Bacterial Diversity in Clay

For a long time, no in situ active life could be found in clay subsurface environments as potential host rocks for nuclear waste disposal, which seems to be unfavorable to microbial activity. However, the presence of bacteria in deep clay sediment of the Boom clay formation (Mol, Belgium) was shown in 1996 (Boivin-Jahns et al. 1996). In the Meuse/Haute-Marne Underground Research Laboratory located at Bure (300 km east of Paris), the Callovo–Oxfordian argillite formation was evaluated for its use as a potential host rock for a high-level radioactive waste repository in France (Cormenzana et al. 2008), and its microbial diversity was studied by culturing methods in Urios et al. (2012). The bacterial diversity found at the French formations was restricted to three bacterial phyla: *Firmicutes*, *Actinobacteria*, and *Proteobacteria* (Urios et al. 2013).

Over the last years, a couple of studies were performed about the microbial diversity in the Opalinus clay from the Mont Terri URL, Switzerland (Mauclaire et al. 2007; Stroes-Gascoyne et al. 2007; Poulain et al. 2008). Cultivation attempts and studies based on polar lipid fatty acid (PLFA) analyses suggested the presence of viable cells and detected PLFA biomarkers for Gram-negative bacteria and sulfate-reducing bacteria (in particular, *Desulfovibrio* spp., *Desulfobulbus* spp., and *Desulfobacter* spp.) in Opalinus clay (Mauclaire et al. 2007; Stroes-Gascoyne et al. 2007). Ribosomal RNA (rRNA) genes sequenced from enrichment cultures from Opalinus clay samples identified unknown species of *Sphingomonas* and *Alicyclobacillus* (Poulain et al. 2008). However, no PCR-amplifiable DNA from core samples could be extracted (Stroes-Gascoyne et al. 2007).

For the first time, DNA from Opalinus clay could be extracted in our laboratory by a method evolved by Selenska-Pobell and co-workers (Selenska-Pobell et al. 2001). This method combines a very effective direct lysis of microorganisms in environmental samples and the precipitation of the extracted DNA with polyethyleneglycol, with the final purification steps based on the use of AXG-100 cartridges (Macherey-Nagel, Düren, Germany). With this method, high molecular weight DNA from Opalinus clay of the Mont Terri URL was successfully isolated by using 50 g of sample material (Moll et al. 2013a). DNA from the inner part of the core and from the surface part of the core was extracted and analyzed. Ribosomal intergenic spacer analysis (RISA) patterns obtained from both samples did not match with each other, which indicated that the core surface was occupied by bacteria not or barely presented in the inner part of the core. A conclusion from this analysis is that clay material from the inner part of the core should be preferentially analyzed to avoid contaminants which might penetrate into the core during the sampling. An unexpected diverse bacterial community represented by five different bacterial phyla *Proteobacteria*, *Firmicutes*, *Bacteroidetes*, *Acidobacteria*, and *Actinobacteria* as well as unclassified bacteria was found in the inner part of the core by analyzing the 16S rRNA gene clone library (Moll et al. 2013a). The largest group in the sample includes rather diverse representatives of *Firmicutes*, which were affiliated with three distinct clostridial and one negativicutes family. The second largest group was, in contrast, more uniform and mainly represented by *Acidovorax* spp., belonging to the *betaproteobacterial* class of the phylum *Proteobacteria*. Their closest relatives were found in seafloor lavas from the East Pacific Rise (Santelli et al. 2008) and in Baltic Sea surface water (*Acidovorax* sp. C34). Representatives of *Acidovorax* are able to reduce nitrate, U (VI) to U(IV), and can couple the oxidation of ferrous iron (Fe(II)) with nitrate reduction (Nyman et al. 2006; Pantke et al. 2012; Carlson et al. 2013). The third predominant group was affiliated with *Bacteroidetes*, which are widely distributed in water, soils, and sediments and are characterized as a bacterial group which is very adaptive to changes in the nutrient conditions in the environment.

These results are in good agreement with previously performed multidisciplinary approaches to study the microbial diversity in Boom clay formation, a deep-subsurface clay deposit in Mol, Belgium (Wouters et al. 2013) and Spanish bentonites (Lopez-Fernandez et al. 2014, 2015). Wouters and colleagues confirmed the presence of a complex microbial community that can persist in subsurface Boom clay borehole water by using an integrated approach of microscopy, metagenomics, activity screening, and cultivation. Despite the presumed low-energy environment, microscopy and molecular analyses showed a large bacterial diversity and richness. Among different borehole water samples, the core bacterial community comprises seven bacterial phyla, namely, the

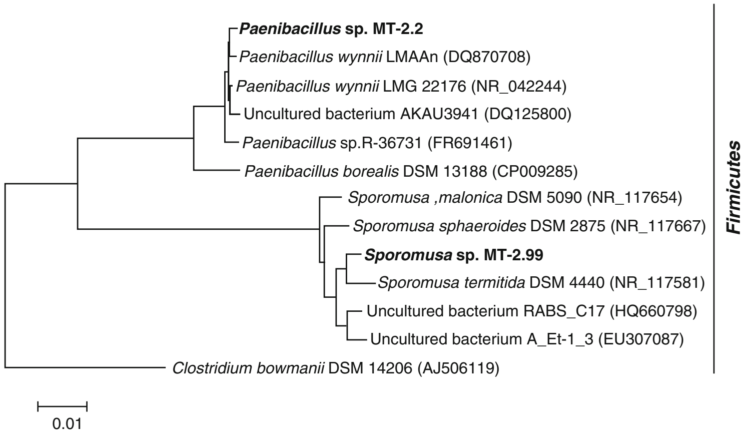

Fig. 2 Phylogenetic dendrogram of the 16S rRNA genes of isolates, obtained from the Mont Terri Opalinus clay sample MT-2 under anaerobic conditions on R2A agar plates

Proteobacteria, *Actinobacteria*, *Chlorobi*, *Firmicutes*, *Bacteroidetes*, *Chloroflexi*, and *Spirochaetes*. *Proteobacteria* made up of 76 % of the community, with the *Acidovorax* genus being highly prominent. In the Spanish bentonites, *Proteobacteria* and *Bacteroidetes* were dominant in clone libraries and Illumina sequencing approaches (Lopez-Fernandez et al. 2015). Culture-dependent analysis of microbial diversity from these clay formations was performed, and bacteria from different phyla were isolated as *Proteobacteria*, *Firmicutes*, and *Actinobacteria* (Lopez-Fernandez et al. 2014).

A culture-dependent approach was also performed in our laboratory with a sample from the inner part of the core from Mont Terri Opalinus clay by using R2A media (Moll et al. 2013a). The 16S rRNA genes of the isolates affiliated within the bacterial phylum *Firmicutes*. Interestingly, the 16S rRNA gene sequence of the isolate MT-2.99 was 96 % similar to the 16S rRNA gene sequences of *Sporomusa* spp. (*Sporomusa malonica* DSM 5090, *Sporomusa sphaeroides* DSM 2875, and *Sporomusa termitida* DSM 4440) (see Fig. 2); the uncultured bacterium clone A_Et-1_3 (EU307087), which was retrieved from Fe(III)-reducing enrichment culture (Hansel et al. 2008); and the uncultured bacterium RABS_C17, which was retrieved from an aquifer sediment where reductive immobilization of U took place (Sharp et al. 2011). *Sporomusa* spp. are obligatory anaerobic and sporulating bacteria (Kuhner et al. 1997). The 16S rRNA gene sequence of isolate MT-2.2 was 99 % similar with the 16S rRNA gene sequence of *Paenibacillus wynnii* LMAAn and *Paenibacillus wynnii* LMG 22176 T, which was found on Mars oasis on Alexander Island, Antarctica (Rodriguez-Diaz et al. 2005) (Fig. 2). Representatives of only one bacterial phylum could be isolated. This limited diversity could be interpreted with the unfavorable living conditions, characterizing the Opalinus clay. However, the capability of representatives of *Firmicutes* to form spores gives them a potential to survive in unfavorable conditions. On the other

Table 1 Protonation constants and site densities of Mont Terri Opalinus clay isolates determined by potentiometric titrations

Type of surface site	pK_a values		Site densities (mmol g^{-1} dry biomass)	
	Sporomusa sp. (Moll et al. 2013a)	*Paenibacillus* sp. (Lütke et al. 2013)	*Sporomusa* sp. (Moll et al. 2013a)	*Paenibacillus* sp. (Lütke et al. 2013)
Carboxyl	4.80 ± 0.06	4.90 ± 0.05	0.53 ± 0.08	0.55 ± 0.06
Phosphoryl	6.68 ± 0.06	6.66 ± 0.10	0.35 ± 0.03	0.24 ± 0.01
Amine/-OH	9.01 ± 0.08	9.20 ± 0.03	0.48 ± 0.05	1.20 ± 0.26

hand, only a small percentage of natural microbial populations can be isolated and studied in the laboratory due to the limited knowledge about their nutrient requirements and other life necessities (Stewart 2012).

The two isolates *Sporomusa* sp. MT-2.99 and *Paenibacillus* sp. MT-2.2 were chosen for further analyses to study how these isolates interact with U(VI) and Cm (III)/Eu(III). Potentiometric titration curves were recovered for the bacterial strains to characterize their cell surface functional groups. The potentiometric titration curves of the bacterial strains were all fitted with a three-site model using HYPERQUAD (Gans et al. 1996). The experimental details are described in detail in Lütke (2013), Lütke et al. (2013), and Moll et al. (2013a, b).

The description of the bacterial cell wall with three major global binding sites is a common approach (Fein et al. 1997; Yee et al. 2004; Dittrich and Sibler 2005; Fang et al. 2009). By comparing the determined values (Table 1) to the pK_a ranges of different bacterial functional groups reported in, e.g., Cox et al. (1999), the respective surface functional groups can be attributed to carboxyl, phosphate, and amine moieties. The determined pK_a values of the major global binding sites are in a very good agreement to those determined for a strain of the Gram-negative genus *Calothrix* (Yee et al. 2004). Our experiments showed that the major surface functional groups of both strains have similar pK_a values, whereas a higher variation could be found in the respective site densities. Both parameter the pK_a values and corresponding site density are necessary to elucidate the An speciation in the presence of these bacteria in terms of surface complexation constants to be used in modeling codes.

3 Determination of Actinide Interactions with Mont Terri Opalinus Clay Isolates

In the following sections of the chapter, the unique potential of bacteria to influence the aqueous speciation of uranium(VI) and curium(III) will be highlighted. The diversity of interaction mechanisms is due to the variety of metabolism and cell surface structures among microbes. The cell walls of bacteria represent a highly efficient matrix for metal sorption offering mainly carboxylic, phosphoryl, and amine moieties for metal complexation (Beveridge and Doyle 1989). It has been proposed that bacteria freely suspended in solution may even have a radionuclide-sorbing capacity higher than that of the surrounding mineral phases (Pedersen and Albinsson 1992; Bencheikh-Latmani et al. 2003; Ohnuki et al. 2005). The composition of the cell wall differs for Gram-negative and Gram-positive bacterial strains. Since strains of the genera *Sporomusa* and *Paenibacillus* differ by that, with the present work, the influence of the cell wall structure on actinide binding can be assessed. The cell walls of Gram-negative bacteria possess an outer membrane of lipopolysaccharide (LPS), a periplasm consisting of a thin layer of peptidoglycan (PG), and an inner cytoplasmic membrane (phospholipid bilayer). The LPS offers carboxyl, phosphoryl, hydroxyl, and amino groups as binding sites for metals (Barkleit et al. 2008). The PG polymeric framework itself is rich in carboxylate groups. In the PG framework, teichoic (basically glycerol phosphate polymers) and teichuronic acids are interconnected, which contain also phosphate groups. The strain *Sporomusa* sp. MT-2.99 showed a Gram-negative staining (Moll et al. 2013a). The *Selenomonas–Megasphaera–Sporomusa* branch unifies members of the *Firmicutes* with Gram-negative-type cell envelopes but still belongs to *Clostridia* (Yutin and Galperin 2013). In contrast to the genus *Sporomusa*, the genus *Paenibacillus* is Gram-positive. In Gram-positive bacteria, the major and very outer cell wall component is PG, which can make up to 90 % of the dry weight of the bacterial cells (Voet et al. 2002).

The thermodynamic data of U(VI) species formed at the bacterial surface were determined with potentiometric titration. Moreover, we assessed the U(VI) and Cm (III) speciation at the cell surface using time-resolved laser-induced fluorescence spectroscopy (TRLFS) as a direct speciation technique. In selected experiments, europium(III) as a nonradioactive analogue for An(III) was used also to validate the Cm(III) TRLFS speciation results by potentiometric titration and also by TRLFS. In Moll et al. (2013a, 2014), we could show that Eu(III) can be used as a nonradioactive analogue to mimic bacterial interactions of An(III). TRLFS has been proven in the past to be a powerful tool especially useful for the determination of the uranium, curium, and europium speciation at low, environmentally relevant concentrations (Geipel 2006; Lütke et al. 2012, 2013; Moll et al. 2014). Furthermore, results on the influence of $[U(VI)]_{initial}$ and pH on the quantities of U(VI) bound and on the bacteria-mediated inorganic phosphate liberation by *Paenibacillus* sp. are presented.

3.1 U(VI) Interaction Studies with Paenibacillus *sp. and* Sporomusa *sp. Cells*

3.1.1 U(VI) Binding by *Paenibacillus* sp. and *Sporomusa* sp. cells as a Function of [U(VI)] and pH Including the Bacteria-Mediated Inorganic Phosphate Release (Lütke et al. 2013; Moll et al. 2013a)

The biosorption efficiency of microbial strains is a key parameter for judging the retardation of the respective actinide caused by the strain. As depicted in Fig. 3,

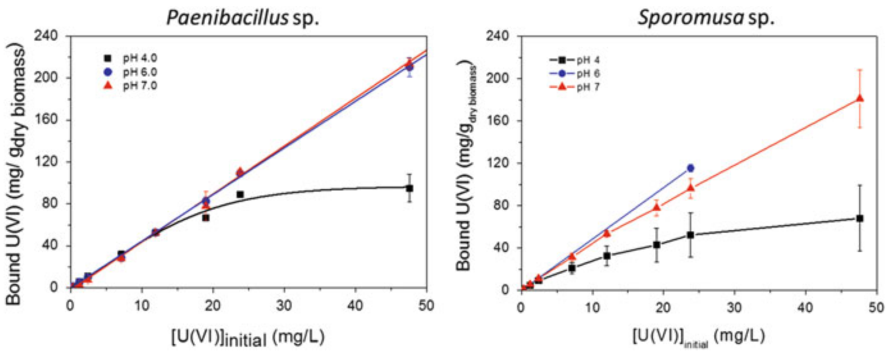

Fig. 3 U(VI) binding onto *Paenibacillus* sp. (left) and *Sporomusa* sp. cells in dependence on $[UO_2^{2+}]_{initial}$ at different pH values in 0.1 M $NaClO_4$, [dry biomass] = 0.2 gL^{-1}

Paenibacillus sp. and *Sporomusa* sp. cells display a strong pH-dependent affinity for U(VI). At both pH values 6 and 7 and an initial [U(VI)] of about 48 mg L^{-1}, more than two times as much U(VI) is bound as at pH 4 for *Paenibacillus* sp. (Lütke et al. 2013). Under similar conditions, almost three times as much as U(VI) is immobilized for *Sporomusa* sp. (Moll et al. 2013a). Interestingly, for pH 6 and 7, the dependency of the sorption on the initial [U(VI)] can be described in both cases by a linear correlation, and almost identical sorption efficiencies were found. At pH 4 on the contrary, the sorption shows an asymptotic behavior with increasing $[U(VI)]_{initial}$. This finding can possibly be explained by a smaller degree of deprotonation of the cell surface functional groups at pH 4 in comparison to pH 6 or 7 resulting in a fewer number of functional groups available for U (VI) complexation.

It has been discovered very early that the release of phosphate can be an active microbial process and altered through external conditions (Shapiro 1967). We could show that the dependency of the inorganic phosphate release by *Paenibacillus* sp. cells depends on the initial U(VI) concentration and pH. The phosphatase activity is maximum (4.8 mg L^{-1}) at pH 6. A pH-dependent bacterial phosphatase activity was also observed for another *Paenibacillus* strain, *Paenibacillus* sp. - JG-TB8 (Reitz et al. 2014), which increased drastically from pH 3 to 6, having maximum activity also at pH 6. At a [U(VI)] as low as 5×10^{-6} M, inorganic phosphate liberation is already markedly decreased in comparison to the samples without any U(VI) added (3.8 mg L^{-1} at pH 6). This effect is strongest at pH 4. The decrease of inorganic phosphate release as response to U(VI) contact was also found for a strain of *P. fluorescens* (Lütke et al. 2012). Upon increasing $[U(VI)]_{initial}$, the phosphate decrease becomes more drastic. Inorganic phosphate release by *Sporomusa* sp. could be also proven. U(VI) phosphate complexes give characteristic luminescence spectra. Thus, the release of inorganic phosphate into the cell supernatants should be observable with TRLFS as described later on.

3.1.2 U(VI) Speciation Explored by Potentiometric Titration (Lütke et al. 2013; Moll et al. 2013a)

The titration data of bacterial cells and UO_2^{2+} were fitted by including the following hydrolytic uranyl species and their stability constants: $(UO_2)_2(OH)_2^{2+}$, $(UO_2)_3(OH)_5^{+}$, and $(UO_2)_4(OH)_7^{+}$(Guillaumont et al. 2003). The titration curves could be modeled with a very good fit result when the bacterial surface complexes R–COO–UO_2^{+}, R–O–PO_3H–UO_2^{+}, R–O–PO_3–UO_2, and (R–O–PO_3)$_2$–UO_2^{2-} were considered. The respective calculated stability constants are summarized in Table 2.

From the stability constants listed in Table 2, it can be seen that overall U (VI) can form fairly stable complexes with the surface functional groups of *Paenibacillus* sp. and *Sporomusa* sp. cells. Furthermore, the interaction with phosphoryl sites is characterized by stability constants several orders of magnitude greater than that of carboxyl site interaction. Our reported stability constant of the *Paenibacillus* sp. R–COO–UO_2^{+} complex is in very good agreement with the stability constant of the 1:1 complex of U(VI) interacting with carboxylic groups of the *Bacillus subtilis* cell surface, log $\beta_{110} = 5.4 \pm 0.2$, published by Fowle et al. (2000). If compared to the results published by Barkleit et al. (2008, 2009) on the U(VI) interaction with PG (R–COO–UO_2^{+} with a log β value of 4.02 was specifically attributed to UO_2^{2+} interacting with glutamic acid groups; R–COO–UO_2^{+} with a log β value of 7.28 was specifically attributed to UO_2^{2+} interacting with diaminopimelic acid groups) and LPS (R–COO–UO_2^{+} with a log β value of 5.93), deviate somewhat from our results. However, it shows the relatively broad range of log β values of U(VI) complexes with carboxyl groups in biological systems. If compared to the results in Table 2 gained with the Äspö isolate *P. fluorescens* (Gram-negative), it becomes obvious that although the same

Table 2 Calculated stability constants of UO_2^{2+}/Eu^{3+}/Cm^{3+} complexes with surface functional groups of *Paenibacillus* sp. and *Sporomusa* sp. cells determined by potentiometric titration (Lütke et al. 2013; Moll et al. 2013a, 2014)

Complex	xyz[a]	log β_{xyz} (±SD) *Paenibacillus* sp.	log β_{xyz} (±SD) *Sporomusa* sp.
R–COO–UO_2^{+}	110	5.33 ± 0.08	4.75 ± 0.98
R–O–PO_3–UO_2	110	8.89 ± 0.04	8.58 ± 0.04
R–O–PO_3H–UO_2^{+}	111	12.92 ± 0.05	13.07 ± 0.06
(R–O–PO_3)$_2$–UO_2^{2-}	120	13.62 ± 0.08	13.30 ± 0.09
R–COO–Eu^{2+}	110	5.70 ± 0.25	6.89 ± 0.62
R–O–PO_3–Eu^{+}	110		7.71 ± 0.33
R–O–PO_3H–Eu^{2+}	111	13.64 ± 0.30	15.49 ± 0.19
R–COO–Cm^{2+}	110		8.06 ± 0.61[b]
R–O–PO_3–Cm^{+}	110		
R–O–PO_3H–Cm^{2+}	111	13.94 ± 0.18[b]	13.90 ± 0.90[b]

[a]Stoichiometry of metal–ligand–H
[b]From TRLFS

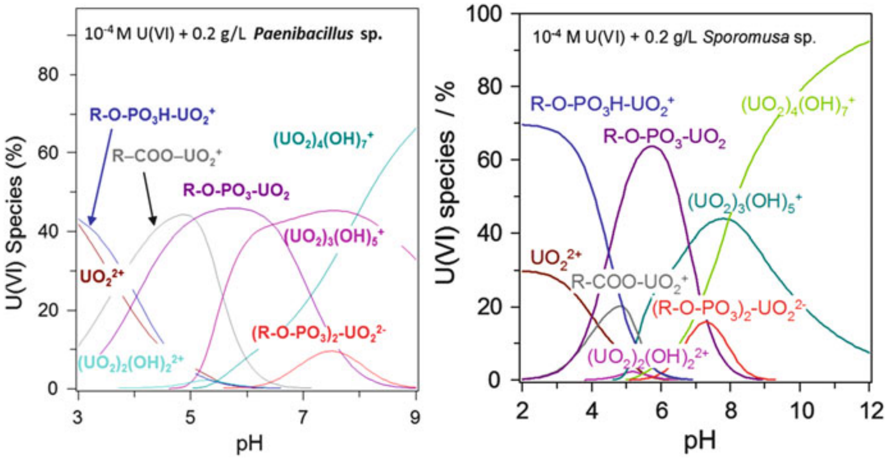

Fig. 4 U(VI) species distributions in the presence of *Paenibacillus* sp. and *Sporomusa* sp. cells in dependence on pH: [U(VI)] = 1 × 10^{-4} M, [dry biomass] = 0.2 gL^{-1}. CO_2-free system

complex stoichiometries could be fitted to the titration data (Lütke et al. 2012), the gained stability constants of the R–COO–UO_2^+ complex displayed a range of 4.75–6.66, indicating the dependency of those on the individual cell wall structure. The comparison of the determined stability constants for phosphoryl interaction, in specific of the R–O–PO_3H–UO_2^+ complex of both strains, to the literature, revealed again a fairly good agreement with the result gained by Fowle et al. (2000) (*B. subtilis*: log β = 11.8) and Barkleit et al. (2008) (LPS: log β = 11.66). An agreement to the literature was observed when comparing the results on U (VI) interaction with deprotonated bacterial phosphoryl sites to the results gained with the model compound LPS (Barkleit et al. 2008: log β_{110} = 7.50 and log β_{120} = 13.80). This might suggest that LPS is a good representative of the phosphoryl properties of the bacterial cell envelope in terms of their binding characteristics toward U(VI).

The discussion of the determined bacterial U(VI) surface complexation constants (Table 2) is illustrated by U(VI) species distribution calculations using the software HySS2009 (Alderighi et al. 1999). The U(VI) speciation in the acidic pH range (pH 3) is determined majorly by UO_2^{2+} being coordinated to hydrogen phosphoryl sites (Fig. 4). This finding coheres well to what was reported by Fowle et al. (2000): the best fit of data obtained from U(VI) binding to *B. subtilis* was achieved by considering U(VI) bound via H-phosphoryl groups at low pH. Nevertheless, at pH 3, for instance, there is a portion of noncomplexed U (VI) in the cell supernatant, which should be detectable using TRLFS.

The species distribution diagram furthermore shows that upon increasing pH, an increasing coordination of UO_2^{2+} to carboxylic and deprotonated phosphoryl sites occurs. Due to the lower stability of the carboxyl bound U(VI) complex in the *Sporomusa* sp. system, here, phosphoryl bound U(VI) dominates compared to

Paenibacillus sp. At a pH greater than 7, uranyl hydroxides dominate the speciation in a CO_2-free system.

3.1.3 U(VI) Speciation Explored by Time-Resolved Laser-Induced Fluorescence Spectroscopy (TRLFS) in the *Paenibacillus* sp. System (Lütke et al. 2013; Moll et al. 2013a)

From both, the cells and the according cell supernatants at pH 4 and 7, U (VI) luminescence spectra were collected and compared (Fig. 5a).

While the band positions of the static spectra give indications for possible U (VI) surface species formed, the time-resolved measurements give insight into the number of present luminescent species. A detailed summary of luminescence emission maxima and calculated lifetimes related to the spectra discussed including the comparison to the appropriate literature is given in Lütke et al. (2013). Also TRLFS affirmed (Fig. 5a) that the speciation at the cell surface changes in dependence on the pH. With a pH shift from 4 to 7, the main luminescence emission band is slightly redshifted by roughly 3 nm, and also the spectral pattern changes. The emission maxima of U(VI) in the supernatant at pH 4 indicate the occurrence of at least two luminescent species having quite distinct emission maxima. An emission band located at 509.7 nm and the associated lifetime of 1.03 ± 0.02 μs clearly indicate a spectral contribution of the free UO_2^{2+} ion. The second spectral feature of U(VI) in the cell supernatant at pH 4 is quite similar to the spectrum of U(VI) in the supernatant at pH 7 in terms of the position of the main luminescence emission band, indicating the presence of a similar species at both pH values. This gives evidence for a cellular ligand being released which coordinates strongly to U(VI); otherwise, the spectral pattern would show a strong pH dependency due to the increasing formation of uranyl hydroxides with increasing pH. Considering also the

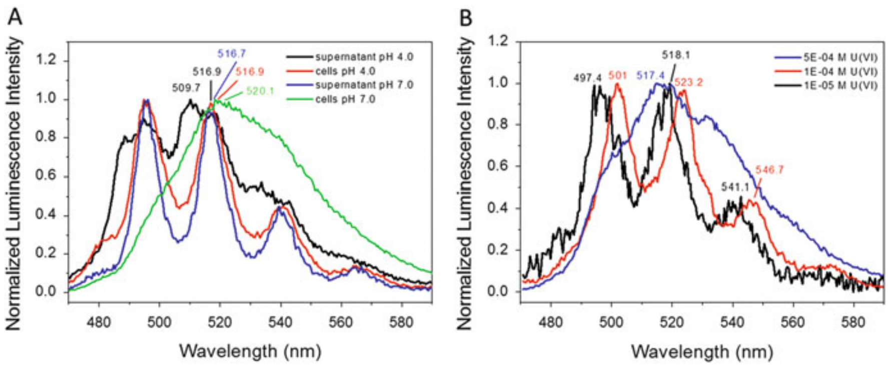

Fig. 5 (**a**) Luminescence spectra of U(VI)-loaded *Paenibacillus* sp. cells and U(VI) in the cell supernatants at pH 4 and 7 in 0.1 M $NaClO_4$ ($[U(VI)]_{initial}$ 1×10^{-4} M, [dry biomass] 0.2 gL^{-1}). (**b**) Luminescence spectra of U(VI)-loaded *Paenibacillus* sp. cells with variation of $[U(VI)]_{initial}$ and at pH 5 in 0.1 M $NaClO_4$, [dry biomass] = 0.2 gL^{-1}

relatively sharp emission bands and the position of the emission maxima of U (VI) in the supernatant at pH 7, the presence of pure U(VI) hydroxide can be excluded. Comparing these band positions to those of model compounds of the literature, especially those of UO_2^{2+} coordinated by $H_2PO_4^-$ and HPO_4^{2-} (Panak et al. 2000), a coordination by inorganic phosphate seems probable. Since inorganic phosphate was already proven to be released into the supernatants in significant amounts by means of ion exchange chromatography, a coordination of UO_2^{2+} by inorganic phosphate seems likely. Comparing the spectrum of U(VI) bound to the cells at pH 4 to that at pH 7, a redshift of 3.2 nm occurs. This significant redshift is in agreement to what was predicted in the calculated U(VI) species distribution. The U(VI) species distribution had shown the increased formation of UO_2^{2+} complexes with deprotonated phosphoryl sites in the neutral pH range, while at low pH around pH 4, uranyl is predominantly coordinated via H-phosphoryl and carboxylic sites. This dependency had also been reported by Barkleit et al. (2008), investigating the interaction of LPS with U(VI). A redshift of the emission maxima occurred when going from UO_2^{2+} complexed by protonated phosphoryl to deprotonated phosphoryl sites. Besides the position of the luminescence emission maxima, also the luminescence lifetimes can be helpful to identify the present species. At pH 4 for U(VI) bound to the cells, two lifetimes could be determined: 0.66 and 2.69 μs. For pH 7, also two lifetimes were found: 0.53 and 2.34 μs. To discriminate here between carboxyl and phosphoryl, and potentially even between deprotonated phosphoryl and H-phosphoryl, a measurement at pH 5 in dependency on $[U(VI)]_{initial}$ was carried out in order to attribute the lifetimes to present U (VI) species (Fig. 5b). In case of a deficit of [U(VI)] compared to the [surface sites], U(VI) should be bound at first via protonated phosphoryl sites. With increasing [U (VI)], an increased amount of $R–O–PO_3–UO_2$ would be formed. If [U(VI)] is increased further, finally, the carboxyl groups as weakest ligand according to the determined stability constants and in accordance to many exemplary cases in the literature (Fowle et al. 2000; Barkleit et al. 2008; Rothstein 1962) will be covered by U(VI). As depicted in Fig. 5b, a significant redshift of about 5 nm occurs at an increased [U(VI)] of 1×10^{-4} M compared to the spectrum at the smallest investigated [U(VI)] of $1 \times \cdot 10^{-5}$ M. The luminescence emission maxima of this spectrum point strongly toward a uranyl phosphoryl interaction (see for comparison Günther et al. 2006). The spectrum at $[U(VI)]_{initial} = 1 \times 10^{-4}$ M accompanied by a short lifetime of in average 0.55 μs can clearly be assigned to phosphoryl-bound U (VI), most likely to deprotonated phosphoryl ($R–O–PO_3–UO_2$). If the [U(VI)] is increased further, the main emission band shifts toward shorter wavelength even below the position of the main emission maximum of the spectrum of the lowest measured [U(VI)]. This finding as well as the spectral pattern observed at this [U (VI)] gives indications for a formation of polynuclear U(VI) species. The data evaluation showed that both species, the $R–O–PO_3H–UO_2^+$ and the $(R–O–PO_3)_2–UO_2^{2-}$ complex, have similar lifetimes and longer than that of the $R–O–PO_3–UO_2$ complex. Similar observations were made by Barkleit et al. (2008) for UO_2^{2+}–LPS complexes. In the U(VI)–*Sporomusa* sp. system, the major contribution of phosphoryl sites on U(VI) speciation could be also confirmed by preliminary TRLFS measurements. TRLFS as a direct speciation technique could successfully prove the following: the pH-dependent cell-mediated inorganic phosphate release, the occurrence of free UO_2^{2+} at acidic pH as predicted by the calculated U(VI) speciation, and the occurrence of different UO_2^{2+} phosphoryl species.

3.2 Cm(III) Interaction Studies with **Paenibacillus** *sp. and* **Sporomusa** *sp. Cells (Lütke 2013; Moll et al. 2013a, 2014)*

In the following paragraph, the change of the Cm^{3+} speciation in the presence of *Sporomusa* sp. cells using TRLFS will be highlighted and compared to findings in the *Paenibacillus* sp. system. For a detailed description of the ongoing process, please refer to the corresponding literature (Lütke 2013; Moll et al. 2013a, 2014).

In the presence of *Sporomusa* sp. cells, a strong decrease in the emission band of the free Cm^{3+} at 593.8 nm could be detected already at pH 1.95 (Fig. 6a). A new redshifted emission band at around 600 nm occurred simultaneously showing the influence of a first Cm^{3+}–*Sporomusa* sp. species. It demonstrates that *Sporomusa* sp. interacts with curium(III) from acidic solutions. The dependencies found in the TRLFS spectra suggested the occurrence of two individual Cm^{3+}–*Sporomusa* sp. species between pH 1.9 and 8.1 having emission maxima at ca. 600 and 601.4 nm. The pH-dependent change of the emission data of the Cm^{3+}–*Sporomusa* sp. system implies the involvement of two functional groups located at the cell envelope structure.

In all bacterial samples, a bi-exponential luminescence decay behavior was measured. The averaged value of the shorter lifetime was calculated to be 108 ± 15 μs, whereas the component with the longer lifetime was calculated to be

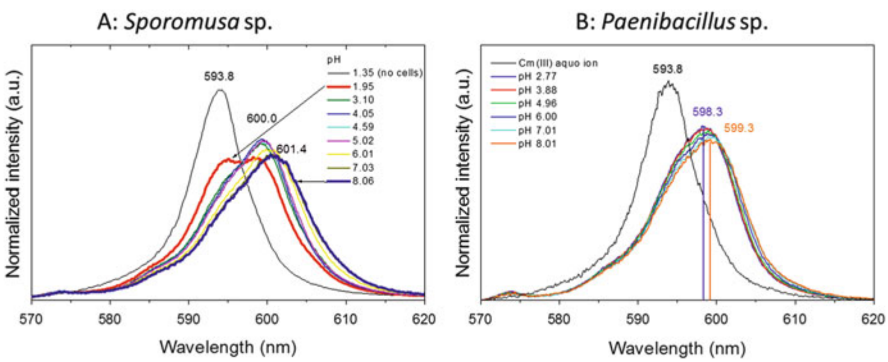

Fig. 6 Luminescence emission spectra of 0.3 μM curium(III) in 0.1 M $NaClO_4$ as a function of pH: (**a**) measured at a fixed *Sporomusa* sp. concentration of 0.02 $g_{dry\ weight}L^{-1}$ and (**b**) measured at a fixed *Paenibacillus* sp. concentration of 0.2 $g_{dryweight}L^{-1}$

252 ± 46 µs. Using the empirical equation given by Kimura and Choppin (1994), these lifetimes correspond to 5.0 and 2.0, respectively, remaining water molecules in the curium(III) first coordination sphere. In general, we found a stronger contribution of the long lifetime to measured sum lifetimes in the acidic pH region. In contrast, the short lifetime contributed most in the neutral to alkaline pH region. Due to these findings and by comparison to relevant literature values (see Moll et al. 2014), the longer lifetime can be assigned to Cm^{3+}−*Sporomusa* sp. species formed in the acidic pH region (phosphoryl interaction), whereas the shorter lifetime corresponds to Cm^{3+}−*Sporomusa* sp. species formed in the neutral to alkaline pH region (carboxyl interaction).

For *Sporomusa* sp., the interaction mechanism with Cm(III) and also Eu(III) is dominated by a major process a reversible biosorption reaction. However, we could identify a certain amount, ca. 30 %, which is irreversibly bound to the cells. This minor process can be described by an immobilization of Cm(III)/Eu(III) within the complex cell envelope structure of *Sporomusa* sp.

The program SPECFIT (Binstead et al. 2004) was used to extract the bacterial curium(III) surface complexation constants (Table 2) and the corresponding single component spectra. The calculation procedure is based on the formal complex formation equation for discrete binding sites and the appropriate mass action law, which represents the complex stability constant log β_{xyz}. The variations observed in the emission data (e.g., shown in Fig. 6a) could be described by the formation of two curium(III) surface complexes. The best fits were obtained with two 1:1 complexes, $R-O-PO_3H-Cm^{2+}$ (Cm^{3+}−*Sporomusa* sp. species 1) and $R-COO-Cm^{2+}$ (Cm^{3+}−*Sporomusa* sp. species 2). The surface complexation constants were calculated to be log $\beta_{111} = 13.90 \pm 0.90$ for the protonated phosphoryl complex and log $\beta_{110} = 8.06 \pm 0.61$ for the carboxyl coordination.

We were able to identify a Eu(III) surface complex with deprotonated phosphoryl groups, $R-O-PO_3-Eu^{+}$, by potentiometric titration in the *Sporomusa* sp. system. Both species $R-COO-Eu^{2+}$ and $R-O-PO_3-Eu^{+}$ coexist between pH 4 and 8. Here, we could see the limitations of TRLFS. A differentiation of two individual species was not possible in this pH range in the spectroscopic titrations by TRLFS. It follows that the stability range of Cm(III)/Eu(III) carboxyl interactions might be overdetermined by TRLFS at least for the *Sporomusa* sp. system.

From Fig. 6b, it becomes obvious that the luminescence spectrum of Cm(III) in the presence of *Paenibacillus* sp. cells is also redshifted compared to that of the Cm (III) aquo ion by approximately 5 nm indicating complex formation. In contrast to the *Sporomusa* sp. system, the spectra of Cm(III) in the presence of the *Paenibacillus* sp. cells undergo only a slight redshift of about 1 nm within pH 3–8. The complex $R–O–PO_3H–Cm^{2+}$ could be extracted having a stability constant log β of 13.94 ± 0.18 using SPECFIT. Obviously, Cm(III) displays high affinity to the phosphoryl sites of the *Paenibacillus* sp. cell surface. No carboxyl interaction could be detected by TRLFS. Investigating the interaction of *Paenibacillus* sp. cells with Eu(III) using potentiometry, a comparatively small stability constant was found for the $R–COO–Eu^{2+}$ complex (Table 2). Taking this into consideration and additionally that the corresponding Cm(III) complex might possess a lower luminescence quantum yield than the corresponding Cm(III) complex with carboxyl sites of *Sporomusa* sp., the failure of detecting a Cm(III) carboxyl complex with *Paenibacillus* sp. cells by TRLFS might be explainable.

Over the whole investigated pH region, two luminescence lifetimes were detected in the *Paenibacillus* sp. system: $\tau_1 = 238 \pm 23$ μs and $\tau_2 = 477 \pm 73$ μs. From both detected lifetimes in the bacterial Cm(III) suspensions at all investigated pH values, the longer lifetime can be clearly assigned to the cell-bound Cm(III). This implies that only one type of functional group is involved in complex formation over the whole investigated pH region. As consequence, the lifetime of in average 238 ± 23 μs belongs to a Cm(III) species in the aqueous phase. At pH 3, hardly any Cm(III) emission decay could be detected due to the low [Cm(III)] remaining in solution after sorption to the biomass. Hence, at pH 3, 95 % Cm(III) was bound, while in the neutral pH range, only 4 % Cm(III) was accumulated due to phosphate release. Therefore, in the presence of Cm(III), *Paenibacillus* sp. cells displayed a pronounced phosphatase activity which was strongly pH-dependent. At pH 8, the time-resolved measurements of the supernatant after 24 h Cm(III) contact revealed two luminescence lifetimes: 183 ± 46 μs and 327 ± 19 μs. The first one might indicate the formation of Cm(III) phosphate, while the second one implies complexation by functional groups of organic origin. Possibly, the second lifetime is attributable to Cm(III) being complexed by cell-released matter. Extraction studies with EDTA showed that binding was completely reversible indicating a pure biosorption process to the cell envelope. In summary and to propose an overall model for Cm(III) interaction with *Paenibacillus* sp. cells affecting the Cm(III) speciation, e.g., at pH 3, Cm(III) initially is present in solution solely as the Cm(III) aqua ion. As such, it must adhere well to the cell surfaces since 95 % Cm(III) gets immobilized, although remarkable cell-mediated phosphate release occurs. It was shown that Cm(III) forms primarily the complex $R–O–PO_3H–Cm^{2+}$ at the cell envelope. At pH 3, in minor amounts, $CmHPO_4^{+}$ and $CmH_2PO_4^{2+}$ coexist with the cell-bound Cm^{3+}. At pH 8, compared to pH 3, the amounts of cell-bound Cm(III) and $CmHPO_4^{+}/CmH_2PO_4^{2+}$ are reversed.

4 Summary and Conclusions

The major aim of our study was to assess the U(VI) and Cm(III) complexation by the bacterial surface functional groups of *Sporomusa* sp. MT-2.99 and *Paenibacillus* sp. MT-2.2 on a molecular level to provide stability constants. Within the investigated pH range (2–8), carboxyl and phosphoryl moieties of the bacterial cell envelope are responsible for An/Ln binding. To detect and characterize the relevant U(VI)/Eu(III)/Cm(III) surface complexes, TRLFS as a direct speciation technique in combination with potentiometric titration for U(VI) and Eu(III) was applied. It could be demonstrated that both methods can complement each other.

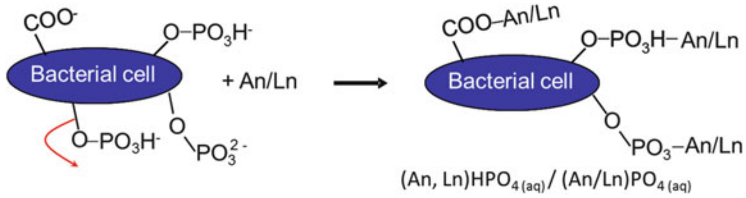

Fig. 7 Simplified scheme of impact of bacterial cells on An/Ln speciation at anaerobic conditions

In view of the versatile possible interaction mechanisms between bacteria and An/Ln, it was found that both strains display indirect interaction in the form of a pronounced pH- and [An]-dependent phosphatase activity and concomitant phosphate release, which was, for example, highest at pH 6 for *Paenibacillus* sp. Using TRLFS, it was proven that phosphate was released into the medium and binds dissolved U(VI).

Using potentiometry for both bacterial species, the following U(VI) surface complexes and their stability constants were determined: R–COO–UO_2^+, R–O–PO_3H–UO_2^+, R–O–PO_3–UO_2, and (R–O–PO_3)$_2$–UO_2^{2-}. Overall, for all strains, the following order of stability can be established for the U(VI) complexes formed at the bacterial cell surfaces: (R–O–PO_3)$_2$–UO_2^{2-} > R–O–PO_3H–UO_2^+ > R–O–PO_3–UO_2 > R–COO–UO_2^+.

In the *Sporomusa* sp. system, the surface species R–COO–Cm^{2+} and R–O–PO_3H–Cm^{2+} could be characterized spectroscopically by TRLFS. For Eu(III) with the bacterial isolates, the surface species R–COO–Eu^{2+} and R–O–PO_3H–Eu^{2+} were identified and characterized thermodynamically. Only in the *Sporomusa* sp. system, a Eu(III) surface complex with deprotonated phosphoryl groups, R–O–PO_3–Eu^+, could be identified by potentiometric titration. Eu(III) can be used as a nonradioactive analogue to mimic bacterial interactions of An(III). TRLFS studies on the interaction of Cm(III) with *Paenibacillus* sp. revealed that Cm(III) is solely bound by the bacterial phosphoryl moieties. The presence of the R–O–PO_3H–Cm^{2+} species over a wide pH range could be demonstrated. Although the existence of a Eu(III) species with carboxylic groups at pH 8 was predicted, no such Cm(III) species could be detected at that pH using TRLFS.

Our results suggested that U(VI)/Eu(III)/Cm(III) complexes with the surface functional groups of the *Sporomusa* sp. and *Paenibacillus* sp. cell envelope dominate their respective speciation over a broad pH and biomass concentration range. To summarize, the following simplified overall schema of the impact of bacterial strains on U(VI), Eu(III), and Cm(III) speciation is proposed (Fig. 7).

In conclusion, Mont Terri Opalinus clay contains a rather diverse bacterial community of representatives of *Proteobacteria*, *Firmicutes*, *Bacteroidetes*, *Acidobacteria*, and *Actinobacteria* as well as unclassified bacteria. However, only representatives of *Firmicutes* could be isolated, namely, *Sporomusa* sp. MT-2.99 and *Paenibacillus* sp. MT-2.2. The isolated Mont Terri Opalinus clay isolates may influence the speciation and hence the migration behavior of selected An/Ln under environmental conditions. The stability constants presented are valuable for modeling the U(VI), Eu(III), and Cm(III) speciation and distribution in the environment. Hence, the results contribute to better estimating the safety of a planned nuclear waste deposition site.

Further studies could focus on the metabolic activity of indigenous microbes in geological formations foreseen for a save storage of nuclear waste. The metabolic activity can affect the physical and geochemical conditions of a geologic repository and hence the speciation of accidentally released An. The quantification of the total microbial DNA in terms of cell numbers in pore waters and cores, for instance, as a function of depth should be addressed further. The performed laboratory experiments in this study could be extended to more environmental conditions (e.g., ternary systems containing the host rock—microbial cells—metals). All this would complete our knowledge of microbial processes influencing the fate of accidentally released An and fission products in the environment.

Acknowledgments The authors thank the BMWi for financial support (contract nos.: 02E10618 and 02E10971), Velina Bachvarova and Sonja Selenska-Pobell for microbial diversity analysis and isolation of the bacteria, Monika Dudek for cultivation of the bacteria, as well as the BGR for providing the clay samples. The authors are indebted to the US Department of Energy, Office of Basic Energy Sciences, for the use of ^{248}Cm via the transplutonium element production facilities at Oak Ridge National Laboratory; ^{248}Cm was made available as part of collaboration between HZDR and the Lawrence Berkeley National Laboratory (LBNL).

References

Alderighi L, Gans P, Ienco A, Peters D, Sabatini A, Vacca A (1999) Hyperquad simulation and speciation (HySS): a utility program for the investigation of equilibria involving soluble and partially soluble species. Coord Chem Rev 184:311–318

Anderson C, Johnsson A, Moll H, Pedersen K (2011) Radionuclide geomicrobiology of the deep biosphere. Geomicrobiol J 28:540–561

Barkleit A, Moll H, Bernhard G (2008) Interaction of uranium(VI) with lipopolysaccharide. Dalton Trans 21:2879–2886

Barkleit A, Moll H, Bernhard G (2009) Complexation of uranium(VI) with peptidoglycan. Dalton Trans 27:5379–5385

Bencheikh-Latmani R, Leckie JO, Bargar JR (2003) Fate of uranyl in a quaternary system composed of uranyl, citrate, goethite, and *Pseudomonas fluorescens*. Environ Sci Technol 37:3555–3559

Bernier-Latmani R, Veeramani H, Vecchia ED, Junier P, Lezama-Pacheco JS, Suvorova EI, Sharp JO, Wigginton NS, Bargar JR (2010) Non-uraninite products of microbial U(VI) reduction. Environ Sci Technol 44:9456–9462

Beveridge TJ, Doyle RJ (1989) Metal ions and bacteria. Wiley, New York

Binstead RA, Zuberbühler AD, Jung B (2004) SPECFIT global analysis system version 3.0.35

Boivin-Jahns V, Ruimy R, Bianchi A, Daumas S, Christen R (1996) Bacterial diversity in a deep-subsurface clay environment. Appl Environ Microbiol 62:3405–3412

Brockmann S, Arnold T, Bernhard G (2014) Speciation of bioaccumulated uranium(VI) by *Euglena mutabilis* cells obtained by laser fluorescence spectroscopy. Radiochim Acta 102:411–422

Brookshaw DR, Pattrick RAD, Lloyd JR, Vaughan DJ (2012) Microbial effects on mineral-radionuclide interactions and radionuclide solid-phase capture processes. Mineral Mag 76:777–806

Carlson HK, Clark IC, Blazewicz SJ, Iavarone AT, Coates JD (2013) Fe(II) oxidation is an innate capability of nitrate-reducing bacteria that involves abiotic and biotic reactions. J Bacteriol 195:3260–3268

Cormenzana JL, García-Gutiérrez M, Missana T, Alonso U (2008) Modelling large-scale laboratory HTO and strontium diffusion experiments in Mont Terri and Bure clay rocks. Phys Chem Earth 33:949–956

Cox JS, Smith DS, Warren LA, Ferris FG (1999) Characterizing heterogeneous bacterial surface functional groups using discrete affinity spectra for proton binding. Environ Sci Technol 33:4514–4521

Dittrich M, Sibler S (2005) Cell surface groups of two picocyanobacteria strains studied by zeta potential investigations, potentiometric titration, and infrared spectroscopy. J Colloid Interface Sci 286:487–495

Fang L, Cai P, Chen W, Liang W, Hong Z, Huang Q (2009) Impact of cell wall structure on the behaviour of bacterial cells in the binding of copper and cadmium. Colloids Surf A 347:50–55

Fein JB, Daughney CJ, Yee N, Davis TA (1997) A chemical equilibrium model for metal adsorption onto bacterial surfaces. Geochim Cosmochim Acta 61:3319–3328

Fowle DA, Fein JB, Martin AM (2000) Experimental study of uranyl adsorption onto *Bacillus subtilis*. Environ Sci Technol 34:3737–3741

Gans P, Sabatini A, Vacca A (1996) Investigation of equilibria in solution. Determination of equilibrium constants with the HYPERQUAD suite of programs. Talanta 43:1739–1753

Geipel G (2006) Some aspects of actinide speciation by laser-induced spectroscopy. Coord Chem Rev 250:844–854

Guillaumont R, Fanghänel T, Fuger J, Grenthe I, Neck V, Palmer DA, Rand MH (2003) Update on the chemical thermodynamics of uranium, neptunium, plutonium, americium and technetium. OECD/NEA, Paris

Günther A, Geipel G, Bernhard G (2006) Complex formation of U(VI) with the amino acid L-threonine and the corresponding phosphate ester O-phospho-L-threonine. Radiochim Acta 94:845–851

Günther A, Raff J, Merroun ML, Roßberg A, Kothe E, Bernhard G (2014) Interaction of U (VI) with Schizophyllum commune studied by microscopic and spectroscopic methods. Biometals 27:775–785

Hansel CM, Fendorf S, Jardine PM, Francis CA (2008) Changes in bacterial and archaeal community structure and functional diversity along geochemically variable soil profile. Appl Environ Microbiol 74:1620–1633

Kalinowski BE, Oskarsson A, Albinsson Y, Arlinger J, Ödegaard-Jensen A, Pedersen K (2004) Microbial leaching of trace elements from Randstad mine tailings. Geoderma 122:177–194

Kelly SD, Wu WM, Yang F, Criddle CS, Marsh TL, O'Loughlin EJ, Ravel B, Watson D, Jardine PM, Kemner KM (2010) Uranium transformations in static microcosms. Environ Sci Technol 44:236–242

Kimura T, Choppin GR (1994) Luminescence study on determination of the hydration number of Cm(III). J Alloys Compd 213–214:313–317

Krawczyk-Bärsch E, Lütke L, Moll H, Bok F, Steudner R, Rossberg A (2015) A spectroscopic study on U(VI) biomineralization in cultivated *Pseudomonas fluorescens* biofilms isolated from granitic aquifers. Environ Sci Pollut Res 22:4555–4565

Kuhner CH, Frank C, Grießhammer A, Schmittroth M, Acker G, Gößner A, Drake HL (1997) *Sporomusa silvacetica* sp. nov., an acetogenic bacterium isolated from aggregated forest soil. Int J Syst Bacteriol 47:352–358

Lloyd JR, Gadd GM (2011) The geomicrobiology of radionuclides. Geomicrobiol J 28:383–386

Lopez-Fernandez M, Fernandez-Sanfrancisco O, Moreno-Garcia A, Martin-Sanchez I, Sanchez-Castro I, Merroun ML (2014) Microbial communities in bentonite formations and their interactions with uranium. Appl Geochem 49:77–86

Lopez-Fernandez M, Cherkouk A, Vílchez-Vargas R, Sandoval R, Pieper D, Boon N, Sánchez-Castro I, Merroun ML (2015) Bacterial diversity in bentonites, engineered barrier for deep geological disposal of radioactive wastes. Microb Ecol. doi:10.1007/s00248-015-0630-7

Lovley DR, Philips EJP, Gorby YA, Landa ER (1991) Microbial reduction of uranium. Nature 350:413–416

Lütke L (2013) Interaction of selected actinides (U, Cm) with bacteria relevant to nuclear waste disposal. Doctoral thesis TU Dresden, Germany

Lütke L, Moll H, Bernhard G (2012) Insights on the Uranium(VI) speciation with *Pseudomonas fluorescens* on a molecular level. Dalton Trans 41:13370–13378

Lütke L, Moll H, Bernhard G (2013) The U(VI) speciation influenced by a novel *Paenibacillus* isolate from Mont Terri Opalinus clay. Dalton Trans 42:6979–6988

Makarova KS, Aravind L, Wolf YI, Tatusov RL, Minton KW, Koonin EV, Daly MJ (2001) Genome of the extremely radiation-resistant bacterium *Deinococcus radiodurans* viewed from the perspective of comparative genomics. Microbiol Mol Biol Rev 65:44–79

Markai S, Andres Y, Montavon G, Grambow B (2003) Study of the interaction between europium (III) and *B*acillus subtilis: fixation sites, biosorption and reversibility. J Colloid Interface Sci 262:351–361

Mauclaire L, McKenzie J, Schwyn B, Bossart P (2007) Detection and identification of indigenous microorganisms in Mesozoic claystone core samples from the Opalinus clay formation (Mont Terri Rock Laboratory). Phys Chem Earth 32:232–240

Merroun ML, Selenska-Pobell S (2008) Bacterial interactions with uranium: an environmental perspective. J Contam Hydrol 102:285–295

Moll H, Merroun ML, Hennig C, Rossberg A, Selenska-Pobell S, Bernhard G (2006) The interaction of *Desulfovibrio äspöensis* DSM 10631^T with plutonium. Radiochim Acta 94:815–824

Moll H, Johnsson A, Schäfer M, Pedersen K, Budzikiewicz H, Bernhard G (2008a) Curium(III) complexation with pyoverdins secreted by a groundwater strain of *Pseudomonas fluorescens*. Biometals 21:219–228

Moll H, Glorius M, Bernhard G, Johnsson A, Pedersen K, Schäfer M, Budzikiewicz H (2008b) Characterization of pyoverdins secreted by a subsurface strain of *Pseudomonas fluorescens* and their interaction with uranium(VI). Geomicrobiol J 25:157–166

Moll H, Glorius M, Johnsson A, Schäfer M, Budzikiewicz H, Pedersen K, Bernhard G (2010) Neptunium(V) complexation by natural pyoverdins and related model compounds. Radiochim Acta 98:517–576

Moll H, Lütke L, Bachvarova V, Steudner R, Geißler A, Krawczyk-Bärsch E, Selenska-Pobell S, Bernhard G (2013a) Microbial diversity in Opalinus clay and interactions of dominant microbial strains with actinides. Wissenschaftlich-Technische Berichte, HZDR-036. Helmholtz-Zentrum Dresden-Rossendorf, Dresden

Moll H, Lütke L, Barkleit A, Bernhard G (2013b) Curium(III) speciation studies with cells of a groundwater strain of *Pseudomonas fluorescens*. Geomicrobiol J 30:337–346

Moll H, Lütke L, Bachvarova V, Cherkouk A, Selenska-Pobell S, Bernhard G (2014) Interactions of the Mont Terri Opalinus clay isolate *Sporomusa* sp. MT-2.99 with Curium(III) and Europium(III). Geomicrobiol J 31:682–696

Nyman JL, Marsh TL, Ginder-Vogel MA, Gentile M, Fendorf S, Criddle C (2006) Heterogeneous response to biostimulation for U(VI) reduction in replicated sediment microcosms. Biodegradation 17:303–316

Ohnuki T, Yoshida T, Ozaki T, Samadfam M, Kozai N, Yubuta K, Mitsugashira T, Kasama T, Francis AJ (2005) Interaction of uranium with bacteria and kaolinite clay. Chem Geol 220:237–243

Oren A (2002) Molecular ecology of extremely halophilic archaea and bacteria. FEMS Microbiol Ecol 39:1–7

Panak PJ, Nitsche H (2001) Interaction of aerobic soil bacteria with plutonium(VI). Radiochim Acta 89:499–504

Panak PJ, Raff J, Selenska-Pobell S, Geipel G, Bernhard G, Nitsche H (2000) Complex formation of U(VI) with *Bacillus*-isolates from a uranium mining waste pile. Radiochim Acta 88:71–76

Pantke C, Obst M, Benzerara K, Morin G, Ona-Nguema G, Dippon U, Kappler A (2012) Green rust formation during Fe(II) oxidation by the nitrate-reducing *Acidovorax* sp. strain BoFeN1. Environ Sci Technol 46:1439–1446

Pedersen K, Albinsson Y (1992) Possible effects of bacteria on trace-element migration in crystalline bed-rock. Radiochim Acta 58–59:365–369

Poulain S, Sergeant C, Simonoff M, Le Marrec C, Altmann S (2008) Microbial investigations in Opalinus clay, an argillaceous formation under evaluation as a potential host rock for a radioactive waste repository. Geomicrobiol J 25:240–249

Reitz T, Rossberg A, Barkleit A, Selenska-Pobell S, Merroun ML (2014) Decrease of U (VI) immobilization capability of the facultative anaerobic strain *Paenibacillus* sp. JG-TB8 under anoxic conditions due to strongly reduced phosphatase activity. PLoS One 9, e102447

Rodriguez-Diaz M, Lebbe L, Rodelas B, Heyrman J, De Vos P, Logan NA (2005) *Paenibacillus wynnii* sp. nov., a novel species harbouring the nifH gene, isolated from Alexander Island, Antarctica. Int J Syst Evol Microbiol 55:2093–2099

Rothstein A (1962) Functional implications of interactions of extracellular ions with ligands of the cell membrane. Circulation 26:1189–1200

Santelli CM, Orcutt BN, Banning E, Bach W, Moyer CL, Sogin ML, Staudigel H, Edwards KJ (2008) Abundance and diversity of microbial life in ocean crust. Nature 453:653–656

Selenska-Pobell S, Kampf G, Flemming K, Radeva G, Satchanska G (2001) Bacterial diversity in soil samples from two uranium waste piles as determined by rep-APD, RISA and 16S rDNA retrieval. Antonie Van Leeuwenhoek 79:149–161

Shapiro J (1967) Induced rapid release and uptake of phosphate by microorganism. Science 155:1269–1271

Sharp JO, Lezama-Pacheco JS, Schofield EJ, Junier P, Ulrich KU, Chinni S, Veeramani H, Margot-Roquier C, Webb SM, Tebo BM, Giammar DE, Bargar JR, Bernier-Latmani R (2011) Uranium speciation and stability after reductive immobilization in aquifer sediments. Geochim Cosmochim Acta 75:6497–6510

Stewart EJ (2012) Growing unculturable bacteria. J Bacteriol 194:4151–4160

Stroes-Gascoyne S, Schippers A, Schwyn B, Poulain S, Sergeant C, Simonoff M, Le Marrec C, Altmann S, Nagaoka T, Mauclaire L, McKenzie J, Daumas S, Vinsot A, Beaucaire C, Matray JM (2007) Microbial community analysis of Opalinus clay drill core samples from the Mont Terri underground research laboratory, Switzerland. Geomicrobiol J 24:1–17

Suzuki Y, Banfield JF (2004) Resistance to, and accumulation of, uranium by bacteria from a uranium-contaminated site. Geomicrobiol J 21:113–121

Takai K, Nakamura K, Toki T, Tsunogai U, Miyazaki M, Miyazaki J, Hirayama H, Nakagawa S, Nunoura T, Horikoshi K (2008) Cell proliferation at 122°C and isotopically heavy CH_4 production by a hyperthermophilic methanogen under high-pressure cultivation. Proc Natl Acad Sci USA 105:10949–10954

Texier AC, Andres Y, Illemassene M, Le Cloirec P (2000) Characterization of lanthanide ions binding sites in the cell wall of *Pseudomonas aeruginosa*. Environ Sci Technol 34:610–615

Thury M, Bossart P (1999) The Mont Terri Rock laboratory, a new international research project in a Mesozoic shale formation, in Switzerland. Eng Geol 52:347–359

Urios L, Marsal F, Pellegrini D, Magot M (2012) Microbial diversity of the 180 million-year-old Toarcian argillite from Tournemire, France. Appl Geochem 27:1442–1450

Urios L, Marsal F, Pellegrini D, Magot M (2013) Microbial diversity at iron-clay interfaces after 10 years of interaction inside a deep argillite geological formation (Tournemire, France). Geomicrobiol J 30:442–453

Voet D, Voet JG, Pratt CW (2002) Lehrbuch der Biochemie. Wiley, Germany

Wouters K, Moors H, Boven P, Leys N (2013) Evidence and characteristics of a diverse and metabolically active microbial community in deep subsurface clay borehole water. FEMS Microbiol Ecol 86:458–473

Yee N, Benning LG, Phoenix VR, Ferris FG (2004) Characterization of metal-cyanobacteria sorption reactions: a combined macroscopic and infrared spectroscopic investigation. Environ Sci Technol 38:775–782

Yutin N, Galperin MY (2013) A genomic update on clostridial phylogeny: Gram-negative spore formers and other misplaced clostridia. Environ Microbiol 15:2631–2641

Zhengji Y (2010) Microbial removal of uranyl by uranyl reducing bacteria in the presence of Fe (III) (hydr)oxides. J Environ Radioact 101:700–705

Analysis of Radionuclides in Environmental Samples

A.V. Voronina, N.D. Betenekov, V.S. Semenishchev, and T.A. Nedobukh

Contents

Abstract The main steps of radionuclide determination in environmental samples are presented in this chapter. Details of a sample pretreatment, tracers, and carriers used in radiochemical analysis as well as methods of radionuclide preconcentration and separation are discussed. The comparison of characteristics is given for thin-layer sorbents based on various supports (wood cellulose, copolymer of styrene and divinylbenzene, slices and disks of cellulose triacetate, lavsan film, polyamide disks, polyacrylonitrile), which are used for selective preconcentration and separation of radionuclides. Main applications of extraction chromatographic resins in radiochemical analysis are also shown.

Keywords Radionuclides • Radiochemical analysis • Preconcentration • Separation • Coprecipitation • Sorbents • Extraction chromatographic resins

---

A.V. Voronina (✉) • N.D. Betenekov • V.S. Semenishchev • T.A. Nedobukh
Radiochemistry and Applied Ecology Chair, Physical Technology Institute, Ural Federal University, Mira str., 19, Ekaterinburg, Russia
e-mail: av.voronina@mail.ru

C. Walther, D.K. Gupta (eds.), *Radionuclides in the Environment*,
DOI 10.1007/978-3-319-22171-7_13

1 Introduction

Spontaneous migration of natural radionuclides and anthropogenic dissipation of both natural and artificial radionuclides due to normal activity and accidents at enterprises of nuclear fuel cycle and some other sectors (such as mining, metallurgy, and chemical industry) result in radionuclide transfer to natural water and soils. Determination of natural and artificial radionuclides in environmental samples is an integral part of radioecological monitoring. The radioecological monitoring is greatly important for opportune decision-making and decreasing internal radiation dose that is conditioned by radionuclide accumulation in a human's body. According to the recommendations of the International Commission on Radiological Protection (ICRP 2007), the approaches to normalization and control should be the same for both natural and anthropogenic radionuclides. Obtaining necessary information for modeling of both natural and anthropogenic radionuclide migrations in various landscapes and media, including radioactively contaminated lands, is another purpose of the radioecological monitoring. Currently and especially in cases of an emergency, the radioecological monitoring requires rapid radioanalytical techniques with high precision and reliability of results obtained (Moskvin et al. 2011). In many cases, determination of individual radionuclides may be necessary other than determination of gross alpha or beta activity of a sample.

The following methods are used for identification and quantitative determination of radionuclides:

A. Determination of a Radionuclide Activity Using Intensity, Type, and Energy of Its Emission In the radioecological monitoring, some gamma-emitting radionuclides may be determined directly or after a minimal sample treatment using gamma spectrometry. Gamma spectrometry (especially, in case where semiconductor spectrometer is used) allows for synchronous and independent registration of various radionuclides; therefore, operations of their separation become unnecessary. In some cases, a sample may be measured without any treatment. It is necessary to take into account the influence of geometry and density of a sample as well as contribution of background and other gamma emitters to complete absorption peak of the analyte. Tasks of determination of pure alpha and beta emitters are rather more complicated. If the activity concentration of the analyte or its emission's penetrability is very low, operations of preconcentration and chemical separation are necessary. The analyte should be separated from a sample with known chemical yield to a relatively small volume in a form being suitable for further measurement. For example, operations of separation are still necessary for the determination of the radiotoxic fission product ^{90}Sr (pure beta emitter).

Preparation of a thin alpha source is an indispensable condition of measurement of alpha-emitting radionuclides via both alpha radiometry and especially alpha spectrometry. In case of even relatively thick sources, alpha spectrometry cannot be used for the reliable identification of radionuclides because of self-absorption and dispersion of alpha rays in the source. If the alpha source is prepared using

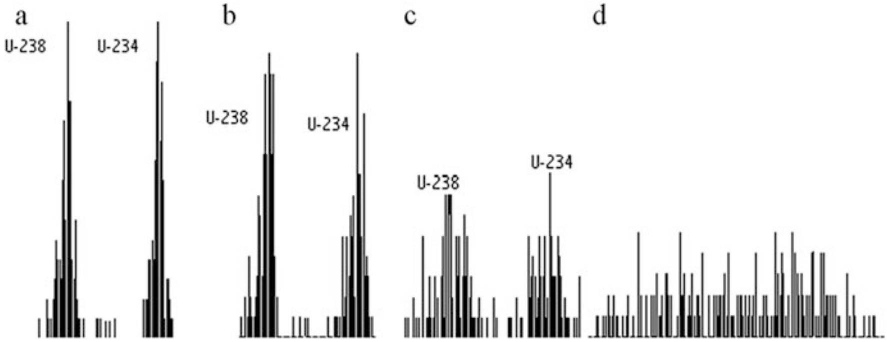

Fig. 1 α-spectra of natural uranium affected by various salt contents in the solution: (**a**) <2 mg, (**b**) 15 mg, (**c**) 75 mg, (**d**) 150 mg

sorption method (e.g., sorption-active disks or films), then additional purification occurs as a result of source preparation. In contrast to that, requirements to purity of the concentrate are very exacting, if the electrodeposition method is used for alpha source preparation. As an example, four alpha spectra of sources obtained via natural uranium electrodeposition from solutions with various salt contains are presented in Fig. 1. Total salt content in a sample up to 75 mg allows for obtaining sources with relatively high uranium yield and spectra with good resolution. Increase of total salt content results in higher uranium yield, but resolution of the spectrum becomes lower because of increasing of thickness of the source. Salt content of 150 mg and more makes obtaining resolved uranium peaks impossible.

The use of liquid scintillation spectrometers allows avoiding the problem of thin source preparation; however, these spectrometers are very expensive and not available for many laboratories performing routine radiochemical analysis. In alpha spectrometric measurements, chemical separation is also necessary for the separate determination of radionuclides with unresolvable peaks, such as ^{241}Am/^{238}Pu or ^{237}Np/^{234}U. The decay scheme should be also taken into account, when a scheme of radiochemical analysis is chosen. For some radionuclides, determination of emission of its radioactive daughter nuclide may be rather easier than determination of its own emission. For example, analysis of pure beta emitter ^{137}Cs via gamma rays of daughter ^{137m}Ba, determination of low-energy beta emitter ^{90}Sr via high-energy beta particles of equilibrium ^{90}Y, and measurement of ^{210}Pb activity via dynamics of daughter ^{210}Bi ingrowth are often used.

B. Determination of Weight of a Radionuclide via Physicochemical Methods This option is reasonable for measurement of very long-lived radionuclides, such as ^{238}U (4.47×10^9 a), ^{232}Th (1.4×10^{10} a), ^{99}Tc (2.1×10^5 a), ^{129}I (1.61×10^7 a), etc. (Bienvenu et al. 2004; Yoshida et al. 2007). Weight of a radionuclide is determined via mass spectrometry (MS); this method allows for the determination of individual isotopes (including stable isotopes) with quite low detection limits. In this case, the main purpose of sample treatment is the maximum possible concentration of analyte and elimination of a limited number of interfering

Fig. 2 A typical generalized radioanalytical scheme for environmental samples

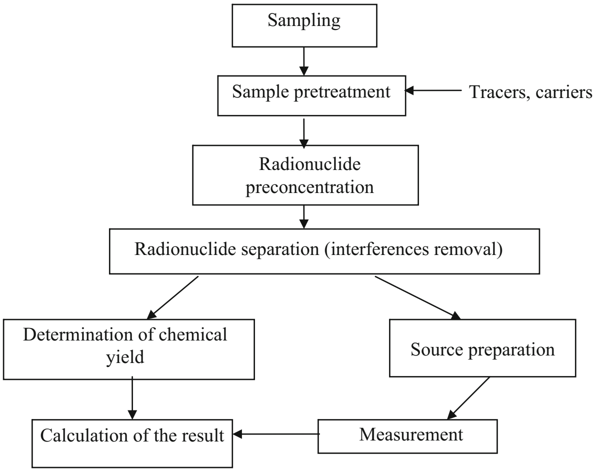

elements. Elimination of isobaric interferences is the most important step of sample treatment in case of long-lived radionuclide determination via MS. For example, stable isotope ^{126}Te interferes MS determination of long-lived fission product ^{126}Sn; in case of ^{226}Ra determination via ICP-MS, isobaric interference of ^{88}Sr and ^{138}Ba may occur (Maxwell and Culligan 2012).

Thus, the main steps of a scheme of radionuclide analysis in environmental samples are sampling (the sample should be representative), sample pretreatment, radionuclide preconcentration and/or separation, source preparation, measurement, and calculation. A typical generalized radioanalytical scheme for environmental samples is given in Fig. 2.

2 Principles of Sampling and Sample Pretreatment

A significant maldistribution is typical for radionuclides in the environment. Therefore, the result of analysis strongly depends on accuracy and carefulness of sampling. Incorrect sampling may result in a serious mistake, especially in cases of analysis of environmental objects. This mistake may be suppressed by the increase of parallel sample quantity and volume; however, in practice the quantity of samples is always limited. Thus, when a sampling is planned and performed, the main purpose is to obtain representative sample containing the analyte concentration corresponding to that average in the studied environmental object.

The next stage is sample conservation and storage before further analysis. During the sample storage (especially in cases of aqueous and biological samples), some undesirable processes may occur affecting the result of analysis. Among these processes are partial loss of a radionuclide due to sorption by a container, formation of complexes and colloids, precipitation (mostly coprecipitation with iron hydroxide), and biological reactions. It is impossible to absolutely avoid these processes; however, there are a number of techniques making minimization of these processes possible. Conservation of aqueous samples is performed by the sample acidifying to pH 2 in order to avoid sorption of the analyte by the container. It is preferable to acidify the sample immediately at the sampling point. Pretreatment of aqueous samples includes boiling for destruction of hydroxide and carbonate complexes and colloids that may bind the analyte as well as sample filtration through a wide-porous filter in order to remove particles of sediments and organic fragments that may contain elevated activity of the analyte.

Bioassays should be analyzed as fast as possible. Storage of bioassays during several days is possible in a refrigerator at the temperature of 4 °C. In some cases a chemical preserving agent (formalin, ethanol, etc.) is added to the bioassay in order to increase its storage life (Teldesi et al. 1985); however, it should be taken into account that the preserving agent may interfere further analysis. Homogeneity is very important for bioassays. Samples of vegetation and animals (meat, fish) are cut, grinded, and averaged. Then these bioassays are dried in a drying oven at the temperature of 100–120 °C; dry samples are transferred into a porcelain cup, carbonized using a hotplate or infrared lamp, and finally ashed in a porcelain crucible at the temperature of 600–700 °C. Ashing time depends on quantity and humidity of a sample. This operation of dry mineralization (ashing) is necessary for removal of all organic compounds from a sample. In cases of radiochemical analysis of biological liquids containing elevated concentration of organic compounds (urine, milk, blood, etc.), sample oxidization via boiling in the presence of nitric acid and hydrogen peroxide ("wet ashing") is often used.

Pretreatment of soil samples usually consists of removing of large components (stones, roots, etc.), grinding and ashing for elimination of organic compounds, and finally sample leaching with the aim of a radionuclide transfer to a solution. Dry ashing of soil samples is performed at the temperature of 300–400 °C. Lower temperature of ashing may be insufficient for complete destruction of organic compounds. On the other hand, higher temperature of ashing may result in loss of a radionuclide due to either evaporation (this is typical for relatively volatile radionuclides such as cesium and ruthenium isotopes) or a radionuclide transformation into a very stable insoluble form [e.g., plutonium transformation into insoluble dioxide PuO_2 as a result of heating (Veselsky 1977)]. Nitric or hydrochloric acid as well as aqua regia are commonly used for sample leaching; hydrofluoric acid is also used if "hot particles" (particles of irradiated nuclear fuel with very high activity concentration) present in a soil sample (Holgye and Burcik 1992).

3 Carriers and Tracers in Radiochemical Analysis

Usually analyzed radionuclides present in environmental samples as a microconstituent. For example, 1 Bq L^{-1} of ^{210}Pb in a water sample corresponds to its concentration of only 6×10^{-14} g L^{-1}. Behavior of a microconstituent may significantly differ from behavior of the same chemical element presenting in relatively high concentration. A significant part of the analyte may be lost as a result of sorption by a container or fixation by colloidal particles; therefore, procedures of preconcentration and separation cannot be performed with a high effectiveness. *A carrier* is added to the sample in the beginning of analysis in order to avoid the undesirable effect of a microconstituent. Stable isotopes of the same chemical element may be used as the carrier (*an isotopic carrier*), for example, stable strontium for the analysis of ^{90}Sr. In the case when the analyzed radionuclide has no stable isotopes, *a nonisotopic carrier* may be used. There are two kinds of nonisotopic carriers: *specific carriers* (stable isotopes of a chemical analogue of the analyte) and *nonspecific carriers* (collector for group separation of several radionuclides). Barium for ^{226}Ra, cerium or lanthanum for ^{241}Am, and tellurium for ^{210}Po are the most typical examples of a specific nonisotopic carrier. Among nonspecific nonisotopic carriers used in radiochemical analysis, there are polyvalent metal hydroxides, iron (III) phosphate and carbonate, manganese (II) hydroxide, etc. The chemical yield of the analyte may be determined on the basis of a carrier's yield. It also should be taken into consideration that an elevated amount of the carrier will make preparation of a high-quality thin alpha or beta source impossible.

Tracer is a radionuclide used in radiochemical analysis for the determination of chemical yield. Yield is the ratio between quantity of an analyte in the final concentrate and its quantity in the initial sample; yield determination is necessary in order to estimate a possible loss of the analyte in preconcentration and separation steps. Chemical yield is determined via addition of a known activity of a tracer and further measurement of its activity in the final concentrate. Radiation of the tracer chosen should not interfere measurement of the analyte. Isotopes with another type or energy of emission as well as short-lived radionuclides are well suitable for this purpose. The use of a stable isotope as a tracer is also possible. Among the examples of tracers, used in radiochemical analysis for the yield determination, there are ^{85}Sr (K-capture, pure gamma emitter) or stable strontium (gravimetry, ICP-MS, or flame photometry) for ^{90}Sr (pure beta emitter), ^{239}Np (2.36 days) for ^{237}Np (2.1×10^6 a), ^{236}U (higher energy of alpha particles, good resolution of peaks) for ^{234}U, and ^{212}Pb (gamma emitter; short half-life (10 h) allows for its total decay during ^{210}Bi in growth) for ^{210}Pb (pure beta emitter) (Sapozhnikov et al. 2006).

4 Methods of Nonselective Preconcentration of Radionuclides

The necessity of determination of very low activities is one of the characteristic properties of routine radiochemical analysis of environmental samples. The operator often has to use large volume of weight of a sample in order to achieve the required detection limit. Typical activities and volumes of real analyzed environmental samples are given in Table 1.

Table 1 Activities and volumes of samples necessary for analysis

Radionuclides	Sample type	Activity level (Bq m^{-3})	Sample volume	References
^{222}Rn	Air	3–9	1 m^3	EL-Hussein et al. (2001)
^{210}Pb	Air	0.0001–0.0008	1,800 m^3	EL-Hussein et al. (2001)
^{7}Be	Air	0.001–0.003	1,800 m^3	EL-Hussein et al. (2001)
^{85}Kr	Air	1.1–1.4	10 m^3	Igarashi et al. (2000)
^{133}Xe	Air	0.001–0.003	100,000 m^3	Bowyer et al. (1997)
^{7}Be	Snow	2800–2900	12–15 L	Sapozhnikov et al. (2006)
^{32}P, ^{33}P	Rainwater	9–68	5–20 L	Benitez-Nelson and Buesseler (1998)
^{32}P, ^{33}P	Seawater	0.05–0.09	>4000 L	Benitez-Nelson and Buesseler (1998)
^{210}Pb	Seawater	0.3–4	3 L	Nozaki et al. (1998)
^{234}Th	Seawater	3–42	2–1000 L	Buesseler et al. (2001)
^{90}Sr	Seawater	>2	10–20 L	Salbu et al. (1997)
^{239}Pu, ^{240}Pu	Seawater	0.0006–0.01	60 L	Sanchez et al. (1991)
^{137}Cs	Seawater	>2	>50 L	Smith et al. (1998)
Pu, Am	Seawater	0.001–0.05	50–500 L	La Rosa et al. (2000)

Since operations of chemical separation of an analyte from a large sample result in a high spending of reagents, labor, and time as well as in producing a high waste volume, a nonselective preconcentration of the analyte and a part of impurities into a minimal volume sounds reasonable. Methods of nonselective preconcentration are based on either coprecipitation of the analyte with a sparingly soluble compound or its sorption by a nonselective ion exchange resin. In the case of aqueous samples when the last option is realized, organic cation exchange resins based on copolymer of styrene and divinylbenzene are used mostly often.

Coprecipitation is a process of joint precipitation of a microconstituent (analyzed radionuclide) with a phase of a sparingly soluble compound due to isomorphous joint cocrystallization or absorption of the microconstituent on the surface of the sediment; in any case, the microconstituent does not form its own phase. The earliest schemes of radiochemical analysis included also methods of radionuclide separation using selective coprecipitation. However, currently these precipitation methods were replaced by more selective sorption and extraction methods, whereas precipitation methods are used mostly for preconcentration. Hydroxides, oxides, phosphates, and some other insoluble salts of polyvalent metals are typical nonselective collectors for radionuclides. Some examples of nonselective collectors and their main applications are given in Table 2.

Quantitative separation of the precipitate from the solution is the most laborious and time-consuming operation of the preconcentration step via coprecipitation. Gravity thickening with further decantation of supernatant, vacuum-assistant filtration, or filtration of the solution through a filter cartridge is used in order to accelerate and simplify this step. The advantages of the last option are a high speed and a low laboriousness of the preconcentration step. The effectiveness of the precipitate separation from the solution may be increased by decrease of a

Table 2 Examples of nonselective collectors for radionuclide coprecipitation

Collector	Radionuclide, coprecipitated with the collector	References
$Fe(OH)_3$, $Al(OH)_3$, $Mn(OH)_4$	Isotopes of heavy metals, actinides, ^{33}P, ^{210}Pb	Qiao et al. (2014); La Rosa et al. (2000)
$BaSO_4$	$^{226, 228}Ra$, ^{210}Pb	Elsinger et al. (1982)
CaC_2O_4	^{90}Sr	Brun et al. (2002)
$Ca_3(PO_4)_2$	^{90}Sr, $^{226, 228}Ra$, ^{210}Pb, U (VI), Th	Maxwell et al. (2013)
$Fe_4[Fe(CN)_6]_3$	$^{137, 134}Cs$	Tananaev et al. (1971)
LaF_3	Actinides (III, IV)	Maxwell et al. (2014)
MnO_2	$^{226, 228}Ra$, ^{210}Pb, ^{228}Th	Grabowski et al. (2010)

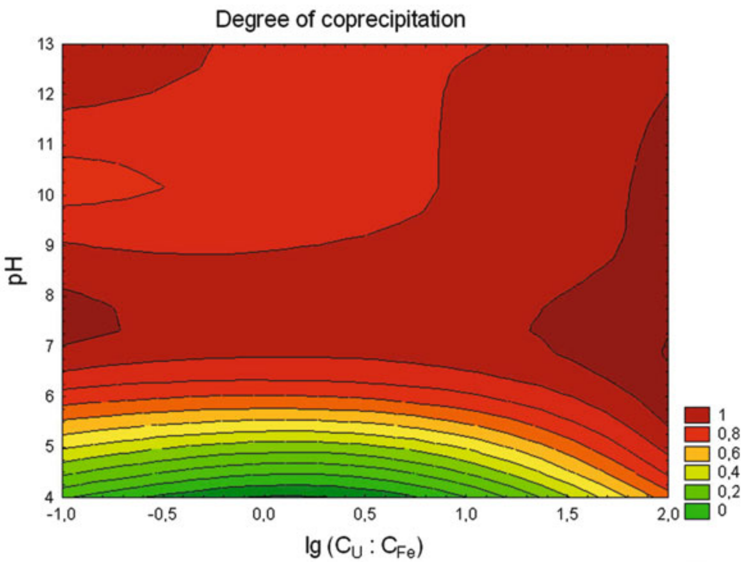

Fig. 3 The dependence of degree of uranium coprecipitation with iron (III) hydroxide on pH and value of $\log(C_U{:}C_{Fe})$

carrier's quantity as well as by selection of parameters of the filter cartridge. Cellulose may be used as the basis for the filter cartridge due to its extended surface area and good filtering property.

Coprecipitation with iron (III) hydroxide and further frontal chromatographic separation of the precipitate on cellulose was suggested by authors of this chapter as a method of uranium and thorium preconcentration. Preliminary experiments have shown that iron naturally occurring in water (0.08–1 mg L^{-1}) was not enough for formation of iron (III) hydroxide phase. Therefore, addition of supplementary iron (III) is required for preconcentration. Optimal conditions of uranium and thorium coprecipitation with iron (III) hydroxide, as a dependence on pH, salt content, and Fe(III), U, and Th concentrations, were found as a result of theoretical and experimental modeling. Typical dependence of degree of uranium coprecipitation with iron (III) hydroxide is presented in Fig. 3.

Conditions of the coprecipitation are somewhat different for uranium and thorium; however, their joint preconcentration is possible. Pretreatment and grain size of the cellulose, size of the cartridge, and flow rate are the main parameters affecting quantitative separation of iron hydroxide on the filtration cartridge. As it has been determined, pretreatment of the cellulose by alkaline solution, the grain size of 0.2–0.4 mm, flow rate of 100–130 mL min^{-1} cm^{-2}, and ratio between height and diameter of the cartridge $H/d = 10{:}1$ are the optimal parameters providing quantitative separation of iron hydroxide. Capacity of the cellulose to iron hydroxide at pH > 6 was 11 ± 2 mg of Fe per gram of the cellulose. The analysis of the breakthrough chromatogram has shown that capacity of the cellulose depends on the quantity of iron added; for example, at the iron concentration of 100 μg L^{-1}, breakthrough was observed after a sample loading volume of 500 bed volumes. Thus, the minimal weight of the cellulose required for filtration of 100 L water sample is only 20 g.

The following method for uranium and thorium preconcentration from samples of natural water was suggested on the ground of the experimental data described above:

1. Sample conservation using nitric acid.
2. Addition of an aliquot of iron (III) chloride in order to achieve iron concentration of 0.1–2.5 mg L^{-1}.
3. PH adjustment to 6.5–7.5 with NaOH solution and further iron hydroxide precipitation during 10–15 min.
4. Frontal chromatographic separation of the precipitate on the cartridge (H/d = 10:1, flow rate = 130 mL min^{-1} cm^{-2}). The cellulose quantity is 1 g per 1 L of a sample.

The method was tested for thorium preconcentration from samples of waters with various salt contents (200–1700 mg L^{-1}). The results have shown that the addition of 0.1 mg of iron (III) per 1 L of a sample was enough quantitatively for both uranium and thorium preconcentration; chemical yields were (92 ± 10) % and (98 ± 8) % for uranium and thorium, respectively.

Thus, the described technique coprecipitation with iron (III) hydroxide and further frontal chromatographic separation of the precipitate on cellulose is an effective method of uranium and thorium preconcentration from samples of fresh natural waters. However, further treatment of the concentrate is necessary for radionuclide separation and purification. For example, the following scheme was suggested for the determination of isotopic ratio of uranium: uranium stripping from the cartridge using $NaHCO_3$ solution, the second concentration and purification step using the strong acid cation exchange resin CU-2 (copolymer of styrene and divinylbenzene with sulfonate groups), desorption, and finally source preparation via electrodeposition or sorption by thin-layer titanium hydroxide; the scheme provides uranium yield as high as 95 ± 12 % and also good separation from iron. Another scheme was suggested for thorium: thorium stripping using ammonium oxalate solution and source preparation via microprecipitation with cerium fluoride. This scheme provides thorium yield of 96 ± 9 % and good separation from uranium: in case of uranium concentration in a sample of 500 μg L^{-1}, the decontamination factor was ~$10^2 - 10^3$.

5 Methods of Selective Preconcentration and Separation of Radionuclides in Radiochemical Analysis

Developing rapid methods of radionuclides, selective separation is one of the most important tasks in modern radiochemical analysis. An intensive development of the theory and practice of separation methods based on processes of interphase distribution has given occasion to the fact that sorption and extraction processes became the main separation processes in the chemical part of radiochemical analysis.

5.1 Use of Selective Sorbents

The use of selective sorbents allows organizing both rapid radionuclide preconcentration from large volumes of natural waters (including fresh surface water, seawater, etc.) and effective separation of the analyzed radionuclide immediately as a result of sorption; this results in a significant simplification and acceleration of the analytical procedure. A wide choice of available sorbents and various techniques of organizing the process of interphase distribution (batch conditions, chromatography, etc.) are the main advantages of sorption methods. Another advantage of sorption methods is the possibility of full separation of a radionuclide that makes determination of its chemical yield unnecessary. The use of sorbents based on ferrocyanides and molybdophosphates for cesium separation and the use of sorbents based on manganese dioxide for radium separation from aqueous samples are typical examples of selective sorbent use for simultaneous preconcentration and separation of radionuclides in radiochemical analysis.

Thin-layer sorbents synthesized by the method of a thin-layer impregnation onto various supports are widely used in radiochemical analysis of environmental samples.

5.1.1 Thin-Layer Inorganic Sorbents

Chemical methods of precipitation of a thin layer of a sparingly soluble compound onto the surface of a carrier are the basis of synthesis of thin-layer sorbents (TLS) (Betenekov et al. 1976). Beads of both organic and inorganic supports may be used for TLS synthesis. Films, slices, and fibers are also interesting supports. For these sorbents, improved kinetic characteristics of sorption are typical due to decrease of the inhibiting influence of internal diffusion. In contrast to sorbents synthesized via the impregnation method, TLS have better mechanical characteristics; the method also allows for precipitation of thin films onto nonporous nonswelling materials (glass, plastic, etc.). TLS based on granulated supports with good mechanical characteristics are widely used for concentration and separation of various elements in both static and dynamic conditions, including schemes of radiochemical analysis (Betenekov et al. 1976, 1979, 1983).

Table 3 summarizes the results of systematic studies of radionuclide speciation and also static, kinetics, and dynamics of radionuclide interphase distribution in systems (TLS—aqueous solution).

The following abbreviations are used in Table 3:

(1) A sorbent type: IPF is iron–potassium ferrocyanide; IP is iron phosphate; BS is barium sulfate; TH is titanium hydroxide; ZnS, CdS, and CuS are zinc, cadmium, and copper sulfides, respectively. Support types are as follows: C is wood cellulose with the grain size of 0.2–0.6 mm; CSD is spherical copolymer of styrene and divinylbenzene; CTA is slices or disks of cellulose triacetate.
(2) Sample type: SW is seawater; FW is freshwater.
(3) Radionuclide speciation: α_d and α_c are parts of dissolved and colloidal forms of a radionuclide (determined using filtration through a 70-nm track membrane).
(4) Characteristics of sorption static: K_{d1} and K_{d2} are distribution coefficients of a radionuclide calculated for gram of a TLS and for gram of a sorption-active layer, respectively, L kg^{-1}.
(5) Characteristics of sorption kinetics: β_1 and β_2 are the sorption rate constants for the first and the second portions of kinetic curves, min^{-1}.
(6) Characteristics of sorption dynamics: V_R is the retention volume, mL.

Radionuclide speciation in natural waters was studied using sorption and ultrafiltration through track membranes. It was shown for seawater at pH 8.2 that cesium, strontium barium, cobalt, and uranium radionuclides present totally in ionic forms, whereas REEs (Y, Ce), ruthenium, and lead radionuclides, besides ionic forms, occurred as pseudocolloidal species due to the sorption on various colloidal particles; radioactive colloids of iron consist of both pseudocolloidal and own colloidal species.

In the case of seawater at pH 5, the major part of uranium and plutonium present in a sample as radioactive colloids and decrease of salt content (freshwater) result in formation of radiocesium pseudocolloids. The presence of these species affects sorption kinetics. After the first linear portion of the kinetic curve conditioned by external diffusion (β_1), other several linear portions were observed; for these conditions sorption rate is limited by the processes of colloids dissolving or the radionuclide redistribution from pseudocolloidal particles to the sorbent. At the second stage, the rate constants (β_2) decrease by an order of two or three magnitudes; the internal diffusion becomes to be a limiting factor that makes rapid sorption of a heterogeneous sorbate under static conditions impossible. A significant increase of a sorbent's weight allows realizing the total extraction of a radionuclide for an acceptable period; however, this results in a dramatic decrease

Table 3 Characteristics of radionuclide interphase distribution in systems (TLS—aqueous solution)

References	TLS	Radionuclides	Characteristics of							
				Radionuclide speciation		Static		Kinetics		Dynamics
			Sample type (pH)	α_d	α_c	K_{d1}	K_{d2}	β_1	β_2	V_R
Betenekov et al. (1987)	IPF-C	^{137}Cs	SW (8.2)	1.0	0.0	6×10^6	3.2×10^5	29.8	–	3.2×10^5
Betenekov and Gubanova (1980)	IP-C	^{90}Sr	FW	1.0	0.0	4×10^4	2×10^3	10^{-2}	10^{-4}	2×10^3
Vinogradov et al. (1985)	BS-C	^{133}Ba	SW (8.2)	1.0	0.0	8×10^6	2×10^4	10^{-2}	10^{-4}	2×10^4
Kaftailov et al. (1985)	TH-C	^{91}Y	SW (8.2)	0.55	0.45	6×10^5	2×10^4	0.14	4×10^{-2}	2×10^4
Denisov (1989)	TH-CSD	^{144}Ce	SW (8.2)	0.1	0.9	6×10^6	2.5×10^4	0.16	5×10^{-2}	$>2 \times 10^4$
Kaftailov et al. (1987)	TH-C	^{59}Fe	SW (8.2)	0.1	0.9	6×10^4	3.2×10^3	0.1	10^{-3}	$>2 \times 10^4$
Betenekov et al. (1986)	ZnS-C	^{60}Co	SW (8.2)	1.0	0.0	2×10^5	2×10^4	0.1	–	2×10^4
Betenekov et al. (1977)	CdS-C	^{106}Ru	SW (8.2)	0.8	0.2	2×10^6	4×10^4	0.1	10^{-2}	$>2 \times 10^4$
Betenekov et al. (1984b)	CuS-C	^{212}Pb	SW (8.2)	0.2	0.8	6×10^4	2×10^3	0.1	10^{-2}	$>2 \times 10^4$
Betenekov et al. (1984a)	TH-C	^{233}U	SW (8.2)	1.0	0.0	6×10^5	1.2×10^4	10^{-2}	10^{-4}	$>10^4$
Faizrakhmanov et al. (1987), Kaftailov et al. (1990)	TH-CTA	^{233}U	SW (5.0) FW (5.0)	0.05	0.95	6×10^6	–	0.1	10^{-2}	–

of the concentration factor, making this variant unpromising for analytical applications. By contrast, radionuclide selective preconcentration under dynamic conditions provides quantitative rapid separation and concentration of both ionic (cesium, cobalt) and colloidal (yttrium, cerium, iron, ruthenium, lead) species of radionuclides even at elevated flow rates (100–300 mL cm^{-2} min^{-1}). The high rate of sorption of ionic species is conditioned by a high rate of the external diffusion mass transfer; in the case of colloidal particles, the separation is also conditioned by mechanical filtration (Kaftailov et al. 1987).

A method for rapid complex radiochemical analysis of uranium, plutonium, cesium, strontium, and REE's radionuclides in natural water was developed using the results of these researches; this method allows for determination of both ionic and colloidal species of radionuclides in a sample (Betenekov and Gubanova 1980; Betenekov 1996). The following principles are in the basis of this method.

1. Only chromatographic regime of sorption is able to provide the total separation of a radionuclide, independently on the selectivity and distribution coefficient of a sorbent.
2. Desorption step is obligatory only for radionuclides that do not possess γ-emission.
3. Determination of the chemical yield is not necessary, if the chosen conditions (e.g., distribution coefficients, flow rates, pH, etc.) provide the radionuclide breakthrough near to zero.

Thus, a scheme of rapid complex radiochemical analysis consists of the following simple steps: the addition of a corrective solution to the sample for radionuclide stabilization in appropriate physicochemical forms, the sample loading through the system of stacked cartridges with various selective sorbents, the sorbent rinse by a rinsing solution and further air blowing, and the transfer of the sorbents to planchets and measurement. Developing of the scheme of rapid complex radiochemical analysis includes the choice of a type and quantity of sorbents, an order of their sequence in the stacked system, and parameters of loading and rinsing solutions; the choice is conditioned by the list of radionuclides to be analyzed, the required detection limits, and physicochemical characteristics of the sample. The required concentration factors are conditioned by the parameters of measuring equipment and the required detection limits.

An analyzing system including a container for a sample, a filter cartridge (polypropylene membrane with the pore size of up to 0.5 μm) for removal of sediments and colloidal particles, and a peristaltic pump and stacked cartridges with various TLS is suggested for rapid radiochemical analysis of uranium, plutonium, cesium, strontium, and REE's radionuclides in natural waters. This system allows for separate analysis of colloidal and ionic species of radionuclides as well as separation of several groups of radionuclides immediately as a result of the sorption step. In the case of natural water with the activity concentration of 0.01 Bq L^{-1}, the main parameters of the analysis are sample volume (100 L), weights of TLS for various radionuclides (10–50 g), and duration of the sample treating (up to 3 h). The total duration of the analysis includes (besides sorption step) the time needed for adjustment of the sample medium (if required) and for measurement. However, for this method, time consumption is significantly less than in cases of traditional analytical methods (Lavrukhina et al. 1963). The concentrate of radioactive colloids, obtained using the membrane filter cartridge, requires the additional chemical treatment. Determination of gamma-emitting radionuclides is possible immediately after ashing of the filter. By contrast, determination of beta and alpha emitters will require further separation and purification using the methods of ion exchange and extraction chromatography (Betenekov et al. 1995; Pin and Zalduegui 1996; Hidaka and Yoneda 2007; McAlister and Horwitz 2012; Hao et al. 2012), including the use of TLS based on granulated supports (Betenekov et al. 1991).

The TLS for separation of any radionuclide should show the maximal selectivity for these radionuclides, but its distribution coefficients for other radionuclides should be $K_d < 1$. The following example of individual cesium and strontium rapid chromatographic separation illustrates the principles of sorbent selection and the order of their disposition in the stacked cartridge system.

Long-term radioactive pollution of extended areas of the former USSR as a result of radiation accidents at Chernobyl NPP and Mayak PA is conditioned mainly by long-lived fission products ^{137}Cs and ^{90}Sr. Analytical schemes including preconcentration, separation, and measurement are suggested for the determination of these radionuclides. The use of ferrocyanides of transition metals is reasonable for ^{137}Cs separation, since they show the best selectivity for cesium (K_d is more than 10^5 L kg^{-1}) among all other organic and inorganic sorbents. Ferrocyanides usually show selectivity for Cs over a wide range of pH and salt content; however, ferrocyanides cannot adsorb alkaline earth metals (including strontium) from aqueous solutions. Also there is no uptake of REEs at a pH range less than 3; the last condition is important for analysis of ^{90}Sr, since the behavior of its daughter ^{90}Y (beta emitter, $T_{½} = 64$) should be taken into account. Traditional schemes of radiochemical analysis do not provide the avoidance of strontium and yttrium separation resulting in analysis time of at least 2 weeks that is necessary for ^{90}Y ingrowth in the concentrate of ^{90}Sr before measurement.

The suggested two-step scheme of complex radiochemical analysis consists of direct selective separation of ^{137}Cs from a sample and further direct joint separation of ^{90}Sr and ^{90}Y using a nonselective sorbent. The CU-2 strong acid cation exchange resin may be used as a nonselective sorbent; it provides distribution coefficients for both strontium and yttrium of approximately 10^4 L kg^{-1} at the pH range of more than 2. The optimal pH range is 2 to 3, because at pH $<$ 2 distribution coefficients dramatically decrease, whereas at pH $>$ 3 yttrium may be sorbed by the ferrocyanide sorbent. Conservation of a sample (in order to avoid loss of radionuclides) is performed via acidifying to pH 2–3 that corresponds to the optimal conditions for chromatographic separation of cesium and strontium.

The developed methods of rapid radiochemical analysis of natural waters were used in oceanographic expeditions in 1974, 1978, and 1980 as well as for radioecological scanning of the lands contaminated by radionuclides including the 30-km zone of the Chernobyl NPP and East Ural Radioactive Trace. The data

Table 4 Activities of various radionuclides in surface water bodies

Sampling location	Activity of suspension matter in Bq L^{-1}					Activity of aqueous phase in Bq L^{-1}				
	^{90}Sr	^{134}Cs	^{137}Cs	^{144}Ce	^{238}U	^{90}Sr	^{134}Cs	^{137}Cs	^{144}Ce	^{238}U
Pripyat River	0.2	0.04	0.16	0.07	0.001	26	0.44	2.1	n/a	0.01
Dnieper River, Kievskoe Reservoir	0.06	0.008	0.07	0.009	0.001	1.1	0.07	0.47	n/a	0.05
Dnieper River, Kanevskoe Reservoir	0.01	0.003	0.01	n/a	0.001	1.3	0.008	0.06	n/a	0.01
Dnieper River, Kremenchug Reservoir	0.01	n/a	0.002	n/a	0.001	0.64	n/a	0.01	n/a	0.03

of the radioecological monitoring (1989) of surface waters contaminated as a result of the Chernobyl disaster, obtained using the methods of rapid radiochemical analysis, are given in Table 4.

Analysis of the obtained results shows that radionuclide speciation extremely affects their migration. Thus, ^{144}Ce presents mostly as colloidal particles; therefore, its activity dramatically decreases down the Dnieper River; it cannot be found even in Kanevskoe Reservoir. Sorption by colloids and sediments is also typical for cesium; therefore, its activity decreases by an order of several magnitudes down the river. By contrast, uranium presents as the stable uranyl tricarbonate complex; thus, its activity was approximately the same at all sample points. Migration of strontium was quite similar to that of uranium. The comparison of the data from Table 4 with the results of monitoring in other regions shows that the aftermath of the Chernobyl disaster insignificantly affected the basins of Volga and Ural rivers, since only traces of ^{134}Cs and ^{144}Ce were found there.

TLS based on plane supports are also useful for some applications in radiochemical analysis. A number of publications cover use of thin-layer hydroxides and sulfides based on plane supports for preparation of alpha sources with an energy resolution less than 20 keV (Denisov 1989) as well as for analytical support of study of alpha emitter sorption from natural waters (Betenekov et al. 1984a, b; Faizrakhmanov et al. 1987). A good energy resolution is conditioned by the very small thickness of a sorption-active layer (up to 50 μg cm^{-2}). The following example illustrates the sensitivity and simplicity of analytical techniques using TLS based on plane supports. The DKPB-20 alpha camera with a semiconductor detector (produced by Joint Institute for Nuclear Research, Dubna City, Russia) allows obtaining the minimal measured activity of 0.02 Bq with a relative error of 30 % for the square of active source of 20 cm^2. The use of thin-layer sorbents TH-CTA and TH-L (titanium hydroxide based on a lavsan film) for selective preconcentration of actinides allows for detection limits as low as

1.7×10^{-5} Bq mL^{-1} and 5×10^{-4} Bq mL^{-1} for natural uranium and ^{239}Pu, respectively. The simplicity and rapidity (the time required for preconcentration at the temperature of 80 °C does not exceed 2 h) of the suggested method of radiochemical analysis combine with an acceptable selectivity of radionuclide separation.

In a number of publications (Moore and Reid 1973; Surbeck 1995; Moon et al. 2003), impregnation of a thin layer of sorption-active MnO_2 onto the surface of polyamide disk is suggested. MnO_2 is well known as the effective sorbent for radium isotopes having a good selectivity even at high calcium concentrations. This thin-layer manganese dioxide is commercially available as Ra-NucfilmDiscs (Eikenberg et al. 2001). Due to their high selectivity for Ra, these disks allow for direct determination of Ra isotopes in aqueous samples without additional separation and purification steps. The disk is immersed into an untreated water sample to be analyzed (pH 4–8, typical sample volume is 100 mL) and stirred for 6 h. The typical Ra yield in these conditions is more than 90 %. Then dried disk may be measured on an alpha spectrometer. The low thickness of active layer provides good resolution of alpha spectra.

The last recent example of thin-layer sorbents used in radiochemical analysis is composite ferrocyanide, and molybdophosphate sorbents based on polyacrylonitrile, described in recent publications (Field et al. 1999; Kamenik et al. 2013; Pike et al. 2013). Kamenik et al. (2013), passed 100 L samples of acidified seawater (and also untreated seawater through KNiFC–PAN) through 25 mL columns with AMP–PAN or KNiFC–PAN sorbents. High flow rates of up to 300 mL min^{-1} allow treating 100 L samples over less than 6 h. Overall, chemical yields are approximately 90 %, being slightly higher for KNiFC–PAN and acidified seawater. Higher flow rates were tested for untreated seawater and KNiFC–PAN; it is shown that Cs chemical yield is more than 85 % even at the flow rate of 470 mL min^{-1}. Detection limit calculated by authors for 100 L samples, average yield, and measurement time of 50–70 h are 0.15 and 0.18 Bq m^{-3} for ^{137}Cs and ^{134}Cs, respectively.

5.1.2 Surface-Modified Sorbents

The surface-modified sorbents also may be used in radiochemical analysis for selective concentration of radionuclides. A chemical modification of a surface of a sorption-active support with an extended surface area is the basis of their synthesis. The method of surface modification consists of change of the porous space of the support as a result of pretreatment and further formation of a sparingly soluble compound, which is selective to any radionuclide, on the surface and in the porous space of the support. The mixed nickel–potassium ferrocyanide based on hydrated titanium dioxide (NPF-HTD sorbent) may be used as a prospective sorbent radiocesium preconcentration and separation in a scheme of radiochemical analysis. The method of synthesis of the NPF-HTD and its sorption properties are described in the work (Voronina et al. 2012).

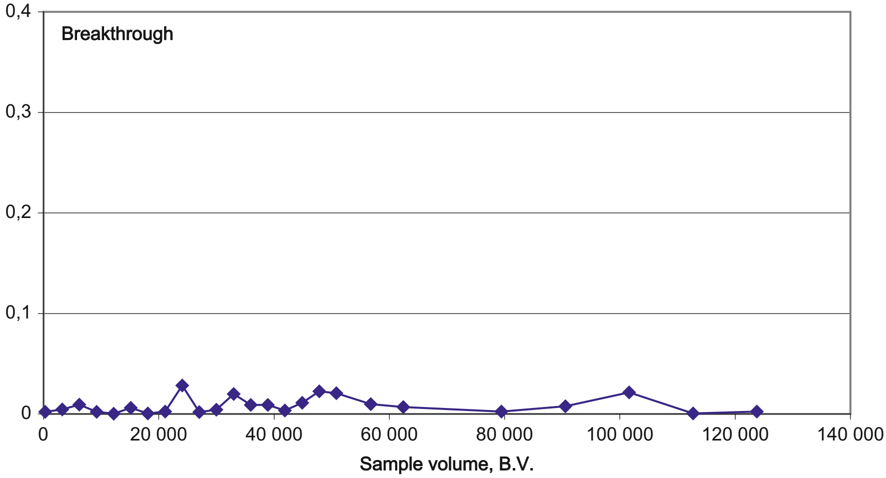

Fig. 4 Breakthrough chromatogram for ^{137}Cs on the NPF-HTD sorbent

The long experiment described in the work (Betenekov et al. 2006) illustrates the possibility of the NPF-HTD use for the selective concentration of cesium from large volumes of natural water. Cesium was separated from spiked tap water using a chromatographic column filled by the NPF-HTD sorbent in order to evaluate the resource of the column and the maximal volume of a sample to be treated. In the experiment more than 120,000 bed volumes (B.V.) of the sample were passed through the NPF-HTD column without any significant breakthrough (less than 3 %) and sorbent destruction. This experiment was stopped before column resource has been exhausted because of high radiocesium activity accumulated in the column. The breakthrough chromatogram is presented in Fig. 4. The maximal resource of the NPF-HTD column about 400,000 B.V. was calculated, taking into account cesium distribution coefficient.

Another experiment was made for cesium yield determination. The chromatographic column containing 2 g of the NPF-HTD sorbent was used for ^{137}Cs separation from 10 L samples of spiked tap water with the flow rate of 30 mL min^{-1}. The same activity of ^{137}Cs was added to a measuring dish of the same weight as the sorbent in order to make a standard source. Calculating the cesium yield was done using data of four replicates; its value was 97.0 ± 2.0 %. In the case of very low activity in a sample, it is possible to increase the sample volume up to 100 L and the sorbent weight up to 20–30 g in order to accelerate the preconcentration step.

As it was mentioned above, the direct gamma spectrometric measurement of cesium immediately in the sorbent is possible after preconcentration. However, in some cases cesium desorption and further measurement of activity in the eluate may be better. Particularly, this approach allows for measurement via beta radiometry instead of gamma spectrometry (beta radiometers have a lower background and a higher efficiency of registration, providing a lower detection limit), avoidance of extraction of the radioactive sorbent from the column, and also elimination of the effect of cesium maldistribution in the column and randomness of the source geometry on the results of measurement. As it is shown for similar sorbents based on nickel–potassium ferrocyanide and ammonium molybdophosphate, cesium elution is possible by strong solutions of ammonium salts; for example, in the tenfold volume of 5 M NH_4Cl strips 92 % of Cs from a column (Sebesta and Stefula 1990), the use of NH_4NO_3 solution is also possible (Brewer et al. 1999). Another elution method is destruction of the sorption-active phase by strong alkaline solutions (e.g., 5 M NaOH).

The possibility of ^{137}Cs quantitative elution from the NPF-HTD sorbent under the dynamic conditions by NH_4Cl and NaOH solutions was studied. It was shown that the use of 20 mL of 5 M NH_4Cl as an eluent for 0.5 g column results in the total degree of ^{137}Cs elution less than 25 %; thus, the use of ammonium chloride was decided to be an unpromising variant. In another experiment NaOH solutions with concentration of 1 mol L^{-1} and 5 mol L^{-1} were tested for ^{137}Cs elution. 5 M NaOH have shown the best results as a stripping agent: the total desorption degree by 20 mL of the solution was 96.5 %, whereas for 1 M NaOH solution, this value was only 14.5 %. However, the sorbent may be used only once, because destruction of the phase of nickel–potassium ferrocyanide occurs as a result of desorption.

5.2 *Use of Extraction Chromatographic Resins*

A wide spectrum of available organic extractants is commonly used in radiochemistry for radionuclide separation and purification. However, liquid–liquid extraction is not an easy-handling technique for a number of reasons, including toxicity and fire risk of extractants. Extraction chromatographic resins (EC resins) combine high selectivity for various radionuclides, rapid kinetics, and high capacity of organic extractants with simplicity of operations of ion exchange chromatography. EC resins consist of an organic extractant impregnated onto a porous inert support (usually, porous silica or an organic polymer).

The advantage of extraction chromatography is a wide choice of available extractants with selectivities for a wide spectrum of radionuclides with well-known extraction characteristics under various conditions. Since EC resin possesses approximately the same selectivity as extractant which was used for its producing, the existing separation methods based on liquid–liquid extraction may be easily replaced by respective methods of EC separation. A wide spectrum of EC resins allows developing rapid methods for radionuclide separation and determination in samples with a high matrix content including methods for simultaneous determination of several radionuclides due to combination of various EC resins. However, the majority of extractants work in strong acidic media (e.g., 3–8 M nitric acid, etc.); therefore, the use of EC resins for direct radionuclide separation from a sample is very complicated in contrast to the case of selective sorbent use. Thus, the separate preconcentration step is usually required in order to reduce sample volume and convert it to a necessary medium, when EC resins are used for a

Table 5 Extractants that are commercially available as extraction chromatographic resins

Extractant	Main application	References
Neutral extractants		
Octyl(phenyl)-*N*,*N*-diisobutyl-carbamoyl-methylphosphine oxide (CMPO)	Isotopes of lanthanides, Y	Dietz and Horwitz (1992)
Dipentyl pentylphosphonate (DP [PP])	Nitrato complexes of U (VI), Th (IV), Np (IV), Pu (IV)	Horwitz et al. (1992a, b)
N,*N*,*N*′,*N*′-tetra-*n*-octyldiglycolamide *N*,*N*,*N*′,*N*′-tetrakis-2-ethylhexyldiglycolamide	Am (III)	Maxwell and Culligan (2006); Maxwell (2008)
Tributyl phosphate (TBP)	U(VI), Pu(IV), ^{126}Sn	Dirks et al. (2014)
Acidic extractants		
Bis(2-ethylhexyl) methanediphosphonic acid (H_2DEH[MDP])	Am (III), Np (IV), U (VI)	Horwitz et al. (1997); Burnett et al. (1997); Croudace et al. (2006)
Di(2-ethylhexyl)orthophosphoric acid (HDEHP)	^{226}Ra, light REEs	Pin and Zalduegui (1996); Benkhedda et al. (2005); Hidaka and Yoneda (2007)
Alkaline extractants		
Aliquat® 336 (quaternary ammonium salt)	Pu(IV), Th(IV), Np (IV), Tc(VII)	Tagami and Uchida (2000); Pimpl and Higgy (2001)
Alamine® 336 (mixture of amines $(C_8H_{17})_3N$, $(C_{10}H_{21})(C_8H_{17})_2N$, $(C_{10}H_{21})_2(C_8H_{17})N$, and $(C_{10}H_{21})N)$	Pu(IV), Tc(VII)	McAlister and Horwitz (2012)
Crown ethers		
4,4′(5′)-di-*t*-butylcyclohexano-18-crown-6	^{90}Sr, ^{210}Pb	Horwitz et al. (1992a); Vajda et al. (1997)
Calix[4]-bis-crown-6	^{137}Cs	Hao et al. (2012)

radionuclide separation in radiochemical analysis. Table 5 gives a brief overview of the main applications of the extractants, which are commercially available as EC resins.

6 Conclusions

Obtaining a representative sample, its correct pretreatment and rapid and quantitative preconcentration and separation of a radionuclide are the most crucial points of the radiochemical analysis of environmental samples. The use of selective sorbents allows organizing simultaneous rapid radionuclide preconcentration from large volumes of natural waters (freshwater, seawater, etc.) and effective separation of the analyzed radionuclide immediately in the sorption step that results in a significant simplification and acceleration of the analytical procedure. Thin-layer sorbents based on various supports (wood cellulose, copolymer of styrene and divinylbenzene, slices and disks of cellulose triacetate, lavsan film, polyamide disks, and polyacrylonitrile) are widely used in radiochemical analysis for selective preconcentration and separation of radionuclides. A number of extraction chromatographic resins are also available for various tasks of radionuclide separation.

References

Benitez-Nelson CR, Buesseler KO (1998) Measurement of cosmogenic ^{32}P and ^{33}P activities in rainwater and seawater. Anal Chem 70:64–72

Benkhedda K, Larivière D, Scott S, Evans D (2005) Hyphenation of flow injection on-line preconcentration and ICP-MS for the rapid determination of ^{226}Ra in natural waters. J Anal At Spectrom 6:523–528

Betenekov ND (1996) A rapid radiochemical analysis of aqueous media using thin-layer inorganic sorbents (TLIS). Conversion 6:20–23

Betenekov ND, Gubanova AN (1980) Dynamics of heterogeneous microconstituents sorption by inorganic sorbents. In: Inorganic ion exchange materials (Book Proceeding). Leningrad, LSU

Betenekov ND, Egorov YV, Popov VI, Puzako VD, Cheremukhin YG (1976) The method of synthesis of a thin-layer sorbent. USSR patent № 526379

Betenekov ND, Egorov YV, Medvedev VP (1977) Static criteria of sorption on microconstituents from aqueous solution. In: Volkhin VV Perm (ed) Inorganic ion exchangers (synthesis, structure and characteristics). Zvezda

Betenekov ND, Egorov YV, Puzako VD, Remez VP, Stepanets OV, Khitrov LM, Cheremukhin YG (1979) The method of preconcentration of caesium radionuclides from seawater. USSR patent № 828464

Betenekov ND, Egorov YV, Puzako VD, Remez VP (1983) The method for radiocaesium separation. USSR patent № 213698

Betenekov ND, Vasilevsky VA, Egorov YV, Nedobukh TA (1984a) Radiochemical study of hydroxide films. Part II. Uranium sorption by a thin-layer titanium hydroxide under static conditions. Radiochemistry 4:432–439

Betenekov ND, Ipatova EG, Poluyakhtov AI (1984) Static and dynamics of sorption of lead microquantities by thin-layer sorbents from salty solutions. In: Researches in chemistry, technology and application of radioactive materials (Book Proceeding). Leningrad, LTI

Betenekov ND, Kaftailov VV, Denisov EI (1986) Radiochemical studies of chalcogenide films. Part X. About cobalt sorption by a thin-layer zinc sulphide from carbonate solutions. Radiochemistry 5:599–603

Betenekov ND, Kaftailov VV, Bushkov IE (1987) Caesium sorption from solutions similar to the seawater. Radiochemistry 1:127–129

Betenekov ND, Buklanov GV, Ipatova EG, Korotkin YS (1991) Ion exchange of alkaline metals on a thin-layer zinc ferrocyanide. Radiochemistry 5:163–168

Betenekov ND, Ipatova EG, Djakov AA, Rostovtsev VY (1995) Highly sensitive method of determination of fissile materials concentration in liquid radioactive waste of NPP. Radiat Measur 1–4:405–407

Betenekov ND, Voronina AV, Nogovitsyna EV, Chopko NN (2006) Dynamic studies of highly selective sorbents. Sorpt Chromato Process 6:1115–1118

Bienvenu P, Brochard E, Excoffier E, Piccione M (2004) Determination of iodine 129 by ICP-QMS in environmental samples. Can J Anal Sci Spectrosc 49:423–428

Bowyer TW, Abel KH, Hensley WK, Panisko ME, Perkins RW (1997) Ambient ^{133}Xe levels in the Northeast US. J Environ Radioact 37:143–153

Brewer KN, Todd TA, Wood DJ, Tullock PA, Sebesta F, John J, Motl A (1999) AMP-PAN column tests for the removal of Cs-137 from actual and simulated INEEL high-activity wastes. Czech J Phy 49:959–964

Brun S, Bessac S, Uridat D, Boursier B (2002) Rapid method for the determination of radiostrontium in milk. J Radioanal Nucl Chem 253:191–197

Buesseler KO, Benitez-Nelson C, van der Loeff MR, Andrews J, Ball L, Crossin G, Charette MA (2001) An intercomparison of small- and large-volume techniques for thorium-234 in seawater. Mar Chem 74:15–28

Burnett WC, Corbett DR, Schultz M, Horwitz EP, Chiarizia R, Diet M, Thakkar A, Fern M (1997) Pre-concentration of actinide elements from soils and large volume water samples using extraction chromatography. J Radioanal Nucl Chem 226:121–127

Croudace IW, Warwick PE, Greenwood RC (2006) A novel approach for the rapid decomposition of Actinide™ resin and its application to measurement of uranium and plutonium in natural waters. Anal Chim Acta 577:111–118

Denisov EI (1989) Separation of cerium microquantities from salty solutions using thin-layer titanium hydroxide. Doctoral (Chemistry) Dissertation, Sverdlovsk, Ural Polytechnical Institute, Russia

Dietz M, Horwitz EP (1992) Improved chemistry for the production of yttrium-90 for medical applications. Int J Radiat Appl Instrum 43:1093–1101

Dirks C, Vajda N, Kovács-Széles E, Bombard A, Happel S (2014) Characterization of a TBP Resin and development of methods for the separation of actinides and the purification of Sn. In: 17th Radiochemistry conference–Book of Abstracts

Eikenberg J, Tricca A, Vezzu G, Bajo S, Ruethi M, Surbeck H (2001) Determination of Ra-228, Ra-226 and Ra-224 in natural water via adsorption on MnO_2-coated discs. J Environ Radioact 54:109–131

EL-Hussein A, Mohamemed A, Abd EL-Hady M, Ahmed AA, Ali AE, Barakat A (2001) Diurnal and seasonal variations of short-lived radon progeny concentration and atmospheric temporal variations of ^{210}Pb and ^{7}Be in Egypt. Atmos Environ 35:4305–4313

Elsinger RJ, King PT, Moore WS (1982) Radium-224 in natural waters measured by γ-ray spectrometry. Anal Chim Acta 144:277–281

Faizrakhmanov FF, Betenekov ND, Egorov YV (1987) Kinetics of uranium sorption by a thin-layer titanium hydroxide from fresh waters. In: Researches in chemistry, technology and application of radioactive materials (Book Proceeding). Leningrad, LTI

Field D, Harding K, Hooper E, Keltos D, Krasny D, Šebesta F (1999) Caesium removal from fuel pond waters using a composite ion exchanger containing nickel hexacyanoferrate. Czech J Phys 49:965–969

Grabowski P, Dlugosz M, Szajerski P, Bem H (2010) A comparison of selected natural radionuclide concentrations in the thermal groundwater of Mszczonów and Cieplice with deep well water from Łódź city, Poland. Nucleonica 55:181–185

Hao X, Tan S, Deng W (2012) The studies on absorption behavior of calix[4]-bis-crown-6 chromatographic resin and its application to the separation of HLW. J Radioanal Nucl Chem 291:1291–1296

Hidaka H, Yoneda S (2007) Sm and Gd isotopic shifts of Apollo 16 and 17 drill stem samples and their implications for regolith history. Geochim Cosmochim Acta 71:1074–1086

Holgye Z, Burcik I (1992) Contribution to the analysis of plutonium originated from the Chernobyl accident in soil. J Radioanal Nucl Chem Lett 165:185–190

Horwitz P, Dietz M, Chiarizia R, Diamond H, Essling AM, Graczyk D (1992a) Separation and preconcentration of uranium from acidic media by extraction chromatography. Anal Chim Acta 266:25–37

Horwitz P, Chiarizia R, Dietz M (1992b) Acid dependency of the extraction of selected metal ions by a strontium-selective extraction chromatographic resin: calculated vs. experimental curves. Solvent Extr Ion Exch 10:337–361

Horwitz EP, Chiarizia R, Dietz ML (1997) DIPEX: a new extraction chromatographic material for the separation and preconcentration of actinides from aqueous solution. React Funct Polym 33:25–36

ICRP (2007) Recommendations of the International Commission on Radiological Protection (Users Edition). ICRP Publication 103 (Users Edition). Ann ICRP 37:2–4

Igarashi Y, Sartorius H, Miyao T, Weiss W, Fushimi K, Aoyama M, Hirose K, Inoue HY (2000) ^{85}Kr and ^{133}Xe monitoring at MRI, Tsukuba and its importance. J Environ Radioact 48:191–202

Kaftailov VV, Betenekov ND, Vasilevsky VA (1985) Radioactive colloids in sorption systems. Part XVII. Kinetics of yttrium sorption by a thin-layer titanium hydroxoperoxide from solutions similar to the seawater. Radiochemistry 27:147–150

Kaftailov VV, Mitrofanova SA, Betenekov ND (1987) Radioactive colloids in sorption systems. Part XIX. Iron preconcentration from salty solutions using filtration. Radiochemistry 29:121–123

Kaftailov VV, Nedobukh TA, Betenekov ND, Egorov YV (1990) An external diffusion kinetics of a sorption in the linear part on an isotherm affected by complexation of a sorbate in the initial solution. J Phys Chem 64:2439–2444

Kamenik J, Dulaiova H, Sebesta F, Stastna K (2013) Fast concentration of dissolved forms of cesium radioisotopes from large seawater samples. J Radioanal Nucl Chem 296:841–846

La Rosa JJ, Burnett W, Lee SH, Levy I, Gastaud J, Povinec PP (2000) Separation of actinides, cesium and strontium from marine samples using extraction chromatography and sorbents. J Radioanal Nucl Chem 248:765–770

Lavrukhina AK, Malysheva TV, Pavlotskaya FI (1963) Radiochemical analysis. Academy of Sciences, Moscow

Maxwell SL (2008) Rapid method for determination of plutonium, americium and curium in large soil samples. J Radioanal Nucl Chem 275:395–402

Maxwell SL, Culligan BK (2006) Rapid column extraction method for actinides in soil. J Radioanal Nucl Chem 270:699–704

Maxwell SL, Culligan BK (2012) Rapid determination of ^{226}Ra in environmental samples. J Radioanal Nucl Chem 293:149–156

Maxwell SL, Culligan BK, Shaw PJ (2013) Rapid determination of radiostrontium in large soil samples. J Radioanal Nucl Chem 295:965–971

Maxwell SL, Culligan BK, Huchinson JB, Utsey RC, McAlister DR (2014) Rapid determination of actinides in seawater samples. J Radioanal Nucl Chem 300:1175–1189

McAlister D, Horwitz P (2012) Separation methods utilizing oxalate and HCl on anion exchange resins. In: Eichrom User Group Meeting. RRMC, Fort Collins, CO

Moon DS, Burnett WC, Nour S, Horwitz EP, Bond A (2003) Preconcentration of radium isotopes from natural waters using MnO_2 resin. Appl Radiat Isot 59:255–262

Moore WS, Reid DF (1973) Extraction of radium from natural waters using manganese impregnated acrylic fibers. J Geophys Res 78:8880–8886

Moskvin LN, Epimakhov VN, Chetverikov VV (2011) Radiochemical monitoring of water and air media in nuclear power industry. Radiochemistry 53:1–12

Nozaki Y, Dobashi F, Kato Y, Yamamoto Y (1998) Distribution of Ra isotopes and the ^{210}Pb and ^{210}Po balance in surface seawaters of the mid Northern Hemisphere. Deep Sea Res I 45:1263–1284

Pike SM, Buesseler KO, Breier CF, Dulaiova H, Stastna K, Sebesta F (2013) Extraction of cesium in seawater off Japan using AMP-PAN resin and quantification via gamma spectroscopy and inductively coupled mass spectrometry (Conference Paper). J Radioanal Nucl Chem 296:369–374

Pimpl M, Higgy RH (2001) Improvement of Am and Cm determination in soil samples. J Radioanal Nucl Chem 248:537–541
Pin C, Zalduegui J (1996) Sequential separation of light rare-earth elements, thorium and uranium by miniaturized extraction chromatography: application to isotopic analyses of silicate rocks. Anal Chim Acta 339:79–89
Qiao J, Shi K, Hou X, Nielsen S, Roos P (2014) Rapid multisample analysis for simultaneous determination of anthropogenic radionuclides in marine environment. Environ Sci Technol 48:3935–3942
Salbu B, Nikitin AI, Strand P, Christensen GC, Chumichev VB, Lind B, Fjelldal H, Bergan TDS, Rudjord AL, Sickel M, Valetova NK, Føyn L (1997) Radioactive contamination from dumped nuclear waste in the Kara Sea – result from the joint Russian – Norwegian expedition in 1992–1994. Sci Total Environ 202:185–198
Sanchez AL, Gastaud J, Noshkun V, Buesseler KO (1991) Plutonium oxidation states in the southwestern Black Sea: evidence regarding the origin of the cold intermediate layer. Deep Sea Res I 38:S845–S854
Sapozhnikov JA, Aliev RA, Kalmykov SN (2006) Radioactivity of the environment. Binom, Moscow
Sebesta F, Stefula V (1990) Composite ion exchanger with ammonium molybdophosphate and its properties. J Radioanal Nucl Chem 140:15–21
Smith JN, Ellis KM, Kilius LR (1998) ^{129}I and ^{137}Cs tracer measurements in the Arctic Ocean. Deep Sea Res I 45:959–984
Surbeck H (1995) Determination of natural radionuclides in drinking water, a tentative protocol. Sci Total Environ 173–174:91–99
Tagami K, Uchida S (2000) Separation of rhenium by an extraction chromatographic resin for determination by inductively coupled plasma-mass spectrometry. Anal Chim Acta 405:227–229
Tananaev IV, Seifer GB, Kharitonov YY, Kuznetsov VG, Korol'kov AP (1971) Khimiya ferrotsianidov (Chemistry of Ferrocyanides). Nauka, Moscow
Teldesi U, Yakovlev YV, Bilimovich GN (1985) Diagnostics of the environment using radioanalytical methods. Energoatomizdat, Moscow
Vajda N, LaRosa J, Zeisler R, Danesi P, Kis-Benedek G (1997) A novel technique for the simultaneous determination of ^{210}Pb and ^{210}Po using a crown ether. J Environ Radioact 37:355–372
Veselsky JC (1977) Problems in the determination of plutonium in bioassay and environmental analysis. Anal Chim Acta 90:1–14
Vinogradov VN, Ipatova EG, Betenekov ND (1985) Synthesis of a thin-layer barium sulphate and the study of its sorption characteristics. In: Researches in chemistry, technology and application of radioactive materials (Book Proceeding). Leningrad, LTI
Voronina AV, Semenishchev VS, Nogovitsyna EV, Betenekov ND (2012) A study of ferrocyanide sorbents on hydrated titanium dioxide support using physicochemical methods. Radiochemistry 54:69–74
Yoshida S, Muramatsu Y, Katou S, Sekimoto H (2007) Determination of the chemical forms of iodine with IC-ICP-MS and its application to environmental samples. J Radioanal Nucl Chem 273:211–214

Uncertainty Analysis and Risk Assessment

Rodolfo Avila

Contents

Abstract This chapter presents an overview of the main concepts and methods that are used in the field of risk and uncertainty analysis. We will explore different definitions of the concept of risk and its relationship with the concepts of uncertainty, probability and hazard. Thereafter, we discuss deterministic and probabilistic methods for risk quantification and illustrate various approaches for presentation of the results of a risk analysis. The chapter also outlines the process for uncertainty analysis, which comprises identifying the sources of uncertainty, quantifying the uncertainties of different components, propagating the different uncertainties to obtain an overall measure of uncertainty and finally performing sensitivity and uncertainty analyses, in order to identify factors that have the highest contribution to the overall uncertainty.

Keywords Risk • Risk analysis • Probability • Uncertainty • Uncertainty analysis • Sensitivity analysis

R. Avila (✉)
Facilia AB, Gustavslundsvägen 151G, 167 51 Bromma, Sweden
e-mail: rodolfo@facilia.se

C. Walther, D.K. Gupta (eds.), *Radionuclides in the Environment*,
DOI 10.1007/978-3-319-22171-7_14

1 Risk Analysis

A risk analysis consists of an answer to the following three questions (Kaplan and Garrick 1981):

1. What can happen? (i.e. what can go wrong?)
2. How likely is it that will happen?
3. If it does happen, what are the consequences?

The above questions could be answered in a qualitative manner, and this is what we often do during our everyday life activities, when we make conscious or unconscious estimates of the risks of different courses of action or inaction. In fact, as expressed by Kaplan and Garrick (1981), we are not able in life to avoid risk but only to choose between risks. At the same time, rational decision-making requires a clear and quantitative way of expressing risk so it can be properly weighted against all costs and benefits in the decision-making process. In Sect. 1.1, we present a formal definition of risk that is fit for the purpose of quantitative risk analysis, i.e. for answering the above questions in a quantitative objective manner. Further, to provide more clarity on the concept of risk, in Sects. 1.2 and 1.3, we provide a discussion of the relationship between risk and other concepts that are also used in the context of risk analysis, namely, the concepts of uncertainty and hazard.

It is evident that risk analysis is not only concerned with estimating adverse consequences of different scenarios but also with estimation of the probability of these scenarios. While the consequence analysis is rather straightforward and easy to understand, probabilities and their estimation are more difficult to grasp intuitively. This is because of the subjective nature of probabilities. Having this in mind, in this chapter we will give more attention to the probability side of the risk assessment.

1.1 *Definition of Risk*

The concept of risk is widely used in many disciplines, and the word risk is used in many different senses. In this book, we will use the definition given in Kaplan and Garrick (1981), where risk is defined as a set of three components: the scenarios consisting of a sequence of events and processes leading to the adverse consequences (s_i), the probability of these scenarios (p_i) and their adverse consequences (c_i). This definition is better fit for the purpose of risk analysis than the often used definition of risk as probability time's consequence. The latter definition implies a loss of important information. For example, two scenarios with very different probabilities and consequences might be assigned the same risk value, which is misleading: a low probability–high consequence scenario is not the same thing as high probability–low consequence scenarios. In the case of multiple scenarios, the probability time consequence view would correspond to the expected value of the consequences, so information about the consequences and probabilities of each scenario is lost. This information is however essential for performing a risk analysis in support to decision-making.

Hence, we will use the following mathematical representation of risk (Kaplan and Garrick 1981):

$$\text{Risk} = \{\langle s_i, p_i, c_i, \rangle\} \tag{1}$$

where

s_i is the identification or description of the *ith* scenario, $i = 1, 2\ldots, N$.
p_i is the probability of the *ith* scenario.
c_i is the adverse consequence of the *ith* scenario.

The brackets are used to denote the "set of" the triplet "scenario, probability and consequence"
and not

$$\text{Risk} = \sum_i p_i{}^* c_i \tag{2}$$

which is actually the expectation of the adverse consequence.

1.2 Relationships Between Risk and Uncertainty

Uncertainty is a concept that describes a state of having limited knowledge where it is impossible to exactly describe the existing state, a future outcome or more than one possible outcome. Intuition tells us that risk and uncertainty should be related. One could argue that a person would not take a risk, i.e. would not voluntarily expose to an adverse consequence, if this person was certain that a scenario leading to the exposure will take place. For example, no rational person would take a risk if it was certain that the scenario will occur and it will certainly have a fatal outcome. At the same time, uncertainty is not the same as risk. For example, you may be highly uncertain about how much your children will like your birthday present, but you would hardly say that you are facing a risk because of that, or? So, the concept of risk involves both uncertainty and an adverse consequence. Indeed, a commonly used definition of risk is a state of uncertainty where some possible outcomes have an undesired effect or significant loss (adverse consequence).

A core element of risk is uncertainty represented by plural outcomes and their likelihood. No risk exists if the future outcome is uniquely known and hence guaranteed. The probability that we will die someday is equal to 1, so there would be no fatal risk if sufficiently long time frame is assumed. Equally, rain risk does not exist if there was 100 % assurance of rain tomorrow, although there would be other risks induced by the rain. In a formal sense, any risk exists if, and only if, more than one outcome is expected at a future time interval.

In their formal definition of risk, Kaplan and Garrick (1981) propose a useful coupling between risk and uncertainty by explicitly including uncertainty in the probability and consequence components of the risk set:

$$\text{Risk} = \{\langle s_i, P(p_i), P(c_i)\rangle\} \tag{3}$$

where

$P(p_i)$ and $P(c_i)$ are the probability density functions for the probability of the scenarios, seen as frequencies, and their consequence, respectively.

Hence, in the risk equation (3), both the probability and the consequence are now regarded as uncertain, and probability density functions are assigned to them, instead of single-point values. The concept of probability and the probability theory provide us with efficient and well-developed approaches for dealing with uncertainty.

1.3 Relationship Between Risk and Hazard

Hazard is defined as "a source of danger" (Webster 1977), and it represents the potential for causing harm, adverse consequences. Hazard is just a source of risk, which does not realise until exposure takes place. Risk is the possibility of the adverse consequence and the degree of probability of such adverse consequence. The risk associated with a low hazard could be high, while the risk associated with a high hazard could be low, depending on what protective measures we take to reduce the probability of exposure and the adverse consequences in case of an exposure. Figure 1 shows an illustrative example of the relationship between hazard and risk.

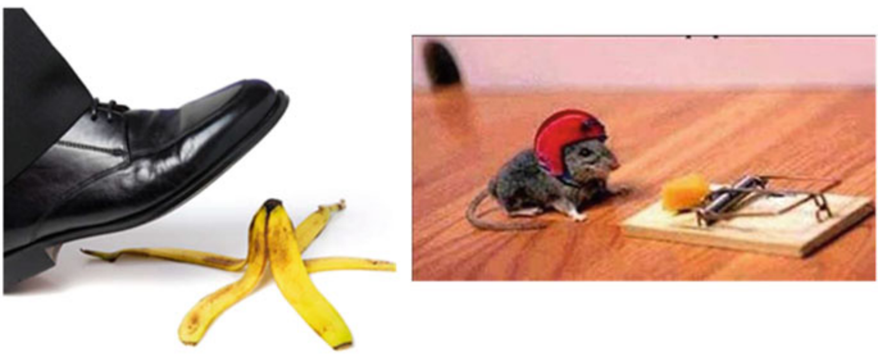

Fig. 1 The banana peel and the trap represent hazards for the man and the mouse, respectively. The risk will depend on the probability of exposure to the hazard and the consequences of the exposure. The latter is influenced by the level of safeguards against the hazard

The hazards here are the banana peel and the mouse trap, for the stressed man and the hungry mouse, respectively. Most people will agree with the idea that the trap is a higher hazard for the mouse than the peel is for the man. This may explain why the man goes unaware and unprotected, whereas the mouse is very aware of the hazard and has taken safety measures. But, what risk is the highest? This will depend on the probability of getting exposed to the hazard and the consequences of this exposure. The latter will depend on the efficiency of safety measures (safeguards) implemented against the hazards. If the efficiency of the safety measures is high, then the risk can be low. In Kaplan and Garrick (1981), the authors explain this idea by symbolically representing risk as hazard/safeguards. This equation shows that by adding safety measures, it is possible to reduce the risk to as low as desired, but we may never bring it to zero. A good strategy, often recommended or required by regulators, is to improve safety until risks are reduced to as low as reasonably practicable, for example, the ALARP principle in the United Kingdom or by implementing standards of good engineering practice. It is worth noting that awareness of risk also reduces risk and can be considered as a safeguard. For instance, if our unlucky man knows that there is a banana peel on the road of his path, then the associated risk is lower than if he is unaware of it.

1.4 Risk Quantification and Presentation

Having agreed on a definition of risk and its relationship with associated concepts, uncertainty and hazard, we can now proceed to discuss how to quantify it and present it in a way that is useful for risk analysis, with the ultimate goal of identifying safety measures that can be used for reducing the risk. The safety measures may have a preventive effect by reducing the probability of exposure or a mitigating effect by reducing the magnitude of the adverse consequences. The following general procedure can be applied for quantification of the risks using Eq. (3).

1.4.1 Identification of Scenarios

A first step for the risk quantification is to develop a list of scenarios to be considered in the quantification. A scenario is a sequence of future events and processes that could result in adverse consequences from exposure to one or more hazards. The scenario definition includes a description of how the system will be affected by the events and how different safety measures are expected to perform, acting as barriers to the exposure. There exist several techniques for systematic identification of scenarios. One example is the use of databases of feature events and processes (FEPs) in order to identify scenarios for assessments of risks of repositories for nuclear waste (IAEA 2004). The subject matter of methods for identification of scenarios is outside the scope of this book chapter and will not be discussed further here. We nevertheless recommend that a systematic approach is used that yields a list of scenarios that is as complete as possible. Moreover, the scenarios, or categories of scenarios, should be chosen so that they are mutually exclusive, and the same event does not show up in more than one category.

It could be argued that the list of scenarios is in reality infinite, and therefore, any risk analysis that is based on a list of scenarios will be incomplete. People can always say that they are worried about scenarios that are not in the list. The work of Kaplan and Garrick (1981) has shown that this issue can be handled by including an additional category (N_{i+1}) of scenarios, which they called the "other" category. They also showed that this category of scenario may be handled by the same process as any other scenario category.

1.4.2 Consequence Analysis

The next step is to quantify the potential adverse consequences associated with each scenario. These are damages or losses that can occur in the future if the scenario realises. Hence, more often than not, the consequence analysis will be done using mathematical models that can predict how the system will evolve under the assumptions inherent to a specific scenario. The consequence analysis will also rely on past experiences from similar situations. The range of models and methods that can be used for the consequence analysis is very broad and will have to be selected on a case by case basis. Hence, here we will not discuss this issue in any more detail, but instead we will focus our discussions on methods for the analysis of uncertainties of model predictions (Sect. 3) and for identifying the uncertainties that have the largest contribution on the overall uncertainty of the model predictions (Sect. 4).

1.4.3 Assignment of Probabilities to the Scenarios

In parallel to the consequence analysis, the probabilities associated with each scenario should be estimated. As mentioned in Sect. 1.2, the estimated probabilities are also uncertain. This can be handled by assigning a probability density function (PDF) to the probability of the scenario, rather than a single value.

1.4.4 Risk Curves and Risk Matrices

As we have mentioned before, the risk associated with a scenario has a least two dimensions and is not well represented with a single number. As shown by Kaplan and Garrick (1981), it takes a whole curve or rather a whole family of curves (if uncertainties are taken into account) to represent risk.

Figure 2 shows an example of a risk curve where the uncertainty in the probability of the scenario is taken into account. Details of how these curves are

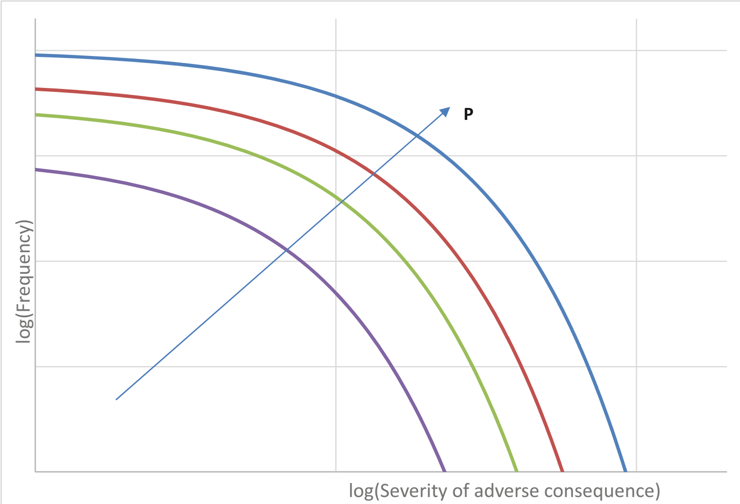

Fig. 2 Family of risk curves that takes into account the uncertainty in the scenario probabilities. *P* is the cumulative probability obtained from the probability density function that was used to quantify the uncertainty in the scenario probabilities

constructed from Eq. (3) can be found in Kaplan and Garrick (1981). Each of the curves in Fig. 2 represents the risk corresponding to one value of the cumulative probability of the scenarios, generated from the probability density functions that are used to represent the uncertainty in the scenario probabilities. The risk refers to adverse consequences of the same type, for example, increased mortality by cancer disease due to exposures to a chemical or radionuclide. In many situations, there might be several types of adverse consequences, like negative impacts of the environment, economical losses, etc. The risk curves would become a risk surface over a multidimensional space, which would be very difficult to interpret and use in practice. So, commonly separate risk curves are constructed for each type of adverse consequence.

The main advantage of the family of curves in Fig. 2 is that all information that the risk encapsulates is preserved. This is the information that is required to analyse the risk from the perspective of decision-making. However, sometimes there is no sufficient information available to construct such risk curves and more simple representations are used. One of the most widely used representations is the so-called risk matrix, although their use is mainly confined to the field of risk management.

In a risk matrix, the probabilities and the adverse consequences are categorised into a small number of levels, typically 5. A matrix can then be built where the different scenarios can be placed. Although many standard risk matrices exist in different contexts (US DoD 2006; NASA 2009; ISO 2003), individual projects and organisations often create their own or tailor an existing risk matrix. An example of

		Adverse Consequences				
		Very Low	Low	Medium	High	Very High
Probabilities	Very High			SC1		
	High				SC3	
	Medium					
	Low					
	Very Low					SC2

Fig. 3 Risk matrix where the risk associated with three different scenarios is qualitatively represented

		Adverse Consequences				
		Very Low	Low	Medium	High	Very High
Probabilities	Very High			SC1		
	High				SC3	
	Medium					
	Low					
	Very Low					SC2

Fig. 4 Risk matrix where the risk associated with three different scenarios (the same as in Fig. 3) is qualitatively represented. In this matrix, scoring of the risks has been introduced by multiplying scores for the probabilities with scores for the adverse consequences. On this basis, three categories for the risk are obtained: low (*green cells*), moderate (*yellow cells*) and high (*red cells*)

such matrix is presented in Fig. 3. Some authors go further, by giving scores to the probability and consequence categories and multiplying these scores with each other. This way the matrix cells also get scores, which are then used to give a score to the risks associated with a scenario, depending on their position in the matrix. An example of such matrix is presented in Fig. 4.

Despite the qualitative nature of the risk matrix, it can be used for making initial decisions on how to manage risks associated with the different scenarios. For example, from Figs. 3 and 4, it is evident that the only viable way of reducing risk for scenario SC2 would be to implement mitigating safety measures, whereas for scenario SC1, preventive measures would be more appropriate, and for SC3, both preventive and mitigating measures could be appropriate.

For the risk matrices to be useful, it is recommended that the arguments made for defining the categories, placing the scenarios in the matrix and doing the scoring are properly justified and documented. The limitations of this type of risk representation should be kept in mind, the matrices should be used with caution, and as far as possible, the results obtained with the matrices should be corroborated by using other risk quantification methods, such as the risk curves presented above. An analysis of mathematical aspects of the use of risk matrices can be found in Cox (2008), where the following limitations are mentioned:

(a) Poor Resolution. Typical risk matrices can correctly and unambiguously compare only a small fraction (less than 10 %) of randomly selected pairs of hazards. They can assign identical ratings to quantitatively very different risks ("range compression").
(b) Errors. Risk matrices can mistakenly assign higher qualitative ratings to quantitatively smaller risks. For risks with negatively correlated frequencies and severities, they can be "worse than useless", leading to worse-than-random decisions.
(c) Suboptimal Resource Allocation. Effective allocation of resources to risk-reducing countermeasures cannot be based on the categories provided by risk matrices.
(d) Ambiguous Inputs and Outputs. Categorisations of severity cannot be made objectively for uncertain consequences. Inputs to risk matrices (frequency and severity categorisations) and resulting outputs (i.e. risk ratings) require subjective interpretation, and different users may obtain opposite ratings of the same quantitative risks.

1.4.5 Risk Quotients

The risk curves and risk matrix discussed above provide an integrated picture of the risk taking into account all scenarios. However, it is also of interest to analyse the risks from each scenario separately. A common approach is to calculate the so-called risk quotients (RQ), defined as the quotient between the adverse consequences, for example, the radiation dose to an organism or the effect on the organism, and a reference level or standard, for example, a dose limit:

$$\mathrm{RQ}_i = \frac{c_i}{\mathrm{Ref}} \tag{4}$$

where

c_i is the adverse consequence of the *ith* scenario.
"Ref" is a reference value used to measure the severity of the adverse consequence.

Depending on the values assigned to c_i, the RQ will have different meanings. For example, if a cautious value is chosen for c_i, then a cautious value of the RQ will be obtained, which could be used for screening purposes. If the expected value of c_i is used, then the expected value of the RQ is obtained. We could also use a probability density function for c_i and in this way incorporate uncertainty in the RQ.

An example of application of the RQ can be found in the ERICA-integrated approach to assessment of radiological impacts on nonhuman biota implemented in the ERICA Tool (Brown et al. 2008), where different RQs are used for implementing a tiered approach to the assessments. Another example is the use of RQs for quantifying risks of chemical to humans and biota by dividing concentrations in the environmental media by the so-called non-observed effect levels (NOEL).

The RQs are calculated for each type of adverse consequences separately; however, since they are a relative magnitude, different RQs can be compared with each other or even combined with each other to obtain a measure of the overall risk; taking into account all adverse consequences.

As mentioned above, in any practical risk assessment, we have to deal with uncertainties associated with the possible outcomes. One way of dealing with the uncertainties is to be conservative in the assessments. For example, we may compare a conservative estimate of the adverse consequences with a conservatively chosen reference value. In this case, if the adverse consequence is below the reference value, then it is possible to assure that the risk is low. Since single values are usually compared, this approach is commonly called "deterministic". Its main advantage lies in the simplicity and in that it requires minimum information. However, problems arise when the reference values are actually exceeded or might be exceeded, as in the case of potential exposures, and when the costs for realising the reference values are high. In those cases, the lack of knowledge on the degree of conservatism involved impairs a rational weighing of the risks against other interests.

An alternative, in our opinion more consistent, approach for dealing with uncertainties is the so-called probabilistic risk assessment. The essence of this approach consists in explicitly quantifying the uncertainties in terms of probabilities. For example, the adverse consequence and the reference value (Eq. 4) can be both treated as random variables. In this case, the RQ is also a random variable that can be described with a probability density function, commonly known as the "risk profile" (Fig. 5). A deterministic RQ is just one value among the universe of all values than the RQ can possibly take. The probability that the RQ is above

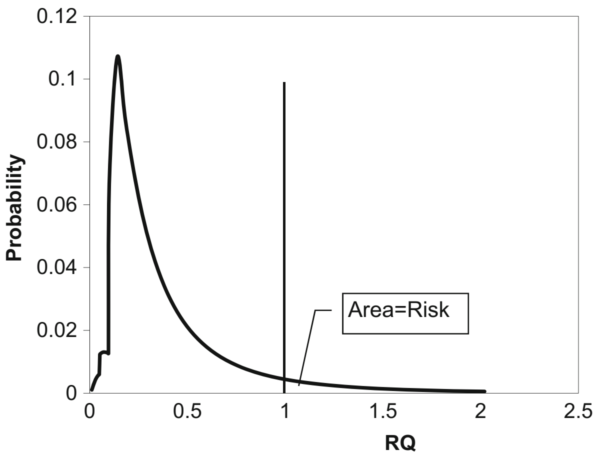

Fig. 5 Example of probability density function corresponding to the risk quotient, commonly known as the "risk profile". The area under the curve for RQ > 1 is a quantitative measure of the risk

1 (indicated area in Fig. 5) is a quantitative measure of the risk. In contrast, the deterministic approach provides only a qualitative risk estimate.

As mentioned above, in the deterministic approach, often conservative values are used in Eq. (4). Given the multiplicative nature of this equation, a substantial magnification (positive bias) of the conservatism may take place. For this reason, values of RQ close to or above 1 will carry very little information about the risks. A common way to deal with this problem is to carry out assessments in tiers. This means that more realistic quotients are estimated whenever a conservative assessment yielded RQ $>$ 1. This approach could be seen as a simplified version of a probabilistic approach. In any case, the interpretation of the results would require knowledge about the distribution of the exposure and the reference value. For example, using mean values in Eq. (4) is meaningful only if the magnitudes follow a normal distribution, which is rarely the case.

2 Probability

The concepts of risk, presented above, and of uncertainty, see below, both rely on the concept of probability. In this context, there are two primary definitions of the concept probability: *relative frequency* and *subjective* interpretation.

The interpretation as a relative frequency defines probability as the number of times that an outcome occurs in N equally likely trials. This means that the probability of an outcome *A* equals the number of outcomes favourable to *A* (within the meaning of the experiment) divided by the total number of possible outcomes. However, what meaning can be associated with the statement: the probability of a scenario consisting of failure of a protective barrier is 0.01? The concept of repeated trials is meaningless, the protective barrier will be built only once, and it will either fail or be successful during its design lifetime. It cannot do both. Here we have an example of the subjective interpretation of probability. It is a measure of our belief on the likelihood of occurrence of an outcome.

In risk assessment applications, subjective probability is generally more useful than the relative frequency concept. However, the basic rules governing both interpretations are identical. Both concepts specify the probability of an outcome to range between, and to include numerical values of, zero and one.

One important property of probabilities is that they are always conditioned to the occurrence of other outcomes and to assumptions made based on available background information. This means that two different persons or the same person at different times can make different subjective estimates of the probability if they have a different experience or are relying on different background information. Hence, probability estimates rely on knowledge and experience of the assessor. This is often used as a criticism to the subjective interpretation of probability. However, if two different persons make an estimate of the probability based on the same information and assumptions, they will arrive at the same probability, if they observe the axioms and theorems of probability theory. So in that sense, the estimate of subjective probabilities is also objective.

3 Uncertainty Analysis

Uncertainty analysis is the process of identifying the sources of uncertainties, quantifying the uncertainty of the different risk components, through a process of quantifying and propagating uncertainties of predictions with models used for estimating the risk components.

3.1 Sources of Uncertainty

The estimates of probabilities of the scenarios and of their adverse consequences are always uncertain. The uncertainty can arise from a number of sources, including system uncertainties, uncertainties in the mathematical models applied, and uncertainty in the model parameter values, caused by the natural variability of the measured variables, measurement errors and biases in the sampling and monitoring.

The sources of uncertainty can be broadly categorised as follows:

System uncertainty refers to uncertainty in the states of the system where the adverse consequences occur, including not only the situation at the moment of the assessment, but also the situation in the past (for retrospective assessments) and in the future (for prospective assessments). It includes uncertainty in the environmental properties and how these change, in the sources of contamination, etc. This type of uncertainty is usually dealt with by making assessments for several alternative scenarios.

Model uncertainty arises from the necessarily imperfect knowledge about processes, which leads to imperfect conceptual models. The mathematical representation of the conceptual models may be oversimplified, also contributing to model uncertainty. Imprecision in the numerical solution of mathematical models is another source of uncertainty falling into this category. This type of uncertainty is usually treated by performing intercomparisons between alternative models and between model predictions and empirical observations.

Data/parameter uncertainty refers to the uncertainty in the values of the parameters used in the models. The methods for characterisation of this type of uncertainty are straightforward and well documented in the literature; see, for example, IAEA (1989) and Morgan and Henrion (1992). They consist of assigning probability distributions to the parameters. The parameter/data uncertainties can then be propagated through the models by different methods, for example by performing Monte Carlo simulations (see Sect. 3.3).

3.2 Assigning Probability Distributions to Model Parameters

Probability distributions (Evans et al. 2000) are a convenient instrument for representing quantitatively the uncertainty in the inputs and parameter values, which facilitates using existing probabilistic techniques for uncertainty and sensitivity analyses. There exist different methods for assigning probability distributions to variables, which are briefly discussed below.

3.2.1 Distribution Fitting

When sufficient empirical data is available, the probability distribution of the inputs and parameters can be directly estimated using standard statistical techniques (Taylor 1993).The task of choosing a specific parametric probability distribution is twofold: first optimal parameters are found for each type of probability distributions, and then the fit is assessed for each type of distributions to find the most appropriate distribution. Commonly used methods to find optimal distribution parameters include the maximum likelihood estimate (MLE) and the least squares method (LSM). To assess the precision of a parametric approximation methods based on the so-called goodness of fits, statistics are usually applied; examples are the χ-test statistics, the Kolmogorov–Smirnov statistics and the Anderson–Darling test.

3.2.2 Maximum Entropy

In cases when data is not available for performing distribution fitting, for example, if only statistical or other generalised information is available, such as mean value and standard deviation or the range of possible values, then the so-called principle of maximum entropy can be applied. The principle of using the entropy concept to derive probability distributions was introduced by Jaynes (1957). The principle infers a distribution function that preserves the maximal level of uncertainty (entropy) given presupposed constraints on the modelled variable. This means that the choice of any other distribution would require making additional assumptions unsupported by the constraints imposed by the available information. The maximum entropy (ME) distribution thus constitutes a mathematically well-founded choice of distribution when there is a lack of knowledge and data. The most commonly encountered sets of constraints yields the maximum entropy distributions presented in Table 1 (Harr 1987).

Table 1 Constraints and corresponding maximum entropy distributions

Case	Constrains from available information	Maximum entropy distribution
1	Mean	Exponential
2	Lower bound = 0 and any percentile	Exponential
3	Lower bound > 0 and any percentile	Shifted exponential or gamma
4	Range	Uniform
5	Range and mean	Beta with standard deviation that maximises the entropy
6	Mean and standard deviation	Normal
7	Range, mean and standard deviation	Beta
8	Mean rate of occurrence	Poisson

3.2.3 Bayesian Inference

When there is few data available, which is not sufficient for doing distribution fitting, Bayesian techniques can be used for deriving probability distributions using available prior information for similar situations, analogues. One example is the case when we need to derive PDFs for a parameter for a chemical element, for which we have only a few data values. In this case, data available for analogue elements can be used to derive an a priori distribution, which can be then updated with the few data available for the element of interest to obtain a posterior distribution. Bayesian techniques provide a framework for continuous updating of probability distributions as data becomes available. A comprehensive description of Bayesian techniques can be found in Gelman et al. (2003). Examples of application of this method for derivation of PDF of radioecological parameters can be found in Hosseini et al. (2013), where different methods that can be applied, depending on the information available, are described in details and are illustrated with examples.

3.2.4 Expert Elicitation

The data available for a given parameter are often limited both in quality and quantity. Moreover, some of the existing data may not be consistent with the assessment context. The process of deriving probability distributions is therefore largely subjective and requires specialised knowledge and judgement of each parameter. Principles for the formal collection and use of expert opinion have received considerable attention (Hofer 1986). Formal techniques have been, for example, developed to study risks of reactor operation (Hora and Iman 1989). However, it should be taken into account that formal expert elicitation is an expensive and time-consuming procedure.

The appropriate distribution type should be selected on a case by case basis using one, or a combination of several, of the above described methods. However, the experience shows that many parameters used in models of the transfer of contaminants in the environment are often well fitted by lognormal distributions. Several explanations for the frequently observed good fit to the lognormal distribution have been put forward (Aitchison and Brown 1957; Crow and Shimizu 1987).

3.3 Propagation of Uncertainties

To estimate the uncertainty in the model simulation endpoints, the uncertainties in the inputs and parameters must be propagated though the model. A good discussion on this subject can be found in IAEA (1989). When simple analytical expressions for the probability distributions are available, variance propagation can sometimes be applied for propagating the uncertainties (Morgan and Henrion 1992; Hoffman and Hammonds 1994). If one has a simple additive model and the input variables are independent, the mean value of the output distribution is the sum of the means of the input variables. Similarly, the variance of the output distribution is the sum of the variances of the input variables. The shape of the resulting output distribution will tend to be normal even if the distributions assigned to the inputs were not. A similar approach can be taken with multiplicative models after first converting the model to its additive form by logarithmically transforming the input variables. The output distribution of a multiplicative model will tend to be lognormal even when the input distributions were not. When the models are more complicated, the propagation of uncertainties can be carried out by means of Monte Carlo simulations.

3.3.1 Monte Carlo Analysis

When analytical methods cannot be applied, the uncertainties can be propagated using Monte Carlo analysis. The bases of the Monte Carlo method are straightforward (Vose 1996): point estimates in a model equation are replaced with probability distributions, samples are randomly taken from each distribution, and the results tallied usually in the form of a probability density function or cumulative distribution. This process is illustrated in Fig. 6 for the case of a simple model with one input, one parameter and one endpoint.

Several variations of the Monte Carlo technique for sampling from input and parameters distributions are available (Morgan and Henrion 1992). The conventional Monte Carlo sampling consists of taking random samples from the PDFs. One variation is importance sampling, where values of particular importance (usually the tails of the input distributions) are sampled more often and then given reduced weight to improve resolution in the tails of the output distribution. In stratified sampling, the input distributions are divided into intervals and input

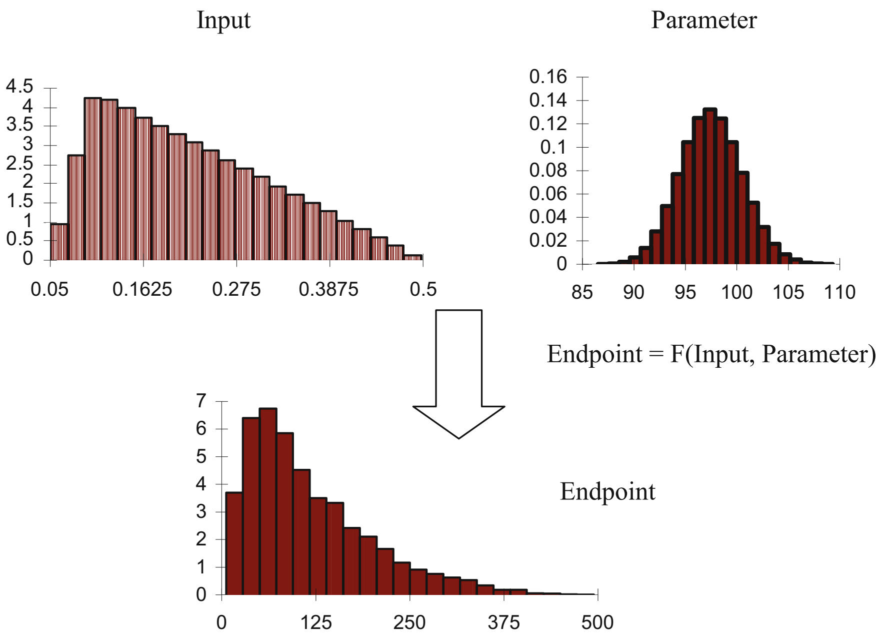

Fig. 6 Monte Carlo probabilistic simulations can be used for propagating the uncertainties in the inputs and parameters through the model. As result, a probability distribution of the endpoints is obtained, which can be used for quantification of the uncertainties of the estimations. In this example, the endpoint is calculated with a function *F* (the model) of one input and one parameter

values obtained by random sampling from within each interval. The most popular version of stratified sampling is Latin hypercube sampling, which divides input distributions into intervals of equal probability. Latin hypercube sampling is more precise than conventional Monte Carlo sampling, because the entire range of the input distributions is sampled in a more even, consistent manner (Iman and Helton 1988).

4 Sensitivity Analysis

Sensitivity analysis is used to apportion the relative effect of the uncertain inputs and parameters on the variation and uncertainty of the model simulation endpoints. Several sensitivity analysis methods of varying degree of complexity have been proposed in the literature (Saltelli et al. 2004). The choice on an appropriate method depends on several factors, such as the time needed for performing a simulation with the model, the number of uncertain parameters and the type of dependency between the inputs/parameters and the simulation endpoints of interest. For linear dependencies, simple methods based on correlations, such as the Pearson correlation coefficient (CC) and the Spearman rank correlation coefficient (SRCC), are sufficient, while for complex non-monotonic dependencies, more advanced methods, based on decomposition of the variance, are required.

The Pearson correlation coefficient is the normalised covariance between the input and output data sets and can take values between −1 and +1. The CC is equal in absolute value to the square root of the model coefficient of determination R^2 associated with the linear regression. The CC measures the linear relationship between two variables without considering the effect that other possible variables might have. Hence, it can be used as a sensitivity measure if the dependency between the inputs and the outputs is linear.

For nonlinear dependencies between inputs and outputs, the Pearson correlation coefficient will perform poorly as a sensitivity measure. Rank transformation of the data can be used to transform a nonlinear but monotonic relationship to a linear relationship. When using rank transformation, the data is replaced with their corresponding ranks. The usual correlation procedures are then performed on the ranks instead of the original data values. The Spearman rank correlation coefficients are calculated in the same way as the CC but on the ranks. The model coefficient of determination R^2 is also computed with the ranked data and measures how well the model matches the ranked data. Rank-transformed statistics are more robust and provide a useful solution in the presence of long-tailed input–output distributions. The SRCC will perform well as a sensitivity measure as long as there is a monotonic dependency between the inputs/parameters and the simulation endpoints.

The results of the sensitivity analysis can be presented in many different ways, for example, as tornado plots (Fig. 7). These are simple bar graphs where the sensitivity statistics, i.e. the CC or the SRCC, is visualised vertically in order of descending absolute value. The longer the bar, the larger the effect of the parameter on the simulation endpoint. The parameters that have positive values of the

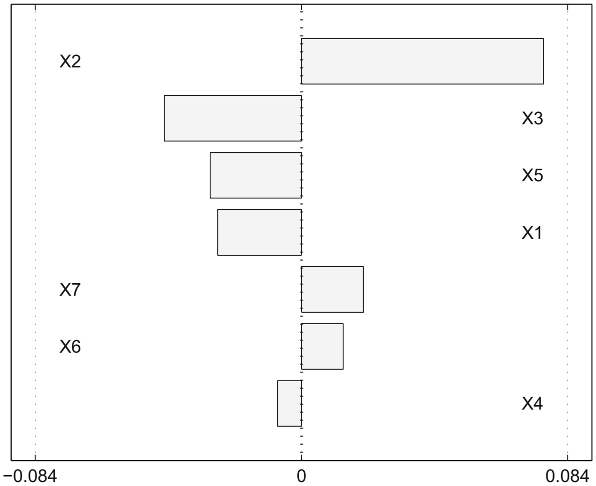

Fig. 7 Example of a tornado plot representing the sensitivity statistics (values of the correlation coefficients given in the *x*-axis). The larger the *bar*, the larger the effect of the parameter on the studied simulation endpoint. In this example, the parameters X2, X6 and X7 have a positive effect on the endpoint, while the parameters X1, X3, X4 and X5 have a negative effect, as indicated by the sign of the correlation coefficients

sensitivity measures have a positive effect on the endpoint, while the ones with negative values have a negative effect.

5 Conclusions

In this chapter, we have provided an overview of the risk and uncertainty analysis processes and of the methods that exist for performing such analyses. Risk and uncertainties are concepts that are related to each other but also with the concept of probability. This creates some difficulties for understanding and presenting the results of risk and uncertainty analysis. At the same time, the use of probability theory provides a way for a scientifically sound quantification of the risks and uncertainties.

References

Aitchison J, Brown JAC (1957) The Log-normal distribution. Cambridge University Press, Cambridge, UK

Brown JE, Alfonso B, Avila R, Beresford NA, Copplestone D, Pröhl G, Ulanovsky A (2008) The ERICA tool. J Environ Radioact 99:1371–1383

Cox LA Jr (2008) What's wrong with risk matrices? Risk Anal 28:497–512

Crow EL, Shimizu K (1987) Log-normal distributions. Theory and application. CRC, Boca Raton, FL

Evans M, Hastings N, Peacock B (2000) Statistical distributions. Wiley, New York

Gelman A, Carlin JB, Stern HS, Rubin DB (2003) Bayesian data analysis, 2nd edn. CRC, Boca Raton, FL

Harr ME (1987) Reliability-based design in civil engineering. McGraw-Hill, London

Hofer E (1986) On surveys of expert opinion. Nucl Eng Des 93:153–160

Hoffman FO, Hammonds JS (1994) Propagation of uncertainty in risk assessments: the need to distinguish between uncertainties due to lack of knowledge and uncertainties due to variability. Risk Anal 14:707–712

Hora SC, Iman RL (1989) Expert opinion in risk analysis: the NUREG-1150 methodology. Nucl Sci Eng 102:323–331

Hosseini A, Stenberg K, Avila R, Beresford NA, Brown JE (2013) Application of the Bayesian approach for derivation of PDFs for concentration ratio values. J Enviorn Radioact 126:376–387

IAEA (1989) Evaluating the reliability of predictions made using environmental transfer models. Safety Series No. 100. International Atomic Energy Agency, Vienna

IAEA (2004) Safety assessment methodologies for near surface disposal facilities. Results of a co-ordinated research project. Vol 1 Review and enhancement of safety assessment approaches and tools. International Atomic Energy Agency, Vienna

Iman RL, Helton JC (1988) An investigation of uncertainty and sensitivity analysis techniques for computer models. Risk Anal 8:71–90

ISO (2003) Space systems risk management. International Organization for Standardization. ISO 17666. http://www.iso.org/iso/catalogue_detail?csnumber=33149

Jaynes ET (1957) Information theory and statistical mechanics, I and II. Phys Rev 106:620–630; 108:171–190

Kaplan S, Garrick BJ (1981) On the quantitative definition of risk. Risk Anal 1:11–27

Morgan MG, Henrion M (1992) Uncertainty. A guide to dealing with uncertainty in quantitative risk and policy analysis. Cambridge University Press, Cambridge

NASA (2009) Risk management reporting, GSFC-STD-0002. Goddard Space Flight Center, NASA, Greenbelt, MD

Saltelli A, Tarantola E, Campolongo F, Ratto M (2004) Sensitivity analysis in practice – a guide to assessing scientific models. Wiley, Chichester

Taylor AC (1993) Using objective and subjective information to develop distributions for probabilistic exposure assessment. J Expo Anal Environ Epidemiol 3:285–298

UDoD (2006) Risk management guide for DoD acquisition. United States Department of Defense, Washington, DC

Vose D (1996) Quantitative risk analysis–a guide to Monte Carlo simulation modelling. Wiley, New York

Webster (1977) Webster's new collegiate dictionary. G & C Merriam, Springfield